Hydrogeochemische Modellierung der CO_2-Speicherung und -Leckage in geologischen Formationen

Unsicherheiten verursacht durch thermodynamische Datenbanken und numerische Codes

von

Christoph Haase

Kiel, 2015

Hydrogeochemische Modellierung der CO_2-Speicherung und -Leckage in geologischen Formationen

Unsicherheiten verursacht durch thermodynamische Datenbanken und numerische Codes

Dissertation
zur Erlangung des Doktorgrades
der Mathematisch-Naturwissenschaftlichen Fakultät
der Christian-Albrechts-Universität zu Kiel
vorgelegt von

Christoph Haase

Kiel, 2015

Erster Gutachter: PD Dr. Markus Ebert

Zweiter Gutachter: Prof. Dr. Romain Bousquet

Tag der mündlichen Prüfung: 23. März 2016

Zum Druck genehmigt: 23. März 2016

gez. Prof. Dr. Wolfgang J. Duschl, Dekan

Ein Abend, an dem sich alle Anwesenden einig sind,
ist ein verlorener Abend

Einstein (1921)

Kurzfassung

Die geologische CO_2-Speicherung kann dazu beitragen Emissionen von u. a. Kohlekraftwerken zu reduzieren und dabei langfristig CO_2 aus der Atmosphäre zu entfernen. Dabei wird CO_2 von Kraftwerksabgasen abgeschieden und in tiefe geologische Formationen injiziert (CCS, Carbon Capture and Storage). CO_2 kann in verschiedenartigen Reservoiren gespeichert werden, wofür sich ausgebeutete Erdöl- und Erdgasfelder, Kohleflöze und saline Aquifere eignen. Von diesen Reservoirtypen haben die salinen Aquifere die größte CO_2-Speicherkapazität. Ab einer Tiefe von ca. 800 m ist die CO_2-Speicherkapazität maximal, da CO_2 in dieser Tiefe annähernd die höchste Dichte aufweist. Von den salinen Aquiferen sind überwiegend permeable Sandsteinformationen geeignet, die im Rotliegend, Buntsandstein oder Keuper auftreten. Diese permeablen Formationen müssen von undurchlässigen Schichten überlagert werden, um einen CO_2-Aufstieg in oberflächennahe Grundwasserleiter oder in die Atmosphäre zu verhindern (»structural trapping«). In der Speicherformation löst sich das injizierte CO_2 partiell im Formationswasser (»hydrodynamic trapping«) und wird durch Ausfällungsreaktionen in kohlenstoffhaltigen Mineralphasen festgelegt (»mineral trapping«).

Die Auswirkungen einer CO_2-Speicherung auf die Speicherformation können durch numerische Modelle vorhergesagt werden. Diese Modelle koppeln thermische, hydraulische, mechanische und chemische Prozesse (THMC). Für die Berechnung der reaktiven Prozesse können die geochemischen Teilmodelle wie z. B. PHREEQC, THE GEOCHEMIST'S WORKBENCH, EQ3/6 und FACTSAGE/CHEMAPP eingesetzt werden. Diese Modelle verwenden verschiedene thermodynamische Datenbanken, die Unterschiede in den Reaktionsparametern aufweisen. Die Anwendung verschiedener Datenbanken kann aufgrund der Datenvarianzen zu Spannweiten der berechneten Ergebnisse führen. Die Ergebnisspannweite aller angewendeten Datenbanken wird als Unsicherheit des Modellergebnisses definiert.

Für einfache Systeme, beispielsweise für die Reaktion von CO_2 mit einem NaCl-haltigen Formationswasser und mit Calcit, liegen die Unsicherheiten der CO_2- und Calcit-Löslichkeit im Bereich von einer Größenordnung. Dabei steigt die Unsicherheit der Calcit-Löslichkeit von 12 mmol/kgw bei oberflächennahen Bedingungen, d. h. geringe Temperatur, niedriger Druck und Ionenstärke (T-P-I), auf 44 mmol/kgw bei Reservoirbedingungen (hohe T-P-I-Bedingungen) an. Die CO_2-Löslichkeit weist jedoch viel größere Spannweiten als die von Calcit auf, z. B. beträgt die Spannweite des gelösten CO_2 bei geringen T-P-I-Bedingungen 88 mmol/kgw. Die Spannweite der Löslichkeit von CO_2 steigt um einen Faktor von 10 bei Reservoirbedingungen an. Für die Berechnung der hydrodynamischen Speicherung oder der Rückhaltung von CO_2 ist daher die exakte Berechnung der CO_2-Löslichkeit von größerer Bedeuting als die der Calcit-Löslichkeit.

Die Anwendung verschiedener Datenbanken zeigt generell keine signifikanten Unterschiede zwischen Datenbanken mit Debye-Hückel oder Pitzer-Ansatz. Die Anwendung des Pitzer-Ansatzes für Modelle von CO_2-Speicherformationen ist die beste Wahl, da die Formationswässer meist hohe Ionenstärken aufweisen. Die Pitzer-Gleichung berechnet bei solch hohen Ionenstärken Aktivitätskoeffizienten, die gut mit experimentellen Ergebnissen übereinstimmen. Jedoch ist damit die Berechnung der Reaktionen von wichtigen Si- oder Al-haltigen Mineralphasen nicht möglich. Daher wurden von allen Datenbanken diejenigen bestimmt, die die geringsten Abweichungen zu den Ergebnissen des Modells von Duan & Li (2008) zeigen, welches sehr geringe Abweichungen im Vergleich zu experimentellen Ergebnissen der CO_2- und Calcit-Löslichkeit berechnet. Die Datenbanken *phreeqc.dat* und *wateq4f.dat* von PHREEQC und werden daher generell für die Modellierung der CO_2-Speicherung empfohlen.

In reaktiven Transportmodellen werden kinetisch kontrollierte Reaktionen, wie z. B. die Feldspatauflösung, für die Modellierung des CO_2-Einflusses auf Leckage- und Speicherformationen notwendig. Die Anwendung acht thermodynamischer Datenbanken von PHREEQC und THE GEOCHEMIST's WORKBENCH wurde für die Auflösung von Anorthit in einem ein-dimensionalen Transportmodell untersucht. Die Ergebnisunsicherheiten erreichen Maximalwerte von ca. 90 %, wenn die Anorthitauflösung in einem Formationswasser der Buntsandsteinformation mit der höchsten Ionenstärke (6.5 mol/l) und der höchsten Temperatur (58 °C) berechnet wird. Jedoch beträgt die Unsicherheit für Formationswässer, die von einer CO_2-Leckage beeinflusst werden können, wie die des Quartärs, nur 1 %. Durch die CO_2-Lösung nimmt der pH-Wert der Formationswässer auf Werte zwischen 4.0 und 5.5 ab. In diesem pH-Bereich wechselt der Auflösungsmechanismus von Anorthit vom langsamen neutralen Mechanismus zum schnelleren sauren Mechanismus, wodurch die Auflösungszeit stark variiert. Die Variation der initialen pH-Werte und initialen Auflösungsraten berechnet durch die unterschiedlichen Modellprogramme und thermodynamischen Datenbanken nimmt im Verhältnis zur Ionenstärke zu. Eine genaue Untersuchung der Ursachen ergibt, dass die Berechnungsmethode der Aktivitätskoeffizienten der aquatischen Hauptspezies den größten Einfluss auf die simulierten Modellergebnisse hat. Den zweitgrößten Einfluss hat die Berechnungsmethode der Aktivitätskoeffizienten von CO_2. Durch die Kalibration mit experimentellen Daten kann eine bestimmte thermodynamische Datenbank ausgewählt werden, die diese Daten wiedergibt. Jedoch ist die Kalibration der thermodynamischen Datenbanken für alle möglicherweise ablaufenden Reaktionen in komplexen geologischen Systemen bei großen Spannweiten der Temperatur- und Druckbedingungen, wie sie besonders bei der CO_2-Speicherung auftreten, nicht möglich. Die Unsicherheiten, die in dieser Arbeit für CO_2-Speichersysteme quantifiziert wurden, bestehen daher unabhängig von vorher durchgeführten Kalibrationen von thermodynamischen Datenbanken mit experimentellen Daten.

Anhand von Säulenversuchen wurde die kinetisch kontrollierte Auflösung von Calcit bei zwei verschiedenen Partialdrücken bestimmt. Der Vergleich von experimentell ermittelten Calcium-Konzentrationen mit den von PHREEQC simulierten Ergebnissen bei Verwendung der Standard-Datenbank und der Verwendung der Ratengesetze mit der Standard-Parametrisierung ergibt einen zu schnellen Anstieg der Calcium-Konzentration. Bei höheren Partialdrücken von 43 bar ergeben sich zusätzlich zu hohe Gleichgewichtskonzentrationen für Calcium. Die Ursache für die langsamer ablaufende Calcitlösung kann die Diffusionsgrenzschicht (DBL) sein. Daher wurde die reaktive Oberfläche im Ratengesetz angepasst um die Auflösungsrate zu verringern, wodurch der Anstieg der Calciumkonzentration mit den Versuchsergebnissen gut übereinstimmt. Damit kann die Calcitauflösung durch die Verwendung des numerischen Codes gut abgebildet werden.

Die Abweichung der Gleichgewichtskonzentration zwischen Anwendung der *pitzer.dat* und *phreeqc.dat* Datenbank ist bei Partialdrücken von 43 bar in den kleinskaligen Modellen am größten. Daher wurde ein Feldskalamodell mit diesen thermodynamischen Datenbanken berechnet, wobei die kinetisch kontrollierte Calcitauflösung mit den veränderten Parametern der kinetischen Ratengesetze berechnet wurde. Die Varianz betrug bei hohen Partialdrücken (43 bar) in tieferen Aquiferen ca. 35 %. Die berechnete Reaktionsfront von Calcite ist so steil, dass die Verwendung einer Gleichgewichtsreaktion die gleichen Ergebnisse ergibt. Wenn die Strömungsgeschwindigkeit ausreichend hoch ist und die Zellengröße klein genug, so dass die Aufenthaltszeit des Wassers in einer Zelle ca. 2 Stunden nicht unterschreitet, kann eine Gleichgewichtsreaktion angewendet werden. Jedoch ist die Aufenthaltszeit in einer Zelle von großskaligen Modellen, wie sie bei Berechnung einer

CO_2-Leckage verwendet werden, viel größer. Daher wird das Gleichgewicht zu Calcit innerhalb der Aufenthaltszeit einer Zelle problemlos erreicht.

Die geochemische Modellierung ist ein geeignetes Werkzeug um bei einer CO_2-Speicherung die Verteilung von CO_2 zu simulieren, das im Formationswasser gelöst ist oder als Gasphase vorliegt. Ebenso können die Auswirkungen einer CO_2-Injektion oder -Leckage auf geologische Formationen vorhergesagt werden. Jedoch sind die Modellergebnisse nicht genau, denn es treten Unsicherheiten durch die Varianz der thermodynamischen und kinetischen Parameter auf. Durch eine Kalibrierung der Modellberechnungen mit experimentellen Daten kann die Eignung von thermodynamischen Datenbanken und kinetischen Ratengesetzen geprüft werden, jedoch kann nicht für jede Reaktion in komplexen geologischen Systemen eine Kalibrierung durchgeführt werden. Daher bleiben die Unsicherheiten für diese Systeme trotz vorher durchgeführten Kalibrierungen bestehen. Diese Unsicherheiten können insbesondere die Vorhersage der Festlegung von CO_2 in Mineralphasen (»mineral trapping«) und die hydrodynamische Speicherung von CO_2 in Speicher-, Rückhalte-, Transfer- und Schutzgutformationen beeinflussen (»solubility trapping«) und sich somit auf die Bewertung des Risikos eines CO_2-Eintritts in oberflächennahe Grundwasserleiter auswirken. Neben den untersuchten Unsicherheiten spielen in gekoppelten numerischen Modellen weitere Parameter für die Vorhersagesicherheit eine Rolle. Diese Parameter können z. B. die Porosität, hydraulische Durchlässigkeit oder die Mineralzusammensetzung der Formation sein und zu zusätzlichen Unsicherheiten der Modellergebnisse führen.

Abstract

Geologic carbon has been proposed as a technology for reducing large scale CO_2 emissions into the atmosphere. CO_2 can be captured at power plants and stored in different reservoir types, among which the saline aquifers have the largest estimated storage capacity. The storage is efficient in depth larger than 800 m, because the density of CO_2 is very high at the prevailing temperature and pressure conditions. Therefore, at these depth the storage capacity with respect to CO_2 is largest. The formations suitable for CO_2 storage are permeable sandstones, which are overlain by impermeable layers, i. e. fine-grained rocks (mudstones or siltstones, saltrocks). The impermeable layers can prevent CO_2 from migrating into formations overlaying the storage formation (»structural trapping«) and into protected potable aquifers near the surface acidifying the groundwater, which are the major risks of CO_2 storage. In the storage formation CO_2 dissolves in the formation water (»hydrodynamic trapping«) and through mineral reactions the CO_2 can be trapped in carbon bearing mineral (»mineral trapping«).

The effects induced by the injection of CO_2 into geologic reservoirs or by a CO_2 leakage into the overlaying formations can only be predicted by numerical modelling (non-invasive). The numerical model codes couple thermical, hydraulic, mechanical and chemical processes. For the geochemical processes the model codes The Geochemist's Workbench, EQ3/6, Phreeqc and FactSage/ChemApp are commonly applied. The thermodynamic parameters necessary to model these reactions are not determined explicitly through experiments at the total range of temperature and pressure conditions and are thus extrapolated by the simulation code. The model codes include different thermodynamic databases and their application leads to different model code results. Until today, none of the databases was validated for the application to CO_2 storage or leakage models. Thereby, using different thermodynamic databases generated variations in the simulation results referred to as model uncertainty.

Until now the research of CO_2 storage processes has been focused on the geochemical processes of the CO_2 reaction with minerals of storage formations, which mostly consist of sandstones containing quartz, feldspars or calcite. Regarding safety assessment the reactions between CO_2 and overlaying formations in case of a CO_2 leakage are of equal importance as reactions in the storage formation. In particular, limestone formations can react very sensitively to CO_2 intrusion.

The uncertainty study is performed comparing the computed results applying the geochemical model codes The Geochemist's Workbench, EQ3/6, Phreeqc and FactSage/ChemApp and their thermodynamic databases. The input parameters (1) total concentration of the solution, (2) temperature and (3) fugacity are varied within typical values for CO_2 reservoirs, overlaying formations and close-to-surface aquifers. The most sensitive input parameter in the system H_2O-CO_2-NaCl-$CaCO_3$ for the calculated range of dissolved calcite and CO_2 is the fugacity of CO_2. Hence, the largest range of dissolved calcite is calculated at high fugacities and is 210 mmol/kgw. The average deviation of the results using the databases *phreeqc.dat* and *wateq4f.dat* in combination with the Phreeqc code is lowest in comparison to the results of the specific model of Duan and Li (2008), which represents the experimental values at best. Still, the solubility of CO_2 in the formation water is overestimated using these two databases. Therefore, the model results calculate a larger retention capacity, defined as the quantity of CO_2 dissolved in the formation water, than the Duan and Li model would calculate.

Phreeqc and The Geochemist's Workbench codes were used in this study to simulate anorthite dissolution in storage, retention, transfer, and near-surface formation waters represented by respective geological units. For each of the formation waters, a one-dimensional scenario was simulated by using

eight different thermodynamic databases. At a high ionic strength and a high temperature mineral trapping is the most efficient process for long term CO_2 storage. However, among the geological formations and the time needed for anorthite dissolution regarded in this study, model uncertainties caused by using different numerical code and thermodynamic database combinations were largest (ca. 90 %) for the storage formation waters at 58 °C and I = 6.5 mol/l. Conversely, in near-surface formation waters the model uncertainty was less than 1 %. Due to CO_2 dissolution the calculated pH of the formation waters decreased to a range between pH 4.0 and 5.5. In that pH range, the dissolution mechanism of anorthite switches from the slow neutral to the faster acid mechanism causing dissolution time length variations. The calculated pH variation further increased with rising ionic strength. A detailed examination of the reasons revealed the activity coefficient calculation method of the main aquatic species to have the largest impact on the simulated model results. The second largest impact had the calculation method of the CO_2 activity coefficient. By calibration to experimental data, a specific thermodynamic database can be chosen representing these experimental results. However, the calibration of thermodynamic databases is not possible for all potential reactions in more complex geological systems at large ranges of temperature and pressure conditions. The uncertainties quantified in this study for CO_2 storage systems originating from using thermodynamic databases will therefore persist independently from previously conducted calibrations of thermodynamic databases to experimental data.

Among the risks of CO_2 storage is the potential of CO_2 leakage into overlaying formations and near-surface potable aquifers. Through a leakage, the CO_2 can intrude into protected groundwater resources, which can lead to groundwater acidification followed by potential mobilisation of heavy metals and other trace metals through mineral dissolution or ion exchange processes. The prediction of pH buffer reactions in the formations overlaying a CO_2 storage site is essential for assessing the impact of CO_2 leakages in terms of trace metal mobilisation. For buffering the pH-value, calcite dissolution is one of the most important mechanisms. Although calcite dissolution has been studied for decades, experiments conducted under elevated CO_2 partial pressures are rare. In this work the first study for column experiments is presented applying CO_2 partial pressures from 6 to 43 bars and realising a near-natural flow regime. Geochemical calculations of calcite dissolution kinetics were conducted using PHREEQC together with different thermodynamic databases. Applying calcite surface areas, which were previously acquired by N_2-BET or calculated based on grain diameters, respectively, to the rate laws according to Plummer et al. (American Journal of Science 278:179–216, *doi:10.2475/ajs.278.2.179*, 1978) or Palandri and Kharaka (U.S. Geological Survey Open file Report 2004-1068:71, 2004) in the numerical simulations led to an overestimation of the calcite dissolution rate by up to three orders of magnitude compared to the results of the column experiments. Only reduction of the calcite surface area in the simulations as a fitting procedure allowed reproducing the experimental results. A reason may be that the diffusion boundary layer (DBL), which depends on the groundwater flow velocity and develops at the calcite grain surface separating it from the bulk of the solution, has to be regarded: The DBL leads to a decrease in the calcite dissolution rate under natural laminar flow conditions compared to turbulent mixing in traditional batch experiments. However, varying the rate constants by three orders of magnitudes in a field scale PHREEQC model simulating a CO_2 leakage produced minor variations in the pH buffering through calcite dissolution. This justifies the use of equilibrium models when calculating the calcite dissolution in CO_2 leakage scenarios for porous aquifers and slow or moderate groundwater flow velocities. However, the selection of the thermodynamic database has an impact on the dissolved calcium concentration, leading to an

uncertainty in the simulation results. The resulting uncertainty, which applies also to the calculated propagation of an aquifer zone depleted in calcite through dissolution, seems negligible for shallow aquifers of approximately 60 m depth, but amounts to 35 % of the calcium concentration for aquifers at a depth of approximately 400 m.

In general, geochemical modelling is a suitable tool to predict the CO_2 proportion distributed between the formation water and gas phase due to a storage or leackage of CO_2 and to predict the effects of CO_2 on specific geologic formations. However, the model simulations do not result in exact values, because thermodynamic and kinetic parameter variances result in a range of the model predictions referred to as model uncertainty. Calibrating the model simulation using experimental data the suitability of thermodynamic databases and kinetic rate laws can be tested. Uncertainties remain for complex geological systems despite previously conducted calibrations. These uncertainties influence the prediction for »mineral trapping« in storage formations and »solubility trapping« of CO_2 in retention and transfer formations to protect potable aquifers from an intrusion of CO_2. The uncertainties can affect the assessment of the risks of CO_2 intrusion in near-surface aquifers. In addition to the uncertainties investigated in the presented work coupled reactive transport models include further parameters affecting the prediction accuracy. These parameters can be i. e. the porosity, hydraulic permeability and the mineral types and their proportion in the geologic formation and may lead to additional uncertainty of the numerical code results.

Inhaltsverzeichnis

Abbildungsverzeichnis

Tabellenverzeichnis

Abkürzungsverzeichnis

a_i Aktivität a des Ions i [-].
a_0 Parameter zur Aktivitätsberechnung.
b_0 B-dot Parameter zur Aktivitätsberechnung.
c_i Konzentration c des Ions i [mol/kgw].
$\Delta_f G^0$ Standardbildungsenergie eines Stoffes [J].
$\Delta_r G^0$ Differenz der Gibbs-Energien der Reaktanden bei Standardbedingungen [J].
f Fugazität [bar].
G Gibbs-Energie [J].
γ_i Aktivitätskoeffzient γ des Ions i [-].
E_a Aktivierungsenergie kinetisch kontrollierter Reaktionen [kJ/mol].
$\Delta_r H^0$ Reaktionsenthalpie [kJ/mol], Differenz der Standardbildungsenthalpien einer Reaktion bei Standardbedingungen zwischen den Produkten und Edukten.
$\Delta_f H^0$ Standardbildungsenthalpie [kJ/mol], Energie, die bei der Bildung eines Mols einer Substanz aus der allotropisch stabilsten Form der reinen Elemente unter Standardbedingungen frei wird oder zur Bildung erforderlich ist.
ρ Dichte eines Stoffes bei Standardbedingungen [kg/m^3].
I Ionenstärke einer Lösung [mol/kgw].
i Spezies i [-].
K_{eq} Gleichgewichtskonstante einer Reaktion.
P Druck [bar].
R Die universelle Gaskonstante 8.315 J K^{-1}mol^{-1}.
k Kinetische Ratenkonstante [mol s^{-1}l^{-1}].
SI Sättigungsindex einer Mineralphase.
S_A Mineraloberfläche für kinetische Ratengesetze [m^2].
z_i Ladung des Ions i [-].

1. Einleitung

Diese Arbeit wurde im Kontext des vom Bundesministerium für Bildung und Forschung (BMBF) und von den Industriepartnern E.ON Energie AG, E.ON Gas Storage AG, EnBW Energie Baden-Württemberg AG, RWE Dea AG, Stadtwerke Kiel AG, Vattenfall Europe Technology Research GmbH und Wintershall Holding AG geförderten Projekts »Modellierung und Parametrisierung von CO_2-Speicherung in tiefen, salinen Speichergesteinen für Dimensionierungs- und Risikoanalysen« (CO_2-MoPa) durchgeführt. In dem Projekt CO_2-MoPa wurde die Simulation der geologischen CO_2-Speicherung in tiefen, salinen Formationen am Beispiel Norddeutschlands untersucht. Bei den in diesen Formationen bestehenden Druck- und Temperaturbedingungen ($T > 30\,°C$, $P > 80\,bar$) ist die CO_2-Speicherung bei geringer Gasdichte möglich. CO_2 nimmt dabei ein geringes Volumen ein. Bei Vorliegen von undurchlässigen Deckschichten (z. B. Tonstein oder Steinsalz) ist ein CO_2-Aufstieg in oberflächennahe Grundwasserleiter oder in die Atmosphäre nicht möglich. Um die Risiken eines möglichen CO_2-Aufstiegs zu bewerten, ist die Bestimmung der gespeicherten CO_2-Menge, davon besonders der in Mineralphasen festgelegte Anteil, von großer Bedeutung. Zur Quantifzierung dieser Anteile wurden in dem Projekt CO_2-MoPa numerische und prozessorientierte Modellwerkzeuge entwickelt und angewendet, die die großskalige CO_2-Ausbreitung und -Speicherung in tiefen, salinen Formationen vorhersagen können (Bauer et al., 2012). Dabei wurden hydraulische, geochemische und geomechanische Prozesse in die numerischen Modellcodes integriert.

Die Bewertung des Risikos einer CO_2-Speicherung kann im Vorfeld nur mit numerischen Modellcodes vorgenommen werden. Die Modellcodes simulieren die CO_2-Lösung im Formationswasser um dadurch induzierte Mineralreaktionen, z. B. für die pH-Pufferung, zu quantifizieren. Eine genaue Kenntnis der möglichen Spannbreite der CO_2-Lösung in Formationswässern bei verschiedenen Temperatur- und Druckbedingungen ist zum einen für die Vorhersage der gespeicherten CO_2-Menge im Formationswasser der Speicherformation und zum anderen für die Vorhersage der Rückhaltekapazität im Fall einer CO_2-Leckage essentiell. Dadurch kann prognostiziert werden, wie groß der Anteil von CO_2 ist, der als Gasphase zurückbleibt. Die Prognose dieser Prozesse dient dazu, die Möglichkeit eines CO_2-Austritts in die Atmosphäre zu bewerten und damit das Risiko einer CO_2-Speicherung zu analysieren. Da für mögliche CO_2-Speicherstandorte die notwendigen Daten für den Modellaufbau fehlen, wurden in diesem Projekt virtuelle Szenarien simuliert, die mögliche Reaktionsszenarien für eine CO_2-Speicherung und -Leckage darstellen. Anhand dieser Prognoseergebnisse können z. B. Monitoringstrategien bewertet und Risikoanalysen erstellt werden.

Das Ziel dieser Arbeit ist der Vergleich der Simulationsergebnisse verschiedener geochemischer Modellcodes für mögliche Reaktionsszenarien in geologischen Formationen Norddeutschlands bei einer CO_2-Speicherung. In bisherigen Studien der CO_2-Speicherung wurden verschiedene numerische Modellcodes mit thermodynamischen Datenbanken angewendet, jedoch ohne eine Begründung für die Anwendung einer Modellcode-Datenbank-Kombination zu liefern und ohne die Simulationsergebnisse unterschiedlicher Kombinationen dieser zu vergleichen. Nur in einer begrenzten Anzahl von Studien wurden die Ergebnisse verschiedener Modellcode-Datenbank-Kombinationen für eine begrenzte Anzahl Reaktionsszenarien verglichen. In der vorliegenden Arbeit sollen durch Anwendung verschiedener numerischer Codes kombiniert mit thermodynamischen Datenbanken

die Ergebnisspannbreiten bzw. -varianzen für Mineral- und Gaslöslichkeiten bestimmt werden. Der Ergebnisbereich der möglichen Modellcode-Datenbank Kombinationen wird als Modellunsicherheit in Bezug auf das berechnete Modellergebnis definiert. Die Modellunsicherheiten sollen für Reaktionsszenarien bestimmt werden, die die Druck- und Temperaturbedingungen von CO_2-Speicherformationen bis hin zu oberflächennahen Formationen abdecken.

Die vorliegende Arbeit wurde als kumulative Dissertation angefertigt. Nach der Einleitung bilden die Kapitel drei wissenschaftlichen Publikationen (Kapitel 2, 3 und 4). Die Publikationen der Kapitel 2 und 4 wurden in der internationalen wissenschaftlichen Zeitschrift »Applied Geochemistry« veröffentlicht. Die Publikation aus Kapitel 3 wurde in der Zeitschrift »Aquatic Geochemistry« veröffentlicht.

Paper I: »Uncertainties in geochemical modelling of CO_2 and calcite dissolution in NaCl solutions due to different modelling codes and thermodynamic databases« (Kapitel 2)

Das Ziel des ersten Papers ist die Bestimmung von Modellunsicherheiten, die durch Anwendung unterschiedlicher thermodynamischer Datenbanken entstehen. Die Datenbanken enthalten unterschiedliche Parameter, die ihrerseits ebenfalls Varianzen aufweisen. Mögliche Parameter dieser Art sind z. B. Gleichgewichtskonstanten der Reaktionen, Debye-Hückel-Parameter zur Berechnung von Aktivitätskoeffizienten, Art und Anzahl der aquatischen Spezies und die Temperaturkorrektur für die Parameter. Die Ergebnisspannweiten der CO_2- und Calcite-Lösung bei Verwendung der Modellcodes kombiniert mit verschiedenen thermodynamischen Datenbanken sollen zuerst in nulldimensionalen Szenarien (ein Einheitsvolumen Wasser) untersucht werden. Dabei sollen die Spannweiten der Simulationsergebnisse für vereinfachte Systeme bei Verwendung eines synthetischen Formationswassers für verschiedene Salzgehalte (NaCl), CO_2-Partialdrücken und Temperaturbedingungen bestimmt werden.

Paper II: »Uncertainties of geochemical models and thermodynamic databases for predicting geochemical impact of CO_2 on geologic formations« (Kapitel 3)

Im zweiten Paper werden eindimensionale Reaktionsszenarien erstellt, mit denen die Feldspatauflösung induziert durch eine CO_2-Reaktion in CO_2-Speicher- und oberflächennahen Formationen berechnet wird. Dabei soll die zeitabhängige Auflösung von Anorthit in einem eindimensionalen Modell bei Verwendung von zwei numerischen Modellcodes unter Verwendung verschiedener thermodynamischer Datenbanken berechnet werden. Als Vergleichsgröße dient die berechnete Auflösungszeit für Anorthit in der Modellzelle. Durch die Anwendung verschiedener thermodynamischer Datenbanken wird eine Spannbreite der Modellergebnisse für die Auflösungszeit von Anorthit simuliert. Der die Auflösungszeit steuernde Parameter und die für die Unsicherheiten verantwortlichen Datenbankparameter sollen bestimmt werden. Die Spannbreiten der Modellergebnisse sollen für verschiedene Formationswässer untersucht werden.

Paper III: »Suitability of existing numerical model codes and thermodynamic databases for the prognosis of calcite dissolution processes in near-surface sediments due to a CO_2 leakage investigated by column experiments« (Kapitel 4)

Im dritten Paper soll durch den Vergleich von Simulationsergebnissen der numerischen Codes mit experimentellen Daten eine thermodynamische Datenbank bestimmt werden, die für die Modellierung

einer CO_2-Leckage geeignet ist. Calcit ist in potentiellen Speicher- und Leckageformationen ein häufig vorkommendes Mineral und reagiert vergleichsweise schnell unter CO_2-Einfluss. Es soll untersucht werden, wie gut numerische Modellcodes mit Ratengesetzen bei Verwendung der Standardparametrisierung für die Ratengesetze der Calcitauflösung die Ergebnisse eines Säulenversuchs bei verschiedenen CO_2-Partialdrücken simuliert werden kann. Dabei sollen zwei unterschiedliche Ratengesetze für die Calcitauflösung angewendet und es soll überprüft werden, inwieweit sich durch Anpassung kinetischer Parameter die experimentellen Ergebnisse simulieren lassen. Eine für die Berechnung der Auswirkungen einer CO_2-Leckage geeignete Datenbank wird bestimmt.

1.1 Hydrogeochemische Codes

1.1.1 Historische Entwicklung

Die Berechnungsmethoden der Lösung von chemischen Gleichgewichtsproblemen wurde im Zuge der Raketenentwicklung im Zweiten Weltkrieg entwickelt (van Zeggeren & Storey, 1970; Zeleznik, 1962; Zeleznik & Gordon, 1960). Die Technologie der Raketen, wie z. B. der V2, benötigte eine genaue Kenntnis der chemischen Gleichgewichte (Gordon et al., 1959), die in Treibstoffsystemen zwischen den Treibstoffen und den bei der Verbrennung entstehenden Gasen herrschen (Damköhler & Edse, 1943).

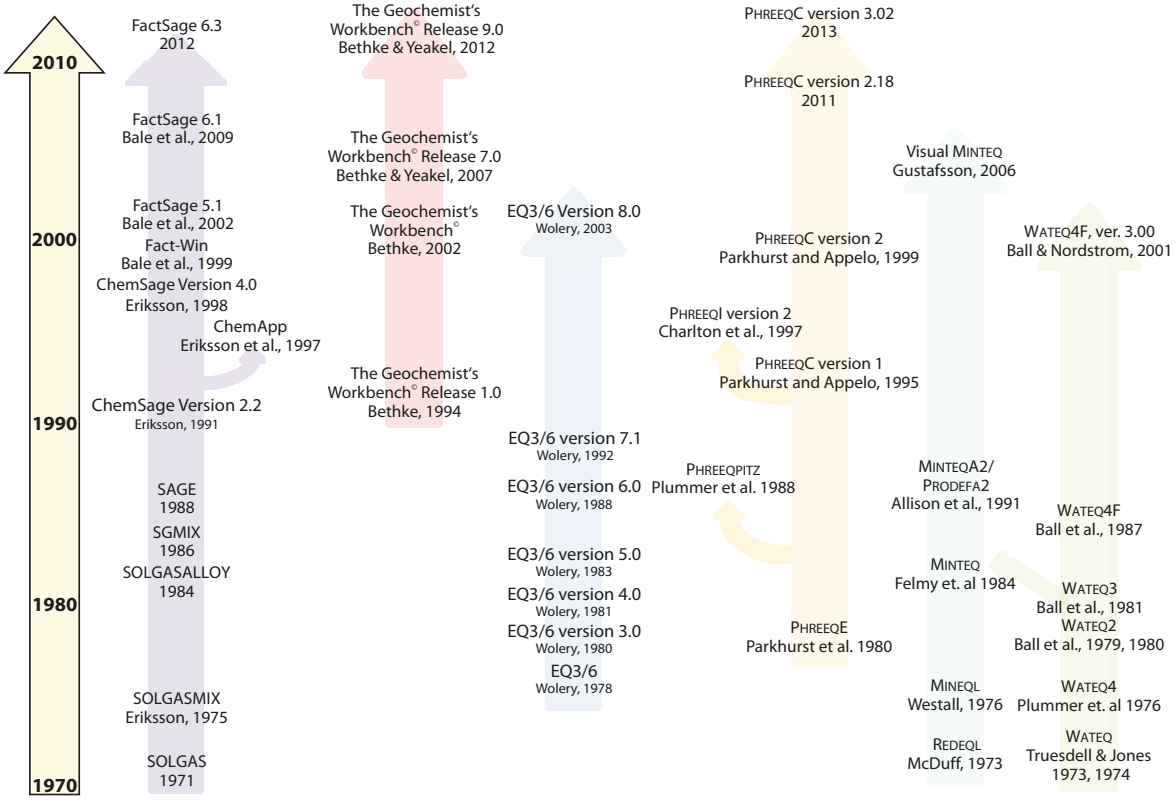

Abbildung 1.1
Entwicklung der Programmgruppen FACTSAGE, THE GEOCHEMIST'S WORKBENCH, EQ3/6, PHREEQC, VISUAL MINTEQ und WATEQ4F.

Damköhler & Edse (1943) und Zeleznik (1962) entwickelten Methoden um nichtlineare Gleichungen, basierend auf Massenbilanz- und Massenerhaltungsgleichungen, mit einer graphischen Abschätzungsmethode zu lösen und wendeten diese Methode auf Gasgemische an. Erste größere Fortschritte wurden nach dem Zweiten Weltkrieg gemacht. Brinkley (1946) entwickelte ein generelles Lösungsschema und ebnete damit den Weg für einen systematischen Ansatz für die Gleichgewichtsberechnungen. Brinkley (1947) wendete verschiedene Methoden an, darunter auch die Newton-Raphson Methode zur Lösung der Gleichungssysteme. Da Anfang der 50er Jahre Computer kommerziell verfügbar wurden und die Methode von Brinkley (1947) für die Anwendung auf Computern optimiert worden war, verbreitete sich diese Methode schnell und Computerprogramme zur Berechnung chemischer Gleichgewichte wurden entwickelt (Gordon et al., 1959; Gordon & Zeleznik, 1963). Ein Programm, das auf Gleichgewichtskontanten für das Massenwirkungsgesetz (»Law-of-Mass-Action«, LMA) basiert, wurde von Morel & Morgan (1972) entwickelt. Parallel dazu wurde von White et al. (1958) der Ansatz der Minimierung der Gibbs-Energie (»Gibbs Energy Minimization«, GEM) entwickelt. Einen Überblick über die beiden Methoden geben Zeleznik & Gordon (1968).

Seit der zunehmenden Verbreitung von Computern in Forschungseinrichtungen wurden von verschiedenen Forschergruppen diverse numerische Codes für die Berechnung geochemischer Gleichgewichtsprobleme entwickelt (Abbildung 1.1). Eines der ersten thermodynamischen geochemischen Rechenprogramme war das Speziierungs-Programm Watchem, das im Jahr 1969 entwickelt wurde. Dieses Programm wurde über Wateq (Truesdell & Jones, 1974) zu Wateq4f (Ball & Nordstrom, 1991) weiterentwickelt. Dessen Daten sind in Phreeqc als Datenbank *wateq4f.dat* verfügbar. Phreeqc (Parkhurst & Appelo, 1999) ging aus dem 1980 entwickelten Programm Phreeqe (Parkhurst et al., 1980) hervor. Das Programm wurde kontinuierlich zur Phreeqc Version 3 weiterentwickelt (Parkhurst & Appelo, 2013). Die Version 3 enthält neue Funktionen wie eine Berechnung der Druckabhängigkeit der Gleichgewichtskonstanten und die Berechnung der Löslichkeit von Gasen unter Verwendung der Redlich-Kwong Zustandsgleichung (Appelo et al., 2014).

Der geochemische Code Minteq wurde aus RedEql (McDuff & Morel, 1973) entwickelt (Peterson et al., 1987; Abbildung 1.1). Der Code Minteq wurde mit einer graphischen Oberfläche versehen und wird daher als Visual Minteq (Gustafsson, 2006) bezeichnet. Die Datenbanken von Minteq liegen im Phreeqc-Format als *minteq.dat* und *minteq.v4.dat* vor, ebenso liegt die Datenbank im Format von The Geochemist's Workbench als *thermo_minteq.dat* vor.

Die Entwicklung des Modellcodes EQ3/6 wurde 1978 vom Lawrence Livermore National Laboratory (LLNL) für die Anwendung in der Endlagerung von radioaktiven Stoffen begonnen und bis zur Version 8.0 weiterentwickelt (Wolery & Jarek, 2003) (Abbildung 1.1). The Geochemist's Workbench ist eine neuere Programmentwicklung ausgehend von EQ3/6. The Geochemist's Workbench wurde 1994 am Department of Geology der University of Illinois at Urbana-Champain begonnen und kontinuierlich weiterentwickelt. Die aktuellste Version ist das Release 10.0 aus dem Jahr 2014 (Bethke & Yeakel, 2014). Die thermodynamischen Datenbanken von EQ3/6 wurden häufig mit dem Code TOUGHREACT verwendet (Pruess et al., 2003, Xu et al., 1997).

Erst seit dem letzten Jahrzehnt ist es möglich den Ansatz der Minimierung der Gibbs-Energie im Programm FactSage (Bale et al., 2002) und ChemApp (Petersen & Hack, 2007) in der hydrogeochemischen Modellierung anzuwenden (Kapitel 1.1.7, 1.2). Das Programm wurde in neueren Studien an das Strömungsprogramm Geosys gekoppelt (Li et al., 2009, Mitiku et al., 2013).

Einen Überblick über geochemische Codes und ihre Datenbanken geben Jenne (1979), Bassett & Melchior (1990), Nordstrom (2007) und Oelkers et al. (2009). Die akutellen Entwicklungen werden von Nordstrom & Campbell (2014) und im Special Issue »Geochemical Speciation Codes and Databases« (Kulik et al., 2015) wiedergegeben. Reaktive Transportcodes wurden von Steefel et al. (2005) beschrieben und der aktuelle Entwicklungsstand wird von Steefel et al. (2014) zusammengefasst.

Die Berechnung von chemischen Reaktionen von Mineralphasen mit Wasser- und Gasphasen (geochemische Modellierung) ist seit mehreren Jahrzehnten ein etabliertes Werkzeug in der Hydrogeologie bzw. Hydrogeochemie (z. B. Appelo & Willemsen, 1987; Appelo et al., 1990, 1998; Bethke, 2008; Merkel & Planer-Friedrich, 2008). Damit wurde die Prognose der Entwicklung der Grundwasserchemie möglich und die ablaufenden Prozesse und Reaktionen konnten in hydrogeochemischen Systemen besser verstanden werden (z. B. van Berk & Hansen, 2006; Postma et al., 1991; van Berk & Wisotzky, 1995; van Berk et al., 2011, 2014; Fu et al., 2012, 2015 a, 2015 a).

1.1.2 Anwendungsbereiche

Heute existiert eine Vielzahl von hydrogeochemischen Modellierungsprogrammen (Merkel & Planer-Friedrich, 2008), die in unterschiedlichen Bereichen der Geowissenschaften Anwendung finden (Abbildung 1.1). Die Anwendungsbereiche reichen dabei von Grundwasserverunreinigungen sowohl organischer als auch anorganischer Natur über die Auswirkungen des Bergbaus auf das Grundwasser (Acid Mine Drainage) und den Transport und die Endlagerung radioaktiver Stoffe und ihre Auswirkungen auf die Umwelt bis hin zur CO_2-Speicherung in geologischen Formationen. Geochemische Modellierungen werden dabei z. B. zur Berechnung der Auswirkungen des Nitrateintrags (Engesgaard & Kipp, 1992), zur Analyse von Grundwasserverunreinigungen durch Stein- und Braunkohlehalden (Ludwig et al., 1999), zur Quantifizierung der Abbauraten von chlorierten Kohlenwasserstoffen (Brun & Engesgaard, 2002), zur Abschätzung der Auswirkungen der Endlagerung radioaktiven Abfalls auf oberflächennahe Grundwasserleiter (Krupka & Serne, 1998), zur Vorhersage von Reaktionen induziert durch geothermische Nutzung von Aquiferen (Møller et al., 1998) und zur Berechnung der Kapazität von CO_2-Speichern (Kumar et al., 2004; Lindeberg et al., 2009; Kopp et al., 2009) sowie zu deren Risikoanalysen durchgeführt (Gaus et al., 2005, 2008; Fahrner et al., 2012 a).

Aus der großen Anzahl geochemischer Modellcodes wurden in dieser Arbeit vier Programme ausgewählt. Diese unterscheiden sich vor allem in ihrem Funktionsumfang (Modelldimensionen reichen von null-dimensionalen Batch-Modellen bis zu zweidimensionalen Modellen, Berechnung von Oberflächenkomplexierung usw.), den Ansätzen zur Berechnung des Gleichgewichtszustands (Law-of-Mass-Action Ansatz oder Gibbs Energy Minimization) und der Verfügbarkeit (kommerzielle von Firmen entwickelte oder von staatlichen Institutionen kostenfrei bereitgestellte Software). Die eingesetzten Programmpakete sind Phreeqc, EQ3/6, The Geochemist's Workbench und ChemApp/FactSage. Der »Law-of-Mass-Action« (LMA) Ansatz wird von Phreeqc, EQ3/6 und The Geochemist's Workbench angewendet, während (ChemApp/FactSage) die »Gibbs Energy Minimization« (GEM) verwendet (White et al., 1958).

1.1.3 Quellen für Unsicherheiten

Die verwendete Software wird bei der hydrogeochemischen Modellierung als numerischer Code bzw. Modellcode bezeichnet. Das damit aufgebaute Abbild der realen Welt ist das Modell; in diesem Fall ist es das hydrogeochemische Modell. Jedes Ergebnis eines Modells enthält eine gewisse Spannbreite,

die aus verschiedenen Faktoren resultieren kann. Diese Ergebnisspannweiten werden in Bezug auf ein einzelnes Ergebnis als Modellunsicherheit definiert. Die Quellen für die Unsicherheiten bei der Modellierung können nach Beck (1987) in vier Kategorien eingeteilt werden: (1) Das konzeptionelle Modell, (2) die abgeschätzten Parameterwerte, (3) die experimentellen Daten zur Kalibrierung der Modelle und (4) die Fehlerfortpflanzung. Bassett & Melchior (1990) unterschieden hingegen die Kategorien (1) verfügbare Daten, (2) Berechnungsverfahren und (3) die menschliche Eingabe als Quellen für Unsicherheiten. Ekberg (1999) identifizierte (1) das konzeptionelle Modell als primäre Quelle der Unsicherheiten bei geochemischer Modellierung, gefolgt von (2) den Varianzen thermodynamischer Daten. Der Autor schlägt vor, verschiedene Ansätze zu verwenden um konzeptionelle Unsicherheiten zu quantifizieren. Zum Beispiel können Sensitivitätsanalysen verwendet werden um den Einfluss thermodynamischer Daten zu untersuchen (Ekberg, 1999).

Der Bedarf einer Fehlerbetrachtung der Modellierung wird von (Bassett & Melchior, 1990) als essentiell betrachtet. Nach Meinung dieser Autoren fehlt die Bewertung der Modellsensitivitäten in Hinblick auf Probenahme, chemische Analyse und Systembedingungen. Die Fehler bei der Lösung von Massenbalancegleichungen und des Massenwirkungsgesetzes bei Verwendung eines mathematischen Modells werden als minimal angesehen (Bassett & Melchior, 1990). Die verwendeten numerischen Methoden werden ebenfalls von INTERA (1983) als eine untergeordnete Quelle für Unsicherheiten angesehen. Bassett & Melchior (1990) empfehlen einen rigorosen Vergleich von berechneten Ergebnissen mit aktuellen Daten um die Größenordnung der Simualtionsunsicherheiten zu bestimmen. Dieser Forderung wurde in der bisherigen Forschung nur wenig nachgekommen. Für die CO_2-Speicherung zeigten (Gaus et al., 2008), dass die Simulationsergebnisse für die Calcitlösung bei Verwendung unterschiedlicher Aktivitätsalgorithmen erhebliche Differenzen zeigten. Thomas et al. (2012) evaluierten verschiedene thermodynamische Sub-Modelle, z. B. zur Berechnung der CO_2-Fugazität (fCO_2), der CO_2-Löslichkeit und der Aktivitätskoeffizienten (γ_{CO_2}) von CO_2. Die Autoren stellten fest, dass die geochemischen Prognosen am stärksten von der Wahl des Berechnungsmodells für die CO_2-Fugazität abhängig sind. Die Verwendung von Scale2000 und Phreeqc zur Berechnung der CO_2-Löslichkeit in salinen Formationswässern wurde von Kervevan et al. (2005) untersucht. Die Autoren stellten fest, dass die Korrektur des CO_2-Partialdrucks die CO_2-Löslichkeit signifikant beeinflusst.

Bisher wurde nur bei speziellen geochemischen Systemen die Größenordnung der Unsicherheiten der Modellcodes bestimmt. Zum Beispiel wurden die Unsicherheiten hervorgerufen durch die Verwendung verschiedener thermodynamischer Daten für Uran(IV)-Spezies für flache Aquifere von Denison & Garnier-Laplace (2005) und Nitzsche et al. (2000), für Metalle und Liganden von Smith et al. (1999) und für das Torium-Phosphat-System von Ekberg (1999) untersucht und quantifiziert. Nitzsche et al. (2000) und Criscenti et al. (1996) wiesen den thermodynamischen Datenbanken einen bedeutenden Einfluss auf die Unsicherheiten von geochemischen Simulationen zu. Diese reichten dabei von einer bis zu mehreren Größenordnungen. Criscenti et al. (1996) untersuchten den Einfluss thermodynamischer Daten durch Monte-Carlo-Analysen und bestimmten signifikante Eingabeparameter, die eine genaue Bestimmung benötigen.

Parameter für kinetische Ratengesetze führen zusätzlich zu den anderen Faktoren zu einer vergrößerten Ergebnisspannweite. Die Ratenkonstanten und reaktive Oberflächen der Mineralphasen variieren um mehrere Größenordnungen (Palandri & Kharaka, 2004; Arvidson et al., 2003).

Zusammenfassend können die Quellen für Unsicherheiten geochemischer Modellierungen in die sechs Kategorien (1) konzeptionelle Modelle, (2) Eingabeparameter für das Modell, (3) numerische

Berechnungsmethoden, (4) thermodynamische Daten, (5) Aktivitätsalgorithmen und -parameter sowie (6) die kinetische Ratengesetze und deren Parameter eingeteilt werden.

1.1.4 PHREEQC

Geschichte und Aufbau

Das thermodynamische Gleichgewichtsprogramm PHREEQC Version 2 wurde als PHREEQE in Fortran geschrieben (Parkhurst et al., 1990), dann zu PHREEQC Version 1 weiterentwickelt (Parkhurst, 1995). Es wurde dabei in der Programmiersprache C geschrieben. Bei der Weiterentwicklung zu PHREEQC Version 2 (Parkhurst et al., 1999) wurde der Code beibehalten, die numerischen Methoden zur Vermeidung von Konvergenzproblemen verbessert und neue Funktionen hinzugefügt.

PHREEQC wurde entwickelt um geochemische Reaktionen in wässrigen Lösungen bei geringen Temperaturen zu berechnen (Parkhurst & Appelo, 1999). PHREEQC kann die Speziierung von aquatischen Lösungen und Sättigungsindizes von Mineralphasen berechnen. Weiterhin kann das Programm Batch-Reaktionen und ein-dimensionale Transportberechnungen durchführen. Die numerische Berechnung beinhaltet Gleichgewichtsberechnungen zwischen aquatischen Spezies, Mineralphasen, Gasen und Solid-Solutions. Weiterhin können mit PHREEQC Oberflächenkomplexierungs-, Ionenaustausch- und irreversible Reaktionsprozesse sowie irreversible Reaktionen wie z. B. kinetisch kontrollierte Reaktionen, Mischungen von Lösungen und Temperaturänderungen berechnet werden.

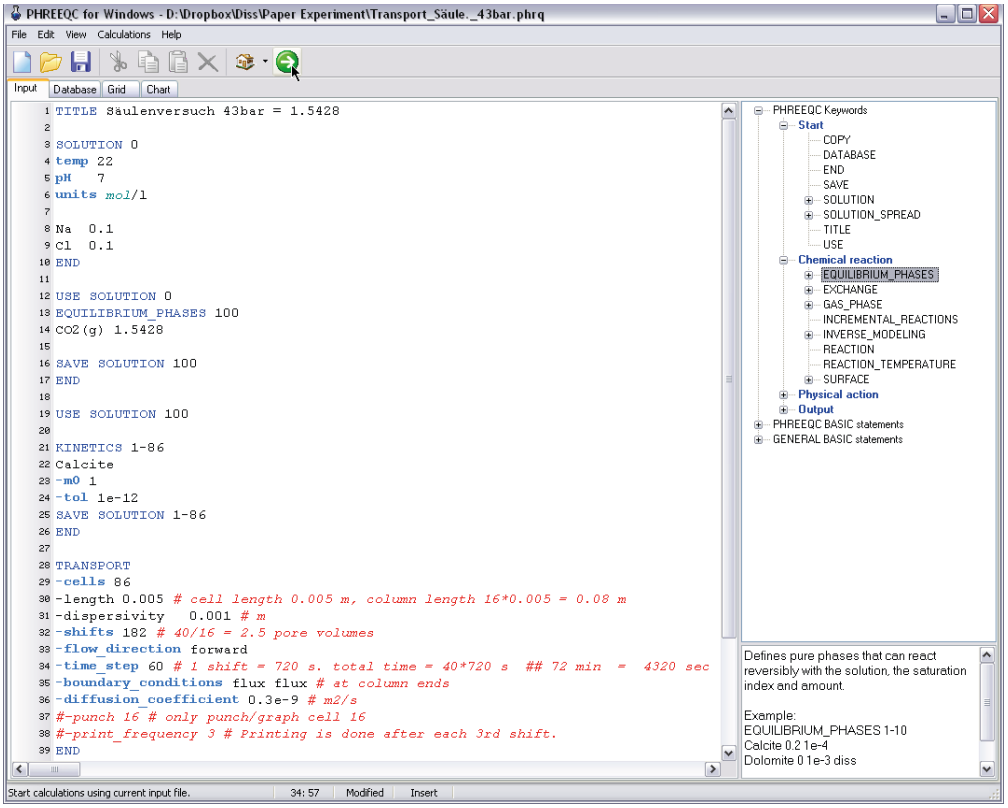

Abbildung 1.2

Windows-Oberfläche des Codes PHREEQC für Windows Version 2 von Vincent Post mit Keyword-Leiste, Input-, Database-, Grid- und Chart-Fenster.

Schließlich ist mit PHREEQC die inverse Modellierung möglich, wodurch Mineral- und Gaszusammensetzungen bestimmt werden können, die zu der Lösungszusammensetzung führen können (Parkhurst & Appelo, 1999).

Die Version 2 von PHREEQC beinhaltet als neue Funktionen z. B. die Simulation von Dispersion oder Diffusion, immobilem Porenwasser in ein-dimensionalen Transportberechnungen und kinetischen Reaktionen mit benutzerdefinierten Ratengesetzen (Parkhurst & Appelo, 1999). Im Jahr 2013 wurde die Version 3 von PHREEQC veröffentlicht (Parkhurst & Appelo, 2013). Damit kann mit PHREEQC die Druckabhängigkeit der Gleichgewichtskonstanten und Gaslöslichkeiten mit der Zustandsgleichung von Peng-Robinson berechnen (Robinson et al., 1985).

PHREEQC verwendet die Gleichungen zur Aktivitätsberechnung dynamisch. Das heißt, je nach den vorhandenen Daten im Datensatz werden die Davies oder die Debye-Hückel Gleichung (Anhang D; Debye & Hückel, 1923) für bestimmte Reaktionen verwendet. PHREEQC verwendet eine erweiterte Form der Debye-Hückel Gleichung, die WATEQ Debye-Hückel Gleichung (Truesdell & Jones, 1974). Sie enthält zur Erweiterung des Gültigkeitsbereichs die ionenspezifischen Parameter a_0 und b_0. Wenn diese beiden Parameter im Datensatz angegeben sind, wird die WATEQ Debye-Hückel Gleichung zur Aktivitätsberechnung eingesetzt (Parkhurst & Appelo, 2013). Ist b_0 nicht angegeben (Truesdell & Jones, 1974), reduziert sich die Gleichung zur erweiterten Debye-Hückel Gleichung (Debye & Hückel, 1923). Wenn keiner der beiden ionenspezifischen Parameter (a_0 und b_0) angegeben ist, dann wird die Davies Gleichung (Davies, 1962) verwendet. Für ungeladene Spezies wird der erste Term der WATEQ Debye-Hückel Gleichung Null und reduziert sich damit zur Setchenow Gleichung ($\log \gamma_i = b_0 \times I$; Setschenow, 1892). Für ungeladene Spezies ist der Parameter $b_0 = 0.1$ (Parkhurst & Appelo, 2013).

Seit 2008 ist mit PHREEQC auch die Berechnung der spezifischen Leitfähigkeit und der Dichte möglich. Für die Berechnung der Dichte wird der Millero-Algorithmus verwendet, der die Konzentrationen der gelösten Spezies verwendet (Millero, 1974, 2000, 2001). Der Algorithmus wurde erfolgreich für Dichteberechnungen von Millero & Lepple (1973), Millero et al. (1976) und Millero (2000) verwendet. Jedoch kann die Dichte nur mit *phreeqc.dat* und *pitzer.dat* berechnet werden (Parkhurst & Appelo, 2013).

In PHREEQC werden Lösungszusammensetzungen und chemische Reaktionen durch Keywords über die Oberfläche definiert (Abbildung 1.2). Der Output des Programms erfolgt über die Programmoberfläche, in einer Datei oder es wird ein Diagramm ausgegeben.

Datenbanken

PHREEQC enthält acht verschiedene Datenbanken, wobei *phreeqc.dat* die Standarddatenbank ist. Die Datenbank ist in sich konsistent und ist für oberflächennahe Temperatur- und Druckbedingungen verwendbar. Die Datenbank des Speziierungs-Programms (WATEQ4F) wurde als Datenbank übernommen. Des Weiteren liegen zwei Datenbanken des Programms MINTEQ vor und eine des Lawrence Livermore National Lab (LLNL) (Delany & Lundeen, 1991). Die *llnl.dat* basiert auf den gleichen Datensätzen wie die Datenbanken des Programms EQ3/6 (*data0.com*). Sie beinhaltet viele Elemente und hat einen größeren Temperatur-Gültigkeitsbereich (bis 300 °C, Delany & Lundeen, 1991). Für höhere Ionenstärken bringt PHREEQC eine Pitzer-Datenbank (Pitzer, 1973) und eine weitere, die das Specific-Ion-Interaction Modell (Ciavatta, 1990) beinhaltet, mit. Weiterhin liegt eine Datenbank vor, die die Verteilung von Wasserstoff-, Sauerstoff-, Stickstoff- und Kohlenstoff-Isotope berechnen kann (*iso.dat*).In den Standard-

Datenbanken sind kinetische Ratengesetze für die Auflösung von Albit, Calcit, Dolomit, Kalifeldspat, Organischem Kohlenstoff, Pyrit, Pyrolusit und Quarz enthalten.

1.1.5 The Geochemist's Workbench

Geschichte und Aufbau

Das Programmpaket The Geochemist's Workbench (GWB) (Bethke, 2008) wurde am Department of Geology der University of Illinois in Urbana-Champain in mehr als 20 Jahren entwickelt. Dabei wurde die Universität von einem Konsortium von Firmen und staatlichen Laboratorien unterstützt. The Geochemist's Workbench besteht aus mehreren einzelnen Programmmodulen. Dazu gehören sowohl die Berechnung von chemischen Reaktionen, Stabilitätsdiagrammen und Gleichgewichtszuständen als auch die Simulation von reaktivem Stofftransport und die Darstellung der Simulationsergebnisse (Bethke & Yeakel, 2009). The Geochemist's Workbench kann als Weiterentwicklung von EQ3/6 mit graphischer Oberfläche angesehen werden. Die Datenbanken wurden von EQ3/6 übernommen und erweitert.

Das Paket GWB Professional beinhaltet die Standardprogramme und Modellierungsprogramme zur Berechnung des eindimensionalen und zweidimensionalen reaktiven Stofftransports sowie ein Programm zur Darstellung der Simulationsergebnisse (Bethke & Yeakel, 2009). Folgende Programme sind in dem Paket enthalten:

Rxn Balanciert automatisch Reaktionen aus, berechnet Gleichgewichtskonstanten und Reaktionsgleichungen und Temperaturen, bei denen Reaktionen im Gleichgewicht sind.

Act2 Berechnet und erstellt Stabilitätsdiagramme.

Tact Berechnet und erstellt Temperatur-Aktivitäts- und Temperatur-Fugazitäts-Diagramme.

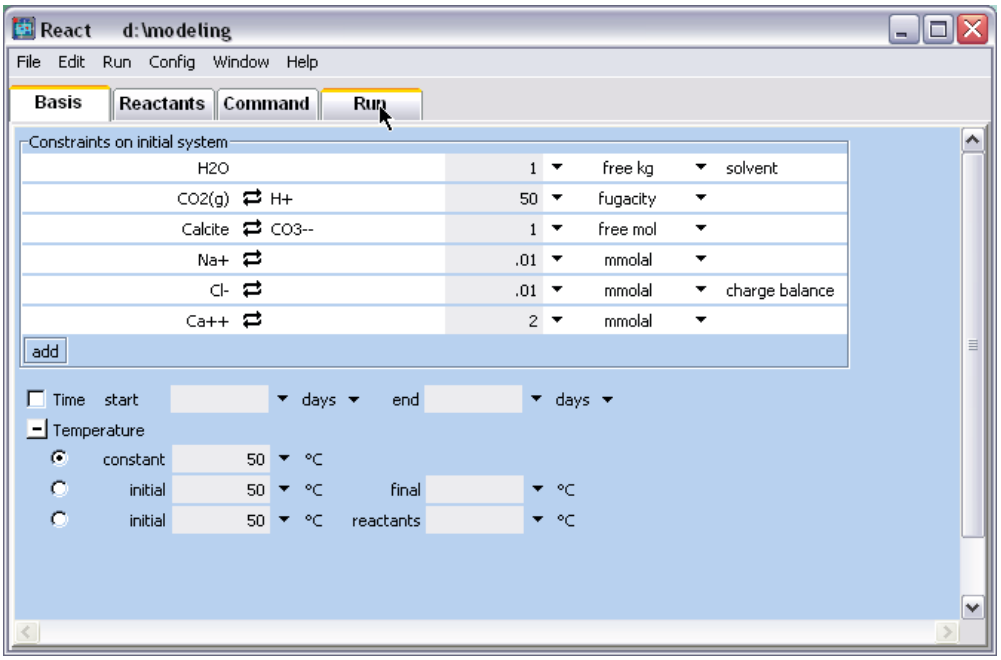

Abbildung 1.3

Windows-Oberfläche des React-Moduls des Softwarepakets The Geochemist's Workbench mit Basis-, Reactants-, Command- und Run-Fenster.

```
|
| Title                  | (utitl(n))
|-------------------------------------------------------------------------------
|EQ3NR input file name= test.3i
|Description= "Test-Eingabe"
|Version level= 8.0
|Revised 02/02/09    Revisor= Christoph Haase
|This is part of the EQ3/6 Test Case Library
|
|Sensitivität NaCl          75°C und pCO2 1bar (Input erst in EQ6)
|-------------------------------------------------------------------------------
|Special Basis Switches (for model definition only)       | (nsbswt)
|-------------------------------------------------------------------------------
|Replace |None                                            | (usbsw(1,n))
|   with |None                                            | (usbsw(2,n))
|-------------------------------------------------------------------------------
|Temperature (C)         | 7.50000E+01| (tempc)
|-------------------------------------------------------------------------------
|Pressure option (jpres3):
|  [ ] ( 0) Data file reference curve value
|  [x] ( 1) 1.013-bar/steam-saturation curve value
|  [ ] ( 2) Value (bars) | 0.00000E+00| (press)
|-------------------------------------------------------------------------------
|Density (g/cm3)         | 1.00000E+00| (rho)
|-------------------------------------------------------------------------------
|Total dissolved solutes option (itdsf3):
|  [x] ( 0) Value (mg/kg.sol) | 0.00000E+00| (tdspkg)
|  [ ] ( 1) Value (mg/L)      | 0.00000E+00| (tdspl)
|-------------------------------------------------------------------------------
|Electrical balancing option (iebal3):
|  [x] ( 0) No balancing is done
|  [ ] ( 1) Balance on species |Cl-                     | (uebal)
|-------------------------------------------------------------------------------
|Default redox constraint (irdxc3):
|  [ ] (-3) Use O2(g) line in the aqueous basis species block
|  [x] (-2) pe (pe units)      | 4.00000E+00| (pei)
|  [ ] (-1) Eh (volts)         | 5.00000E-01| (ehi)
|  [ ] ( 0) Log fO2 (log bars) | 0.00000E+00| (fo2lgi)
|  [ ] ( 1) Couple (aux. sp.)  |None                    | (uredox)
|-------------------------------------------------------------------------------
|Aqueous Basis Species/Constraint Species        |Conc., etc. |Units/Constraint
| (uspeci(n)/ucospi(n))                          | (covali(n))|(ujf3(jflgi(n)))
|-------------------------------------------------------------------------------
|H+                                              |1.00000E+00|Hetero. equil.
|->|CO2(g)                                          |(ucospi(n))
|Ca++                                            |2.00000E-03|Molality
|HCO3-                                           |1.00000E-00|Hetero. equil.
|->|Calcite                                         | (ucospi(n))
|Na+                                             |1.00000E-20|Molality
|Cl-                                             |1.00000E-20|Molality
|-------------------------------------------------------------------------------
```

Abbildung 1.4

Ausschnitt aus einer Eingabedatei für EQ3 im Menü-Style-Format einer Textdatei.

SpecE8 Berechnet die Verteilung von Spezies in wässrigen Lösungen, Sättigungszustände von Mineralen und Fugazitäten von Gasen. Berechnet weiterhin die Sorption von Spezies an Mineraloberflächen mit verschiedenen Berechnungsmethoden, Oberflächenkomplexierung und Ionenaustausch.

Gtplot Stellt SpecE8-Ergebnisse als x-y Diagramme, ternäre Diagramme, Piper-, Durov-, und Stiff-Diagramme dar (Abbildung 1.3).

React Berechnet über SpecE8 hinausgehend Reaktionspfade von Fluid-, Mineral- und Gasphasen. Sagt die Fraktionierung von stabilen Isotopen während des Reaktions-Prozesses vorher. Darstellung der Ergebnisse mit Gtplot.

X1t Simulation von reaktivem Transport in eindimensionalen Systemen. Das Programm hat die gleichen geochemischen Modellierungsfähigkeiten wie React, mit Ausnahme der Isotopenfraktionierung. Kopplung der geochemischen Prozesse mit Grundwasserströmung und Stofftransport gekoppelt.

X2t Simulation von reaktivem Transport in zweidimensionalen Systemen.

Xtplot Darstellung der Ergebnisse der Xt1- und Xt2-Berechnungen als Kartenansicht und als X-Y-Diagramm.

Das Programmpaket wurde ursprünglich von Craig Bethke im Hydrogeologie-Programm der University of Illinois entwickelt und geschrieben. Verschiedene Programmierer haben die Programmoberfläche (User Interface) weiterentwickelt und das Programmmodul zur Darstellung der Ergebnisse verbessert (Xtplot). In dieser Arbeit wurde das im Jahr 2008 veröffentlichte Release 7.0 angewendet.

In The Geochemist's Workbench sind in den thermodynamischen Datenbanken eine bestimmte Anzahl an Basisspezies enthalten. Die Basisspezies können durch einen Austausch (»swapping«) mit anderen aquatischen Spezies, Mineralen oder Gasen modifiziert werden um die geochemischen Bedingungen wiederzugeben. Um z. B. ein Gleichgewicht mit Quarz einzustellen, wird Quarz gegen die Basisspezies $SiO_2(aq)$ getauscht. Ein anderes Beispiel ist die Einstellung einer CO_2-Fugazität eines geochemischen Systems, wobei $CO_2(g)$ entweder gegen HCO_3^- oder H^+ ausgetauscht wird.

Datenbanken

Mit dem Programmpaket werden 17 Datenbanken zur Verfügung gestellt, wovon neun zur Simulation von wässrigen Lösungen eingesetzt werden können. Die Standard-Datenbank ist *thermo.dat*, die auf einem Datensatz von EQ3/6 des Lawrence Livermore National Labratory (LLNL) basiert (*thermo.dat*; Delany & Lundeen, 1991). Die Datenbank *thermo.com.v8.r6+.dat* wurde direkt aus den Datensätzen des LLNL erstellt und ist aktueller als die *thermo.dat* Datenbank. Die *thermo.dat* und *thermo.com.v8.r6+.dat* Datenbank verwenden für den Parameter b_0 den gleichen Wert wie für alle aquatischen Spezies. Zwei Datenbanken von Phreeqc wurden in das GWB-Format konvertiert (*thermo_phreeqc.dat* und *thermo_phreeqc.dat*). Die Pitzer Datenbank von Phreeqc wurde ebenfalls in The Geochemist's Workbench übernommen und in *phrqpitz.dat* umbenannt. Daneben hat The Geochemist's Workbench auch eine eigene *thermo_pitzer.dat* Datenbank und eine *thermo_hmw.dat* Datenbank (Harvie et al., 1980). The Geochemist's Workbench enthält ebenfalls eine Datenbank von dem Code Minteq (*thermo_minteq.dat*). Weitere Datenbanken können nur zur Berechnung von speziellen Problemen, wie Oberflächenkomplexierung (z. B. von $FeOH^+$), Sorption mit Verteilungskoeffizienten, Freundlich-Isothermen oder wie dem Langmuir-Modell, Isotopen oder Ionenaustauschern eingesetzt werden (Bethke, 2008).

1.1.6 EQ3/6

Geschichte und Aufbau

Das Programmpaket EQ3/6 wurde vom Lawrence Livermore National Labratory (LLNL) für die Anwendung in der Endlagerung vor allem für das Yucca-Mountain-Projekt entwickelt. Die aktuelle Version ist die Version 8.0 (Wolery & Jarek, 2003). EQ3/6 besteht, wie der Name andeutet, aus zwei Teilmodulen. Dies ist zum einen EQ3NR, womit die Speziierung der Lösung, und zum anderen EQ6, womit Reaktionspfade berechnet werden können. Weiterhin enthält das Programmpaket den Datenbank-Prozessor EQPT, der die formatierten Datenbankdateien einliest (*data0*-Datei) und eine EQ3/6-spezifische Datei (*data1*-Datei) ausgibt.

Das Teilmodul EQ3NR kann vor allem für die Berechnung von Grundwasseranalysen verwendet werden. Das Programmmodul berechnet die Speziierung einer Lösung, Sättigungszustände und Minerallöslichkeiten. Es muss immer zuerst eine EQ3NR-Berechnung durchgeführt werden, bevor eine Reaktionspfadberechnung mit EQ6 beginnt.

Das Teilmodul EQ6 berechnet die Reaktionen einer Lösung mit irreversibel reagierenden Reaktanden. Das Programmmodul kann aber auch Mischungen von Lösungen oder Auswirkungen einer Temperaturänderung auf die Lösungszusammensetzung berechnen. Die Berechnungen können sowohl als Reaktionsprozess als auch zeitabhängig durchgeführt werden. Bei einer zeitabhängigen Berechnung muss der Benutzer ein Ratengesetz für die Reaktionen definieren.

Tabelle 1.1

Datenbanken von EQ3/6 mit Angabe des Datenbanksystems und des Gültigkeitsbereichs bezüglich Druck und Temperatur (Wolery, 1992).

Kurzname	Vollständiger Name	Datensatz	Jahr	Gültigkeitsbereich
cmp	*data0.com.V8.R6*	R5[b]	1996	[c], bis 300 °C
hmw	*data0.hmw.V8.R6*	R5[b]	1996	[c], nur 25 °C
pit	*data0.pit.V8.R6*	R5[b]	1996	[c], bis 100 °C
shv	*data0.shv.V8.R6*	R7[a]	1997	[c], bis 300 °C
skb	*data0.skb.V8.R6*	R5[b]	1996	[c], bis 300 °C
sub	*data0.sup.V8.R6*	R5[b]	1996	[c], bis 300 °C
ymp	*data0.ymp.R2*			[c], bis 200 °C
ypf	*data0.ypf Version 1.0*		2003	[c], bis 200 °C
500	*data0.500.V8.R6*	R7[a]	1997	500 bar, bis 350 °C,[d]
1kb	*data0.kb.V8.R6*	R7[a]	1997	1 kbar, bis 600 °C,[d]
2kb	*data0.2kb.V8.R6*	R7[a]	1997	2 kbar, bis 900 °C,[d]
5kb	*data0.5kb.V8.R6*	R7[a]	1997	5 kbar, bis 1000 °C,[d]

[a] GEMBOCHS.V2-Jewel.src.R7
[b] GEMBOCHS.V2-Jewel.src.R5
[c] log_K_{Eq} entlang der Dampfdruckkurve von Wasser
[d] basiert auf *data0.shv.V8.R6*

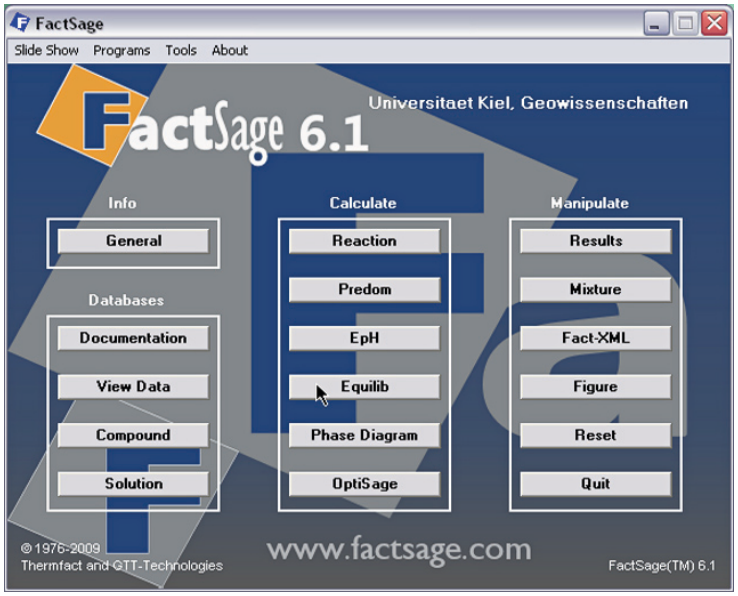

Abbildung 1.5
Windows-Oberfläche des Programmpakets FactSage mit den drei Modulen Databases, Calculate und Manipulate in der Version 6.1.

Datenbanken

Die Datenbanken werden ebenfalls vom Lawrence Livermore National Labratory (LLNL) verwaltet. Es verwendet ein Datenbanksystem mit dem Namen GEMBOCHS Geologic and Engineering Materials: Bibliography of Chemical Species (Johnson & Lundeen, 1994). Die Datenbank enthält über 2000 chemische Spezies, darunter aquatische Spezies und thermodynamische Daten in vielen Formen: Parameter für Zustandsgleichungen, Spezieseigenschaften (z. B. $\Delta_r G^0$, $\Delta_f G^0$, $\Delta_r H^0$ oder $\Delta_f H^0$) und Reaktionseigenschaften (z. B. log_K_{Eq} oder ΔH_r^0), Parameter zur Bestimmung von Aktivitätskoeffizienten (z. B. Debye-Hückel-Parameter A und B, Ionendurchmesser a_0, Interaktionskoeffizienten λ_i, μ_i). Das Datenbanksystem kann auch dazu benutzt werden, verschiedene Daten bestehender Datensammlungen zu mischen (z. B. SUPCRT92, NEA92; Johnson et al., 1992; Grenthe et al., 1992; Mompeán & Wanner, 2003).

EQ3/6 in der Version 8.0 wird mit 12 Datenbanken geliefert. Vier Datenbanken enthalten bei höheren Drücken berechnete Gleichgewichtskonstanten (500 bar bis 5000 bar). Die Datenbanken sind jeweils mit dem Druck bezeichnet, für die die Gleichgewichtskonstanten berechnet wurden *data0.500*, *data0.1kb*, *data0.2kb* und *data0.5kb* (Tabelle 1.1). Neun der Datensätze basieren auf der Aktivitätsberechnung mit der Debye-Hückel und Davies Gleichung. Nur die Datensätze *data0.hmw*, *data0.pit* und *data0.ypf* basieren auf dem Pitzer-Ansatz.

1.1.7 FactSage/ChemApp

Geschichte und Aufbau

Das Softwarepaket ChemApp (Petersen & Hack, 2007; Eriksson & Königsberger, 2008) wurde von der Firma GTT Technologie und der Firma CRCT entwickelt. Dazu wurde eine graphische Oberfläche programmiert, die mehrere Programme unter dem thermochemischen Datenbanksystem

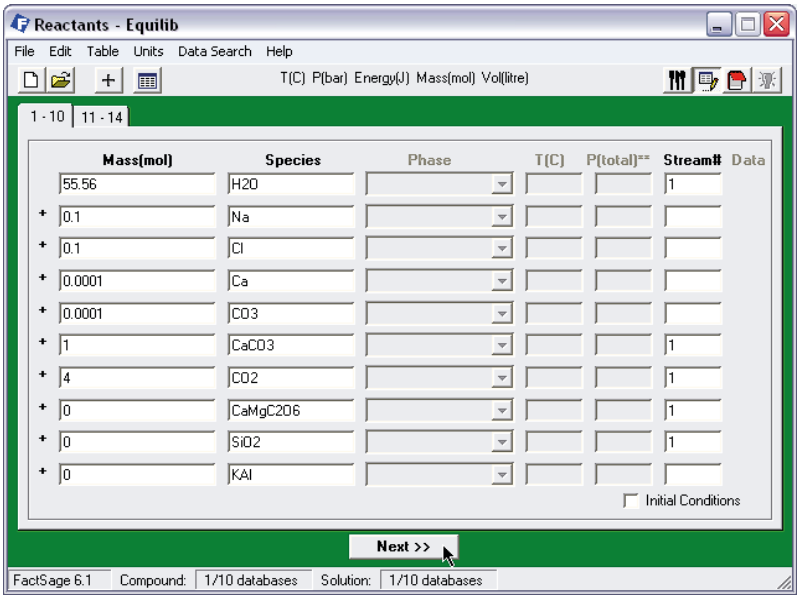

Abbildung 1.6
Windows-Oberfläche des Modules Equilib des Programmpakets FactSage mit Eingabe der chemischen Elemente.

FactSage (Eriksson & Königsberger, 2008) vereint. FactSage mit erweitertem Funktionsumfang entstand 2001 durch die Fusion von F*A*C*T Facility for the Analysis of Chemical Thermodynamics und ChemSage (Version 5.0) (Bale et al., 2002). Das originale F*A*C*T-Paket wurde für die Simulation thermochemischer Prozesse in der Pyrometallurgie eingesetzt (Bale et al., 2009). Mit der Migration zu Fact-Win und zu FactSage sind die Einsatzgebiete vielfältiger geworden. So reicht das Anwendungsspektrum von FactSage von Problemstellungen der Hydrometallurgie, Elektrometallurgie, Korrosion, Glastechnologie, Verbrennung, Keramik und Geologie bis hin zu den Umwelt- und Geowissenschaften.

Das Hauptfenster erlaubt die Auswahl aus den verschiedenen Modulen des Programmpakets. Die Module sind in vier Kategorien gruppiert: 1. Info 2. Databases 3. Calculate 4. Manipulate (Abbildung 1.5). FactSage enthält zwei Arten thermochemischer Datenbanken: Compound- und Solution-Datenbanken. Die Datenbanken von FactSage (*FToxid*, *FTsalt*, *FThall*, *FThelg*, *FTmisc*, *FTpulp*) beinhalten die weltweit größte Sammlung optimierter thermochemischer Datenbanken für anorganische Systeme (Bale et al., 2009). Sie werden seit mehr als 25 Jahren entwickelt, wobei große Veränderungen zwischen 2001 und 2003 stattfanden. Die aktuellen Datenbankversionen wurden 2004 veröffentlicht. Für aquatische Systeme einsetzbar sind jedoch nur sechs Datenbanken.

FactSage benutzt den Ansatz der Minimierung der Gibbs-Energie (G) zur Berechnung des Gleichgewichtszustands (White et al., 1958). Der Gibbs-Energie Minimierer ist in den Modulen Equilib, Phase Diagram und OptiSage enthalten und wurde ebenfalls in ChemApp integriert (Bale et al., 2009). Mit FactSage wurden technische Prozesse modelliert und bereits existierende Prozesse optimiert (Almpanis-Lekkas et al., 2014; Lessard et al., 2015; Reinmöller et al., 2015). FactSage wurde auch zur Simulation von CO_2-Speicherung eingesetzt (z. B. Béarat et al., 2006) und ChemApp wurde mit OpenGeoSys (OGS) gekoppelt, wodurch reaktive Transportmodellierungen durchgeführt werden konnten (z. B. Li & Bauer, 2009; Li et al., 2013; Beyer et al., 2012; Mitiku et al., 2013; Xie et al., 2011).

Equilib führt komplexe Gleichgewichtsberechnungen für Mulitkomponenten- und Multiphasensysteme unter unterschiedlichen Randbedingungen wie Lösungskonzentrationen, Temperatur- oder Druckbedingungen aus. Eines der Eingabefenster von Equilib findet sich in Abbildung 1.6. Verschiedene Zielgrößen können berechnet werden, wie z. B. extensive Eigenschaften, Bildung oder Auflösung einer Zielphase, Ausfällung aus einer Zielphase oder Gleichgewichtskonzentrationen oder -aktivitäten. Mögliche Aufgaben sind die Berechnung von bei adiabatischen Bedingungen vorherrschenden Temperaturen und Löslichkeiten von Mineralphasen in Wasser. Ebenso kann die HCl-Menge bestimmt werden, die einem System zugegeben werden muss, um einen bestimmtem pH-Wert einzustellen (Bale et al., 2002; 2009).

Datenbanken

Das Programm FactSage enthält sechs Datenbanken, die zur Berechnung von aquatischen Lösungen verwendet werden können. Dazu gehören die Standard-Datenbanken *Fact* und *Fact53*, drei *FT_Helg*-Datenbanken die Pitzer Datenbank *Fact-Pitz*. Die Pitzer Datenbank enthält eine geringe Anzahl von Elementen und nur bei 25 °C gültige Pitzer-Parameter. Die Daten für 49 Kationen und 36 Anionen wurden Literaturquellen bis zum Jahr 1996 entnommen. Weiterhin enthält FactSage drei Helgeson-Datenbanken *FT_Helg_AQID*, *FT_Helg_AQDH* und *FT_Helg_AQDD*. Diese Datenbanken basieren auf Daten der GEOPIG-SUPCRT Helgeson Datenbank und beinhalten mehr als 1400 aquatische Spezies. Die Datenbanken verwenden die Helgeson Zustandsgleichung und deren Gültigkeitsbereich reicht bis zu Temperaturen von 350 °C und bis zu Drücken von 165 bar. Die Helgeson Datenbanken haben verschieden Gültigkeitsbereiche für die Ionenstärken. Die Datenbank *FT_Helg_AQID* ist in ideal verdünnten Lösungen bis zu einer Ionenstärke von 0.001 mol/l gültig. *FT_Helg_AQDH* enthält die Debye-Hückel Gleichung zur Aktivitätsberechnung und reicht bis zu einer Ionenstärke von 0.02 mol/l. Die Datenbank *FT_Helg_AQDD* verwendet die Davies-Gleichung und ist bis 0.5 mol/l gültig.

1.2 Anwendung der Codes für die CO_2-Speicherung

PHREEQC (Parkhurst & Appelo, 1999) wurde in verschiedenen Studien angewendet um die Mineralfestlegung in CO_2-Speicherformationen zu berechnen, (z. B. Allen et al., 2005; Cantucci et al., 2009; Dethlefsen et al., 2012; Tomas et al., 2012; Hellevang & Aagaard, 2013), den Einfluss von CO_2 auf die Speicherformation und das Deckgestein zu simulieren (Cantucci et al., 2014; Huq et al., 2015; Tambach et al., 2015), den Einfluss von CO_2 auf Transfer- und Retentionsformationen oder auf oberflächennahe Grundwasserleiter zur Risikoabschätzung zu bestimmen (z. B. Gaus et al., 2005; Zheng et al., 2009a; Keating et al., 2009; Fahrner et al., 2012 b; Cahill & Jakobsen, 2015) oder um Monitoringstrategien zu entwickeln (z. B. Schäfer et al., 2013).

THE GEOCHEMIST'S WORKBENCH wurde bisher eher für Berechnungen bei oberflächennahen Bedingungen eingesetzt. Zum Beispiel wurde die Bedeutung von Karbonatpuffern für das Monitoring von Newell et al. (2008), die Speziierung von NaCl-Lösungen bei hohen CO_2-Konzentrationen (Tutolo et al., 2015) und geochemische Einflüsse auf das Grundwasser durch eine CO_2-Leckage bestimmt (Wilkin & Digiulio, 2010).

EQ3/6 wurde z. B. von Apps et al. (2010), Zheng et al. (2009 a) und Zheng et al. (2012) eingesetzt, um die Folgen von CO_2-Leckagen für die Qualität von oberflächennahem Grundwasser zu simulieren. Zwingmann et al. (2005) prognostizierten mögliche geochemische Reaktionen im Vorfeld einer CO_2-Injektion. Datenbanken von EQ3/6 wurde von Thomas et al. (2012) verwendet um die CO_2-Löslichkeit unter Verwendung verschiedener thermodynamischer Modelle zu vergleichen. Xu et al. (1997) koppelten EQ3/6 an das Mehrphasensimulationsprogramm TOUGH2 um damit reaktive Transportberechnungen zu ermöglichen. Daher wurde die Datenbank von EQ3/6 verwendet um CO_2-Injektionen in die Utsira Formation des Sleipner-Felds (Gaus et al., 2005), die Alteration von Deckgesteinen eines Gasspeichers (Gherardi et al., 2007), Änderung der oberflächennahen Grundwasserchemie infolge CO_2-Eintrags (Zheng et al., 2012) oder die CO_2-Festlegung durch Mineralausfällung zu simulieren (Xu et al., 2005). Daneben wurden auch Kombinationen von PHREEQC und einer EQ3/6-Datenbank eingesetzt um die Integrität von Deckgesteinen für Sicherheitsbewertungen vorherzusagen (Bildstein et al., 2010).

Gundogan et al. (2011) verglichen die geochemischen Modellcodes PHREEQC und TOUGHREAT für die Modellierung der CO_2-Speicherung in Sandsteinformationen und führten die Unterschiede der Ergebnisse vorwiegend auf die thermodynamischen Datenbanken und Aktivitätsmodelle zurück.

Seltener wurde bisher FACTSAGE/CHEMAPP (Eriksson & Königsberger, 2008; Petersen & Hack, 2007; Bale et al., 2009) für die Berechnung von CO_2-Speicherszenarien angewendet. Dabei wird CHEMAPP an OpenGeoSys (OGS) gekoppelt (Li & Bauer, 2009; Li et al., 2013). Beyer et al. (2012) und Kolditz et al. (2012) simulierten mit GEOSYS und CHEMAPP die CO_2-Injektion in das Erdgasfeld Altensalzwedel und Mitiku et al. (2013) simulierten die CO_2-Speicherung in die Buntsandstein und Rhät-Formation des Norddeutschen Beckens.

Zumeist wurden in den zuvor genannten Studien wenige Angaben zu den Gründen für die gewählten Datenbanken gemacht. Meistens wurde einfach die Standard-Datenbank des verwendeten Modellcodes genutzt. Generell fehlt eine Bewertung der Ergebnisse, die bei Anwendung unterschiedlicher thermodynamischer Datenbanken entstehen können.

PHREEQC und THE GEOCHEMISTS'S WORKBENCH wurden bisher sehr häufig zur Simulation von verschiedenen Aspekten der CO_2-Speicherung eingesetzt. Die Datenbanken von EQ3/6 wurden in Kombination mit anderen numerischen Codes verwendet. Aus diesen Gründen wurden diese Modellcodes ausgesucht um die simulierten Ergebnisse in dieser Arbeit zu vergleichen. Dazu wurde der Code CHEMAPP/FACTSAGE ausgesucht, der mit der Minimierung der Gibbs-Energie einen neuen Ansatz zur Berechnung chemischer Reaktion beinhaltet.

1.3 CO_2-Speicherung

Seit Mitte des 19. Jahrhunderts erwärmt sich die Erdoberfläche schneller, als bis zu diesem Zeitpunkt beobachtet wurde. Die globale Erwärmung wird durch den Treibhauseffekt verursacht, der durch erhöhte Treibhausgasemissionen verstärkt wird. Große Anteile der Treibhausgasemissionen sind anthropogen verursacht (IPPC, 2013). Von den verschiedenen Treibhausgasen hat CO_2 einen vergleichsweise großen Einfluss auf den Treibhauseffekt. Die CO_2-Konzentration in der Atmosphäre stieg auf ca. 404 ppm im Mai 2015 (Tans & Keeling, 2015). Um die Emissionen von CO_2 zu reduzieren, werden verschiedene Technologien angewendet um CO_2 langfristig aus der Atmosphäre zu entfernen (Metz et al., 2005; Holloway, 2001). Die CO_2-Speicherung in tiefen geologischen Formationen, die als saline Aquifere bezeichnet werden, stehen im Fokus der vorliegenden Arbeit.

1.3.1 Carbon Capture and Storage

Die CO_2-Abscheidung und -Speicherung (Carbon Capture and Storage, CCS) ist eine Technologie um CO_2 z. B. an Kraftwerken abzuscheiden, zu einer Speicherstätte zu transportieren und geologisch

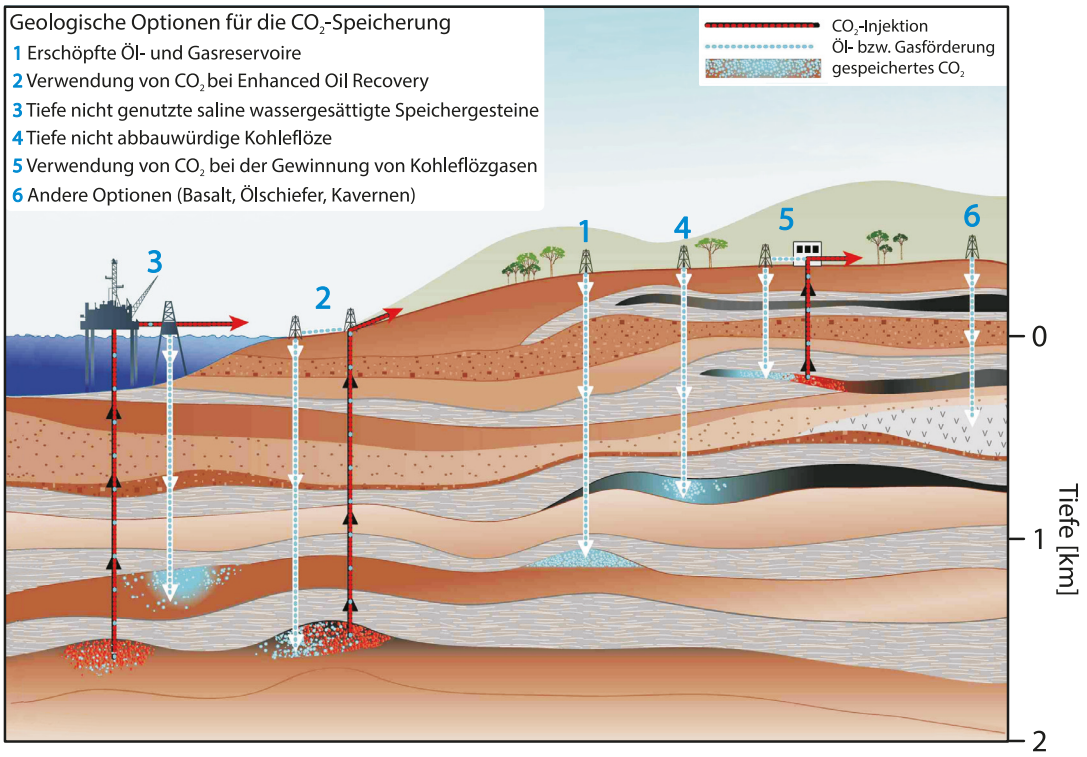

Abbildung 1.7
Möglichkeiten der geologischen Speicherung von CO_2 (Benson & Cook, 2005).

Tabelle 1.2
CO_2-Speicherprojekte in Erdöl- und Erdgasfeldern und salinen Aquiferen (Global CCS Institute, 2014).

Projekt	Leiter	Speichertyp	Projektart	Tiefe [m]	Projekt-start	Quelle
		Algerien				
In Salah CO_2 storage	BP	saliner Aquifer	Erdgasauf-bereitung	1800	2004	Wright (2007), Riddiford et al. (2005)
		Kanada				
Great Plains Synfuel Plant and Wey-burn-Midale Feld	Cenovus Energy, Apache Canada	EOR	Industrie	> 1500	2000	Whittaker et al. (2011)
Boundary Dam Integra-ted CCS Demonstration Project	SaskPower	EOR	Energiege-winnung	1500	2014	Stephenne (2014)
		Norwegen				
Sleipner	StatoilHydro	saliner Aquifer	Erdgasauf-bereitung	1500	1995	Torp & Gale (2004)
Snoevhit	StatoilHydro	saliner Aquifer	Industrie	2600	2008	Maldal & Tappel (2004)
		USA				
Century Plant	Occidental Petrole-um, Sandridge Energy	EOR	Industrie	> 900	2010	
Coffeyville Gasification Plant, Kansas	Chaparral Energy	EOR	Düngemittel-herstellung		2013	
Enid Fertilizer CO_2-EOR Project, Oklohoma	Koch Fertilizer	EOR	Düngemittel-herstellung		1982	
Lost Cabin Gas Plant/Bell Creek Oil field, Wyoming	Conoco Phillips	EOR	Ergasauf-bereitung	2200	2013	
Val Verde Natural Gas Plants , Texas	Altura E&P	EOR	Erdgasauf-bereitung	700/ 950	1972	
Port Arthur, Texas	Air Products	EOR	Industrie		2012	
Shute Creek Gas Processing Facility, LaBarge,Wyoming	ExxonMobil	EOR	Industrie		1986/ 2008/ 2010	
		Brasilien				
Lula Oil Field	Petrobas	Gasproduktion	Industrie		2008	Pizarro & Branco (2012)

zu speichern (Abbildung 1.7). Obwohl CO_2 in der Vergangenheit bereits für Enhanced Oil Recovery (EOR, z. B. Blunt et al., 1993; Malik & Islam, 2000) oder für Enhanced Gas Recovery (EGR, z. B. Oldenburg et al., 2001; Koide & Yamazaki, 2001) in geologische Formationen injiziert wurde, ist die Langzeitspeicherung von CO_2 ein relativ neues Konzept (Benson & Cook, 2005; Chadwick et al., 2008). Erste Ideen finden sich in den frühen 90er Jahren (Dunsmore, 1992; van der Meer, 1992; Gunter et al., 1993; Hitchon, 1996; Gunter et al., 1997). Die ersten kommerziellen Beispiele für die CO_2-Speicherung im Rahmen des Enhanced Oil Recovery (EOR) sind das Weyburn-Feld (White, 2009) in Boundary Dam, Saskatchewan, Kanada, in dem die Injektion in den 80er Jahren und das Sleipner-Feld (Korbøl & Kaddour, 1995) in Norwegen, in dem die Injektion in den 90er Jahren begonnen wurde. Im Jahr 2014 wurde das Kohlekraftwerk »Boundary Dam« mit CO_2-Abscheideanlage in Post-Combustion-Technologie als erstes CCS-Projekt in Betrieb genommen.

CO_2 kann entweder von anderen Abgasen aus Punktquellen abgeschieden werden, wie z. B. von mit fossilen Energieträgern betriebenen Kraftwerken (White et al., 2003), oder bei industriellen Verfahren, bei denen CO_2 prozessbedingt abgeschieden wird, wie bei der H_2- oder Ammoniaksynthese (Bara, 2012). Da Kohlekraftwerke den größten Anteil am CO_2-Ausstoß haben, können sie bevorzugt mit einer Abscheidetechnik ausgerüstet werden (Yang et al., 2008). Für die Abscheidung wird jedoch Energie benötigt, wodurch der Wirkungsgrad um maximal 10 % verringert wird (Rubin et al., 2005).

1.3.2 Speicherprojekte

Projekte zur CO_2-Speicherung in tiefen geologischen Formationen liefern Erkenntnisse und Felddaten, wodurch die Berechnung durch geochemische Codes und Datenbanken verbessert werden kann. Weltweit waren 13 CO_2-Speicherprojekte im Jahr 2014 in Betrieb, 9 Projekte befanden sich in der Ausführung (Global CCS Institute, 2014). Führend war die USA mit 7 sich im Betrieb befindenden Projekten, darauf folgen Kanada und Norwegen mit jeweils 2 Projekten. Algerien betrieb ein Speicherprojekt (In Salah, Tabelle 1.2).

Im industriellen Maßstab führen die USA, Kanada, Norwegen und Algerien CO_2-Speicherprojekte in salinen Formationen durch. Die USA betreiben vier Speicherprojekte im industriellen Maßstab, jedoch wurde erst bei einem Projekt die Injektion begonnen. In Kanada ist die Injektion von CO_2 in zwei saline Formationen geplant. In Norwegen wurde bisher ein Speicherprojekt in salinen Formationen verwirklicht. CO_2, das bei Förderung aus dem Sleipner-Feld anfällt, wird in eine saline Formation über dem Erdölfeld injiziert. In Deutschland wurde bisher ein Projekt zur Speicherung von CO_2 als Forschungsanlage in Ketzin, Brandenburg, betrieben.

1.3.3 Speicherformationen

Für die geologische CO_2-Speicherung kommen verschiedene Formationen in Frage: Ausgebeutete Kohleflöze, Erdöl- und Erdgaslagerstätten und saline Aquifere. Saline Aquifere in tiefen geologischen Formationen treten besonders in Sedimentbecken, wie z. B. dem Norddeutschen Becken zahlreich auf. Verschiedene Studien belegen, dass die salinen Aquifere von diesen Formationen die größte CO_2-Speicherkapazität aufweisen (Knopf et al., 2010; Höller & Viebahn, 2011; Liebscher et al., 2013). Weltweit liegt die geschätzte CO_2-Speicherkapazität geologischer Formationen zwischen 100-200 000 Gigatonnen CO_2. Benson & Cook (2005) schätzen die Gesamtspeicherkapazität für CO_2 auf mindestens 1700 Gigatonnen CO_2 (Abbildung 1.8). Davon haben die tiefen salinen Formationen einen Anteil von

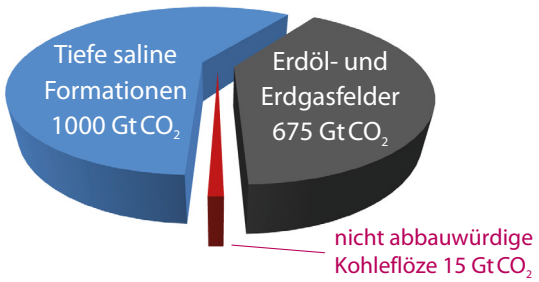

Abbildung 1.8

Geschätzte weltweite Kapazität in Gigatonnen CO_2 für die Speicherformationstypen saline Formationen, Erdöl- und Erdgasfelder und Kohleflöze (Benson & Cook, 2005).

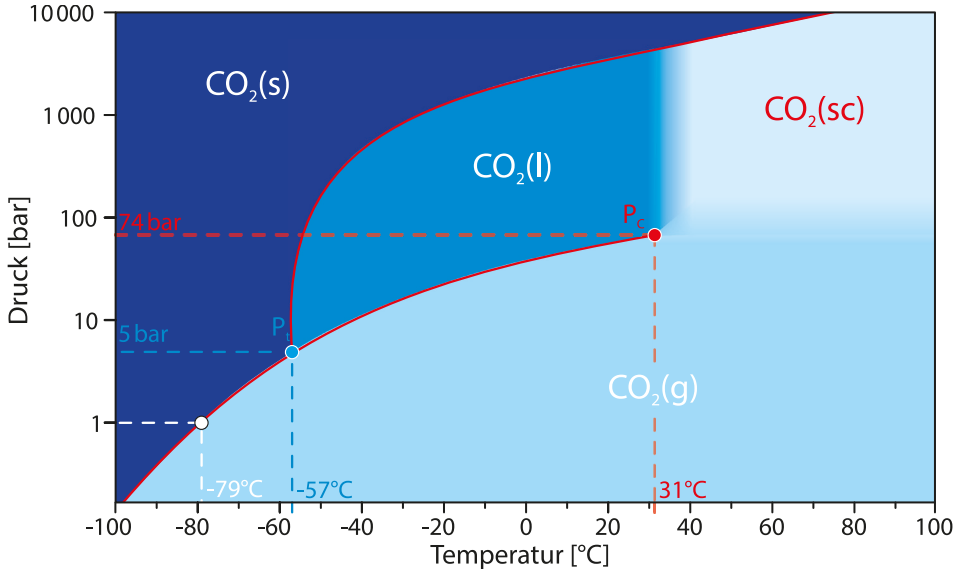

Abbildung 1.9

Phasendiagramm für CO_2 mit den Phasenzuständen flüssig, gasförmig, fest und überkritisch. Tripelpunkt P_t und überkritischer Punkt P_c.

1000 Gigatonnen (Benson & Cook, 2005), die Erdöl- und Erdgasfelder 675–900 Gigatonnen CO_2 (Gale, 2002) und die Kapazität nicht abbauwürdiger Kohleflöze liegt bei ca. 15 Gigatonnen (Freund, 2001). May et al. (2005) schätzen das Speicherpotential in Deutschland auf ca. 19–48 Gigatonnen CO_2, wovon die Kapazität der salinen Formationen ca. 12–28 Gigatonnen beträgt. Die Speicherkapazität der salinen Aquifere wurde von Kopp et al. (2009) auf ca. 9 Gigatonnen CO_2 reduziert.

Zur Speicherung wird CO_2 in Formationen, die sich in Tiefen von mehr als 800 m befinden, injiziert, da CO_2 bei den dort vorherrschenden Druck- und Temperaturbedingungen die höchste Dichte hat. Dadurch kann die größtmögliche CO_2-Menge gespeichert werden. Bei diesen Druck- und Temperaturbedingungen (überkritischer Punkt P_c bei $P > 74$ bar und $T > 31$ °C) liegt CO_2 im überkritischen Zustand vor (Abbildung 1.9).

Als CO_2-Speicherformationen sind vor allem poröse Sandsteine mit hoher Permeabilität geeignet (Zweigel et al., 2004, Kharaka et al., 2006). In Norddeutschland sind dies z. B. Sandsteinformationen aus dem Rotliegend, Buntsandstein oder Keuper. Die Permeabilitäten und Porositäten der Volpriehausen Formation des Mittleren Buntsandsteins zeigen z. B. Schwankungen zwischen 0.1 und 10 mD bzw. zwischen 5 und 10 % (Dethlefsen et al., 2014). Geeignete geologische Strukturen sind Sedimentbecken oder Antiklinalstrukturen (Gunter et al., 2004) z. B. an Salzstöcken. Die Speicherformation muss dabei von undurchlässigen Deckschichten überdeckt werden, wie z. B. von Tonsteinen oder Evaporiten, um einen Aufstieg von CO_2 und Formationswasser mit hohen Gesamtkonzentrationen aus der Speicherformation zu verhindern (»structural trapping«, Abbildung 1.11). Durch kapillare Bindungskräfte kann in den Poren der Speicherformation CO_2 zurückbleiben, das nach Abschluss der CO_2-Injektion nicht wieder vom Formationswasser verdrängt werden kann. Dadurch wird CO_2 als Residualphase in den Porenhohlräumen gespeichert (»residual trapping«, Abbildung 1.11). Krevor et al. (2012) bestimmten residuale CO_2-Sättigungen in verschiedenen Speicherformationen von ca. 20 bis 30 %. Die Lösung von CO_2 im Formationswasser hängt von der Temperatur, Druck und dem Salzgehalt des Formationswassers ab (Dubacq et al., 2013). und dissoziiert zur Kohlensäure (H_2CO_3, Gleichung 1.1).

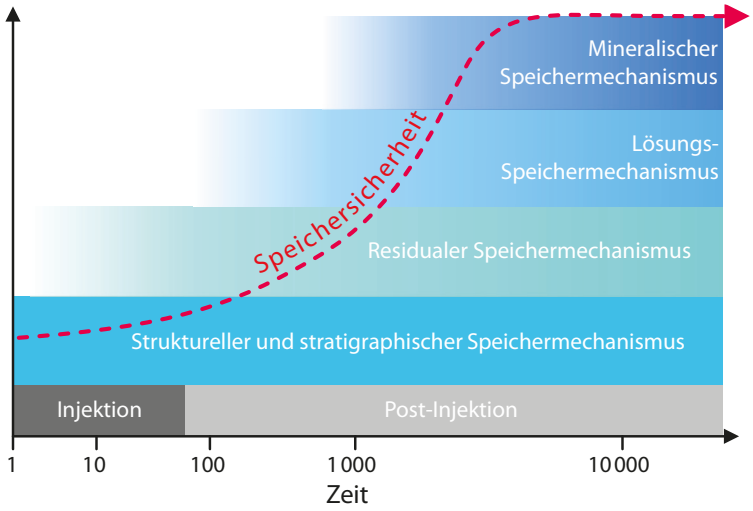

Abbildung 1.10

Verschiedene Speichermechanismen und deren Beiträge zur Speichersicherheit während einer CO_2-Injektion und der Zeiträume nach der Injektion (verändert nach CO2CRC, 2011).

Dieser Mechanismus wird als »solubility trapping« bezeichnet (Gunter et al., 2004). Ein Drittel des injizierten CO_2 wird durch Residualsättigung und Lösung im Formationswasser gespeichert (Suekane et al., 2008). Korbøl & Kaddour (1995) berechneten am Beispiel der Utsira-Formation (Sleipner-Feld, Norwegen) einen im Formationswasser gelösten CO_2-Anteil von 18 %. Nach Johnson et al. (2001) werden zwischen 10 und 20 % des injizierten CO_2 im Formationswasser gelöst. Gilfillan et al. (2009) weisen der CO_2-Lösung im Formationswasser die größte Speicherkapazität in untersuchten natürlichen Gasfeldern zu. Durch die Mineralauflösung und folgende Ausfällung von kohlenstoffhaltigen Sekundärmineralen wie z. B. Karbonaten (Dawsonit, Magnesit oder Dolomit) kann CO_2 durch »mineral trapping« langfristig gespeichert werden (z. B. Bachu et al., 1994; Knauss et al., 2001; Knauss et al., 2005; Kumar et al., 2004; Oelkers et al., 2008; Matter & Kelemen, 2009). Xu et al. (2003 a) stellten fest, dass die gespeicherte CO_2-Menge durch Mineralausfällung bei Verwendung verschiedener Gesteinszusammensetzungen sehr unterschiedlich sein kann. Die Autoren fanden heraus, dass bei günstigen Bedingungen die Menge an gespeichertem CO_2 vergleichbar oder sogar größer sein kann als die im Formationswasser gelöste CO_2-Menge. In einigen Studien wurde eine in Mineralen gespeicherte CO_2-Menge von weniger als 5 % berechnet (Audigane et al., 2007; Bickle et al., 2013), andere Studien zeigen hingegen in Simulationen, dass ca. 50 % des CO_2 in Festphasen umgewandelt wird (Zhang et al., 2013).

1.3.4 Reaktionen

In dieser Arbeit werden zum einen die Unsicherheiten für CO_2-Speicherprozesse und zum anderen die Unsicherheiten bei Prozessen, die CO_2 in über der Speicherformation liegenden Formationen zurückhalten können, untersucht. Die numerischen Codes berechnen dabei die in der Formation ablaufenden Reaktionen zwischen dem Formationswasser sowie den Mineralen der Formation und einer CO_2-Gasphase.

Für die Bewertung der Speichersicherheit ist die Bestimmung des CO_2-Anteils wichtig, der in der Speicherformation nicht mehr als Gasphase vorliegt und dauerhaft in Mineralphasen gespeichert wird. Zur Speichersicherheit tragen verschiedene geochemische Reaktionen bei. Der erste Reaktionsschritt

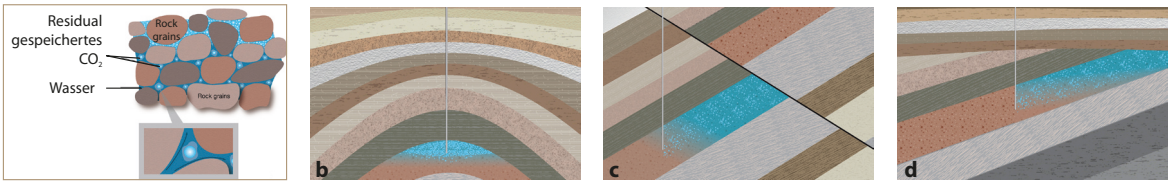

Abbildung 1.11

Residualer Speichermechanismus (a) und strukturelle Speichermechanismen (b, c, d). Als Strukturen können Falten (b), Störungen (c) und Diskordanzen (d) dienen (CO2CRC, 2011).

ist die CO_2-Lösung im salinen Formationswasser, wodurch der pH-Wert sinkt (Gilfillan et al., 2009). Im zweiten Schritt folgen Auflösungsreaktionen von Mineralen. Der niedrige pH-Wert treibt Reaktionen zwischen den Mineralphasen, die in der Formation enthalten sind, und dem Formationswasser an. Zumeist werden karbonatische und silikatische Mineralphasen aufgelöst. Im dritten Schritt können sekundäre Mineralphasen aus dem Formationswasser ausgefällt werden. Wenn diese Kohlenstoff enthalten, kann dadurch ein Teil des Kohlenstoffs aus dem CO_2 in Mineralphasen fixiert werden.

Die Simulation der CO_2-Lösung im Formationswasser wird von geochemischen numerischen Codes mit Ausnahme von FactSage unter Verwendung des Henry-Gesetzes (Henry, 1803) ausgeführt. Da das Henry-Gesetz nur für ideale Gase und geringe Drücke gültig ist, muss das nicht-ideale Verhalten von CO_2 berücksichtigt werden (King, 1969; Weiss, 1974). Daher werden verschiedene Zustandsgleichungen, wie die Peng-Robinson (Peng & Robinson, 1976) oder Redlich-Kwong-Zustandsgleichung (Redlich & Kwong, 1949) verwendet, um die CO_2-Lösung in wässrigen Phasen exakt zu berechnen. Weiterhin wurden Modelle entwickelt, mit denen die CO_2-Lösung bei hohen Drücken und hohen Ionenstärken genau berechnet werden können. Diese Modelle beruhen entweder auf dem Henry-Gesetz (Carroll et al., 1991) oder auf Zustandsgleichungen (Duan & Sun, 2003; Duan et al., 2006).

$$CO_2(g) + H_2O \rightleftarrows CO_2(aq) + H_2O \tag{1.1}$$

$$CO_2(aq) + H_2O \rightleftarrows H_2CO_3 \tag{1.2}$$

$$CO_2(aq) + H_2CO_3 \triangleq H_2CO_3{}^* \tag{1.3}$$

$$H_2CO_3{}^* \rightleftarrows H^+ + HCO_3^- \tag{1.4}$$

$$HCO_3^- + H^+ \rightleftarrows 2H^+ + CO_3^{-2} \tag{1.5}$$

Bolin (1960) und Borges (2004) zeigten, dass der Gastransfer von CO_2 von der Atmosphäre in Meerwasser ein relativ schneller Prozess ist. Die ermittelten Gastransferraten liegen zwischen ca. 1.0×10^{-3} und 2.0×10^{-2} cm s^{-1}. In einer CO_2-Speicherformation beeinflussen weitere Faktoren die Geschwindigkeit des CO_2-Transfers wie z. B. die im Kontakt zur Gasphase stehende Wasseroberfläche, der CO_2-Partialdruck und die Zusammensetzung des Formationswassers. Czernichowski-Lauriol et al. (1996) gehen davon aus, dass sich das injizierte CO_2 bei hohen Drücken relativ schnell im Formationswasser löst. Dieser Mechanismus verhindert einen Aufstieg der CO_2-Gasphase (Rochelle et al., 2004). Durch die CO_2-Reaktion mit dem Formationswasser der Speicherformation bildet sich Kohlensäure (H_2CO_3), die weiter in Hydrogencarbonat- und Carbonat-Ionen dissoziiert (Gleichung 1.1-1.5; z. B. King et al., 1992). In wässrigen Lösungen ist der Anteil von CO_2(aq) viel größer als der Anteil an Kohlensäure (ca. 99 %; Eldik & Palmer, 1982), weshalb CO_2(aq) und Kohlensäure zu $H_2CO_3{}^*$ zusammengefasst werden können.

Eine CO_2-Injektion in einen salinen Aquifer führt aufgrund der CO_2-Lösung und anschließender Dissoziation zu Kohlensäure zu einer pH-Wert-Abnahme des Formationswassers (Trautz et al., 2013; Peter et al., 2012; Kharaka et al., 2010; Lu et al., 2010; Little & Jackson, 2010; Humez et al., 2013; Zheng et al., 2009 a; Carroll et al., 2009; Birkholzer et al., 2008). In karbonatischen Formationen nimmt der pH-Wert induziert durch eine CO_2-Injektion um 1 und in siliziklastischen Formationen um 2 ab (Lu et al., 2010). In Formationen mit siliziklastischen Gesteinen sinkt der pH-Wert auf Werte zwischen 5.0 und 5.8 (Gilfillan et al., 2009). Espinoza & Santamarina (2010) bestimmten pH-Werte zwischen 3.0 und 4.0 in ungepufferten Systemen bei Abwesenheit von Calcit und CO_2-Drücken bis 200 bar und in Calcit-gepufferten Systemen pH-Werte zwischen 4.8 und 4.9. Dabei hängt der pH-Wert von der Mineralzusammensetzung, dem Druck bzw. der CO_2-Fugazität und der Temperatur in der Formation ab (Espinoza & Santamarina, 2010). Wenn der pH-Wert nicht von Calcit gepuffert wird, können Minerale wie z. B. Oxide, Sulfide, Feldspäte, Tonminerale oder Gibbsit als pH-Puffer dienen (Kjøller et al., 2004).

$$CaCO_3 \rightleftarrows CO_3^{-2} + Ca^{+2} \tag{1.6}$$

Die am häufigsten untersuchten Reaktionen sind die Lösung von Karbonaten und verschiedenen Silikaten (Rochelle et al., 2004; DePaolo & Cole, 2013; Gunter et al., 1997). Die Lösungsraten von Calcit (Gleichung 1.6) und Dolomit sind vergleichsweise hoch (Gleichung 1.2; Palandri & Kharaka, 2004; Kharaka, 2006; Lions et al., 2014), wodurch das Gleichgewicht zwischen den Mineralen und dem Formationswasser in mehreren Stunden oder Tagen erreicht werden kann (Svensson & Dreybrodt, 1992). Erst später setzt die Lösung anderer Mineralphasen wie z. B. der Silikate ein. Gunter et al. (1997) simulierten die Auflösung von Plagioklas und Annit in einer glaukonitischen Sandsteinformation (Alberta Basin, Canada), wodurch CO_2 im Formationswasser gespeichert und in Mineralphasen festgelegt werden kann (Gleichung 1.3-1.5). Durch die Auflösung von Anorthit werden Ca^{2+}-Ionen in die Lösung freigesetzt, wodurch Calcit und Kaolinit ausfallen (Gleichung 1.3). Die Auflösung von Annit führt zur Freisetzung von Fe^{2+} und damit zur Ausfällung von Siderit (Gleichung 1.9).

$$\underset{\text{Anorthit}}{CaAl_2Si_2O_8} + 2H_2O \rightleftarrows \underset{\text{Calcit}}{CaCO_3} + \underset{\text{Kaolinit}}{Al_2Si_2O_5(OH)_4} \tag{1.7}$$

$$7\,\underset{\text{Albit}}{NaAlSi_3O_8} + 6H_2O + 6CO_2 \rightleftarrows 6HCO_3^- + 6Na^+ + \text{Na-Smektit} + SiO_2 \tag{1.8}$$

$$3\,\underset{\text{Annit}}{KFe_3^{2+}(AlSi_3)O_{10}(OHF)} + 11CO_2 \rightleftarrows 9\,\underset{\text{Siderit}}{FeCO_3} + 2HCO_3^- + 2K^+ + \underset{\text{Muskovit}}{KAl_3Si_3O_{10}(OH)_2} + 6\,\underset{\textit{Quarz}}{SiO_2} + H_2O \tag{1.9}$$

Xu et al. (2001) modellierten das gleiche System wie Gunter et al. (1997) unter Verwendung von TOUGHREACT. Dabei veränderten Xu et al. (2001) jedoch die mineralogische Zusammensetzung der Festphasen, damit diese das Gestein besser darstellen können. Die Autoren berechneten ebenfalls eine Ausfällung von Calcit, Dolomit und Siderit. Der größte Anteil von CO_2 wird als Siderit gespeichert. Xu et al. (2003 a) berechneten die Mineralreaktionen, die bei einer CO_2-Injektion in Sandsteinformationen im Bereich der Golfküste (USA) auftreten. Die Autoren simulierten die Ausfällung von Calcit, Siderit und Dawsonit für »mineral trapping« bedingt durch die Auflösung von Oligoklas und Daphnit. Die Simulationen zeigen, dass die festgelegte CO_2-Menge stark von der Gesteinszusammensetzung und den Lösungsraten abhängt. Die Mineralausfällung von Karbonatphasen verändert sich in Abhängigkeit von der Porosität, Gasdruck, Temperatur und Redoxbedingungen der Speicherformation (Xu et al., 2003 a).

Kharaka et al. (2006) interpretierten chemische Analysen der Frio Formation (Golfküste, USA) und folgerten, dass Calcit, Eisenoxyde und -hydroxide durch die CO_2 bedingte Abnahme des pH-Werts aufgelöst werden. Die Autoren folgerten aus der Anwendung geochemischer Modelle, dass Plagioklas aufgelöst werden kann (Gleichung 1.10), wodurch Dawsonit, Gibbsit und amorphe Kieselsäure ausfallen können.

$$\underset{\text{Plagioklas}}{0.4H^+ + Ca_{0.2}Na_{0.8}Al_{1.2}Si_{2.8}O_8} + 0.8CO_2 \rightleftarrows 0.2Ca^{+2} + \underset{\text{Dawsonit}}{0.8\,NaAlCO_3(OH)_2} + \underset{\text{Gibbsit}}{0.4\,Al(OH)_3} + \underset{\text{Kieselsäure}}{2.8\ SiO_2} \tag{1.10}$$

Dawsonit wurde in vielen Simulationsstudien für Speicherformationen verwendet, wodurch Kohlenstoff in einer Festphase ausfällt (z. B. Dethlefsen et al., 2012; Xu et al., 2003 b; Mitiku et al., 2013; Kharaka et al., 2006; Gaus, 2010; Hellevang et al., 2013; Yu et al.; 2015). Dabei wird Natrium z. B. durch die Auflösung von Albit freigesetzt und kann mit CO_3^{-2} als Dawsonit ausfallen (Gleichung 1.11; Gaus, 2010; Hellevang et al., 2005). Nach thermodynamischen Berechnungen ist Dawsonit bei hohen CO_2-Partialdrücken stabil und kann bei bestimmten chemischen Randbedingungen ausfallen, bei sinkenden Partialdrücken kann Dawsonit jedoch wieder aufgelöst werden (Hellevang et al., 2005). Die Auflösung von Dawsonit ist bei ca. 80 °C und pH 4 vergleichsweise schnell ($10^{-6.7}$ mol m^{-2} s^{-1}) und kann daher bei zu geringen CO_2-Partialdrücken zu einer kurzen Stabilitätszeit führen (Hellevang et al., 2010). In natürlichen Analoga – wie Erdgasfeldern mit CO_2-Gehalten bis zu 50 % – konnten Wilkinson et al. (2009) jedoch nur maximal 0.9 vol % Dawsonit nachweisen. In triassischen Gesteinen in Yemen kommt Dawsonit bei fCO_2 bis 50 bar mit bis zu 8 vol % vor (Worden, 2006). Die Autoren folgern, dass Dawsonit hauptsächlich in feldspatreichen Sandsteinen mit Formationswässern, die viel Natrium enthalten, auftritt.

$$\underset{\text{Albit}}{7\,NaAlSi_3O_8} + CO_2 + H_2O \rightleftarrows \underset{\text{Dawsonit}}{NaAlCO_3(OH)_2} + 3SiO_2 \tag{1.11}$$

Eine weitere Reaktion für die CO_2-Festlegung ist die Auflösung von Olivin (Forsterit) und die Ausfällung von Kohlenstoff als Magnesit (Gleichung 1.8; Giammar et al., 2005).

$$\underset{\text{Forsterit}}{MgSiO_4} + H^+ \rightleftarrows 2Mg^{2+} + H_4SiO_4 \tag{1.12}$$

$$Mg^{2+} + CO_3^{-2} \rightleftarrows \underset{\text{Magnesit}}{MgCO_3} \tag{1.13}$$

Experimentell wurde die Auflösung von Kalifeldspat nach Gleichung 1.14 nachgewiesen (Shiraki & Dunn, 2000; Ketzer et al., 2009; Yu et al., 2012; Huq et al., 2015). Durch die Auflösung werden Aluminium- und Siliziumionen freigesetzt, wodurch aluminiumhaltige Mineralphasen wie z. B. Kaolinit ausgefällt werden können (Gleichung 1.14). Reaktive Transportmodellierungen zeigen, dass die Rate der Kalifeldspatauflösung signifikant durch die Ausfällungsraten von Sekundärmineralen beeinflusst wird (Tutolo et al., 2015). Die ausgefällten Mineralphasen können die Permebilität der Formation verringern (Yu et al., 2012).

$$\underset{\text{K-feldspar}}{2\,KAlSi_3O_8} + 2H^+ + 9H_2O \rightleftarrows \underset{\text{Kaolinite}}{Al_2Si_2O_5(OH)_4} + 2K^+ + 4H_4SiO_4 \tag{1.14}$$

In Transfer- und Rückhalteformationen im Hangenden der Speicherformation sowie in oberflächennahen Schutzgutformationen kann bei einer CO_2-Leckage aus der Speicherformation durch einen CO_2-Eintrag der pH-Wert des Formationswassers abgesenkt werden, wodurch Karbonate wie z. B. Calcit oder Dolomit aufgelöst werden können (Lu et al., 2010; Wilkin & Digiulio, 2010). In

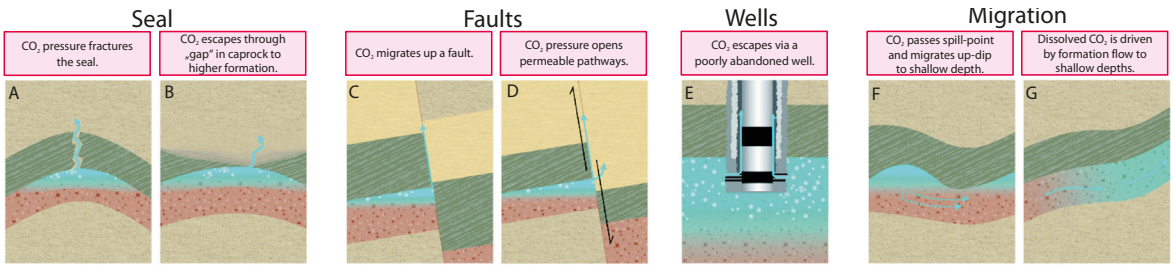

Abbildung 1.12
Mögliche Leckagepfade für CO_2 (CO2CRC, 2011).

oberflächennahen Grundwasserleitern erwarten Wilkin & Digiulio (2010) die Reaktion von Albit zu Kaolinit (Gleichung 1.15), der wiederum durch Auflösung Aluminium- und Hydrogencarbonat-Ionen in das Grundwasser freisetzen kann (Gleichung 1.16). Weiterhin kann CO_2 die Auflösung von Eisenoxiden und -hydroxiden fördern (Gleichung 1.17; Kharaka et al., 2006).

$$\underset{\text{Albit}}{2NaAlSi_3O_8} + 11H_2O + 2CO_2(aq) \rightleftarrows \underset{\text{Kaolinit}}{Al_2Si_2O_5(OH)_4} + 2Na^+ + 2HCO_3^- + 4H_4SiO_4 \quad (1.15)$$

$$\underset{\text{Kaolinit}}{Al_2Si_2O_5(OH)_4} + 5H_2O + 6CO_2(aq) \rightleftarrows 2Al^{3+} + 6HCO_3^- + 2H_4SiO_4 \quad (1.16)$$

$$FeOOH + 2CO_2(aq) + 0.4H_2(g) \rightleftarrows Fe^{2+} + 2HCO_3^- \quad (1.17)$$

In der Speicherformation können durch eine CO_2-Injektion Karbonate und Silikate gelöst werden, wodurch der pH-Wert gepuffert wird. In verschiedenen Studien werden, abhängig von der Zusammensetzung der Speicherformationen, unterschiedliche Silikat-Auflösungsreaktionen verwendet, dadurch sind verschiedene Reaktionen möglich. Diese Reaktionen können dann zur Festlegung von Kohlenstoff in Karbonaten (z. B. Calcit, Dolomit, Magnesit, Siderit und Dawsonit) führen. In den überlagernden Formationen ist die Auflösung von Karbonaten für die pH-Pufferung eine wichtige Reaktion um z. B. die Freisetzung von Schwermetallen berechnen zu können.

1.3.5 Leckagen aus CO_2-Speicherformationen

Neben den in Speicherformationen ablaufenden Reaktionen werden in dieser Arbeit auch Prozesse in Leckage- und Transferformationen simuliert, die die Bewertung der Risiken in Bezug auf CO_2-Leckagen verbessern können. Die Risiken der CO_2-Speicherung sind: (1) Leckagen von CO_2 aus der Speicherformation, (2) der Aufstieg von salinem Formationswasser in oberflächennahe Formationen und (3) Seismizität und Bodenbewegungen (Damen et al., 2006; Newmark et al., 2010). In der vorliegenden Arbeit werden in Kapitel 4 die Unsicherheiten der Vorhersage der Calcitauflösung durch eine CO_2-Leckage in oberflächennahe Formationen untersucht.

CO_2 kann über Leckagepfade wie Deckgesteine, Störungen oder Bohrungen in Formationen aufsteigen, die sich über der Speicherformation befinden. Die Formationen über der Speicherformation werden als Rückhalteformation bezeichnet (Großmann et al., 2011; Dethlefsen et al., 2013). Im Fall einer CO_2-Leckage gelangt CO_2 aus dem Speicher zuerst in die Rückhalteformation (Lions et al., 2014). Wenn CO_2 aus der Rückhalteformation weiter aufsteigt, kann es über die Transferpfadformation in oberflächennahe Schutzgutformationen gelangen (Abbildung 1.13; Oldenburg, 2007; Großmann et al., 2011; Dethlefsen et al., 2013). Durch injiziertes CO_2 kann der Druck in der Formation so groß werden, dass sich Störungen in den Deckgesteinen ausbilden oder dass undurchlässige Störungen

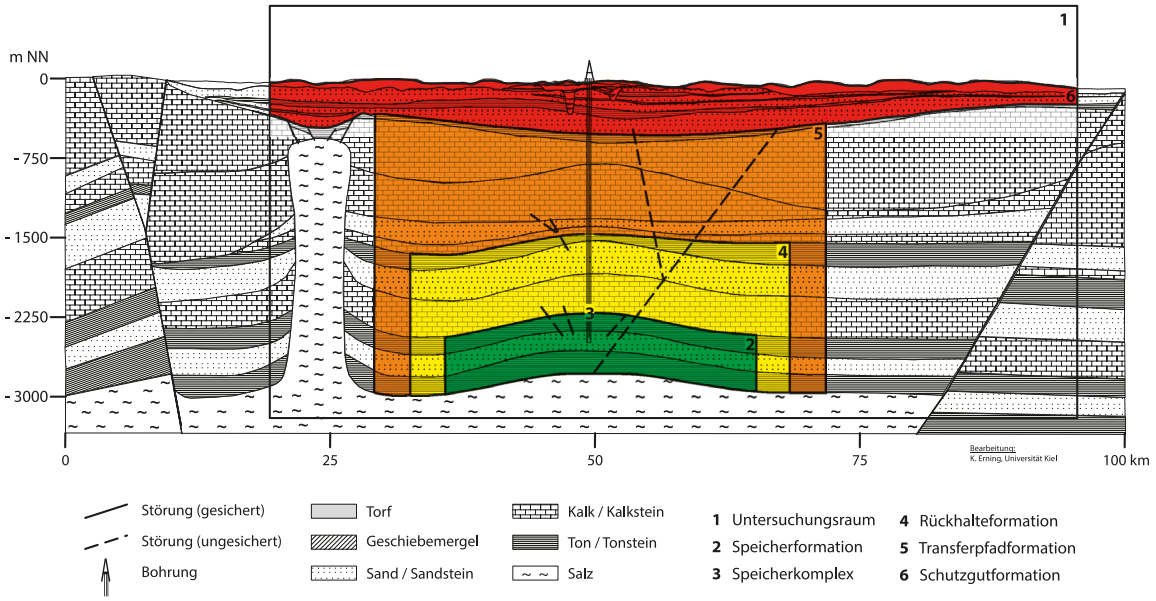

Abbildung 1.13

Untersuchte Teilräume beim Monitoring einer CO_2-Speicherung am Beispiel des geologischen Aufbaus Norddeutschlands (Großmann et al., 2011; Dethlefsen et al., 2013).

wieder geöffnet werden (»hydraulic fracturing«; Damen et al., 2006). Die Deckgesteine bestehen z. B. aus undurchlässigen feinkörnigen Gesteinsschichten (z. B. Tonsteine) oder Salzgesteinen (Holloway, 2005). Wenn jedoch der Druck in der Speicherformation unterhalb dem Druck gehalten wird, bei dem das Deckgestein brechen könnte (initialer Reservoirdruck), ist das Leckagerisiko gering (Damen et al., 2006; Over et al., 1999). CO_2 kann dann nur noch über offene Störungen oder durch Diffusion in darüber liegenden Formationen gelangen (Abbildung 1.12). Das Formationswasser, dessen pH-Wert durch die Reaktion mit CO_2 sehr niedrig ist (pH-Werte zwischen 3 und 6), kann die Zementierung oder Verrohrung der Bohrungen angreifen. Dadurch kann die Injektionsbohrung undicht werden und an dieser das injizierte CO_2 wieder aufsteigen (Watson & Bachu, 2009; Celia et al., 2011; Nordbotten et al., 2009). Weiterhin können im Gebiet des CO_2-Speichers bestehende Bohrungen z. B. der Erdölindustrie vorkommen, die unbekannt oder undicht sein können (Damen et al., 2006). Eine CO_2-Leckage über Störungen oder Bohrungen kann sehr schnell sein, wogegen die Leckage durch die Porenhohlräume des Deckgesteins langsamer ist (Lewicki et al., 2007).

Das Risiko einer CO_2-Leckage birgt die größte Gefahr, wenn CO_2 aufsteigt und an der Erdoberfläche austritt. Da CO_2 schwerer als Luft ist, kann durch eine CO_2-Leckage an der Erdoberfläche eine hohe CO_2-Konzentration entstehen, die für den Menschen und die Umwelt gefährlich sind (Benson & Myer, 2002).

Bevor CO_2 an der Erdoberfläche austreten kann, migriert es – im Fall einer CO_2-Leckage – nach Passage der Leckage- und Transferformation in oberflächennahe Grundwasserleiter. Die Qualität des Grundwassers ist durch eine CO_2-Leckage gefährdet, da der durch CO_2 erniedrigte pH-Wert zur Mobilisierung von natürlich vorkommenden Spurenelementen oder Schwermetallen führen kann, die in den Grundwasserleitern enthalten sind (Cahill et al., 2013; Dafflon et al., 2013; Kharaka et al., 2006; Little & Jackson, 2010; Varadharajan et al., 2013; Wang & Jaffe, 2004; Zheng et al., 2009a; Lions et al., 2014; O'Mullen et al., 2015). Spurenelemente können mobilisiert werden, ohne dass Grenzwerte der Grundwasserqualität überschritten

werden (Birkholzer et al., 2008; Carroll et al., 2009; Apps et al., 2010; Lions et al., 2014). Die Mobilisierung der Spurenelemente und Schwermetalle kann durch Mineral- oder Austauschreaktionen stattfinden (z. B. Bacon et al., 2015). Für die Berechnung des Schwermetalltransports sind Austauschreaktionen an Mineraloberflächen mit großen Austauschkapazitäten, wie z. B. Tonmineraloberflächen, von Bedeutung (Apps et al., 2010; Wilkin & Digiulio, 2010). Wenn in der Formation Karbonate vorkommen, können diese maßgeblich zur Änderung der Grundwasserqualität beitragen, da durch die Reaktion mit CO_2 die Konzentration vieler Kationen ansteigen können (Smyth et al., 2009; Lu et al., 2010; Bacon et al., 2015).

Der Aufstieg von Formationswasser aus einer CO_2-Speicherformation in oberflächennahe Grundwasserleiter kann zur Versalzung des Grundwassers führen (Gale, 2002; Walter et al., 2013; Dethlefsen et al., 2013). In der Speicherformation mobilisierte Spurenelemente und Schwermetalle können durch den Formationswasseraufstieg in oberflächennahe Grundwasserleiter transportiert werden (Lions et al., 2014). Jedoch zeigten Icenhauer et al. (2015), dass in Experimenten unter Verwendung von Sandsteinen der Frio Formation die mobilisierte Konzentration der Schwermetalle mit Ausnahme von Barium, Chrom und Blei gering sind und die Gefahr des Überschreitens von Schwellenwerten unwahrscheinlich ist. Durch die Mobilisierung von Schwermetallen besteht die Gefahr, dass die nutzbaren Grundwasservorräte dezimiert werden können und die ausreichende Versorgung mit Trinkwasser in der Zukunft gefährdet sein könnte. Um diesen Risiken vorzubeugen, muss eine CO_2-Speicherstätte überwacht werden.

1.3.6 Monitoring einer Speicherstätte

Das Monitoring einer CO_2-Speicherstätte muss während einer CO_2-Injektion und der Zeiträume danach durchgeführt werden. Die Untersuchungsergebnisse der in der vorliegenden Arbeit durchgeführten Studien, z. B. die aus Kapitel 2, wirken sich ebenfalls auf die Erstellung von Monitoringkonzepten einer CO_2-Speicherstätte aus. Die Ausbreitung einer Reaktionsfront infolge einer CO_2-Leckage wurde in oberflächennahen Formationen in Kapitel 4 simuliert. Die Ergebnisse aus Kapitel 2 und 4 können dazu beitragen geeignete Monitoringparameter und deren Spannbreiten zu bestimmen, wodurch die Erstellung erfolgreicher Monitoringkonzepte gelingen kann.

Um einen Aufstieg des CO_2 in Transfer-, Rückhalte- und Schutzgutformationen oder in die Atmosphäre frühzeitig zu erkennen und möglicherweise Gegenmaßnahmen einzuleiten, muss eine CO_2-Speicherstätte überwacht werden. Dabei können verschiedene Teilräume unterschieden werden, in denen unterschiedliche Methoden eingesetzt werden können (Abbildung 1.13; Dethlefsen et al., 2013). Das Monitoring einer CO_2-Speicherstätte wird bisher durch die Richtlinie 2009/31 EG über die geologische Speicherung von Kohlendioxid für die Europäische Union geregelt. Die Richtlinie besagt, dass ein standortspezifisches Monitoringkonzept entwickelt werden muss, das alle Bereiche von der Speicherformation bis zur Atmosphäre umfasst. Verschiedene Monitoringkonzepte wurden vom National Energy Technology Laboratory (NETL, U. S. Department of Energy; NETL, 2009), Umweltbundesamt (UBA) (Großmann et al., 2011), CLEAN-Projekt (Köber et al., 2011), der Bundesanstalt für Geowissenschaften und Rohstoffe (BGR) und der U. S. Environmental Protection Agency (USEPA) erstellt. Daneben wurden die zur Verfügung stehenden Monitoringmethoden und Monitoringkonzepte bewertet (z. B. Benson et al., 2002; Benson et al., 2004; Benson, 2006; Davis et al., 2003; Oldenburg et al., 2003; Dethlefsen et al., 2013; Schäfer et al., 2013; Peter et al., 2012).

Abbildung 1.14
Aeroelektromagnetik (airborne electromagnetics, AEM; BGR, 2013).

Das Monitoring einer CO_2-Speicherstätte hat im Wesentlichen zwei Ziele: Erstens muss nachgewiesen werden, dass die Speicherung ordnungsgemäß abläuft, und zweitens muss die Ausbreitung ausgetretener Stoffe und der Einfluss dieser auf die betreffende Formation im Fall einer Betriebsstörung der Speicherstätte überwacht werden (Dethlefsen et al., 2013). Bei einem Austritt von Stoffen aus der Speicherformation wird von Großmann et al. (2011) ein schrittweises Konzept vorgeschlagen, womit auf unerwartete Ereignisse reagiert werden kann. Die Basis dafür bildet die Einteilung der Speicherstätte in Teilräume (Abbildung 1.13). Dabei ist es besonders wichtig Leckagen von CO_2 oder von salinen Formationswässern festzustellen. Solche Leckagen können dabei im Umfang von mehreren zehner Kilometern auftreten. Wenn der Verdacht besteht, dass CO_2 oder Formationswässer in oberflächennahe Schutzgutformationen eingetreten sind, müssen Monitoring-Technologien bereitstehen um die Quelle und Quantität der Leckage großflächig innerhalb eines kurzen Zeitraums zu messen (Dethlefsen et al., 2013).

Vor der CO_2-Speicherung müssen Baselinemessungen der Teilräume vorgenommen werden, wobei die geogenen Werte mit verschiedenen Monitoringmethoden bestimmt werden. Diese Messungen benötigen einen Zeitraum von zwei Jahren, da es starke regionale und saisonale Schwankungen geben kann (Schäfer et al., 2013). Für das weitere Monitoring können die Messwerte mit den Referenzwerten der Baselinemessung verglichen werden. Da für jede möglicherweise einzusetzende Monitoringmethode Referenzwerte vorliegen müssen, sollte die Basismessung möglichst viele Methoden enthalten und die räumliche Ausdehnung sollte entsprechend groß gewählt werden (Köber et al., 2011).

Das Monitoring von offenen und verfüllten Bohrungen ist unterschiedlich. Offene Bohrungen können durch etablierte Methoden, die auf dem neuesten Stand der Technik sind, überwacht werden. Dabei sollten besonders die Bohrlochkopfdrücke und Ringraumdrücke, Injektionsraten und Temperaturen gemessen und die Zusammensetzung des Fluids im Bohrloch überwacht werden. Weiterhin sollten regelmäßig Kalibermessungen (Bohrungsdurchmesser) durchgeführt werden. Die Kontrolle von verfüllten Bohrungen ist jedoch wesentlich schwieriger, verglichen mit der Überwachung von offenen Bohrungen. Vorhandene Bohrungen werden im Rahmen der Speichererkundung in verschiedene Risikoklassen eingeteilt (Köber et al., 2011). Bohrungen, die ein hohes Leckagerisiko aufweisen, da z. B. die Verfüllung nicht mehr stabil ist, müssen saniert werden. Die Umgebung von Bohrungen mit hohem Leckagerisiko soll besonders überwacht werden, wobei ein Radius von mindestens 400 m angesetzt wird (Ide, 2006).

In der Speicherformation sollten Druck- und Temperaturmessungen (Liebscher, 2013), seismische Untersuchungen, wie z. B. die passive Mikroseismik, die Analyse des Formationswassers und der Gase durchgeführt werden. Mit diesen Methoden kann eine mögliche Reaktivierung von Störungen, die CO_2-Druckwelle detektiert und die Verteilung und Migration des CO_2 in der Speicherformation beobachtet werden (Chadwick, 2008). Außerdem geben geophysikalische Messungen Aufschluss über die Bildung von Störungen im Deckgestein der Speicherformation. Während der CO_2-Injektion wird ebenfalls die Injektionsbohrung überwacht, um den ordnungsgemäßen Ablauf der CO_2-Speicherung sicherzustellen (Liebscher, 2013).

Die Beobachtung der Rückhalteformationen ergibt Hinweise auf die Dichtigkeit der Deckschichten und auf mögliche Leckagen in die die Speicherformation überlagernden Formationen. Der Austritt von Formationswasser und anderen Gasen in die Rückhalteformation kann durch seismische und elektromagnetische Methoden sowie durch Formationswasseranalysen kontrolliert werden.

Die Transferpfadformation schützt als letzter Teilraum die oberflächennahen Schutzgüter (Grundwasser und Bodenzone) vor einem CO_2-Aufstieg. Daher müssen diese Formationen besonders intensiv überwacht werden. Die Methoden gleichen denen für die Rückhalteformation. Die Überprüfung der Transferpfadformation kann durch die geringere Tiefenlage und dadurch verursachte höhere Sensitivität der Methoden genauer und mit höherer Sicherheit erfolgen.

Das oberflächennahe Grundwasser ist ein Schutzgut, weshalb dieses nach der EU-Grundwasserrichtlinie zum Schutz des Grundwassers vor Verschmutzung und Verschlechterung (Richtlinie 2006/118/EG) des Europäischen Parlaments und des Rates vor einer Qualitätsverschlechterung und chemischer Verschmutzung geschützt werden soll. Nach der Richtlinie ist Grundwasser das größte Süßwasservorkommen in der EU und eine Hauptquelle für die Trinkwasserversorgung. Essentiell für das Monitoring ist die Grundwasserprobenahme in Grundwassermessstellen, wobei besonders der pH-Wert, elektrische Leitfähigkeit, Total Inorganic Carbon (TIC), Total Dissolved Solids (TDS) und die Calcium-Konzentration geeignete Monitoringparameter für das Feststellen einer CO_2-Beeinflussung sind (Wilkin, 2010; Schäfer et al., 2013; Fahrner et al., 2012 a; Dethlefsen et al., 2013; Zhu et al., 2015). Es wurden Sonden entwickelt, die diese Parameter permanent überwachen können. Die elektrische Leitfähigkeit der Grundwasserleiter lässt sich flächenhaft und schnell durch die hubschraubergestützte Aeroelektromagnetik überwachen (Abbildung 1.14; BGR, 2013, Siemon et al., 2009; Kirsch, 2006; Christensen et al., 2009). Dabei kann bis in eine Tiefe von 300 m der Widerstand gemessen werden und dadurch CO_2 als Gasphase oder die durch CO_2 verursachte Erhöhung der Leitfähigkeit detektiert werden (Dethlefsen et al., 2013). In der Bodenzone kann CO_2 gemessen werden, bevor es in die Atmosphäre entweicht. Im Projekt DEMO-CO_2 war es möglich eine CO_2-Leckage mit Hilfe von mit dem CO_2 injizierten Edelgasen zu detektieren (Rillard et al., 2015). Die CO_2-Messung in der Bodenluft ist jedoch schwierig, da der CO_2-Gehalt aufgrund mikrobiellen Abbaus von organischem Kohlenstoff sehr stark schwankt (Schäfer et al., 2013). Die CO_2-Konzentration in der Luft kann mit CO_2-Detektoren, Eddy-Kovarianz-Messtürmen oder Laser-Systemen durchgeführt werden (Köber et al., 2011). Flächenhaft kann CO_2 nur durch Fernerkundung oder durch ein Ökosystem-Stress-Monitoring detektiert werden.

Literaturverzeichnis

Allen, D. E., Strazisar, B. R., Soong, Y. & Hedges, S. W. 2005. Modeling carbon dioxide sequestration in saline aquifers: Significance of elevated pressures and salinities. Fuel Processing Technology. 86 (14–15), 1569–1580. *doi:10.1016/j.fuproc.2005.01.004*

Almpanis-Lekkas, O., Wukovits, W. & Weiss, B. 2014. Development of an Industrial Iron-Making Melter Gasifier Model with Multiphase Equilibrium Calculations. Chemical Engineering Transactions. 39 (2014) 823–828. *doi:10.3303/CET1439138*

Appelo, C. A. J. & Willemsen, A. 1987. Geochemical calculations and observations on salt water intrusions, I. A combined geochemical/mixing cell model. Journal of Hydrology. 94 (3), 313–330. *doi:10.1016/0022-1694-(87)90058-8*

Appelo, C. A. J., Willemsen, A., Beekman, H. E. & Grifoen, J. 1990. Geochemical calculations and observations on salt water intrusions. II. Validation of a geochemical model with laboratory experiments. Journal of Hydrology. 120 (1–4), 225–250. *doi:10.1016/0022-1694(90)90151-M*

Appelo, C. A. J., Verweij, E. & Schäfer, H. 1998. A hydrogeochemical transport model for an oxidation experiment with pyrite/calcite/exchangers/organic matter containing sand. Applied Geochemistry. 13 (2), 257–268. *doi:10.1016/S0883-2927(97)00070-X*

Appelo, C. A. J., Parkhurst, D. L. & Post, V. E. A. 2014. Equations for calculating hydrogeochemical reactions of minerals and gases such as CO_2 at high pressures and temperatures. Geochimica et Cosmochimica Acta. 125 (15 January 2014), 49–67. *doi:10.1016/j.gca.2013.10.003*

Apps, J. A., Zheng, L., Zhang, Y., Xu, T. & Birkholzer, J. T. 2010. Evaluation of Potential Changes in Groundwater Quality in Response to CO_2 Leakage from Deep Geologic Storage. Transport in Porous Media. 82 (1), 215–246. *doi:10.1007/s11242-009-9509-8*

Arvidson, R. S., Ertan, I. E., Amonette, J. E. & Luttge, A. 2003. Variation in calcite dissolution rates. Geochimica et Cosmochimica Acta. 67 (9), 1623–1634. *doi:10.1016/S0016-7037(02)01177-8*

Audigane, P., Gaus, I., Czernichowski-Lauriol, I., Pruess, K. & Xu, T. 2007. Two-dimensional reactive transport modeling of CO_2 injection in a saline aquifer at the Sleipner site, North Sea. American Journal of Science. 307 (7), 974–1008. *doi:10.2475/07.2007.02*

Bachu, S., Gunter, W. D. & Perkins, E. H. 1994. Aquifer disposal of CO_2: Hydrodynamic and mineral trapping. Energy Conversion and Management. 35 (4), 269–279. *doi:10.1016/0196-8904(94)90060-4*

Bacon, D. H., Qafoku, N. P., Dai, Z., Keating, E. H. & Brown, C. F. 2015. Modeling the impact of carbon dioxide leakage into an unconfined, oxidizing carbonate aquifer. Internation Journal of Greenhouse Gas Control. In press. *doi:10.1016/j.ijggc.2015.04.008*

Bale, C. W., Chartrand, P., Degterov, S. A., Eriksson, G., Hack, K., Mahfoud, R. B., Melançon, J., Pelton, A. D. & Petersen, S. 2002. FactSage Termochemical Sofware and Databases. Calphad. 26 (2), 189–228. *doi:10.1016/S0364-5916(02)00035-4*

Bale, C. W. W., Bélisle, E., Chartrand, P., Decterov, S. A., Eriksson, G., Hack, K., Jung, I.-H., Kang, Y.-B., Melançon, J., Pelton, A. D., Robelin, C. & Petersen, S. 2009. FactSage Termochemical Sofware and Databases–Recent Developments. Calphad. 33 (2), 295–311. *doi:10.1016/j.calphad.2008.09.009*

Ball, J. W. & Nordstrom, D. K. 1991. User's Manual for Wateq4f, with revised thermodynamic Data Base and Test Cases for Calcualting Speciation of Major, Trace, and Redox Elements in natural Waters–USGS Open File Report 91–183. Technical report. U. S. Geological Survey, Menlo Park, California.

Bara, J. E. 2012. What chemicals will we need to capture CO_2? Greenhouse Gases Science and Technology. 171 (2), 162–171. *doi:10.1002/ghg.1279*

Bassett, R. L. & Melchior, D. C. 1990. Chemical Modeling of Aqueous Systems II: An Overview. ACS Symposium Series, vol. 416. Washington, DC: American Chemical Society. *doi:10.1021/bk-1990-0416*

Bauer, S., Class, H., Ebert, M., Feeser, V., Götze, H., Holzheid, A., Kolditz, O., Rosenbaum, S., Rabbel, W., Schäfer, D. & Dahmke, A. 2012. Modeling, parameterization and evaluation of monitoring methods for CO_2 storage in deep saline formations: The CO_2-MoPa project. Environmental Earth Sciences. 67 (2), 351–367. *doi:10.1007/s12665-012-1707-y*

Béarat, H., McKelvy, M. J., Chizmeshya, A. V. G., Gormley, D., Nunez, R., Carpenter, R. W., Squires, K. & Wolf, G. H. 2006. Carbon Sequestration via Aqueous Olivine Mineral Carbonation: Role of Passivating Layer Formation. Environmental Science & Technology. 40(15), 4802–4808. *doi:10.1021/es0523340*

Beck, M. B. 1987. Water Quality Modeling: A Review of the Analysis of Uncertainty. Water Resources Research. 23 (8), 1393–1442. *doi:10.1029/WR023i008p01393*

Benson, S. M. 2006. Monitoring carbon dioxide sequestration in deep geological formations for inventory verifcation and carbon credits. Page 14 of: SPE Annual Technical Conferenceand Exhibition. San Antonio, Texas, USA: Society of Petroleum Engineers. *doi:10.2118/102833-MS*

Benson, S. M. & Myer, L. 2002. Monitoring to ensure safe and effective geologic sequestration of carbon dioxide. Pages 137–151 of: Workshop on Carbon Dioxide Storage, Proceedings. Regina, Canada: ECN.

Benson, S. M., Gasperikova, E. & Hoversten, G. M. 2004. Monitoring protocols and life-cycle costs for geologic storage of carbon dioxide. In: Rubin, E. S., Keith, D. W., Gilboy, C. F., Wilson, M., Morris, T., Gale, J. & Tambimuthu, K. (eds), Proceedings of the 7th International Conference on Greenhouse Gas Control Technologies 5 September 2004.

Benson, S. M., & Cook, P. 2005. Underground geological storage (Chapter 5): IPCC special report on carbon dioxide capture and storage. Technical report. Intergovernmental Panel on Climate Change, Cambridge.

Bethke, C. M. 2008. Geochemical and Biogeochemical Reaction Modeling. Cambridge: Cambridge University Press.

Bethke, C. M., & Yeakel, S. 2014. The Geochemist's Workbench Release 10.0.

Bethke, C. M., & Yeakel, S. 2009. The Geochemist's Workbench: A Users Guide to Rxn, Act2, Tact, React, and Gtplot. Technical report. University of Illinois, Urbana, Illinois.

Beyer, C., Li, D., Lucia, M. D., Kühn, M. & Bauer, S. 2012. Modelling CO_2-induced fluid-rock interactions in the Altensalzwedel gas reservoir. Part II: Coupled reactive transport simulation. Environmental Earth Sciences. 67 (2), 573–588. *doi:10.1007/s12665-012-1684-1*

Bickle, M., Kampman, N. & Wigley, M. 2013. Natural Analogues. Reviews in Mineralogy and Geochemistry. 77 (1), 15–71. *doi:10.2138/rmg.2013.77.2*

Bildstein, O., Kervévan, C., Lagneau, V., Delaplace, P., Crédoz, A., Audigane, P., Perfetti, E., Jacquemet, N. & Jullien, M. 2010. Integrative modeling of caprock integrity in the context of CO_2 storage: Evolution of transport and geochemical properties and Impact on Performance and Safety Assessment. Oil & Gas Science Technology. 65 (3), 485–502. *doi:10.2516/ogst/2010006*

Birkholzer, J., Apps, J., Zheng, L., Zhang, Y., Xu, T. & Tsang, C.-F. 2008. Research Project on CO_2 Geological Storage and Groundwater Resources: Water Quality Efects Caused by CO_2 Intrusion into Shallow Groundwater, Technical Report, October 2008. Technical report. Lawrence Berkeley National Laboratory, Berkeley, California, USA.

Blunt, M., Fayers, F. J. & Orr, F. M. 1993. Carbon dioxide in enhanced oil recovery. Energy Conversion and Management. 34 (9–11), 1197–1204. *doi:10.1016/0196-8904(93)90069-M*

Bolin, B. 1960. On the Exchange of Carbon Dioxide between the Atmosphere and the Sea. Tellus XII. 1 (3), 274–281. *doi:10.1111/j.2153-3490.1960.tb01311.x*

Borges, A. V., Delille, B., Schiettecatte, L.-S., Gazeau, F., Abril, G. & Frankignoulle, M. 2004. Gas transfer velocities of CO_2 in three European estuaries (Randers Fjord, Scheldt, and Thames). Limnology and Oceanography. 49 (5), 1630–1641. *doi:10.4319/lo.2004.49.5.1630*

Brinkley, S. R. 1946. Note on the Conditions of Equilibrium for Systems of Many Constituents. The Journal of Chemical Physics. 14 (9), 563. *doi:10.1063/1.1724195*

Brinkley, S. R. 1947. Calculation of the Equilibrium Composition of Systems of Many Constituents. The Journal of Chemical Physics. 15 (2), 107. *doi:10.1063/1.1746420*

Brun, A. & Engesgaard, P. 2002. Modelling of transport and biogeochemical processes in pollution plumes: literature review and model development. Journal of Hydrology. 256 (3–4), 211–227. *doi:10.1016/S0022-1694(01)00547-9*

Cahill, A. G., Jakobsen, R., Mathiesen, T. B. & Jensen, C. K. 2013. Risks attributable to water quality changes in shallow potable aquifers from geological carbon sequestration leakage into sediments of variable carbonate content. International Journal of Greenhouse Gas Control. 19 (November 2013), 117–125. *doi:10.1016/j.ijggc.2013.08.018*

Cahill, A. G. & Jakobsen, R. 2015. Geochemical modeling of a sustained shallow aquifer CO_2 leakage field study and implications for leakage and site monitoring. International Journal of Greenhouse Gas Control. 37 (June 2015), 127–141. *doi:10.1016/j.ijggc.2015.03.011*

Cantucci, B., Montegrossi, G., Vaselli, O., Tassi, F., Quattrocchi, F. & Perkins, E. H. 2009. Geochemical modeling of CO_2 storage in deep reservoirs: The Weyburn Project (Canada) case study. Chemical Geology. 265 (1–2), 181–197. *doi:10.1016/j.chemgeo.2008.12.029*

Cantucci, B., Montegrossi, G., Buttinelli, M., Vaselli, O., Scrocca, D. & Quattrocchi, F. 2014. Geochemical Barriers in CO_2 Capture and Storage Feasibility Studies. Transport in Porous Media. 106 (1), 107–143. *doi:10.1007/s11242-014-0392-6*

Carroll, J. J., Slupsky, J. D. & Mather, A. E. 1991. The Solubility of Carbon Dioxide in Water at Low Pressure. Journal of physical and chemical Reference Data. 20 (6), 1201–1209. *doi:10.1063/1.555900*

Carroll, S., Hao, Y. & Aines, R. 2009. Geochemical detection of carbon dioxide in dilute aquifers. Geochemical transactions. 10 (4), 1–18. *doi:10.1186/1467-4866-10-4*

Celia, M. A., Nordbotten, J. M., Court, B., Dobossy, M. & Bachu, S. 2011. Field-scale application of a semi-analytical model for estimation of CO_2 and brine leakage along old wells. International Journal of Greenhouse Gas Control. 5 (2), 257–269. *doi:10.1016/j.ijggc.2010.10.005*

Chadwick, A., Arts, R., Bernstone, C., May, F., Thibeau, S. & Zweigel, P. 2008. Best practice for the storage of CO_2 in saline aquifers - observations and guidelines from the SACS and CO2STORE projects. British Geological Survey. Retrieved from http://nora.nerc.ac.uk/2959/1/0812_CO2STORE_BPM_book_V7.pdf

Christensen, N. B., Steuer, A., Siemon, B. & Auken, E. 2009. A comparison of helicopter-borne electromagnetics in frequency- and time-domain at the Cuxhaven valley in Northern Germany. Journal of Applied Geophysics. 67 (3), 194–205. *doi:10.1016/j.jappgeo.2007.07.001*

Ciavatta, L. 1990. The specifc interaction theory in equilibrium analysis. Some empirical rules for estimating interaction coeffcients of metal ion complexes. Annali di Chimica. 80, 255–263.

CO2CRC. 2011. Cooperative Research Centre for Greenhouse Gas Technologies. http://www.co2crc.com.au/. Accessed at 03.10.2014.

Criscenti, L. J., Lafniak, G. F. & Erikson, R. L. 1996. Propagation of uncertainty through geochemical code calculations. Geochimica et Cosmochimica Acta. 60 (19), 3551–3568. *doi:10.1016/0016-7037(96)00188-3*

Czernichowski-Lauriol, I., Sanjuan, B., Rochelle, C., Lindeberg, E. & Bateman, K. 1996. Analysis of the geochemical aspects of the underground disposal of CO_2. In: Apps, J. A. & Tsang, C.-F. (Ed.). Deep Injection Disposal of Hazardous and Industrial Waste (pp. 565–583). Academic Press.

Dafon, B., Wu, Y., Hubbard, S. S., Birkholzer, J. T., Daley, T. M., Pugh, J. D., Peterson, J. E. & Trautz, R. C. 2013. Monitoring CO_2 intrusion and associated geochemical transformations in a shallow groundwater system using complex electrical methods. Environmental Science & Technology. 47 (1), 314–21. *doi:10.1021/es301260e*

Damen, K., Faaij, A. & Turkenburg, W. 2006. Health, Safety and Environmental Risks of Underground CO_2 Storage–Overview of Mechanisms and Current Knowledge. Climatic Change. 74 (1-3), 289–318. *doi:10.1007/s10584-005-0425-9*

Damköhler, G. & Edse, R. 1943. Zusammensetzung dissoziierender Verbrennungsgase und die Berechnung simultaner Gleichgewichte. Zeitschrift für Elektrochemie und angewandte physikalische Chemie. 49 (3), 178–186. *doi:10.1002/bbpc.19430490309*

Davies, C. W. 1962. Ion association. International Association for Great Lakes Research. Butterworths, London.

Davis, T. L., Terrell, M. J. & Benson, R. D. 2003. Multicomponent seismic characterization and monitoring of the CO_2 flood at Weyburn Field, Saskatchewan. The Leading Edge. 22 (7), 696–697. *doi:10.1190/1.1599699*

Debye, P. & Hückel, E. 1923. Zur Theorie der Elektrolyte. Physikalische Zeitschrift, 24 (9), 185–205.

Delany, J. M. & Lundeen, S. R. 1991. The LLNL Termochemical Data Base-Revised Data and File Format for the EQ3/6 Package, Report UCID-21658. Technical report. Lawrence Livermore National Laboratory, Livermore, California.

Denison, F. H. & Garnier-Laplace, J. 2005. The effects of database parameter uncertainty on uranium (VI) equilibrium calculations. Geochimica et Cosmochimica Acta. 69 (9), 2183–2191. *doi:10.1016/j.gca.2004.09.033*

DePaolo, D. J. & Cole, D. R. 2013. Geochemistry of Geologic Carbon Sequestration: An Overview. Reviews in Mineralogy and Geochemistry. 77 (1), 1–14. *doi:10.2138/rmg.2013.77.1*

Dethlefsen, F., Haase, C., Ebert, M. & Dahmke, A. 2012. Uncertainties of geochemical modeling during CO_2 sequestration applying batch equilibrium calculations. Environmental Earth Sciences. 65 (4), 1105–1117. *doi:10.1007/s12665-011-1360-x*

Dethlefsen, F., Köber, R., Schäfer, D., al Hagrey, S. A., Hornbruch, G., Ebert, M., Beyer, M., Großmann, J. & Dahmke, A. 2013. Monitoring Approaches for Detecting and Evaluating CO_2 and Formation Water Leakages into Near-Surface Aquifers. Energy Procedia. 37 (2013) 4886–4893. *doi:10.1016/j.egypro.2013.06.399*

Dubacq, B., Bickle, M. J. & Evans, K. A. 2013. An activity model for phase equilibria in the H_2O–CO_2–NaCl system. Geochimica et Cosmochimica Acta. 110 (1 June 2013) 229–252. *doi:10.1016/j.gca.2013.02.008*

Duan, Z. & Sun, R. 2003. An improved model calculating CO_2 solubility in pure water and aqueous NaCl solutions from 273 to 533 K and from 0 to 2000 bar. Chemical Geology. 193 (3–4), 257–271. *doi:10.1016/S0009-2541(02)00263-2*

Duan, Z., Sun, R., Zhu, C. & Chou, I.-M. 2006. An improved model for the calculation of CO_2 solubility in aqueous solutions containing Na^+, K^+, Ca^{2+}, Mg^{2+}, Cl^-, and SO_4^{2-}. Marine Chemistry. 98 (2–4), 131–139. *doi:10.1016/j.marchem.2005.09.001*

Dunsmore, H. E. 1992. A geological perspective on global warming and the possibility of carbon dioxide removal as calcium carbonate mineral. Energy Conversion and Management. 33 (5–8), 565–572. *doi:10.1016/0196-8904(92)90057-4*

Ekberg, C. 1999. Sensitivity Analysis and Simulation Uncertainties in Predictive Geochemical Modelling: A Case Study. Dissertation, Chalmers University of Technology, Göteborg, Sweden.

Engesgaard, P. & Kipp, K. L. 1992. A geochemical transport model for redox-controlled movement of mineral fronts in groundwater fow systems: A case of nitrate removal by oxidation of pyrite. Water Resources Research. 28 (10), 2829. *doi:10.1029/92WR01264*

Eriksson, G. & Königsberger, E. 2008. FactSage and ChemApp: Two tools for the prediction of multiphase chemical equilibria in solutions. Pure and Applied Chemistry. 80 (6), 1293–1302. *doi:10.1351/pac200880061293*

Espinoza, D. N. & Santamarina, J. C. 2010. Water-CO_2-Mineral systems: Interfacial tension, contact angle, and diffusion-Implications to CO_2 geological storage. Water Resources Research. 46 (7), 1–10. *doi:10.1029/2009WR008634*

Fahrner, S., Schäfer, D. & Dahmke, A. 2012 a. A monitoring strategy to detect CO_2 intrusion in deeper freshwater aquifers. International Journal of Greenhouse Gas Control. 9 (July 2012), 262–271. *doi:10.1016/j.ijggc.2012.03.016*

Fahrner, S., Schäfer, D., Dethlefsen, F. & Dahmke, A. 2012b. Reactive modelling of CO_2 intrusion into freshwater aquifers: current requirements, approaches and limitations to account for temperature and pressure effects. Environmental Earth Sciences. 67 (8), 2269–2283. *doi:10.1007/s12665-012-1673-4*

Freund, P. 2001. Progress in understanding the potential role of CO_2 storage. Pages 272–277 of: Williams, D. J., Durie, R. A., McMullan, P., Paulson, C. A. J. & Smith, A. Y. (eds), Proceedings of the 5th International Conference on Greenhouse Gas Control Technologies (GHGT-5).

Fu, Y., van Berk, W. & Schulz, H.-M. 2012. Hydrogeochemical modelling of fluid-rock interactions triggered by seawater injection into oil reservoirs: Case study Millerfield (UK North Sea). Applied Geochemistry. 27 (6), 1266–1277. *doi: 10.1016/j.apgeochem.2012.03.002*

Fu, Y., van Berk, W., Schulz, H.-M. & Mu, N. 2015 a. Berthierine formation in reservoir rocks from the Siri Oilfield (Danish North Sea) as a result of fluid-rock interactions: Part III. Determining mineral stability and CO_2-sequestering capacity of glauconitic sandstones. Marine and Petroleum Geology. 65 (August 2015), 327–333. *doi 10.1016/j.marpetgeo.2015.01.008*

Fu, Y., van Berk, W., Schulz, H.-M. & Mu, N. 2015 b. Berthierine formation in reservoir rocks from the Siri oilfield (Danish North Sea) as result of fluid-rock interactions: Part II. Deciphering organic-inorganic processes by hydrogeochemical modeling. Marine and Petroleum Geology. 63 (August 2015), 317–326. *doi:10.1016/j.marpetgeo.2015.01.007*

Gale, J. 2002. Overview of CO_2 emissions sources, potential, transport and geographical distribution of storage possibilities. Page 15–29 of: IPCC Workshop on Carbon Dioxide Capture and Storage.

Gaus, I., Azaroual, M. & Czernichowski-Lauriol, I. 2005. Reactive transport modelling of the impact of CO_2 injection on the clayey cap rock at Sleipner (North Sea). Chemical Geology. 217 (3–4), 319–337. *doi:10.1016/j.chemgeo.2004.12.016*

Gaus, I., Audigane, P., André, L., Lions, J., Jacquemet, N., Durst, P., Czernichowski-Lauriol, I. & Azaroual, M. 2008. Geochemical and solute transport modelling for CO_2 storage, what to expect from it? International Journal of Greenhouse Gas Control. 2 (4), 605–625. *doi:10.1016/j.ijggc.2008.02.011*

Gaus, I. 2010. Role and impact of CO_2-rock interactions during CO_2 storage in sedimentary rocks. International Journal of Greenhouse Gas Control. 4 (1), 73–89. *doi:10.1016/j.ijggc.2008.02.011*

Gherardi, F., Xu, T. & Pruess, K. 2007. Numerical modeling of self-limiting and self enhancing caprock alteration induced by CO_2 storage in a depleted gas reservoir. Chemical Geology. 244 (1-2), 103–129. *doi:10.1016/j.chemgeo.2007.06.009*

Giammar, D. E., Bruant, R. G. & Peters, C. A. 2005. Forsterite dissolution and magnesite precipitation at conditions relevant for deep saline aquifer storage and sequestration of carbon dioxide. Chemical Geology. 217 (3–4), 257–276. *doi:10.1016/j.chemgeo.2004.12.013*

Gilfillan, S. M. V., Lollar, B. S., Holland, G., Blagburn, D., Stevens, S., Schoell, M., Cassidy, M., Ding, Z., Zhou, Z., Lacrampe-Couloume, G. & Ballentine, C. J. 2009. Solubility trapping in formation water as dominant CO_2 sink in natural gas felds. Nature. 458 (7238), 614–618. *doi:10.1038/nature07852*

Global CCS Institute 2014. The Global Status of CCS 2014. Technical Report. Melbourne, Australia.

Gordon, S. & Zeleznik, F. J. 1963. A general IBM704 or 7090 computer program for computation of chemical equilibrium compositions, rocket performance, and Chapman-Jouguet detonations. Technical report. NASA, Springfeld, Washington.

Gordon, S., Zeleznik, F. J. & Huf, V. N. 1959. A general method for automatic computation of equilibrium compositions and theoretical rocket performance of propellants. Technical report. NASA.

Großmann, J., Naue, G., Schreck, A., Woiwode, R., Bauer, S., Dahmke, A., Ebert, M., Schäfer, D., Reinicke, K. M., Schilling, F. & Krawczyk, C. 2011. Sicherheit und Umweltverträglichkeit der CO_2-Speicherung – Speicherprozesse. Report for the German Federal Environmental Agency. Technical report. German Federal Environmental Agency (Umweltbundesamt), Dessau-Roßlau.

Grenthe, I., Fuger, J., Konings, R. J. M., Lemire, R. J., Muller, A. B., Nguyen-Trung Cregu, C., Wanner, H. & Forest, I. 1992. Chemical thermodynamics of uranium. Technical report. Nuclear Energy Agency.

Gundogan, O., Mackay, E. & Todd, A. 2011. Comparison of numerical codes for geochemical modelling of CO_2 storage in target sandstone reservoirs. Chemical Engineering Research and Design. 89 (9), 1805–1816. *doi:10.1016/j.cherd.2010.09.008*

Gunter, W. D., Wiwchar, B. & Perkins, E. H. 1997. Aquifer disposal of CO_2-rich Greenhouse Gases: Extension of the time scale of experiment for CO_2-sequestering reactions by geochemical modelling. Mineralogy and Petrology. 59 (1–2), 121–140. *doi:10.1007/BF01163065*

Gunter, W. D., Bachu, S. & Benson, S. 2004. The role of hydrogeological and geochemical trapping in sedimentary basins for secure geological storage of carbon dioxide. Geological Society, London, Special Publications. 233 (1), 129–145. *doi:10.1144/GSL.SP.2004.233.01.09*

Gunter, W. D., Perkins, E. H. & McCann, T. J. 1993. Aquifer disposal of CO_2-rich gases: Reaction design for added capacity. Energy Conversion and Management. 34 (9–11), 941–948. *doi:10.1016/0196-8904(93)90040-H*

Gustafsson, J. P. 2006. Visual MINTEQ 2.51.

Harvie, C. E., Weare, J. H. & Harvie, E. 1980. The prediction of mineral solubilities in natural waters: The Na-K-M-Ca-Cl-SO_4-H_2O system from zero to high concentration at 25 °C. Geochimica et Cosmochimica Acta. 44 (7), 981–997. *doi:10.1016/0016-7037(80)90287-2*

Hellevang, H. & Aagaard, P. 2013. Can the long-term potential for carbonatization and safe long-term CO_2 storage in sedimentary formations be predicted? Applied Geochemistry. 39 (December 2013), 108–118. *doi:10.1016/j.apgeochem.2013.09.012*

Hellevang, H., Declercq, J., Kvamme, B. & Aagaard, P. 2010. The dissolution rates of dawsonite at pH 0.9 to 5 and temperatures of 22, 60 and 77 °C. Applied Geochemistry. 25 (10), 1575–1586. *doi:10.1016/j.apgeochem.2010.08.007*

Hellevang, H., Aagaard, P., Oelkers, E. H. & Kvamme, B. 2005. Can dawsonite permanently trap CO_2? Environmental Science & Technology. 39 (21), 8281–8287. *doi:10.1021/es0504791*

Hellevang, H., Pham, V. T. H. & Aagaard, P. 2013. Kinetic modelling of CO_2-water-rock interactions. International Journal of Greenhouse Gas Control. 15 (July 2013), 3–15. *doi:10.1016/j.ijggc.2013.01.027*

Henry, W. 1803. Experiments on the quantity of gases absorbed by water, at different temperatures, and under different pressures. Philosophical Transactions of the Royal Society of London. 93, 29–42 + 274–276.

Hitchon, B. (ed). 1996. Aquifer disposal of carbon dioxide: Hydrodynamic and mineral trapping – proof of concept. Alberty, Canada: Geoscience Publishing Ltd.

Höller, S. & Viebahn, P. 2011. Assessment of CO_2 storage capacity in geological formations of Germany and Northern Europe. Energy Procedia. 4 (2011), 4897–4904. *doi:10.1016/j.egypro.2011.02.458*

Holloway, S. 2001. Storage of fossil fuel-derived carbon dioxide beneath the surface of the earth. Annual Review of Energy and the Environment. 26 (November 2001), 145–166. *doi:10.1146/annurev.energy.26.1.145*

Holloway, S. 2005. Underground sequestration of carbon dioxide – A viable greenhouse gas mitigation option. Energy. 30 (11), 2318–2333. *doi:10.1016/j.energy.2003.10.023*

Humez, P., Lagneau, V., Lions, J. & Negrel, P. 2013. Assessing the potential consequences of CO_2 leakage to freshwater resources: A batch-reaction experiment towards an isotopic tracing tool. Applied Geochemistry. 30 (March 2013), 178–190. *doi:10.1016/j.apgeochem.2012.07.014*

Huq, F., Haderlein, S. B., Cirpka, O. A., Nowak, M., Blum, P. & Grathwohl, P. 2015. Flow-through experiments on

water–rock interactions in a sandstone caused by CO_2 injection at pressures and temperatures mimicking reservoir conditions. Applied Geochemistry. 58 (July 2015), 136–146. *doi:10.1016/j.apgeochem.2015.04.006*

Icenhower, J. P., Saldi, G. D., Daval, D., Knauss, K. G. 2015. Experimental determination of the reactivity of the Frio Sandstone, Texas, and the fate of heavy metals resulting from carbon dioxide sequestration. Environmental Earth Sciences. In press. *doi: 10.1007/s12665-015-4560-y*

Ide, T., Friedmann, S. J. & Herzog, H. 2006. CO_2 leakage through existing wells: Current technology and regulations. Page 6 of: Proceedings of the 8th International Conference on Greenhouse Gas Control Technologies.

INTERA. 1983. Geochemical models suitable for performance assessment of nuclear waste storage: Comparison of PHREEQE and EQ3/EQ6. ONWI-473. Technical report. INTERA, Houston, Texas.

Intergovernmental Panel on Climate Change. 2013. Climate Change 2013: The Physical Science Basis: Working Group I. Contribution to the Fifth Assessment Report of the Intergovernmental Panel on Climate Change. Cambridge, United Kingdom and New York, NY, USA: Cambridge University Press.

Jenne, E. A. 1979. Chemical Modeling - Goals, Problems, Approaches, and Priorities. In: Jenne, E. A. (ed). Chemical Modeling of Aqueous Systems. American Chemical Society, Washington, D.C., pp 3–21. *doi:10.1021/bk-1979-0093*

Johnson, J. W., Nitao, J. J., Steefel, C. I. & Knauss, K. G. 2001. Reactive transport modeling of geologic CO_2 sequestration in saline aquifers: the influence of intra-aquifer shales and the relative effectiveness of structural, solubility, and mineral trapping during prograde and retrograde sequestration. Page 60 of: Proceedings of the 1st National Conference on Carbon Sequestration.

Johnson, J. W. & Lundeen, S. R. 1994. GEMBOCHS thermodynamic data files for use with the EQ3/6 software package. Technical report. Lawrence Livermore National Laboratory, Livermore, California.

Keating, E. H., Fessenden, J., Kanjorski, N., Koning, D. J. & Pawar, R. 2009. The impact of CO_2 on shallow groundwater chemistry: Observations at a natural analog site and implications for carbon sequestration. Environmental Earth Sciences. 60 (3), 521–536. *doi:10.1007/s12665-009-0192-4*

Kervévan, C., Azaroual, M. & Durst, P. 2005. Improvement of the Calculation Accuracy of Acid Gas Solubility in Deep Reservoir Brines: Application to the Geological Storage of CO_2. Oil & Gas Science Technology. 60 (2), 357–379. *doi:10.2516/ogst:2005022*

Ketzer, J. M. M., Iglesias, R., Einloft, S., Dullius, J., Ligabue, R. & de Lima, V. 2009. Water-rock-CO_2 interactions in saline aquifers aimed for carbon dioxide storage: Experimental and numerical modeling studies of the Rio Bonito Formation (Permian), southern Brazil. Applied Geochemistry. 24 (5), 760–767. *doi:10.1016/j.apgeochem.2009.01.001*

Kharaka, Y. K., Cole, D. R., Hovorka, S. D., Gunter, W. D., Knauss, K. G. & Freifeld, B. M. 2006. Gas-water-rock interactions in Frio Formation following CO_2 injection: Implications for the storage of greenhouse gases in sedimentary basins. Geology. 34 (7), 577. *doi:10.1130/G22357.1*

Kharaka, Y. K., Tordsen, J. J., Kakouros, E., Ambats, G., Herkelrath, W. N., Beers, S. R., Birkholzer, J. T., Apps, J. A., Spycher, N. F., Zheng, L., Trautz, R. C., Rauch, H. W. & Gullickson, K. S. 2010. Changes in the chemistry of shallow groundwater related to the 2008 injection of CO_2 at the ZERT field site, Bozeman, Montana. Environmental Earth Sciences. 60 (2), 273–284. *doi:10.1007/s12665-009-0401-1*

King, M. B. 1969. Phase Equilibrium in mixture. 1st edition. Oxford: Pergamon Press.

King, M. B., Mubarak, A., Kim, J. D. & Bott, T.R. 1992. The mutual solubilities of water with supercritical and liquid carbon dioxides. The Journal of Supercritical Fluids. 5 (4), 296–302. *doi:10.1016/0896-8446(92)90021-B*

Kirsch, R. (ed). 2006. Groundwater Geophysics: A Tool for Hydrogeology. Berlin: Springer-Verlag.

Kjøller, C., Postma, D. & Larsen, F. 2004. Groundwater Acidification and the Mobilization of Trace Metals in a Sandy Aquifer. Environmental Science & Technology. 38 (10), 2829–2835. *doi:10.1021/es030133v*

Knauss, K. G., Johnson, J. W., Steefel, C. I. & Nitao, J. J. 2001. Evaluation of the Impact of CO_2, Aqueous Fluid, and Reservoir Rock Interactions on the Geologic Sequestration of CO_2, with Special Emphasis on Economic Implications. Page 11 of: Proceedings of the 1st National Conference on Carbon Sequestration. Retrieved from https://e-reports-ext.llnl.gov/pdf/240135.pdf

Knauss, K. G., Johnson, J. W., Steefel, C. I. 2005. Evaluation of the impact of CO_2, co-contaminant gas, aqueous fluid and reservoir rock interactions on the geologic sequestration of CO_2. Chemical Geology. 217 (3–4), 339–350. *doi: 10.1016/j.chemgeo.2004.12.017*

Knopf, S., May, F., Müller, C. & Gerling, P. 2010. Neuberechnung möglicher Kapazitäten zur CO_2-Speicherung in tiefen Aquifer-Strukturen. Energiewirtschafliche Tagesfragen. 60 (4), 76–80.

Köber, R., Wiegers, C., Schäfer, D., Dahmke, A., Großmann, J., Tischer, L. & Beyer, M. 2011. Ableitung eines standortspezifschen Langzeit-Monitoringkonzepts für EGR unter Einbeziehung der rechtlichen und sicherheitstechnischen Vorgaben sowie hydrogeochemisches Monitoring im fachen Grundwasserleiter. Endberichtdes BMBF-Forschungsvorhabens CLEAN. Technical report. Institut für Geowissenschafen, Christian-Albrechts-Universität zu Kiel, Kiel.

Koide, H. & Yamazaki, K. 2001. Subsurface CO_2 Disposal with Enhanced Gas Recovery and Biogeochemical Carbon Recycling. Environmental Geosciences. 8 (1), 218–224. *doi:10.1046/j.1526-0984.2001.008003218.x*

Kolditz, O., Bauer, S., Beyer, C., Böttcher, N., Dietrich, P., Görke, U.-J., Kalbacher, T., Park, C.-H., Sauer, U., Schütze, C., Shao, H., Singh, A., Taron, J., Wang, W. & Watanabe, N. 2012. A systematic benchmarking approach for geologic CO_2 injection and storage. Environmental Earth Sciences. 67 (2), 613–632. *doi:10.1007/s12665-012-1656-5*

Kopp, A., Class, H. & Helmig, R. 2009. Investigations on CO_2 storage capacity in saline aquifers. International Journal of Greenhouse Gas Control. 3 (3), 263–276. *doi:10.1016/j.ijggc.2008.10.002*

Korbøl, R. & Kaddour, A. 1995. Sleipner vest CO_2 disposal-injection of removed CO_2 into the Utsira formation. Energy Conversion and Management. 36 (6), 509–512. *doi:10.1016/0196-8904(95)00055-I*

Krevor, S. C. M., Pini, R., Zuo, L. & Benson, S. M. 2012. Relative permeability and trapping of CO_2 and water in sandstone rocks at reservoir conditions. Water Resources Research. 48 (2), 1-16. *doi:10.1016/0196-8904-(95)00055-I*

Krupka, K. M. & Serne, R. J. 1998. Effects on radionuclide concentrations by cement/groundwater interactions in support of performance assessment of low-level radioactive waste disposal facilities. Technical report. U. S. Nuclear Regulatory Commission, Washington, DC.

Kulik, D. A., Hummel, W., Lützenkirchen, J. & Lefèvre, G. 2015. Preface: SI: Geochemical Speciation Codes and Databases. Applied Geochemistry. 55 (April 2015), 1–198. *doi:10.1016/j.apgeochem.2014.12.019*

Kumar, A., Noh, M., Pope, G. A., Sepehrnoori, K., Bryant, S. & Lake, L. W. 2004. Reservoir simulation of CO_2 storage in deep saline aquifers. In: SPE/DOE Fourteenth Symposium on Improved Oil Recovery. *doi:10.2118/89343-PA*

Lessard, J. D., Shekhter, L. N., Gribbin, D. G., Blagoveshchensky, Y. & McHugh, L. F. 2015. A new technology platform for the production of electronic grade tantalum nanopowders from tantalum scrap sources. International Journal of Refractory Metals and Hard Materials. 48 (January 2015), 408–413. *doi:10.1016/j.ijrmhm.2014.09.027*

Lewicki, J. L., Birkholzer, J. & Tsang, C.-F. 2007. Natural and industrial analogues for leakage of CO_2 from storage reservoirs: identification of features, events, and processes and lessons learned. Environmental Geology. 52 (3), 457–467. *doi:10.1007/s00254-006-0479-7*

Li, D. & Bauer, S. 2009. Development of a coupled transport and geochemical reaction code and a first application to CO_2 sequestration. Pages 59–66 of: Proceedings of the Workshop TRePro II. Karlsruhe: Forschungszentrum Karlsruhe GmbH. Retrieved from http://bibliothek.fzk.de/zb/berichte/FZKA7482.pdf#page=69

Li, D., Bauer, D., Benisch, K., Graupner, B. & Beyer, C. 2013. OpenGeoSys-ChemApp: A coupled simulator for reactive transport in multiphase systems and application to CO_2 storage formation in Northern Germany. Acta Geotechnica. 9 (1), 67–79. *doi:10.1007/s11440-013-0234-7*

Liebscher, A., Möller, F., Bannach, A., Köhler, S., Wiebach, J., Schmidt-Hattenberger, C., Weiner, M., Pretschner, C., Ebert, K. & Zemke, J. 2013. Injection operation and operational pressure-temperature monitoring at the CO_2 storage pilot site Ketzin, Germany - Design, Results, Recommendations. International Journal of Greenhouse Gas Control. 15 (July 2013), 163–173. *doi:10.1016/j.ijggc.2013.02.019*

Lindeberg, E., Vuillaume, J.-F. & Ghaderi, A. 2009. Determination of the CO_2 storage capacity of the Utsira formation. Energy Procedia. 1 (1), 2777–2784. *doi:10.1016/j.egypro.2009.02.049*

Lions, J., Devau, N., de Lary, L., Dupraz, S., Parmentier, M., Gombert, P. & Dictor, M.-C. 2014. Potential impacts of leakage from CO_2 geological storage on geochemical processes controlling fresh groundwater quality: A review. International Journal of Greenhouse Gas Control. 22 (March 2014), 165–175. *doi:10.1016/j.ijggc.2013.12.019*

Little, M. G. & Jackson, R. B. 2010. Potential impacts of leakage from deep CO_2 geosequestration on overlying freshwater aquifers. Environmental Science & Technology. 44 (23), 9225–32. *doi:10.1021/es102235w*

Lu, J., Partin, J. W., Hovorka, S. D. & Wong, C. 2010. Potential risks to freshwater resources as a result of leakage from CO_2 geological storage: A batch-reaction experiment. Environmental Earth Sciences. 60 (2), 335–348. *doi:10.1007/s12665-009-0382-0*

Ludwig, B., Khanna, P., Balkenhol, R., Friedrich, G. & Dohrmann, R. 1999. Pyrite oxidation in a sediment sample of an open-cut brown coal mine: Mineral formation, buffering of acidity and modeling of cations and sulfate. Journal of Plant Nutrition and Soil Science. 162 (5), 499–509. *doi:10.1002/(SICI)1522-2624(199910)162:5<499::AID-JPLN499>3.0.CO;2-4*

Maldal, T. & Tappel, I. M. 2004. CO_2 underground storage for Snøhvit gas field development. Energy. 29 (9–10), 1403–1411. *doi: 10.1016/j.energy.2004.03.074*

Malik, Q. M. & Islam, M. R. 2000. CO_2 Injection in the Weyburn Field of Canada: Optimization of Enhanced Oil Recovery and Greenhouse Gas Storage With Horizontal Wells. In SPE/DOE Improved Oil Recovery Symposium. Tulsa, Oklahoma, USA: Society of Petroleum Engineers. *doi:10.2118/59327-MS*

Matter, J. M., & Kelemen, P. B. 2009. Permanent storage of carbon dioxide in geological reservoirs by mineral carbonation. Nature Geoscience. 2 (12), 837–841. *doi:10.1038/ngeo683*

May, F., Müller, C. & Bernstone, C. 2005. How Much CO_2 can be Stored in Deep Saline Aquifers in Germany? Das Potential tiefer salinarer Aquifere zur CO_2-Speicherung in Deutschland. VGB PowerTech, 85 (6), 32–37.

McDuff, R. E. & Morel, F. M. 1973. REDEQL: A general program for the computation of chemical equilibrium in aqueous systems. California Institute of Technology, Keck Lab Technical Report. EA-73-02.

Merkel, B. J., & Planer-Friedrich, B. 2008. Grundwasserchemie – Praxisorientierter Leitfaden zur numerischen Modellierung von Beschaffenheit, Kontamination und Sanierung aquatischer Systeme. Heidelberg: Springer-Verlag.

Metz, B., Davidson, O., Coninck, H. D., Loos, M. & Meyer, L. 2005. IPCC special report on carbon dioxide capture and storage. Geneva, Switzerland. Retrieved from http://www.osti.gov/energycitations/product.biblio.jsp?osti_id=20740954

Millero, F. J. 2001. The physical chemistry of natural waters. New York: Wiley-Intersciences.

Millero, F. J. 2000. The activity coeffcients of non-electrolytes in seawater. Marine Chemistry. 70 (1–3), 5–22. *doi:10.1016/S0304-4203(00)00011-6*

Millero, F. J. 1974. Seawater as a Multicomponent Electrolyte Solution. Miami: Defense Technical Information Center.

Millero, F. J. & Lepple, F. K. 1973. The density and expansibility of artificial seawater solutions from 0 to 40 °C and 0 to 21 chlorinity. Marine Chemistry. 1 (2), 89–104. *doi:10.1016/0304-4203(73)90009-1*

Millero, F. J., Lawson, D. & Gonzalez, A. 1976. The density of artificial river and estuarine waters. Journal of Geophysical Research. 81 (6), 1177–1179. *doi:10.1029/JC081i006p01177*

Mitiku, A. B., Li, D., Bauer, S. & Beyer, C. 2013. Geochemical modelling of CO_2-water-rock interactions in a potential storage formation of the North German sedimentary basin. Applied Geochemistry. 36 (September 2013), 169–186. doi: *10.1016/j.apgeochem.2013.06.008*

Møller, N., Greenberg, J. P. & Weare, J. H. 1998. Computer Modeling for Geothermal Systems: Predicting Carbonate and Silica Scale Formation, CO_2 Breakout and H_2S Exchange. Transport in Porous Media. 33 (1-2), 173–204. *doi:10.1023/A:1006501927827*

Mompeán, F. J. & Wanner, H. (2003). The OECD nuclear energy agency thermochemical database project. Radiochimica Acta. (**91**), 617–622. *doi:10.1524/ract.91.11.617.23468*

NETL. 2009. Monitoring, Verifcation, and Accounting of CO_2 stored in deep geologic Formations. Technical report. National Energy Technology Laboratory, Alberta.

Newell, D. L., Kaszuba, J. P., Viswanathan, H. S., Pawar, R. J. & Carpenter, T. 2008. Significance of carbonate buffers in natural waters reacting with supercritical CO_2: Implications for monitoring, measuring and verification (MMV) of geologic carbon sequestration. Geophysical Research Letters. 35 (23), L23403. *doi:10.1029/2008GL035615*

Newmark, R. L, Friedmann, S. J. & Carroll, S. 2010. Water challenges for geologic carbon capture and sequestration. Environmental Management. 45 (4), 651–661. *doi:10.1007/s00267-010-9434-1*

Nitzsche, O., Meinrath, G. & Merkel, B. 2000. Database uncertainty as a limiting factor in reactive transport prognosis. Journal of Contaminant Hydrology. 44 (3–4), 223–237. *doi:10.1016/S0169-7722(00)00106-6*

Nordbotten, J. M., Kavetski, D., Celia, M. A. & Bachu, S. 2009. Model for CO_2 Leakage including multiple geological Layers and multiple leaky Wells. Environmental Science & Technology. 43 (3), 743–749. *doi:10.1021/es801135v*

Nordstrom, D. K. 2007. Modeling Low-Temperature Geochemical Processes. In: Holland, H. D. & Turekian, K. K. (eds). Treatise on Geochemistry. Elsevier, Oxford, pp 1–38. *doi: 10.1016/B0-08-043751-6/05074-X*

Nordstrom, D. K. & Campbell, K. M. 2014. Modeling Low-Temperature Geochemical Processes. In: Holland, H. D. & Turekian, K. K. (eds). Treatise on Geochemistry (Second Edition). Elsevier, Oxford, pp 27–68. *doi:10.1016/B978-0-08-095975-7.00502-7*

Oelkers, E. H., Benezeth, P. & Pokrovski, G. S. 2009. Thermodynamic Databases for Water-Rock Interaction. Reviews in Mineralogy and Geochemistry 70 (1). 1–46. *doi: 10.2138/rmg.2009.70.1*

Oelkers, E. H., Gislason, S. R. & Matter, J. 2008. Carbon Dioxide Sequestation: Mineral Carbonation of CO_2. Elements. 4 (5), 333–337. *doi:10.2113/gselements.4.5.333*

Oldenburg, C. M. 2003. Carbon Sequestration in natural Gas Reservoirs: Enhanced Gas Recovery and natural Gas Storage. Pages 1–8 of: TOUGH Symposium 2003. Berkeley, California: Lawrence Berkeley National Laboratory. Retrieved from http://escholarship.org/uc/item/61b1pogk

Oldenburg, C. M., Pruess, K. & Benson, S. M. 2001. Process Modeling of CO_2 Injection into Natural Gas Reservoirs for Carbon Sequestration and Enhanced Gas Recovery. Energy & Fuels. 15 (2), 293–298. *doi:10.1021/ef000247h*

Oldenburg, C. M. 2007. Screening and ranking framework for geologic CO_2 storage site selection on the basis of health, safety, and environmental risk. Environmental Geology. 54 (8), 1687–1694. *doi:10.1007/s00254-007-0947-8*

O'Mullan, G., Dueker, M. E., Clauson, K., Yang, Q., Umemoto, K., Zakharova, N., Matter, J., Stute, M., Takahashi, T. & Goldberg, D. 2015. Microbial Stimulation and Succession following a Test Well Injection Simulating CO_2 Leakage into a Shallow Newark Basin Aquifer. PLOS One. 10 (1), 1–25. *doi: 10.1371/journal.pone.0117812*

Over, J. A., de Vries, J. E. & Stork, J. 1999. Removal of CO_2 by Storage in the Deep Underground, Chemical Utilization and Biofixation: Options for the Netherlands. Utrecht, Netherlands: Novem. Retrieved from https://inis.iaea.org/search/searchsinglerecord.aspx?recordsFor=SingleRecord&RN=31023342

Palandri, J. L. & Kharaka, Y. K. (2004). A compilation of rate parameters of water-mineral interaction kinetics for application to geochemical modeling. U. S. Geological Survey Open File Report 2004-1068 (Vol. 1068). Retrieved from http://www.dtic.mil/cgi-bin/GetTRDoc?Location=U2&doc=GetTRDoc.pdf&AD=ADA440035

Parkhurst, D. L. 1995. User's guide to PHREEQC: A computer program for speciation, reaction-path, advective-transport, and inverse geochemical calculations, Water-Resources Investigations Report 95–4227. Technical report. U. S. Department of the Interior, U. S. Geological Survey, Lakewood, Colorado.

Parkhurst, D. L. & Appelo, C. A. J. 1999. User's Guide to PHREEQC (Version 2): A Computer Program for Speciation, Batch-Reaction, One-Dimensional Transport, and Inverse Geochemical Calculations. Technical report. Water-Resources Investigations Report 99–4259. U. S. Geological Survey, Denver, Colorado, USA.

Parkhurst, D. L. & Appelo, C. A. J. 2013. PHREEQC (Version 3)-A Computer Program for Speciation, Batch-Reaction, One-Dimensional Transport, and Inverse Geochemical Calculations. Modeling Techniques, Book 6. U. S. Department of the Interior, U. S. Geological Survey. Retrieved from http://pubs.usgs.gov/tm/06/a43/

Parkhurst, D. L., Torstenson, D. C. & Plummer, L. N. 1980. PHREEQE - A computer program for geochemical calculations. U. S. Geological Survey. Water-Resources Investigations Report 80–96.

Parkhurst, D. L., Torstenson, D. C. & Plummer, L. N. 1990. PHREEQE: A computer program for geochemical calculations. Technical report. U. S. Geological Survey. Water-Resources Investigations Report 80–96.

Peng, D.-Y. & Robinson, D. B. 1976. A New Two-Constant Equation of State. Industrial & Engineering Chemistry Fundamentals. 15 (1), 59–64. *doi:10.1021/i160057a011*

Peter, A., Lamert, H., Beyer, M., Hornbruch, G., Heinrich, B., Schulz, A., Geistlinger, H., Schreiber, B., Dietrich, P., Werban, U., Vogt, C., Richnow, H.-H., Großmann, J. & Dahmke, A. 2012. Investigation of the geochemical impact of CO_2 on shallow groundwater: Design and implementation of a CO_2 injection test in Northeast Germany. Environmental Earth Sciences. 67 (2), 335–349. *doi:10.1007/s12665-012-1700-5*

Petersen, S. & Hack, K. 2007. The thermochemistry library ChemApp and its applications. International Journal of Materials Research. 98 (10), 935–945. *doi:10.3139/146.101551*

Peterson, S. R., Opitz, B. E., Graham, M. J. & Eary, L. E. 1987. An overview of the geochemical code MINTEQ: Applications to Performance Assessment for Low-Level Wastes. Technical report. Pacifc Northwest Laboraty, Richland, WA, USA.

Pitzer, K. S. 1973. Termodynamics of electrolytes. I.Theoretical basis and general equations. The Journal of Physical Chemistry. 77 (2), 268–277. *doi:10.1021/j100621a026*

Pizarro, J. O. & Branco, C. 2012. Challenges in Implementing an EOR Project in the Pre-Salt Province in Deep Offshore Brasil. SPE EOR Conference at Oil and Gas West Asia. *doi:10.2118/155665-MS*

Postma, D., Boesen, C., Kristiansen, H. & Larsen, F. 1991. Nitrate Reduction in an Unconfned Sandy Aquifer: Water Chemistry, Reduction Processes, and Geochemical Modeling. Water Resources Research. 27 (8), 2027–2045. *doi:10.1029/91WR00989*

Pruess, K, Xu, T, Apps, J. & Garcia, J. 2003. Numerical modeling of aquifer disposal of CO_2. Society of Petroleum Engineers Journal. 8 (1), 12. *doi:10.2118/66537-MS*

Redlich, O. & Kwong, J. N. S. 1949. On the Termodynamics of Solutions. V. An Equation of State. Fugacities of Gaseous Solutions. Chemical Reviews. 44 (1), 233–244.

Reinmöller, M., Klinger, M., Schreiner, M. & Gutte, H. 2015. Relationship between ash fusion temperatures of ashes from hard coal, brown coal, and biomass and mineral phases under different atmospheres: A combined FactSage(TM) computational and network theoretical approach. Fuel. 151 (1 July 2015), 118–123. *doi:10.1007/s12665-012-1700-5*

Riddiford, F., Wright, I., Bishop, C., Espie, T. & Tourqui, A. 2005. Monitoring geological storage the In Salah Gas CO_2 storage project. Pages 1353–1359 of: Proceedings of the 7th International Conference on Greenhouse Gas Control Technologies. *doi:10.1016/B978-008044704-9/50149-X*

Rillard, J., Loisy, C., Le Roux, O., Cerepi, A., Garcia, B., Noirez, S., Rouchon, V., Delaplace, P., Willequet, O. & Bertrand, C. 2015. The DEMO-CO_2 project: A vadose zone CO_2 and tracer leakage field experiment. International Journal of Greenhouse Gas Control. 39 (August 2015), 302–317. *doi:10.1016/j.ijggc.2015.04.012*

Robinson, D. B., Peng, D.-Y. & Chung, S. Y.-K. 1985. The development of the Peng-Robinson equation and its application to phase equilibrium in a system containing methanol. Fluid Phase Equilibria. 24 (1–2), 25–41. *doi:10.1016/0378-3812(85)87035-7*

Rochelle, C. A., Czernichowski-Lauriol, I. & Milodowski, A. E. (2004). The impact of chemical reactions on CO_2 storage in geological formations: A brief review. Geological Society, London, Special Publications. 233 (1), 87–106. *doi:10.1144/GSL.SP.2004.233.01.07*

Rubin, E. S, Rao, A. B. & Chen, C. 2005. Comparative Assessments of Fossil Fuel Power Plants with CO_2 Capture and Storage. Pages 1–9 of: Proceedings of the 7th International Conference on Greenhouse Gas Control Technologies (GHGT-7), Vol. 1.

Schäfer, D., Hagrey, S. A., Auken, E., Bahr, A., Beyer, M., Dahmke, A., Dumke, I., Foged, N., Furche, M., Gräber, M., Großmann, J., Helkjaer, M., Köber, R., Poggenburg, J., Naue, G., Schlömer, S., Seeger, C., Tischer, L., Vidal, A., Wiegers, C. & Wöhrl, C. 2013. Environmental and Process Monitoring. Pages 131–167 of: Kühn, M. & Münch, U. (eds), CLEAN – CO_2 Large-Scale Enhanced Gas Recovery in the Altmark Natural Gas Field - GEOTECHNOLOGIEN Science Report No. 19. Advanced Technologies in Earth Sciences. Berlin: Springer Verlag.

Setschenow, M. 1892. Action de l'acide carbonique sur les solutions des sels a acides fort. Annales de Chimie et des Physique. 25, 226–270.

Siemon, B., Christiansen, A. V. & Auken, E. 2009. A review of helicopter-borne electromagnetic methods for groundwater exploration. Near Surface Geophysics. 7 (5-6), 629–646. *doi:10.3997/1873-0604.2009043*

Siemon, B. 2013. http://www.bgr.bund.de/DE/Themen/GG_Geophysik/Aerogeophysik/Aeroelektromagnetik/aeroelektromagnetik_node.html. Accessed on 15th March 2014. Aeroelektromagnetik: Erfassung der Leitfähigkeit des oberflächennahen Untergrunds aus der Luft. Bundesgesellschaft für Geowissenschaften und Rohstoffe (BGR).

Shiraki, R. & Dunn, T. L. 2000. Experimental study on water-rock interactions during CO_2 flooding in the Tensleep Formation, Wyoming, USA. Applied Geochemistry. 15 (3), 265–279. *doi:10.1016/S0883-2927(99) 00048-7*

Smith, D. S., Adams, N. W. H. & Kramer, J. R. 1999. Resolving uncertainty in chemical speciation determinations. Geochimica et Cosmochimica Acta. 63 (19–20), 3337–3347. *doi:10.1016/S0016-7037(99)00255-0*

Smyth, R. C., Hovorka, S. D., Lu, J., Romanak, K. D., Partin, J. W., Wong, C. & Yang, C. 2009. Assessing risk to fresh water resources from long term CO_2 injection-laboratory and feld studies. Energy Procedia. 1 (1), 1957–1964. *doi:10.1016/j.egypro.2009.01.255*

Suekane, T., Nobuso, T., Hirai, S. & Kiyota, M. 2008. Geological storage of carbon dioxide by residual gas and solubility trapping. International Journal of Greenhouse Gas Control. 2 (1), 58–64. *doi:10.1016/S1750-5836(07)00096-5*

Svensson, U. & Dreybrodt, W. 1992. Dissolution kinetics of natural calcite minerals in CO_2-water systems approaching calcite equilibrium. Chemical Geology. 100 (1–2), 129–145. *doi:10.1016/0009-2541(92)90106-F*

Steefel, C. I., DePaolo, D. J. & Lichtner, P. C. 2005. Reactive transport modeling: An essential tool and a new research approach for the Earth sciences. Earth and Planetary Science Letters. 240 (3–4), 539–558. *doi:10.1016/j.epsl.2005.09.017*

Steefel, C. I., Appelo, C. A. J., Arora, B., Jacques, D., Kalbacher, T., Kolditz, O., Lagneau, V., Lichtner, P. C., Mayer, K. U., Meeussen, J. C. L., Molins, S. Moulton, D., Shao, H., Šimůnek, J., Spycher, N., Yabusaki, S. B. & Yeh, G. T. 2014. Reactive transport codes for subsurface environmental simulation. Computational Geosciences. 19 (3), 445–478. *doi: 10.1007/s10596-014-9443-x*

Stéphenne, K. 2014. Start-Up of World's First Commercial Post-Combustion Coal Fired CCS Project: Contribution of Shell Cansolv to SaskPower Boundary Dam ICCS Project. Energy Procedia. 63 (2014), 6106–6110. *doi:10.1016/j.egypro.2014.11.642*

Tambach, T. J., Koenen, M., Wasch L. J. & van Bergen, F. 2015. Geochemical evaluation of CO_2 injection and containment in a depleted gas field. International Journal of Greenhouse Gas Control. 32 (January 2015), 61–80. *doi:10.1016/j.ijggc.2014.10.005*

Tans, P. & Keeling, C. D. 2015. http://www.esrl.noaa.gov/gmd/ccgg/trends/. Accessed on 24th of June 2015. Last updated on 5th of June 2015. Trends in atmospheric carbon dioxide: Recent Monthly Average Mauna Loa CO_2. Earth System Research Laboratory (Global Greenhouse Gas Reference Network).

Tomas, M. W., Stewart, M., Trotz, M. & Cunningham, J. A. 2012. Geochemical modeling of CO_2 sequestration in deep, saline, dolomitic-limestone aquifers: Critical evaluation of thermodynamic sub-models. Chemical Geology. 306-307 (May), 29–39. *doi:10.1016/j.chemgeo.2012.02.019*

Torp, T. A. & Gale, J. 2004. Demonstrating storage of CO_2 in geological reservoirs: The Sleipner and SACS projects. Energy. 29 (9–10), 1361–1369. *doi:10.1016/j.energy.2004.03.104*

Trautz, R. C., Pugh, J. D., Varadharajan, C., Zheng, L., Bianchi, M., Nico, P. S., Spycher, N. F., Newell, D. L., Esposito, R. A., Wu, Y., Dafflon, B., Hubbard, S. S. & Birkholzer, J. T. 2013. Effect of dissolved CO_2 on a shallow groundwater system: A controlled release field experiment. Environmental Science & Technology. 47 (1), 298–305. *doi:10.1021/es301280t*

Truesdell, A. H. & Jones, B. F. 1974. WATEQ, a computer program for calculating chemical equilibria of natural waters. Technical report. Lawrence-Livermore National Laboratory, Livermore, California.

Tutolo, B. M., Luhmann, A. J., Kong, X.-Z., Saar, M. O. & Seyfried, W. E. 2015. CO_2 sequestration in feldspar-rich sandstone: Coupled evolution of fluid chemistry, mineral reaction rates, and hydrogeochemical properties. Geochimica et Cosmochimica Acta. 160 (1 July 2015), 132–154. *doi:10.1016/j.gca.2015.04.002*

van Berk, W. & Hansen, C. 2006. Hydrogeochemische Stoffussmodelle: Leitfaden zur Modellierung der Beschaffenheitsentwicklung von Grund- und Rohwässern (German Edition). Berlin: Springer.

van Berk, W. & Wisotzky, F. 1995. Sulfide oxidation in brown coal overburden and chemical modeling of reactions in aquifers influenced by sulfide oxidation. Environmental Geology. 26 (3), 192–196. *doi:10.1007/BF00768742*

van Berk, W., Ilger, J.-M., Fu, Y. & Hansen, C. 2011. Decreasing CO_2 partial pressure triggered Mg-Fe-Ca carbonate formation in ancient Martian crust preserved in the ALH84001 Meteorite. Geofluids. 11 (1), 6–17. *doi:10.1111/j.1468-8123.2010.00296.x*

van Berk, W., Fu, Y. & Schulz, H.-M. 2014. Creation of pre-oil-charging porosity by migration of source-rock-derived corrosive fluids through carbonate reservoirs: One-dimensional reactive mass transport modelling. Petroleum Geoscience. 21 (1), 35–42. *doi:10.1144/petgeo2014-065*

van der Meer, L. G. H. 1992. Investigations regarding the storage of carbon dioxide in aquifers in the Netherlands. Energy Conversion and Management. 33 (5-8), 611–618. *doi:10.1016/0196-8904(92)90063-3*

van Eldik, R. & Palmer, D. A. 1982. Effects of pressure on the kinetics of the dehydration of carbonic acid and the hydrolysis of CO_2 in aqueous solution. Journal of Solution Chemistry. 11 (5), 339–346. *doi:10.1007/BF00649292*

van Zeggeren, F. & Storey, S. H. 1970. The Computation of Chemical Equilibria. Cambridge: Cambridge University Press.

Varadharajan, C., Tinnacher, R. M., Pugh, J. D., Trautz, R. C., Zheng, L., Spycher, N. F., Birkholzer, J. T., Castillo-Michel, H., Esposito, R. A. & Nico, P. S. 2013. A laboratory study of the initial effects of dissolved carbon dioxide (CO_2) on metal release from shallow sediments. International Journal of Greenhouse Gas Control. 19 (November 2013) 183–211. *doi:10.1016/j.ijggc.2013.08.017*

Walter, L., Binning, P. J. & Class, H. 2013. Predicting salt intrusion into freshwater aquifers resulting from CO_2 injection – A study on the influence of conservative assumptions. Advances in Water Resources. 62,

Part C (December 2013), 543–554. *doi:10.1016/j.advwatres.2013.09.017*

Wang, S. & Jaffe, P. R. 2004. Dissolution of a mineral phase in potable aquifers due to CO_2 releases from deep formations; effect of dissolution kinetics. Energy Conversion and Management. 45 (18), 2833–2848. *doi:10.1016/j.enconman.2004.01.002*

Watson, T. L., & Bachu, S. 2009. Evaluation of the potential for gas and CO_2 leakage along wellbores. E&P Environmental and Safety Conference, 5-7 March, Galveston, Texas, U.S.A. pp 11–1. *doi:10.2118/106817-MS*

Weiss, R. F. F. 1974. Carbon dioxide in water and seawater: The solubility of a non-ideal gas. Marine Chemistry. 2 (3), 203–215. *doi:10.1016/0304-4203(74)90015-2*

White, C. M., Strazisar, B. R., Granite, E. J., Hofman, J. S. & Pennline, H. W. 2003. Separation and Capture of CO_2 from Large Stationary Sources and Sequestration in Geological Formations—Coalbeds and Deep Saline Aquifers. Journal of the Air & Waste Management Association. 53(6), 645–715. *doi:10.1080/10473289.2003.10466206*

White, D. 2009. Monitoring CO_2 storage during EOR at the Weyburn-Midale Field. The Leading Edge. 28 (7), 838–842. *doi:10.1190/1.3167786*

White, W. B., Johnson, S. M. & Dantzig, G. B. 1958. Chemical Equilibrium in Complex Mixtures. The Journal of Chemical Physics. 28 (5), 751. *doi: 10.1063/1.1744264*

Whittaker, S., Rostron, B., Hawkes, C., Gardner, C., White, D., Johnson, J., Chalaturnyk, R. & Seeburger, D. 2011. A decade of CO_2 injection into depleting oil fields: Monitoring and research activities of the IEA GHG Weyburn-Midale CO_2 Monitoring and Storage Project. Energy Procedia, 4 (2011), 6069–6076. *doi:10.1016/j.egypro.2011.02.612*

Wilkin, R. T. & Digiulio, D. C. 2010. Geochemical impacts to groundwater from geologic carbon sequestration: controls on pH and inorganic carbon concentrations from reaction path and kinetic modeling. Environmental Science & Technology. 44 (12), 4821–7. *doi:10.1021/es100559j*

Wilkinson, M., Haszeldine, R.S., Fallick, A. E., Odling, N., Stoker, S. J. & Gatlif, R. W. 2009. CO_2-Mineral Reaction in a Natural Analogue for CO_2 Storage-Implications for Modeling. Journal of Sedimentary Research. 79 (7), 486–494. *doi:10.2110/jsr.2009.052*

Wolery, T. J. 1992. EQ3/6, A Sofware Package for Geochemical Modeling of Aqueous Systems: Package Overview and Installation Guide (Version 7.0).

Wolery, T. W., & Jarek, R. L. 2003. Sofware User's Manual: EQ3/6, Version 8.0.

Worden, R. H. 2006. Dawsonite cement in the Triassic Lam Formation, Shabwa Basin, Yemen: A natural analogue for a potential mineral product of subsurface CO_2 storage for greenhouse gas reduction. Marine and Petroleum Geology. 23 (1), 61–77. *doi:10.1016/j.marpetgeo.2005.07.001*

Wright, I. W. 2007. The In Salah Gas CO_2 Storage Project. International Petroleum Technology Conference, IPTC 2007.

Xie, M., Kolditz, O. & Moog, H. C. 2011. A geochemical transport model for thermo-hydro-chemical (THC) coupled processes with saline water. Water Resources Research. 47 (W02545), 1–14. *doi:10.1029/2010WR009270*

Xu, T., Gerard, F., Pruess, K., & Brimhall, G. 1997. Modeling non-isothermal multiphase multi-species reactive chemical transport in geologic media. Technical report LBNL-40504. Berkeley, California, USA. *doi:10.2172/589221*

Xu, T., Apps, J. A. & Pruess, K. 2003 a. Reactive geochemical transport simulation to study mineral trapping for CO_2 disposal in deep arenaceous formations. Journal of Geophysical Research. 108 (B2),13. *doi:10.1029/2002JB001979*

Xu, T., Sonnenthal, E., Spycher, N. & Pruess, K. 2003 b. TOUGHREACT: A New Code of the TOUGH Family for Non-isothermal Multiphase Reactive Geochemical Transport in Variably Saturated Geologic Media. Technical report. Lawrence Berkeley National Laboratory, University of California, Berkeley, California, USA.

Xu, T., Apps, J. A. & Pruess, K. 2001. Analysis of Mineral Trapping for CO_2 Disposal in Deep Aquifers. Technical report. Lawrence Berkeley National Laboratory, Berkeley, California.

Xu, T., Apps, J. A. & Pruess, K. 2005. Mineral sequestration of carbon dioxide in a sandstone-shale system. Chemical Geology. 217 (3-4), 295–318. *doi:10.1016/j.chemgeo.2004.12.015*

Yang, H., Xu, Z., Fan, M., Gupta, R., Slimane, R. B., Bland, A. E. & Wright, I. 2008. Progress in carbon dioxide separation and capture: A review. Journal of Environmental Sciences. 20 (1), 14–27. *doi:10.1016/S1001-0742(08)60002-9*

Yu, Z., Liu, L., Yang, S., Li, S. & Yang, Y. 2012. An experimental study of CO_2-brine-rock interaction at in situ pressure-temperature reservoir conditions. Chemical Geology. 326-327 (9 October 2012), 88–101. *doi:10.1016/j.chemgeo.2012.07.030*

Yu, Z., Liu, L., Liu, K., Yang, S. & Yang, Y. 2015. Petrological characterization and reactive transport simulation of a high-water-cut oil reservoir in the Southern Songliao Basin, Eastern China for CO_2 sequestration. International Journal of Greenhouse Gas Control 37 (2015), 191–212. *doi: 10.1016/j.ijggc.2015.03.021*

Zeleznik, F. J. & Gordon, S. 1960. An analytical investigation of three general methods of calculating chemical-equilibrium compositions. Technical report. NASA TN D–473.

Zeleznik, F. J. & Gordon, S. 1968. Calculation of Complex Chemical Equilibria. Industrial and Engineering Chemistry. 60 (6), 27–57. *doi:10.1021/ie50702a006*

Zeleznik, F. J. 1962. Calculation of Detonation Properties and Efect of Independent Parameters on Gaseous Detonations. American Rocket Society Journal. 32 (4), 606–615. *doi:10.2514/8.6080*

Zhang, S., DePaolo, D. J., Xu, T. & Zheng, L. 2013. Mineralization of carbon dioxide sequestered in volcanogenic sandstone reservoir rocks. International Journal of Greenhouse Gas Control. 18 (October 2013), 315–328. *doi:10.1016/j.ijggc.2013.08.001*

Zheng, L., Apps, J. A., Zhang, Y., Xu, T. & Birkholzer, J. T. 2009 a. On mobilization of lead andarsenic in groundwater in response to CO_2 leakage from deep geological storage. Chemical Geology. 268 (3–4), 281–297. *doi:10.1016/j.chemgeo.2009.09.007*

Zheng, L., Apps, J. A., Zhang, Y., Xu, T. & Birkholzer, J. T. 2009 b. Reactive transport simulations to study groundwater quality changes in response to CO_2 leakage from deep geological storage. Energy Procedia. 1 (1), 1887–1894. *doi:10.1016/j.egypro.2009.01.246*

Zheng, L., Apps, J. A., Spycher, N., Birkholzer, J. T., Kharaka, Y. K., Tordsen, J., Beers, S. R., Herkelrath, W. N., Kakouros, E. & Trautz, R. C. 2012. Geochemical modeling of changes in shallow groundwater chemistry observed during the MSU-ZERT CO_2 injection experiment. International Journal of Greenhouse Gas Control. 7 (March 2012), 202–217. *doi:10.1016/j.ijggc.2011.10.003*

Zhu, Q., Li, X., Jiang, Z. & Wei, N. 2015. Impacts of CO_2 leakage into shallow formations on groundwater chemistry. Fuel Processing Technology. 135 (July 2015), 162–167. *doi:10.1016/j.fuproc.2014.11.042*

Zweigel, P., Arts, R., Lothe, A. E. & Lindeberg, E. B. G. 2004. Reservoir geology of the Utsira Formation at the first industrial-scale underground CO_2 storage site (Sleipner area, North Sea). Geological Society, London, Special Publications. 233 (1), 165–180. *doi:10.1016/j.ijggc.2009.10.016*

Zwingmann, N., Mito, S., Sorai, M. & Ohsumi, T. 2005. Preinjection Characterisation and Evaluation of CO_2 Sequestration Potential in the Haizume Formation, Niigata Basin, Japan. Geochemical Modelling of Water-Minerals-CO_2 Interaction. Oil & Gas Science and Technology. 60 (2), 249–258. *doi:10.2516/ogst:2005015*

2. Uncertainty in geochemical modelling of CO_2 and calcite dissolution in NaCl solutions due to different modelling codes and thermodynamic databases

Christoph Haase*[1], Frank Dethlefsen[1], Markus Ebert[1], Andreas Dahmke[1]

[1] Kiel University, Institute of Geosciences, Ludewig-Meyn-Straße 10, 24118 Kiel, Germany

Published in Applied Geochemistry (Editor: R. Fuge) *doi:10.1016/j.apgeochem.2013.03.001*
Article history: Received 6 September 2012, Accepted 1 March 2013

Abstract

A prognosis of the geochemical effects of CO_2 storage induced by the injection of CO_2 into geologic reservoirs or by CO_2 leakage into the overlaying formations can be performed by numerical modelling (non-invasive) and field experiments. Until now the research has been focused on the geochemical processes of the CO_2 reacting with the minerals of the storage formation, which mostly consists of quartzitic sandstones. Regarding the safety assessment the reactions between the CO_2 and the overlaying formations in the case of a CO_2 leakage are of equal importance as the reactions in the storage formation. In particular, limestone formations can react very sensitively to CO_2 intrusion. The thermodynamic parameters necessary to model these reactions are not determined explicitly through experiments at the total range of temperature and pressure conditions and are thus extrapolated by the simulation code. The differences in the calculated results lead to different calcite and CO_2 solubilities and can influence the safety issues. This uncertainty study is performed by comparing the computed results, applying the geochemical modelling software codes The Geochemist's Workbench, EQ3/6, Phreeqc and FactSage/ChemApp and their thermodynamic databases. The input parameters (1) total concentration of the solution, (2) temperature and (3) fugacity are varied within typical values for CO_2 reservoirs, overlaying formations and close-to-surface aquifers. The most sensitive input parameter in the system H_2O-CO_2-NaCl-$CaCO_3$ for the calculated range of dissolved calcite and CO_2 is the fugacity of CO_2. Hence, the largest range of dissolved calcite is calculated at high fugacities and is 210 mmol/kgw. The average deviation of the results using the databases *phreeqc.dat* and *wateq4f.dat* in combination with the code Phreeqc is lowest in comparison to the results of the specific model of Duan and Li, which represents the experimental values at best. Still, the solubility of CO_2 is overestimated in the formation water using these two databases. Therefore, the model results calculate a larger retention capacity, defined as the quantity of CO_2 dissolved in the formation water, than the Duan and Li model would do.

* corresponding author

2.1 Introduction

2.1.1 Scope of the work

The storage of CO_2 in deep saline aquifers is a technology to reduce CO_2 emissions into the atmosphere to abate global warming. The injection of CO_2 into a geological reservoir leads to geochemical reactions between CO_2, groundwater and the mineral phases in the subsurface. The calculation of the amount of dissolved CO_2 in the aqueous phase is important to predict the CO_2 distribution and the CO_2 capacity of a reservoir in terms of the hydrodynamic trapping of CO_2. The dissolution of silicates and subordinately of carbonates is important for predicting the effects of the CO_2 storage on the geologic formation and the quantification of mineral trapping processes. Furthermore, in the case of a CO_2 leakage the retention and transfer formations overlaying the storage formation can hold back the CO_2 through dissolution, whereby it is prevented from migrating into aquifers used for drinking water supply or into the atmosphere (Großmann et al., 2011; Dethlefsen et al., 2013). The retention capacity of the overlaying formations is the maximum quantity of CO_2 dissolved in the aqueous phase in the formation. Through the leakage of CO_2 into near-surface aquifers, the consequential groundwater acidification can be attenuated by the dissolution of carbonates like calcite. In this way, the calculation of the amounts of dissolved CO_2 and calcite in the storage, retention and transfer formations as well as in near-surface aquifers is especially important for an effective risk assessment based on the use of geochemical models.

The aim of the study is to evaluate the range of the calculated amounts of the dissolved phases, calcite and CO_2, applying different model codes and thermodynamic databases, whereby the calculation uncertainty is quantified. Thereupon, statements are made about the reliability of the calculation of the CO_2 capacity of the storage formation, the retention capacity and the risk assessment in the case of a CO_2 leakage. Therefore, a very simple geochemical model including CO_2 and calcite dissolution applying the pressure and temperature range to be expected in the reservoir, intermediate depths and in near-surface aquifers is set up in this study. The simple model includes only the equilibrium calculation between the aqueous solution, calcite and gaseous CO_2 and neglects, for instance, sorption processes, sulfate complexes, kinetic reactions and transport processes.

The results produced by using the geochemical modelling software packages PHREEQC, EQ3/6, THE GEOCHEMIST'S WORKBENCH, and FACTSAGE/CHEMAPP in combination with the provided 30 thermodynamic databases are compared at various pressure and temperature conditions (Tables 2.2 and 2.3). The databases differ in the included gas phases, mineral phases and aquatic species, as well as in the thermodynamic parameters for the equilibrium reactions. The model codes using the thermodynamic databases can be divided into two groups, which apply either the law of mass action approach (LMA) or the Gibbs energy minimization approach (GEM). Applying different databases at temperature and pressure conditions near the surface can lead to uncertainties in the dimension of one order of magnitude (Denison and Garnier-Laplace, 2005). However, at near-surface conditions the standard databases of PHREEQC *phreeqc.dat* and *wateq4f.dat* are validated for modelling geochemical reactions (Appelo et al., 1990; 1998).

2.1.2 Uncertainties in geochemical modelling

The sources of the uncertainties in geochemical modelling are distinguished after Ekberg (1999) into the three categories thermodynamic data, formation water composition, and the conceptual model.

In contrast, Beck (1987) groups the problems of prediction into four main categories, which are: the model structure, the estimated model parameter values, design of the experiments to calibrate the model, and the propagation of prediction errors. The main categories are classified in this work into (a) the model approach, (b) the thermodynamic data, and (c) the input parameters for the model.

The model approach was identified as the most important factor for uncertainties in the calculated solubilities by Ekberg (1999), but it is difficult to quantify the uncertainties arising from the model approach due to the dependence on the modeller. Smith et al. (1999) also indicate a need of uncertainty assessment for the system definition. Nitzsche et al. (2000), for example, investigated the uncertainties due to different thermodynamic databases for the U speciation by reactive transport modelling and observed a range of several orders of magnitude in the model results. Criscenti et al. (1996), Bassett and Melchior (1990) and Dethlefsen et al. (2012) also attribute a large impact to the uncertainty of the thermodynamic databases. Criscenti et al. (1996) evaluated the uncertainties arising from thermodynamic databases by sensitivity analyses in the predicted pH value. Uncertainties arising from the input parameters were also evaluated by Criscenti et al. (1996). The authors defined significant key parameters that require precise measurement and thus give guidance on the collection of field data.

The physical and chemical conditions in CO_2 reservoirs and overlaying retention formations, which include solutions with ionic strength of up to 6 mol/kgw, pressures up to 300 bars and temperatures up to 150 °C, are beyond the validity range of these established geochemical software codes and their databases causing the expected uncertainties to be even higher than at near-surface conditions. However, these databases have been applied for modelling the impact of CO_2 storage and leakage on geologic formations (Carroll et al., 2011; Gaus et al., 2005; Gundogan et al., 2011) as the databases, which are valid at high ionic strength, do not include the required elements and minerals, i. e. the Pitzer database does not include Si and Al. Furthermore, the Pitzer database is not valid at temperatures higher than 25 °C. In conclusion, a database valid for all conditions of deep saline formations does not exist.

The databases including the LMA approach incorporate mainly the Debye-Hückel theory offering the largest number of species and phases available for the calculation of equilibrium reactions. The application of the databases including the Debye-Hückel theory to model geochemical reactions at conditions in a CO_2 reservoir or in a CO_2 leakage scenario has not been validated against field or experimental data, rather the application of the Pitzer databases is recommended due to their validity at high ionic strengths. However, the virial coefficients used in the Pitzer equations are only determined at 25 °C (Pitzer and Mayorga, 1973; Kim and Frederick, 1988a, b) and are then extrapolated to higher temperatures. Furthermore, the limited number of elements in the Pitzer database restricts this approach to simple systems, as the parameters are not available for instance for Al and Si, what makes the calculation of silicate dissolution impossible. Still the calculation results using the Pitzer approach can be compared to the results using the Debye-Hückel theory in the case of CO_2 and calcite dissolution.

The *sit.dat* database of PHREEQC is based on the specific ion interaction theory (Brönsted, 1922; Scatchard, 1936; Guggenheim and Turgeon, 1955) and the database can calculate activity coefficients at high concentrations of the solute. The theory has been tested up to a concentration of 3 mol/kg (Elizalde, 1995). The theory requires interaction coefficients, but not as much as the Pitzer approach. Using a different approach, Duan et al. (2006) and Duan and Li (2008) developed an even more specific model for calculating equilibrium concentrations in the H_2O-CO_2-NaCl-$CaCO_3$ system

Tabelle 2.1
Software and the 30 provided databases including different activity models depending on the database.

Activity model	PHREEQC	EQ3/6	THE GEOCHEMIST'S WORKBENCH	FACTSAGE
	Law of mass action approach (LMA)			Gibbs energy minimization (GEM)
Ion dissociation	*phreeqc.dat*	*data0.cmp*	*thermo_phreeqc.dat*	*Fact*
	wateq4f.dat	*data0.skb*	*thermo_wateq4f.dat*	*Fact53*
	minteq.dat	*data0.shv*	*thermo_minteq.dat*	*FT_Helg_AQDH*
	minteq.v4.dat	*data0.sup*	*thermo.dat*	*FT_Helg_AQID*
	llnl.dat	*data0.ymp*	*thermo.com.v8.r6+.dat*	*FT_Helg_AQDD*
Ion association	*pitzer.dat*	*data0.hmw*	*thermo_phrqpitz.dat*	*Fact-Pitz*
	sit.dat	*data0.ypf*	*thermo_hmw.dat*	
		data0.pit	*thermo_hdata.dat*	
			thermo_pitzer.dat	

and producing modelling results in excellent agreement with experimental data (Duan and Li, 2008). However, this model is restricted to this four component system, so that it cannot replace the application of the geochemical model codes mentioned earlier. Still the model of Duan and Li (2008) can serve as a reference in the discussed system, especially for the amount of dissolved CO_2.

2.2 Methods

2.2.1 Software and databases

The geochemical software packages THE GEOCHEMIST'S WORKBENCH, EQ3/6, PHREEQC and FACTSAGE/CHEMAPP were applied for the uncertainty analyses in this study (Table 2.1). PHREEQC is widely used in geochemical reaction modelling (Zhu et al., 2003; Hansen and van Berk, 2004; Postma et al., 2007), THE GEOCHEMIST'S WORKBENCH is a recently developed software package (Bethke, 2008), EQ3/6 was developed for radioactive waste disposal (Wolery, 1992), and CHEMAPP (Eriksson and Königsberger, 2008) was originally developed to calculate phase equilibria in metallurgical processes (Tanaka et al., 2000) and has applied recently to geochemical modelling in hydrogeology (Li and Bauer, 2009; Xie et al., 2011). The library CHEMAPP (Petersen and Hack, 2007) provides the thermodynamic data for the tool FACTSAGE, which is operated via the graphical user interface. The module Equilib includes the FACTSAGE Gibbs energy minimizer (Eriksson and Königsberger, 2008).

All these software packages except FACTSAGE are based on a calculation method to resolve systems of equations, which are based on the law of mass action (Table 2.1). The law of mass action approach (LMA) was compared to the Gibbs energy minimization approach (GEM) to gain the state of equilibrium, which is used by FACTSAGE (Karpov et al., 1997). The two methods are regarded as mathematically equivalent (Zeleznik and Gordon, 1968). FACTSAGE using the *Fact* and *Fact53* databases, however, is only based on the calculation of the molality. The activity is set to unity by the code.

The thermodynamic data for the geochemical reactions are provided in databases, which are available as ASCII text files (Table 2.2). The databases contain geochemical reactions, associated equilibrium

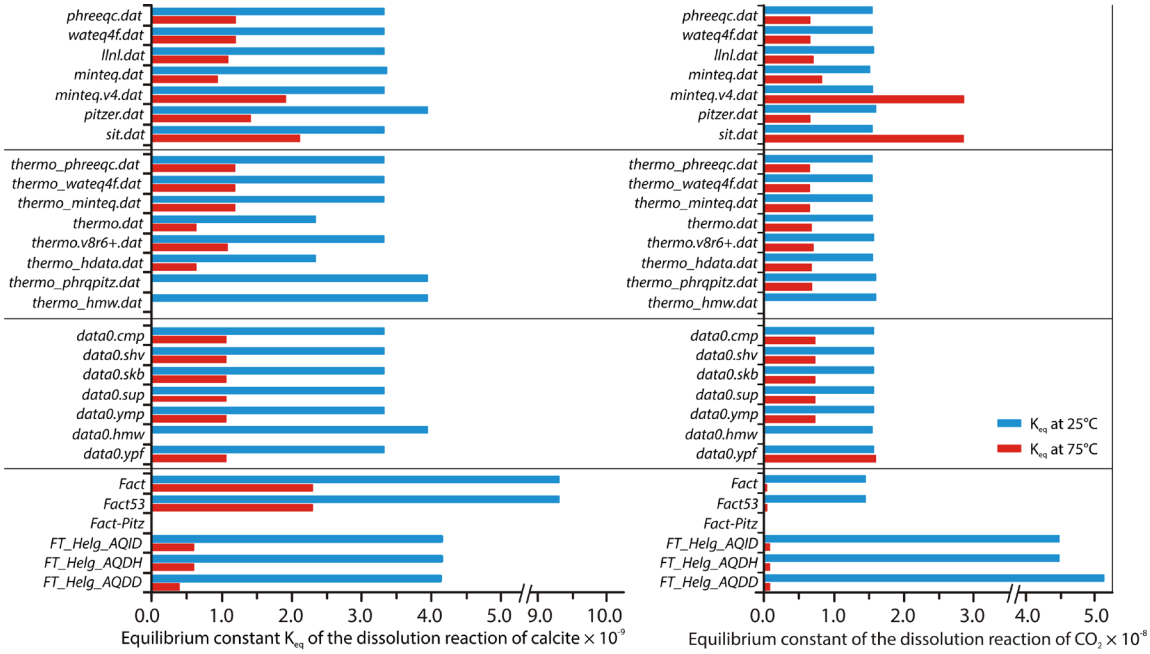

Figure 2.1
Equilibrium constants of the calcite and CO_2 dissolution reaction at 25 °C and 75 °C of all applied databases. The data of the *Fact-Pitz* database was not accessible.

constants and parameters for the activity calculation of the species. The thermodynamic data included in the databases has been collected usually through experiments performed at standard conditions. To apply the models to CO_2 storage scenarios the data has to be extrapolated to the site specific conditions by built-in algorithms, which can lead to increasing uncertainties.

Firstly, when extrapolating the data in terms of temperature the codes use the Van't Hoff method, an empirical analytical function, a temperature grid, or an equation of state. These methods result

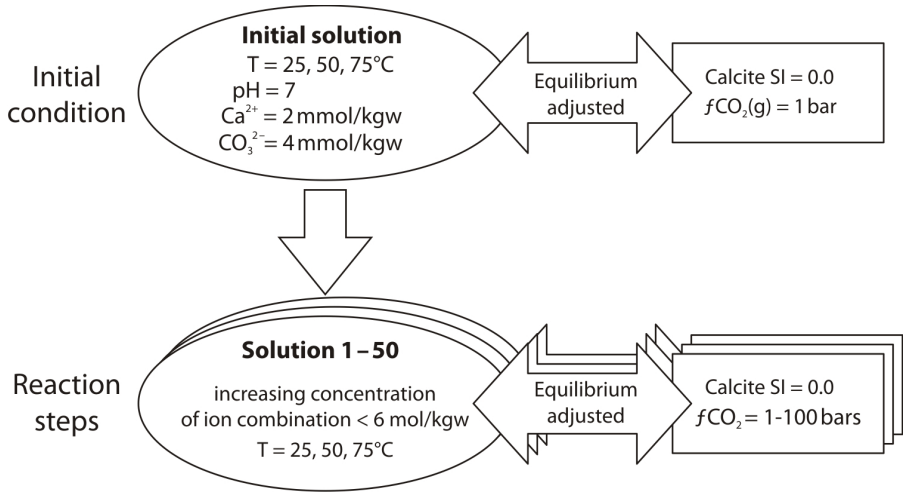

Figure 2.2
Scheme of the thermodynamic model setup with the initial conditions and the reaction steps. The steps include the equilibration with calcite and the fugacity of CO_2.

Table 2.2
Limitations of the databases concerning ionic strength (I), temperature (T) and the contained elements and aqueous complexes. Numbers mark databases including thermodynamic data from the same source.

Database	I (mol/L)	T (°C)	Elements	Aqueous complexes with Na, Cl, C, Ca	Special issues/source of data
phreeqc.dat[1]	<1.0	100	27	5	Valid at higher ionic strength in NaCl dominated solutions
wateq4f.dat[2]	<1.0	100	36	5	Valid at higher ionic strength in NaCl dominated solutions
minteq.dat[3]	<0.1	100	73	5	Data from Visual Minteq
minteq.v4.dat[3]	<0.1	100	72	5	Data from Minteq
llnl.dat[4]	300	89	7		Based on data from Lawrence Livermore National Lab, data from *thermo.com.V8.R6.230*
pitzer.dat[5]	<10	100	16	1	Data from Pitzer (1973) and Pitzer and Mayorga (1974)
sit.dat	<10	100	65	5	Corresponding to ThermoChimie v.7.b
data0.cmp[4]	<1.0	300	81	9	
data0.skb[4]	<1.0	300	81	9	
data0.shv	<1.0	300	63	7	
data0.sup	<1.0	300	69	7	SUPCRT92 data
data0.ymp	<1.0	200	86 (with Si and Al)	9	Data from Yucca-Mountain-Project
data0.hmw[6]	<10	25	9	1	Harvie–Møller–Weare activity model (Harvie et al., 1984)
data0.ypf	<10	200	26 (with Si and Al)	3	Data from Yucca-Mountain-Project
data0.pit[5]	<10	100	52 (with Al, without C)	1	
thermo_phreeqc.dat[1]	<1.0	100	25	5	Based on *phreeqc.dat*
thermo_wateq4f.dat[2]	<1.0	100	35	5	Based on *wateq4f.dat*
thermo_minteq.dat[3]	<0.1	100	75	7	Based on *minteq.dat*
thermo.dat[4]	300	46	8		Based on dataset of Delany, (1986)
thermo.com. v8.r6+.dat[4]	300	81	9		Based on LLNL V8 R6 dataset from 1996 (*data0.cmp*), includes more radionuclides and organic species
thermo_phrqpitz.dat[5]	<10	300	16	1	Based on the *phrqpitz.dat* file
thermo_hmw.dat[6]	<10	25	9	1	Harvie–Møller–Weare activity model
thermo_pitzer.dat[5]	<10	300	30 (with Al, without C)	1	Based on *data0.pit* from 1986; dataset is outdated
thermo_hdata.dat	<10	300	10 (with Si)		Based on *data0.hmw* from 1986; dataset is outdated
Fact[7]	–		79	1	FACT Database Consortium Project
Fact53[7]	–		79	1	FACT Database Consortium Project
FT_Helg_AQID[8]	0.001	350	49	7	165 bar GEOPIG-SUPCRT data (Aqueous Helgeson ideal dilute solution)
FT_Helg_AQDH[8]	0.02	350	49	7	165 bar GEOPIG-SUPCRT data (Debye-Hückel equation)
FT_Helg_AQDD[8]	0.5	350	49	7	165 bar GEOPIG-SUPCRT data (Extended Debye–Hückel equation)
Fact-Pitz[5]	<10			0	

in different outputs based on the same thermodynamic data. The majority of the databases are valid up to temperatures of 100 °C (Table 2.2). Despite this limitation the databases have to be applied to models including formation waters of CO_2 storage sites with higher temperatures as there are no available databases including the required elements.

Secondly, the extrapolation of the data in terms of concentration will be performed by using different activity models for those software packages incorporating the equilibrium constant approach. The activity is calculated according to the ion dissociation and ion association approach. The equations used to calculate activities applying the ion dissociation approach are the Davies equation, Debye-Hückel equation, and extended Debye-Hückel as well as the WATEQ Debye-Hückel equation. If databases incorporating the Pitzer formalism (Pitzer, 1973) are applied a large number of equations with experimentally determined virial-coefficients have to be solved, which is referred to as ion interaction approach. The validity of the Debye-Hückel expression is limited to an ionic strength of 0.7 mol, which is in the range of seawater (Parkhurst and Appelo, 1999). In NaCl-dominated solutions the range can be higher through the use of an ionic strength term included in the WATEQ Debye-Hückel equation of PHREEQC (Truesdell and Jones, 1974). At higher ionic strength the Debye-Hückel theory is not valid (Merkel and Planer-Friedrich, 2008). However, databases that incorporate the ion interaction approach are valid at ionic strength up to 6 mol/kgw (Pitzer and Mayorga, 1973). Therefore, the majority of the databases is only valid up to the low ionic strength of 1.0 mol/L, but despite these restrictions these databases have been applied to CO_2 storage models (i. e. Gaus et al., 2005; Ketzer et al., 2009; Bildstein et al., 2010; Gundogan et al., 2011).

Thirdly, when modelling CO_2 storage the CO_2 solubilities have to be calculated at high CO_2 fugacities. The calculation of the solubility of gases in the aqueous solution is done by using Henry's law. The law describes the solubility of gases in an ideal solution to be proportional to the partial pressure neglecting the non-ideal behaviour of the CO_2 gas. The partial pressure can be corrected to the effective pressure by calculating the fugacity coefficient. The databases include the constants for Henry's law to calculate the solubility of gases.

The four software packages THE GEOCHEMIST'S WORKBENCH, EQ3/6, PHREEQC and FACTSAGE/CHEMAPP include 30 databases, which are all applied in this study (Table 2.2); 18 of these databases, such as *wateq4f.dat* and *phreeqc.dat*, incorporate the theory of ion dissociation (Tables 2.1 and 2.2). Nine databases use the Pitzer formalism (Pitzer, 1973) and the database *sit.dat* of PHREEQC incorporates the Specific Ion Interaction Theory (Guggenheim and Turgeon, 1955) to calculate the activity. The databases *Fact* and *Fact53* set the activity to unity. Some of these databases were converted by the software company for use in a different software package, for example *phreeqc.dat* from PHREEQC was converted for THE GEOCHEMIST'S WORKBENCH and was renamed *thermo_phreeqc.dat*. Therefore, the number of the databases based on different thermodynamic datasets was only 21, but the databases using the same thermodynamic data differ in the activity model used and Debye-Hückel parameters (Table 2.2). The number of aquatic complexes included in the databases is from zero to nine complexes. The databases of EQ3/6 include the largest number of complexes, i. e. the *data0.cmp* and *data0.skb* have nine complexes, because they include the NaCl(aq), NaOH, $CaCl_2$(aq) and $CaCl^+$(aq) complexes. In general, the databases using the Pitzer approach include fewer complexes compared to the remaining databases, i. e. the *pitzer.dat* and *thermo_phrqpitz.dat* include only the $CaCO_3$(aq) complex and *Fact-Pitz* does not include a complex at all (Table 2.2).

Table 2.3

Parameters for the scenario studies. The increase of the NaCl concentration is linear.

Software packages with 30 databases	System regarding CO_2	Temperature	Ionic concentration	Dissolved mineral
PHREEQC	Fugacity of CO_2			
phreeqc.dat				
wateq4f.dat				
minteq.dat	1 bar			
minteq.v4.dat				
llnl.dat		25°C		
pitzer.dat				
sit.dat				
THE GEOCHEMIST'S WORKBENCH	10 bars			
thermo_phreeqc.dat				
thermo_wateq4f.dat				
thermo_minteq.dat				
thermo.dat				
thermo.com.v8.r6+.dat	50 bars			
thermo_phrqpitz.dat				
thermo_hmw.dat				
thermo_hdata.dat		50 °C	Increasing NaCl concentration 0–4 mol/kgw in 50 steps	Calcite
thermo_pitzer.dat				
EQ3/6				
data0.cmp	100 bars			
data0.skb				
data0.shv				
data0.sup	Concentration of CO_2			
data0.ymp				
data0.ypf				
data0.hmw				
data0.pit	0.5 mol CO_2/kgw			
FACTSAGE		75 °C		
Fact				
Fact53				
FT_HelgAQDH				
FT_HelgAQID	1.0 mol CO_2/kgw			
FT_HelgAQDD				
Fact-Pitz				

Open system

Closed system

The equilibrium constants of the calcite dissolution and CO_2(g) dissolution reaction differ throughout the databases (Figure 2.1). The equilibrium constant of calcite dissolution varies from 190 % at 25 °C and decreases to 135 % at 75 °C. The variation for the equilibrium constant of CO_2 dissolution was only 10 % and ca. 300 % at 25 °C and 75 °C, respectively. For this comparison the equilibrium constants of the *Fact-Pitz* database and the *FT_Helg*-databases of FactSage were not assessed, as the data could not be accessed, as the data for FactSage is not stored in an ASCII file.

In general, the databases contain information on elements, redox couples and reaction data for aqueous species, mineral phases and gas phases (Table 2.2). In some cases (i. e. *wateq4f.dat*, *phreeqc.dat*) they include data for exchange species, surface species and kinetic data.

2.2.2 Base case and scenario setup

The scenario models are set up as zero-dimensional models including only thermodynamic equilibrium reactions. The initial conditions are based on standard conditions (25 °C, 1 bar). The initial solution of every model contains 2 mmol Ca^{2+}/kgw and 4 mmol HCO_3^-/kgw; the values for the concentration of Ca^{2+} and HCO_3^- were selected, because The Geochemist's Workbench did not converge at lower concentrations. The pH was always set to a starting value of 7 and equilibrium was adjusted with calcite at a fugacity of CO_2 of 1 bar thereafter (Figure 2.2). In the evaluated scenarios, NaCl was added in 50 reaction steps thereby increasing the concentrations up to 4 mol/kgw. This range of the NaCl concentration represents the majority of the formation waters in saline aquifers suitable for CO_2 storage through to near-surface aquifers, as most of the deep groundwaters in northern Germany contain Na^+ and Cl^- as major ions (Hebig et al., 2012). In each reaction step the equilibrium with calcite was adjusted and the fugacity of CO_2 was fixed (Figure 2.2).

In this way, the scenarios are based on a simplified formation water composition. Different scenarios were set up by varying temperature, CO_2 fugacity or rather the amount of CO_2 as well as by varying the NaCl-concentration of the solution (Table 2.3). The standard scenario was defined at 25 °C and 1 bar fugacity of CO_2 with a low concentration of 0.1 mol NaCl/kgw. Every scenario was calculated firstly at a fixed fugacity of CO_2 (open system) and secondly with a defined concentration of CO_2 (closed system, Table 2.3).

The open system in terms of CO_2 represents a section of the reservoir where the CO_2 is present as a gas phase, since the geochemical models cannot handle supercritical gas phases. This case might occur within a CO_2 plume, where the reservoir of CO_2 is large enough to equilibrate the aqueous phase in relation to CO_2. Another setting is the leakage of CO_2, in which large amounts of CO_2 migrate into the retention or transfer formation saturating the aqueous phase in terms of CO_2.

The closed system in terms of CO_2 constitutes a domain of the reservoir, where the gaseous CO_2 phase is not in contact with the aqueous phase or the gas phase is not present any more and the whole residual gas phase is already dissolved in the aqueous phase. Another possible scenario can be the retention or transfer formations, in which a small amount of CO_2 migrates through a low leakage rate so that the formation water is not saturated for CO_2. The pressure in this system is only represented by the CO_2 fugacity. The effect of the pressure on the equilibrium constant of the calcite dissolution reaction and on the equilibrium constants of the reaction of the aquatic species are neglected by the databases and model codes. Only applying FactSage with *Fact* and *Fact53* the effect of the pressure on the Gibbs energy is calculated by this code. Altogether, four different software packages and 30

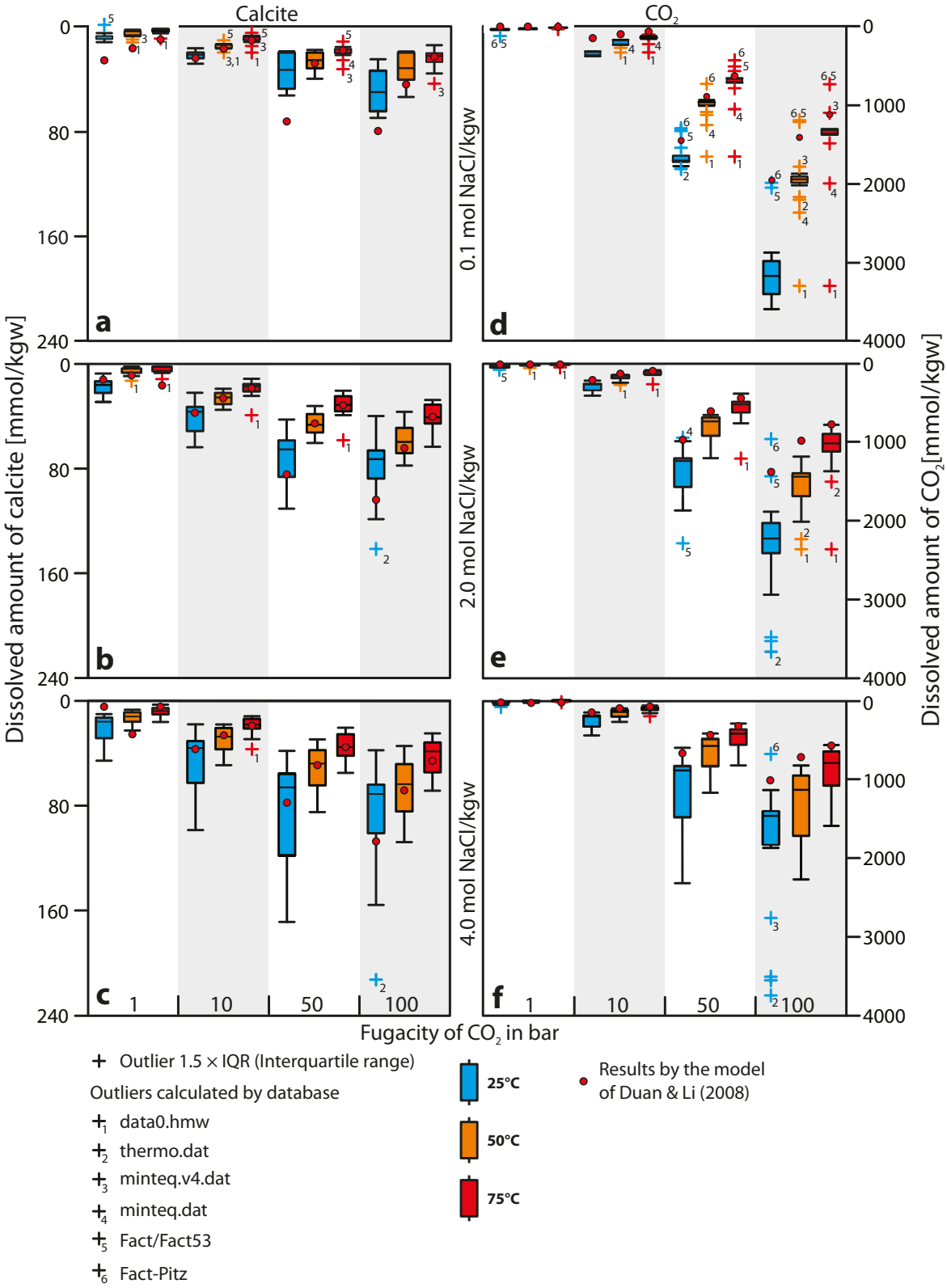

Figure 2.3 a–f

Box plots of the calcite and CO_2 solubility in the open system. Each box plot contains 30 data points derived from the 30 databases. Calcite solubility (left, a–c) and CO_2 solubility (right, d–f) at temperatures of 25, 50 and 75 °C and CO_2 fugacities of 1, 10, 50 and 100 bars (gray marked regions). The box is the 25th to 75th percentile of the data and the whiskers represent the upper and lower quartile. The crosses are values outside the range of 1.5 IQR of the lower or upper quartile and are classified as outliers.

databases at three temperatures with NaCl concentrations reaching to 4 mol/kgw, four fugacities of CO_2 (1, 10, 50 and 100 bars) and two concentrations of CO_2 (0.5 mol/kgw and 1.0 mol/kgw) depending on the open or closed system were investigated (Table 2.3).

2.2.3 Data analyses

The resulting data of the simulations using the combinations of software packages and databases are analysed via box plots. The calculated concentrations are compared at different concentrations, at different temperatures and at different CO_2 fugacities or rather concentrations of CO_2. The parameters chosen for the analysis are the amount of calcite dissolved and the amount of CO_2 dissolved.

The results are described as the range R of dissolved CO_2 and dissolved calcite, which includes the outliers (Equation 2.1). For each mineral or gas phase the following order in the description is maintained: Firstly, the behaviour of the results including the median and the range in dependence of the varied parameters is described. Secondly, the behaviour of the dissolved species in relation to ionic strength, fugacity and temperature is specified. Thirdly, the minimum and maximum values are associated to the databases and fourthly, the outliers visualised by the box plots are described.

$$R = x_{\max} - x_{\min} \tag{2.1}$$

The deviations of the results of the scenario analyses of the thermodynamic databases to the model of Duan and Li (2008), which is in good agreement to experimental solubilities with average deviations < 5 %, are analysed using box plots. For every calculated value of dissolved CO_2 and dissolved calcite, the deviations from the value worked out by the Duan and Li model are calculated (Equation 2.2). The deviations at all temperature, concentration and fugacity conditions are compiled in box plots for every database (Appendix A). An order of the databases with the smallest average deviations to the Duan and Li model is created separately for dissolved calcite and dissolved CO_2 to determine which database is in best agreement with experimental values.

$$f = \frac{\left| x_{Duan\&Li} - x_i \right|}{\left| x_{Duan\&Li} \right|} \tag{2.2}$$

2.3 Results

2.3.1 Calcite dissolution in the open system

The results applying the open system with respect to CO_2 for the scenario containing NaCl show amounts of dissolved calcite between 1–213 mmol (Figure 2.3 a–c). The median of the amount of calcite dissolved in the standard scenario is 9 mmol/kgw and the range (R) averages 12 mmol/kgw. The maximum median is 71 mmol calcite/kgw and thereby is eight times higher than the median of the standard scenario. The maximum range is 175 mmol calcite/kgw, which is 15 times higher than the range of the standard scenario.

Ionic strength. The median of the calcite solubility increases from 0.1 to 2 mol NaCl/kgw and remains constant at higher NaCl-concentration. For example, at 10 bars and 25 °C the median is 22 mmol calcite/kgw and increases up to a NaCl concentration of 2 mol/kgw to a median of 36 mmol calcite/kgw. In contrast to the median, the range continues to increase. For example, at 25 °C and a CO_2-fugacity

of 10 bars the range is 12 mmol calcite/kgw at low ionic concentrations (Figure 2.3 a) in contrast to 74 mmol calcite/kgw at a NaCl concentration of 4 mol/kgw (Figure 2.3 c). Hence the range increases to a value of 62 mmol/kgw, which corresponds to a factor of 6. The increase in the range of calcite dissolution is smaller at higher temperatures. At 75 °C the range of calcite increases from 14 mmol/kgw to 23 mmol/kgw, corresponding to a factor of 1.6.

Fugacity. The second trend is the increase of the solubility of calcite correlating to the increase in the CO_2 fugacity (Figure 2.3 b). At 2 mol NaCl/kgw the range of dissolved calcite increases from 5 mmol/kgw at 1 bar to 41 mmol/kgw at 100 bars. The increase corresponds to a factor of 8.2. The increase due to higher CO_2 fugacity is most significant at 50 °C and a concentration of 2 mol/kgw of NaCl.

Temperature. The third trend is the decrease in the range of dissolved calcite in relation to the elevation of the temperature from 25 to 75 °C (e. g. Figure 2.3 c). For example, the range of calcite solubility is 131 mmol calcite/kgw at 25 °C and at 4.0 mol NaCl/kgw and 50 bars CO_2-fugacity. When the temperature is changed to 75 °C the range of dissolved calcite is only 35 mmol calcite/kgw. Hence, the range decreases in factor 4 due to the temperature increase. At the same time the median of the calcite solubility decreases from 66 to 34 mmol/kgw corresponding to a of factor 2. In general The Geochemist's Workbench using *thermo.dat* calculates the highest solubility of calcite at concentrations of 2 mol NaCl and larger concentrations, for example at 25 °C and 100 bars the maximum value is 213 mmol calcite/kgw. EQ3/6 computes maximum values with the use of *data0.hmw* at 75 °C (Figure 2.3 b and c). At low concentrations the maximum solubility of calcite is calculated by Phreeqc using *minteq.v4.dat* and by EQ3/6 using *data0.hmw*. The statistical analyses of the results of the different databases through box plots show that there are less outliers at high NaCl concentrations than at lower concentrations (compare Figure 2.3 c with a). EQ3/6 applying *data0.hmw* shows outliers at concentrations of 2 and 4 mol NaCl/kgw and high temperatures of 75 °C (Figure 2.3 b, marked with [1]). At low NaCl concentration and 75 °C outliers are calculated by Phreeqc using *minteq.v4.dat* (Figure 2.3 a, marked with [3]). Additionally, The Geochemist's Workbench produces outliers applying *thermo.dat* at fugacities of 100 bars and 25 °C (Figure 2.3 b and c, marked with [2]).

2.3.2 CO_2 dissolution in the open system

The amount of dissolved CO_2 ranges from 12–3730 mmol (Figure 2.3 d–f). The median of the CO_2 solubility in the standard scenario is 41 mmol/kgw and the range averages 88 mmol CO_2/kgw. The maximum range is achieved at 25 °C and 100 bars CO_2 fugacity and amounts to 3060 mmol CO_2/kgw and is, therefore, 35 times higher in comparison to the standard scenario (Figure 2.3 f).

Ionic strength. The range of the CO_2 solubility increases in correlation with higher ionic concentration. For example, at 0.1 mol NaCl/kgw the range of CO_2 dissolved is 46 mmol/kgw at 10 bars CO_2 fugacity and a temperature of 25 °C. The range increases to 309 mmol CO_2/kgw at 4 mol NaCl/kgw. The increase in the range is by a factor of 7 (compare Figure 2.3 d and f).

Fugacity. As for calcite, the range of CO_2 increases relative to the fugacity of CO_2 (Figure 2.3 d–f). At concentrations of 0.1 mol NaCl/kgw the range of dissolved CO_2 is 14 mmol/kgw at 1 bar and 50 °C and increases to 2105 mmol/kgw at 100 bars. The range increases by a factor of 155 and is most significant at the conditions of 50 °C and 0.1 mol NaCl/kgw.

Temperature. The amount of CO_2 dissolved decreases in relation to temperature. For example, the median of the CO_2 solubility at 50 bars and high NaCl concentration is 889 mmol/kgw at a temperature

of 25 °C. However, at 75 °C the median of the CO_2 solubility reduces to only 430 mmol/kgw. Hence the median decreases by a factor of 2.1 due to the increase in the temperature (Figure 2.3 f). The range of dissolved CO_2 increases in relation to higher temperature at low NaCl concentrations, but decreases due to increasing temperature at higher NaCl concentrations. For example, at high NaCl concentrations and at a fugacity of 100 bars the range of dissolved CO_2 averages 3059 mmol/kgw at 25 °C and decreases to a range of 1030 mmol/kgw at 75 °C. The decrease in the range of dissolved CO_2 is by a factor of 3.

The maximum solubilities of CO_2 are calculated by The Geochemist's Workbench with the use of *thermo.dat* at 25 °C (Figure 2.3 f). The database *data0.hmw* of EQ3/6 produces the highest values at 50 °C and 75 °C at low and medium ionic concentrations (< 2 mol NaCl/kgw). At 25 °C the databases *thermo.dat* and *thermo.com.V8.R6+.dat* of The Geochemist's Workbench and *sit.dat* provided by Phreeqc and also *Fact-Pitz* by FactSage are determined as outliers through the box plots.

In general, the results for the CO_2 solubility show more outliers compared to the results for the calcite solubility. More outliers occur at low ionic concentrations in comparison to high ionic concentrations (compare Figure 2.3 a, d with c, f). In particular, at low ionic concentrations FactSage using *Fact*, *Fact53* and *Fact-Pitz* are defined as outliers while calculating the lowest values. That is due to the fact that FactSage does not include activity calculations and the solubility of gases is computed at a fixed system pressure. Also *minteq.dat*, *minteq.v4.dat* and *sit.dat* provided by Phreeqc are determined as outliers at these conditions. Additionally, outliers occur occasionally calculated by *thermo.dat* of The Geochemist's Workbench and by *data0.hmw* of EQ3/6.

Applying FactSage using the databases *FT_Helg_AQID*, *FT_Helg_AQDH* and *FT_Helg_AQDD*, the results of the dissolution of CO_2, especially at higher pressures are higher to a maximum factor of 5 in relation to the maximum values calculated by the remaining software codes and databases. For example, at 50 bars and 25 °C a CO_2 solubility of more than 4 mol CO_2/kgw is calculated and even at

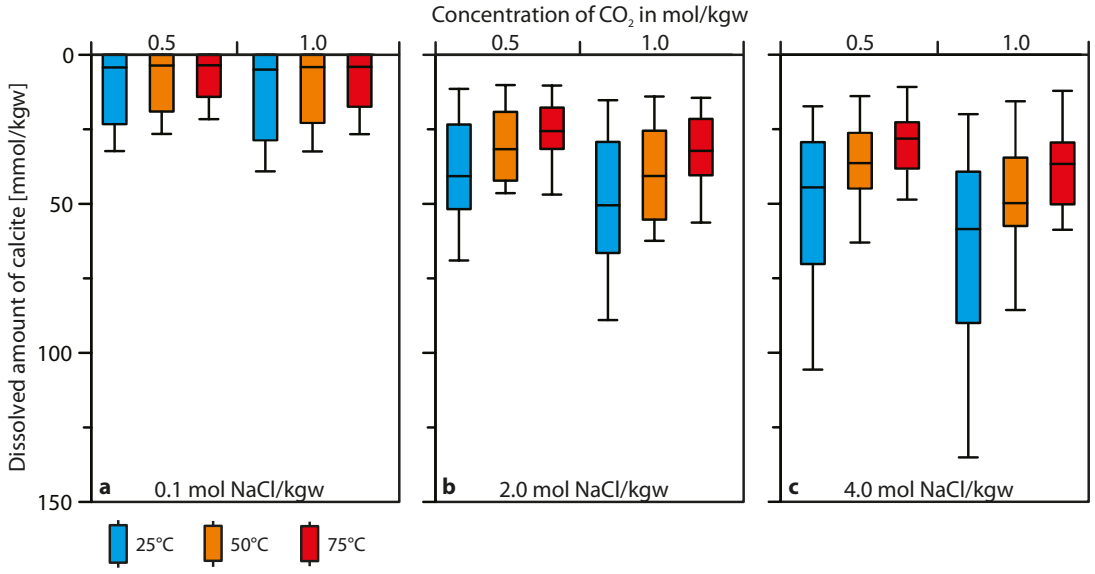

Figure 2.4 a–c

Box plots of calcite solubility in the closed system at temperatures of 25, 50 and 75 °C and at CO_2 concentrations of 0.5 and 1.0 mol/kgw. The plots are only shown at 0.1, 2.0 and 4.0 mol NaCl/kgw.

100 bars and 25 °C the solubility amounts to 10 mol CO_2/kgw. Dissolution of this amount is unrealistic under these conditions. In general, the three Helgeson databases of FactSage were found to calculate unrealistic results for the system with a CO_2 gas phase. Furthermore, the databases including the Harvie-Møller-Weare (hmw) activity model (Harvie et al., 1984), which is also based on the Pitzer equations (Harvie and Weare, 1980), either do not perform calculations at temperatures higher than 25 °C, as the *thermo_hmw.dat* of The Geochemist's Workbench, or produce results classified as outliers as the *data0.hmw* of EQ3/6.

2.3.3 Calcite dissolution in the closed system

The range of calcite dissolution calculated for the closed system with respect to CO_2 reaches up to 135 mmol/kgw. In relation to increasing NaCl concentration the range of calcite solubility increases (Figure 2.4 c). For example, at low ionic concentration of NaCl the range of calcite is 39 mmol/kgw at 1.0 mol CO_2/kgw (Figure 2.4 a). The range increases to 115 mmol calcite/kgw at 4 mol NaCl/kgw (Figure 2.4 c).

Temperature. The range of calcite solubility decreases with respect to rising temperature. For example, the range for calcite of 115 mmol/kgw halves from 25 °C to 75 °C and then amounts to 47 mmol/kgw. The reduction is similar at both CO_2 concentrations. Applying Phreeqc and using *minteq.v4.dat* and *pitzer.dat* minimum values are calculated in every scenario. The maximum values are produced by EQ3/6 applying *data0.hmw*, *data0.skb*, *data0.cmp* and *data0.ymp* at 50 °C and 75 °C. At a temperature of 25 °C the maxima are calculated by The Geochemist's Workbench with the use of *thermo.dat*.

Ionic strength. The trends of the closed system with respect to increasing NaCl concentration and temperature are similar to the trends of the open system. In contrast to the open system, the box plots of the closed system do not show any outliers. In contrast to the open system scenario the databases *FT_Helg_AQID*, *FT_Helg_AQDH* and *FT_Helg_AQDD* delivered by FactSage are included in the box plots, because they calculate plausible values.

The possibility of precipitating halite is only calculated by the database *minteq.v4.dat* provided by Phreeqc. Halite is only precipitated at concentrations beyond 3.5 mol NaCl/kgw. The maximum amount of halite precipitated is up to 485 mmol/kgw at 25 °C, a CO_2 fugacity of 100 bars and a concentration of 4 mol NaCl/kgw. The precipitation of halite does not have a significant impact on the amount of dissolved calcite. In comparison to the system without halite precipitation, the amount of dissolved calcite decreases to 10 mmol/kgw at maximum (data not shown).

Table 2.4

Order of the databases with the lowest average deviation in comparison to the Duan and Li (2008) model for CO_2 and calcite dissolution. The box plots of the deviations can be found in the Appendix A.

Order	CO_2	Calcite	Average deviation	Average deviation in %
1	*wateq4f.dat*	*phreeqc.dat*	*wateq4f.dat*	28.9
2	*phreeqc.dat*	*wateq4f.dat*	*phreeqc.dat*	29.4
3	*pitzer.dat*	*thermo_phreeqc.dat*	*pitzer.dat*	34.3
4	*thermo_wateq4f.dat*	*thermo_wateq4f.dat*	*thermo_wateq4f.dat*	35.1
5	*data0.shv/data0.sup*	*pitzer.dat*	*data0.shv*	35.3

2.3.4 Comparison with the Duan and Li model

The calcite solubility could only be calculated for the open system with respect to CO_2 by the model of Duan and Li (2008). The results of this model match in almost every case the range of dissolved calcite calculated by the applied modelling codes with the thermodynamic databases (Figure 2.3 a–c). In many cases the results of the Duan and Li model are in good agreement with the median of the database results. Only at 25 °C and high CO_2 fugacities are the solubilities of calcite calculated by the Duan and Li model larger (Figure 2.3 a). The comparison of the amount of dissolved CO_2 shows a different correlation. The results of the Duan and Li model are in most cases within the range of the database results. At 1 bar and 10 bars of CO_2 fugacity the values of the Duan and Li model and the results from the databases are in very good agreement (Figure 2.3 d–f). But at higher fugacities the values of the Duan and Li model are always at the lower limit of the range calculated in this study or the values are slightly lower than the minimum values of this study (Figure 2.3 e and f; 100 bars).

2.4 Discussion and Conclusions

2.4.1 Accuracy and reasons for ranges in calculated CO_2 and calcite solubilities

Four approaches to calculate the CO_2 and calcite solubilities were applied: using (1) the ion-dissociation (Debye-Hückel) approach, (2) the ion-association (Pitzer) approach, (3) the Gibbs energy minimization method (GEM), and (4) the Duan and Li model, which is assumed to be the most accurate model for using these simplified scenarios. The Debye–Hückel (1) and the Pitzer approach (2) are grouped into the law of mass action approach (LMA).

The CO_2 solubility calculated by the Duan and Li (2008) model is lower or at the bottom of the range of the solubilities calculated using the LMA and GEM approaches. The main reason for the overestimation of the CO_2 solubility using the LMA approach is that the solubility of CO_2 in the Debye-Hückel and the Pitzer approaches is calculated applying Henry's Law. Although the fugacity is used instead of the partial pressure of CO_2 in this study, the subsequent reactions of the dissolved CO_2 to HCO_3^- and CO_2 ions are not regarded adequately by Henry's Law (Yurteri et al., 1987). The statistical median of the calcite solubility calculated using the LMA approach agrees well with the results of the specific model of Duan and Li (2008). However, the results of the Debye-Hückel approach reach higher amounts of dissolved calcite than calculated using the Pitzer approach. Concerning the calcite solubility, the Debye-Hückel approach produced results more in accordance with the model of Duan and Li (2008) than the Pitzer approach, which seems remarkable due to the general propagation of Pitzer models for solutions with high ionic strengths. The results using the GEM approach are not significantly different from the results of the software packages applying the Debye-Hückel and the Pitzer approach at the conditions chosen for the scenarios in this study. Hence, with none of the tested models and databases including the LMA or GEM approaches, the CO_2 solubility could be calculated adequately at the conditions chosen for the scenarios. The implementation of equations of state to describe the solubility of CO_2 in the geochemical models is, therefore, recommended. In this simple system with only one mineral phase dissolving, the uncertainty (the range of results divided by their median) for the amount of dissolved CO_2 is 210 % and for dissolved calcite is 250 % at maximum.

Since the Duan and Li model (2008) can be used to calculate CO_2 and calcite solubilities in the chosen scenarios, their results were compared with the results of the model codes and thermodynamic databases applied in this study. The databases *phreeqc.dat* and *wateq4f.dat* show the lowest average

deviations from the model of Duan and Li (2008) for CO_2 dissolution and calcite dissolution calculated according to Equation 2.2 (Table 2.4, for box plots see Appendix A). The applications of the Pitzer databases, which are valid at high ionic strength, do not show smaller deviations in general.

In general, the reasons for the variations within the results using the Debye-Hückel and Pitzer approaches result from different (a) aqueous species, minerals and gases, (b) thermodynamic data for reactions, (c) activity models and input parameters, and (d) calculation methods of the temperature dependency of equilibrium constants and different standard enthalpies of reactions in the databases.

The variation of the amount of dissolved calcite cannot be correlated to the variation of the thermodynamic data. For example, the equilibrium constant of calcite varies by 190 % in relation to the average at 25 °C. However, the amount of dissolved calcite varies only by 150 % at 25 °C and increases to 200 % at higher temperature. The variation of the equilibrium constant decreases at higher temperature. The variation of the amount of dissolved CO_2(g) correlates with the variation of the equilibrium constant of the CO_2(g) dissolution reaction at low NaCl-concentrations. But at high NaCl-concentrations the variation of dissolved CO_2(g) decreases in relation to higher temperatures and does not correlate with the variation of the equilibrium constant. Therefore, the equilibrium constant of calcite alone does not have an impact on the variation of dissolved calcite. The equilibrium constant of CO_2(g) has an impact on the variation of the solubility of CO_2(g), but only at low and medium NaCl-concentrations. At higher concentrations the different activity models are responsible for the variations in the dissolved phases.

The differences caused by the different activity models become clear in the case of the *minteq.v4.dat* databases of Phreeqc. Using the *minteq.v4.dat* database, outliers are calculated generally showing lower dissolved calcite amounts. The activity of the aqueous complex $CaHCO_3^+$ calculated by using the *minteq.v4.dat* database differs by an order of magnitude compared to using the *phreeqc.dat* database. The Debye-Hückel parameters a_0 and b_0 for the aqueous complexes of the *minteq.v4.dat* database deviate from the parameters in the phreeqc.dat database by the same order of magnitude. Additionally, the Debye-Hückel parameters a_0 and b_0 for ions like Ca^{2+} and Na^+ are missing in the *minteq.v4.dat* database. Consequently, the Davies equation is used by the code instead of the WATEQ Debye-Hückel equation, which is postulated as the main reason for the outliers using the *minteq.v4.dat* database.

2.4.2 Evaluation of the impact of uncertainties and limits of the applied scenario approach

The amount of total inorganic C (TIC) dissolved in the solution is strongly influenced by the solubilities of CO_2 and calcite. The contribution of dissolved CO_2 to the amount of dissolved TIC in the scenarios representing the storage formation is larger by a factor of 10 compared to the amount of dissolved TIC generated by calcite dissolution. Therefore, the CO_2 fugacity, as the main influencing factor of the calculated amount of dissolved TIC, is most important for calculating the retention of the CO_2 by dissolution. However, at 25 °C the uncertainty through the application of different thermodynamic databases already amounts to a range of a factor of 2 in terms of dissolved CO_2. This result is in good agreement with the study of Kervévan et al. (2005), who defined the error for calculating dissolved C as 50 % by using Phreeqc in comparison to their model.

In this study the effect of the pressure on the equilibrium constants and aquatic species was neglected by using PHREEQC, THE GEOCHEMIST'S WORKBENCH, and EQ3/6. EQ3/6 has a database including pressure corrections but only for 500 bars at minimum (*data0.500*). Only FACTSAGE performed a pressure correction of the equilibrium constants. To include a pressure correction in the codes using the LMA approach the equilibrium constants must be recalculated using programs like SUPCRT92 (Johnson et al., 1992). The use of this program would lead to a completely new database, including different thermodynamic data. However, Dethlefsen et al. (2012) showed that the effect of the pressure correction on the equilibrium constants of the minerals and species at 125 bars was low compared to the variations in using different databases. Consequently, this issue was not a focus in this study. Furthermore the knowledge of whether the system is open or closed in terms of CO_2 is essential. Regarding calcite solubility, the CO_2 fugacity has the largest impact by a factor of 8 applying CO_2 fugacities between 1 and 100. Subordinately, the NaCl concentration influences the range of the calcite solubility by a factor of 6. The temperature has the smallest impact, and leads to a decrease of the range of dissolved calcite by a factor of 4. In near-surface aquifers the dissolution of calcite becomes more important as the contribution of dissolved calcite to the dissolved TIC is only smaller by a factor of 4 compared to the contribution of CO_2 dissolution. Through these uncertainties the calculated retention capacity for the formations cannot be determined exactly, which is important for risk assessment on drinking water aquifers or the biosphere.

According to the simulations the variation in the dissolved calcite leads to different calculated pH values. At 25 °C and 50 bars, these vary from 4.6 to 5.0, for instance. This can have an important impact on further geochemical reactions, regardless of the geological compartment. Although the variation in the quantity of dissolved calcite seems not to be crucial for CO_2 retention capacity, variations in the Ca concentration can lead to differences in the calculated saturation states of further Ca-bearing minerals, such as anorthite, gypsum, or dolomite. The differences in the saturation states can either enhance or impede dissolution or precipitation of these minerals and can, therefore, limit the availability of other cations in the solution such as Al, Si or Mg. For instance, if the amount of dissolved calcite increases, the amount of dissolved anorthite may decrease, while variation in the dissolved or precipitated amounts of gypsum can cause a variation in the ionic strength influencing activity coefficients in the solution.

2.4.3 Implications for the application to natural systems

The study presents a very simplified model, which is calculated over a wide range of physical conditions, but is not representative for each geochemical scenario. For example, the formation waters can contain SO_4 as a main component, but the model solution only includes Na, Ca, Cl and HCO_3. Hence, for instance S complexes are neglected causing a higher calculated ionic strength in solution, as Ca is not ligated in S complexes. Furthermore, in the case of a leakage of CO_2 through a fault in a limestone, calcite can be dissolved and clay within the limestone could remain as a residual mineral phase. This process can lead to the passivation of calcite surfaces and in this way could inhibit further calcite dissolution. Another more complex scenario is CO_2 leakage through a borehole, where the minerals of the cement of the casing can be dissolved. As the cement consists of silicate, Fe, Al and SO_4 phases, this study does not cover these more complex leakage scenarios.

The uncertainty analyses demonstrated the application limits of common geochemical model codes and their thermodynamic databases on the prognosis of geochemical reactions based on these

models. With respect to the risk assessment and safety concepts for CO_2 storage these limits should be considered. In the latest state-of-the-art the application of the *phreeqc.dat* or *wateq4f.dat* database of PHREEQC is recommended to model scenarios of CO_2 storage or leakage. Using these databases the smallest average deviations to the Duan and Li (2008) model were calculated. The use of the Pitzer databases did not result in a smaller average deviation and hence is not necessary for modelling CO_2 storage.

Acknowledgements

This study was funded by the German Federal Ministry of Education and Research (BMBF), EnBW Energie Baden-Württemberg AG, E.ON Energie AG, E.ON Gas Storage AG, RWE Dea AG, Vattenfall Europe Technology Research GmbH, Wintershall Holding AG and Stadtwerke Kiel AG as part of the CO_2-MoPa joint project in the framework of the Special Program GEOTECHNOLOGIEN. The authors thank two anonymous reviewers for their helpful comments.

Appendix A

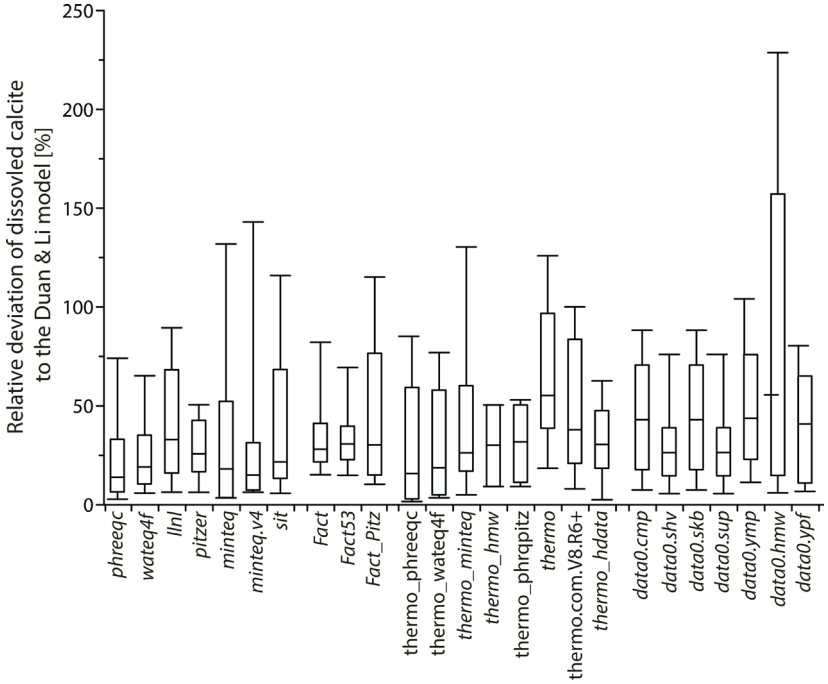

Figure A1

Relative deviation (f) of dissolved CO_2 in relation to the Duan and Li model for the single databases. The deviation is combined at the fugacity and temperature conditions.

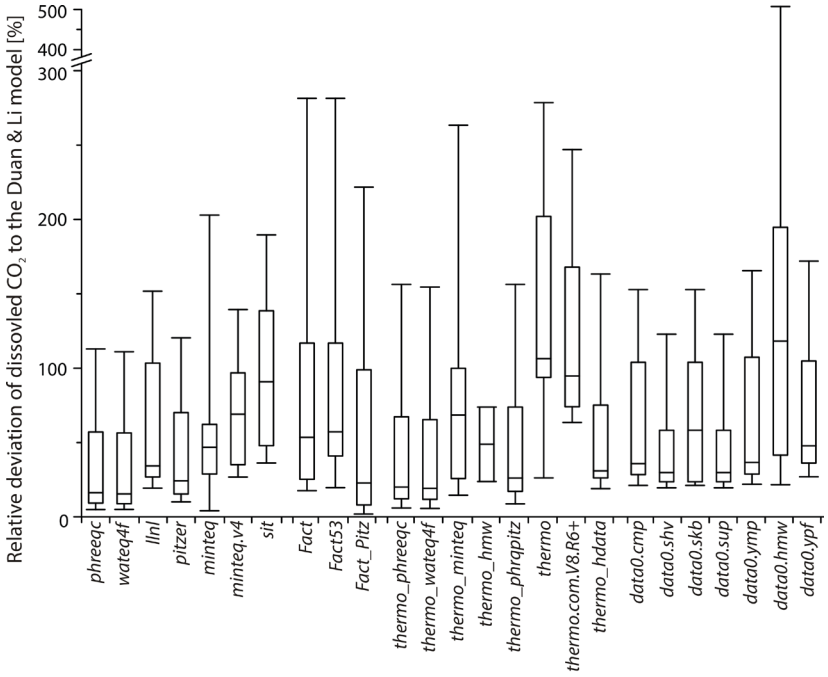

Figure A2

Relative deviation (f) of dissolved calcite in relation to the model of Duan and Li (2008).

References

Appelo, C. A. J., Willemsen, A., Beekman, H. E. & Griffioen, J. 1990. Geochemical calculations and observations on salt water intrusions. II. Validation of a geochemical model with laboratory experiments. Journal of Hydrology 120(1–2), 225–250. *doi:10.1016/0022-1694(90)90151-M*

Appelo, C. A. J., Verweij, E. & Schäfer, H. 1998. A hydrogeochemical transport model for an oxidation experiment with pyrite/calcite/exchangers/organic matter containing sand. Applied Geochemistry 13(2), 257–268. *doi:10.1016/S0883-2927(97)00070-X*

Bassett, R. L. & Melchior, D. C. 1990. Chemical modeling of aqueous systems: An Overview. In: Melchior, D. C. & Bassett, R. L. (Eds.), Chemical Modeling of Aqueous Systems. American Chemical Society Symposium Series. 416, pp. 1–12.

Beck, M. B. 1987. Water quality modeling: a review of the analysis of uncertainty. Water Resourources Research 23(8), 1393–1442. *doi:10.1029/WR023i008p01393*

Bethke, C. M. 2008. Geochemical and Biogeochemical Reaction Modeling. Cambridge University Press, Cambridge.

Bildstein, O., Kervévan, C., Lagneau, V., Delaplace, P., Crédoz, A., Audigane, P., Perfetti, E., Jacquemet, N. & Jullien, M. 2010. Integrative modeling of caprock integrity in the context of CO_2 storage: evolution of transport and geochemical properties and impact on performance and safety assessment. Oil & Gas Science & Technology 65(3), 485–502. *doi:10.2516/ogst/2010006*

Brönsted, J. N., 1922. Studies on solubility. IV. The principle of the specific interaction of ions. Journal of the American Chemical Society 44, 877–898. *doi:10.1021/ja01426a001*

Carroll, S. A., McNab, W. W. & Torres, S. C. 2011. Experimental study of cement sandstone/shale-brine-CO_2 interactions. Geochemical Transactions 12(1), 9. *doi:10.1186/1467-4866-12-9*

Criscenti, L. J., Laniak, G. F. & Erikson, R. L., 1996. Propagation of uncertainty through geochemical code calculations. Geochimica et Cosmochimica Acta 60(19), 3551–3568. *doi:10.1016/0016-7037(96)00188-3*

Delany, J. M. 1986. EQ3/6 Data Base–Ongoing Development at Lawrence Livermore National Laboratory. In: Jackson, K. J. & Bourcier B. L. (Eds.). Proceedings of the Workshop on Geochemical Modeling, Lawrence Livermore National Laboratory, Fallen Leaf Lake, California, pp. 162–166. Retrieved from http://www.osti.gov/energycitations/servlets/purl/6317833-DdHgru/6317833.pdf.

Denison, F. H. & Garnier-Laplace, J. 2005. The effects of database parameter uncertainty on uranium (VI) equilibrium calculations. Geochimimica Cosmochimica Acta 69(9), 2183–2191. *doi:10.1016/j.gca.2004.09.033*

Dethlefsen, F., Haase, C., Ebert, M. & Dahmke, A. 2012. Uncertainties of geochemical modeling during CO_2 sequestration applying batch equilibrium calculations. Environmental Earth Sciences 65(4), 1105–1117. *doi:10.1007/s12665-011-1360-x*

Dethlefsen, F., Köber, R., Schäfer, D., al Hagrey, S. A., Hornbruch, G., Ebert, M., Beyer, M., Großmann, J. & Dahmke, A. 2013. Monitoring approaches for detecting and evaluating CO_2 and formation water leackages into near-surface aquifers. Energy Procedia 37, 4886-4893. *doi:10.1016/j.egypro.2013.06.399*

Duan, Z. & Li, D. 2008. Coupled phase and aqueous species equilibrium of the H_2O-CO_2-NaCl-$CaCO_3$ system from 0 to 250 °C, 1 to 1000 bar with NaCl concentrations up to saturation of halite. Geochimica et Cosmochim. Acta 72(20), 5128–5145. *doi:10.1016/j.gca.2008.07.025*

Duan, Z., Sun, R., Zhu, C. & Chou, I.-M. 2006. An improved model for the calculation of CO_2 solubility in aqueous solutions containing Na^+, K^+, Ca^{2+}, Mg^{2+}, Cl^-, and SO_4^{2-} Marine Chemistry 98(2–4), 131–139. *doi:10.1016/j.marchem.2005.09.001*

Ekberg, C., 1999. Sensitivity analysis and simulation uncertainties in predictive geochemical modelling. Freiberg On-line Geoscience 2.

Elizalde, M. 1995. Current theories in the calculation of activity coefficients–II. Specific interaction theories applied to some equilibria studies in solution chemistry. Talanta 42(3), 395–400. *doi:10.1016/0039-9140-(95)01422-8*

Eriksson, G. & Königsberger, E. 2008. FactSage and ChemApp Two tools for the prediction of multiphase chemical equilibria in solutions. Pure and Applied Chemistry 80(6), 1293–1302. *doi:10.1351/pac200880061293*

Gaus, I., Azaroual, M. & Czernichowski-Lauriol, I. 2005. Reactive transport modelling of the impact of CO_2 injection on the clayey cap rock at Sleipner (North Sea). Chemical Geology 217(3–4), 319–337. *doi:10.1016/j.chemgeo.2004.12.016*

Großmann, J., Naue, G., Schreck, A., Woiwode, R., Bauer, S., Dahmke, A., Ebert, M., Schäfer, D., Reinicke, K. M., Schilling, F. & Krawczyk, C. 2011. Sicherheit und Umweltverträglichkeit der CO_2-Speicherung. Report of the Research and Development Project (Funding Code 3708 49 112 2) for the German Federal Environmental Agency (Umweltbundesamt).

Guggenheim, E. A. & Turgeon, J. C. 1955. Specific interaction of ions. Transitions of the Faraday Society 51, 747–761.

Gundogan, O., Mackay, E. & Todd, A. 2011. Comparison of numerical codes for geochemical modelling of CO_2 storage in target sandstone reservoirs. Chemical Engineering Research and Design 89(9), 1805–1816.

Hansen, C. & van Berk, W. 2004. Retracing the development of raw water quality in water works applying reactive controlled material flux analyses. Aquatic Sciences 66(1), 60–77.

Harvie, C. E. & Weare, J. H. 1980. The prediction of mineral solubilities in natural waters: The Na–K–Mg–Ca–Cl–SO_4–H_2O system from zero to high concentration at 25 °C. Geochimica et Cosmochimica Acta 44(7), 981–997. *doi:10.1016/0016-7037(80)90287-2*

Harvie, C. E., Møller, N. & Weare, J. H. 1984. The prediction of mineral solubilities in natural waters: the Na–K–Mg–Ca–H–Cl–SO_4–OH–HCO_3–CO_3–CO_2–H_2O system to high ionic strengths at 25 °C. Geochimica et Cosmochimica Acta 48(4), 723–751. *doi:10.1016/0016-7037(84)90098-X*

Hebig, K.H., Ito, N., Scheytt, T. & Marui, A. 2012. Review: deep groundwater research with focus on Germany. Hydrogeology Journal 20(2), 227–243. *doi:10.1007/s10040-011-0815-1*

Johnson, J. W., Oelkers, E. H. & Helgeson, H. C. 1992. SUPCRT92: a software package for calculating the standard molal thermodynamic properties of minerals, gases, aqueous species, and reactions from 1 to 5000 bar and 0 to 1000 °C. Computational Geosciences 18(7), 899–947. *doi:10.1016/0098-3004(92)90029-Q*

Karpov, I. K., Chudnenko, K. V. & Kulik, D. A. 1997. Modeling chemical mass transfer in geochemical processes: thermodynamic relations, conditions of equilibria, and numerical algorithms. American Journal of Science 297(April 2012), 767–806. *doi:10.2475/ajs.302.4.281*

Kervévan, C., Azaroual, M. & Durst, P. 2005. Improvement of the calculation accuracy of acid gas solubility in deep reservoir brines: application to the geological storage of CO_2. Oil & Gas Science and Technology 60(2), 357–379. doi:10.2516/ogst:2005022

Ketzer, J. M., Iglesias, R., Einloft, S., Dullius, J., Ligabue, R. & De Lima, V. 2009. Water-rock-CO_2 interactions in saline aquifers aimed for carbon dioxide storage: experimental and numerical modeling studies of the Rio Bonito Formation (Permian), southern Brazil. Applied Geochemistry 24(5), 760–767. *doi:10.1016/j.apgeochem.2009.01.001*

Kim, H. T. & Frederick Jr, W. J., 1988 a. Evaluation of Pitzer ion interaction parameters of aqueous electrolytes at 25 °C. 1. Single salt parameters. Journal of Chemical & Engineering Data 33(2), 177–184. *doi:10.1021/je00052a035*

Kim, H. T., Frederick Jr, W. J., 1988 b. Evaluation of Pitzer ion interaction parameters of aqueous mixed electrolyte solutions at 25 °C. 2. Ternary mixing parameters. Journal of Chemical & Engineering Data 33(3), 278–283. *doi:10.1021/je00053a017*

Li, D. & Bauer, S. 2009. Development of a coupled transport and geochemical reaction code and a first application to CO_2 sequestration, Workshop TRePro II.

Merkel, B. J. & Planer-Friedrich, B. 2008. Groundwater Geochemistry: A Practical Guide to Modeling of Natural and Contaminated Aquatic Systems. Springer Verlag, Heidelberg.

Nitzsche, O., Meinrath, G. & Merkel, B. J. 2000. Database uncertainty as a limiting factor in reactive transport prognosis. Journal of Contaminant Hydrology 44(3–4), 223–237. *doi:10.1016/S0169-7722(00)00106-6*

Parkhurst, D. L. & Appelo, C. A. J. 1999. User's guide to PHREEQC (Version 2): a computer program for speciation, batch-reaction, one-dimensional transport, and inverse geochemical calculations. U. S. Geol. Surv. Water-Resour. Invest. Rep. 99–4259.

Petersen, S. & Hack, K. 2007. The thermochemistry library ChemApp and its applications. International Journal of Materials Research 98(10), 935–945. *doi:10.3139/146.101551*

Pitzer, K. S. 1973. Thermodynamics of electrolytes. I. Theoretical basis and general equations. The Journal of Physical Chemistry 77(2), 268–277. *doi:10.1021/j100621a026*

Pitzer, K. S. & Mayorga, G. 1973. Thermodynamics of electrolytes. II. Activity and osmotic coefficients for strong electrolytes with one or both ions univalent. The Journal of Physical Chemistry 77(19), 2300–2308. *doi:10.1021/j100638a009*

Pitzer, K. S. & Mayorga, G. 1974. Thermodynamics of electrolytes. III. Activity and osmotic coefficients for 2–2 electrolytes. Journal of Solution Chemistry 3(7), 539–546. *doi:10.1007/BF00648138*

Postma, D., Larsen, F., Minh Hue, N. T., Duc, M. T., Viet, P. H., Nhan, P. Q. & Jessen, S. 2007. Arsenic in groundwater of the Red River floodplain, Vietnam: controlling geochemical processes and reactive transport modeling. Geochimica et Cosmochimica Acta 71(21), 5054–5071. *doi:10.1016/j.gca.2007.08.020*

Scatchard, G. 1936. Concentrated solutions of strong electrolytes. Chemical Reviews 19(3), 309–327. *doi:10.1021/cr60064a008*

Smith, D. S., Adams, N. W. H., Kramer, J. R., 1999. Resolving uncertainty in chemical speciation determinations. Geochimica et Cosmochimica Acta 63(19–20), 3337–3347. *doi:10.1016/S0016-7037(99)00255-0*

Tanaka, T., Hack, K. & Hara, S. 2000. Calculation of surface tension of liquid Bi–Sn alloy using thermochemical application library ChemApp. Calphad 24(4), 465–474. *doi:10.1016/S0364-5916(00)85001-4*

Truesdell, A. H., Jones, B. F., 1974. WATEQ, a computer program for calculating chemical equilibria of natural waters. Journal of Research of the U. S. Geological Survey 2(2), 233–245.

Wolery, T. J. 1992. EQ3/6, A Software Package for Geochemical Modeling of Aqueous Systems: Package Overview and Installation Guide (Version 7.0). Lawrence Livermore National Laboratory, Livermore, California.

Xie, M., Kolditz, O. & Moog, H. C. 2011. A geochemical transport model for thermo-hydro-chemical (THC) coupled processes with saline water. Water Resources Research. 47(W02545), 1–14. *doi:10.1029/2010WR009270*

Yurteri, C., Ryan, D. F., Callow, J. J. & Gurol, M. D. 1987. The effect of chemical composition of water on Henry's law constant. Journal (Water Pollution Control Federation) 59(11), 950–956.

Zeleznik, F. J. & Gordon, S. 1968. Calculation of complex chemical equilibria. Industrial Engineering Chem. 60(6), 27–57. *doi:10.1021/ie50702a006*

Zhu, Y., Merkel, B. J., Stober, I. & Bucher, K. 2003. The hydrogeochemistry of arsenic in the Clara mine, Germany. Mine Water and the Environment 22(3), 110–117. *doi:10.1007/s10230-003-0011-1*

3. Uncertainties of geochemical codes and thermodynamic databases for predicting geochemical impact of carbon dioxide on geologic formations

Christoph Haase*[1], Markus Ebert[1], Frank Dethlefsen[1]

[1]Kiel University, Institute of Geosciences, Ludewig-Meyn-Straße 10, 24118 Kiel, Germany

Submitted to Applied Geochemistry

Abstract

Numerical codes are applied in order to calculate chemical reactions following geologic carbon sequestration in deep formations. Thereby, using different thermodynamic databases generated variations in the simulation results referred to as model uncertainty. PHREEQC and THE GEOCHEMIST'S WORKBENCH codes were used in this study to simulate anorthite dissolution in storage, retention, transfer, and near-surface formation waters represented by respective geological units. For each of the formation waters, a one-dimensional scenario was simulated by using eight different thermodynamic databases. At a high ionic strength and a high temperature mineral trapping is the most efficient process for long term CO_2 storage. However, among the geological formations and the time needed for anorthite dissolution regarded in this study, model uncertainties caused by using different numerical code and thermodynamic database combinations were largest (ca. 90 %) for the storage formation waters at 58 °C and I = 6.5 mol/l. Conversely, in near-surface formation waters the model uncertainty was less than 1 %. Due to CO_2 dissolution the calculated pH of the formation waters decreased to a range between pH 4.0 and 5.5. In that pH range, the dissolution mechanism of anorthite switches from the slow neutral to the faster acid mechanism causing dissolution time length variations. The calculated pH variation further increased with rising ionic strength. A detailed examination of the reasons revealed the activity coefficient calculation method of the main aquatic species to have the largest impact on the simulated model results. The second largest impact had the calculation method of the CO_2 activity coefficient. By calibration to experimental data, a specific thermodynamic database can be chosen representing these experimental results. However, the calibration of thermodynamic databases is not possible for all potential reactions in more complex geological systems at large ranges of temperature and pressure conditions. The uncertainties quantified in this study for CO_2 storage systems originating from using thermodynamic databases will therefore persist independently from previously conducted calibrations of thermodynamic databases to experimental data.

*corresponding author

3.1 Introduction

Geologic carbon storage in deep saline aquifers has been proposed as a strategy to reduce CO_2 emissions from power plants and industrial processes. Quantifying the chemical implications of CO_2 injected in saline aquifers referred to as storage formations is crucial to estimate the storage capacity of geologic formations and to appraise safety issues for geological storage sites. The knowledge of chemical reactions of CO_2 with highly mineralized formation water and minerals is important for identifying prevalent mechanisms responsible for long-term and safe carbon storage. For example, mineral dissolution can provide cations followed by precipitation of secondary mineral phases such as carbonates or silicates improving mineral trapping for permanent and long term CO_2 storage (Bachu et al., 2007; Gunter et al., 1993; Matter and Kelemen, 2009; Metz et al., 2005). A proportion of the injected CO_2 can remain as a supercritical phase and may migrate into overlying formations in case of a CO_2 leakage. These overlaying formations referred to as retention formations can hold back CO_2 by dissolution in the formation water (Dethlefsen et al., 2013; Großmann et al., 2011). The remaining supercritical or gaseous phase, depending on pressure and temperature, can potentially migrate further upward via transfer formations into near-surface formations, where protected potable water resources can be acidified (Peter et al. 2012; Trautz et al. 2013). Due to a pH decrease, the quality of potable water of near-surface aquifers can be endangered by the release of trace and heavy metals (Zheng et al., 2009 a; Zheng et al., 2009 b; Lu et al., 2010). The hazard for protected water resources is one of the major risks of the CCS (Carbon Capture and Storage) technology.

Numerical codes were applied to predict the impact of injected CO_2 on geologic formations (Audigane et al., 2006; Gaus et al., 2005; Gherardi et al., 2007; Zheng et al., 2009 a; Carroll et al., 2009). The codes can calculate long-term reactions at large spatial dimensions, which cannot be reproduced by laboratory experiments and for which an upscaling of experimental results is not feasible. Until today, it is not known which thermodynamic database produces the most reliable results for CO_2 storage and leakage scenarios (Dethlefsen et al., 2012; Haase et al., 2013). The databases can only be calibrated by experiments for simple reaction systems. Therefore, by selecting a thermodynamic database a model uncertainty is involved in the calculation results, which is reflected by the range of the results simulated using available thermodynamic databases (Haase et al., 2013; 2014). Several thermodynamic databases were applied until now for reactive transport models simulating CO_2 injection in storage formations, which are i.e. the database *phreeqc.dat* or *llnl.dat* from PHREEQC (Cantucci et al., 2009; Gaus et al., 2005; Gundogan et al., 2011; Hellevang et al., 2013) and EQ3/6 databases adapted to TOUGHREACT (Pruess et al., 2003; Xu et al., 2003; Xu et al., 2005; Xiao et al., 2009; Xu et al., 2014), and finally the *thermo.dat* database from THE GEOCHEMIST'S WORKBENCH (Moore et al., 2005; Berger et al., 2009; Johnson et al., 2001). However, the so far applied databases are not valid at high ionic strength, as the equations calculating the activity coefficients only provide reliable results at ionic strengths of up to about 1 molal (i. e. Davies, Debye-Hückel, or WATEQ-Debye-Hückel equation). At ionic strength higher than 1 molal, only the WATEQ-Debye-Hückel equation can probably provide accurate activity coefficients in NaCl-dominated solutions (Parkhurst and Appelo, 1999; Truesdell and Jones, 1974). Bethke and Yeakel (2012) and Helgeson (1969) indicate a validity up to ionic strengths of 3 molal for the WATEQ-Debye-Hückel equation. At higher ionic strengths, the Pitzer model can calculate accurate activity coefficients (Pitzer and Mayorga, 1974; Pitzer, 1973). However, interaction coefficients for the Pitzer databases are usually limited to 25 °C and to geochemical systems excluding Si and Al mineral phases, which does not allow for regarding silicates being essential for the simulation of reactions occurring during CO_2 storage in sedimentary formations.

Additionally to model uncertainties caused by thermodynamic data, model parameterisations—i. e. mineral reactions or concentrations, kinetic rate constants, surface areas and activation energies—cause variations in simulation results of numerical codes. For example, the selection of the kinetic parameters can influence mineral dissolution rates (Balashov et al., 2013; Black et al., 2014; Haase et al., 2014). To determine calcite dissolution rates, a large number of experiments has been conducted, i. e. by Berner and Morse (1974), Compton and Daly (1987), Plummer et al. (1978), Reddy et al. (1981), and Svensson and Dreybrodt (1992). Within these experiments, the rate constants for calcite dissolution differ by one order of magnitude (Arvidson et al., 2003), mostly due to differences in the experimental design (Hellmann, 1994). Anorthite dissolution has been examined intensively by Busenberg and Clemency (1976), Chou and Wollast (1985), Knauss and Wolery (1986), Holdren and Speyer (1987), Casey et al. (1991), Amrhein and Suarez (1992), Hellmann (1994; 1995), Oelkers and Schott (1995) and Berg and Banwart (2000). Comparing different experimental studies, the rate constant of anorthite dissolution varies in four orders of magnitude (Palandri and Kharaka, 2004). However, the impact of the model parameterisation on predictions of numerical codes was not quantified so far.

CO_2 dissolution in formation waters causes the pH to drop to values around 5.0 in siliciclastic formations of naturally occurring CO_2 systems and induces mineral reactions (Gilfillan et al. 2009). Anorthite dissolution can lead to increased Ca^{2+} concentrations in the formation waters. Increasing Ca^{2+} concentrations can cause the formation water to be supersaturated with respect to carbonate mineral phases like dawsonite, which may immobilize the injected CO_2 by precipitation (Bachu et al., 1994; Hellevang et al., 2005; Johnson, 2004). This process is especially important for CO_2 storage and is referred to as mineral trapping facilitating long-term storage of CO_2. Mineral trapping provides large storage capacity in certain geochemical settings (Matter and Kelemen, 2009).

Plagioclase dissolution strongly depends on formation water pH (Amrhein and Suarez, 1988; Sverdrup, 1990). At acid pH values, the dissolution rate, especially for anorthite, is faster compared to dissolution at neutral pH conditions (Blum, 1994; Casey et al., 1991; Holdren and Speyer, 1987; Oelkers and Schott, 1995). The aim of this study is to compare the results of two geochemical codes for predicting anorthite dissolution in formation waters reacting with CO_2 and using well-defined input data. The model uncertainties were quantified applying different thermodynamic databases using storage to near-surface formation waters. In addition to these model uncertainties, the range of the anorthite dissolution time length was specified using rate constants in the range of experimental values in the same scenario setup.

3.2 Methods

3.2.1 Numerical codes and thermodynamic databases

The CO_2 reaction scenario simulations were performed applying The Geochemist's Workbench (Release 7; Bethke, 2008) and Phreeqc version 2 (Parkhurst and Appelo, 1999). The geochemical codes use thermodynamic databases to calculate aquatic speciation and gas-mineral-water reactions. In this study, eight databases are used: *thermo_phreeqc.dat*, *thermo_wateq4f.dat*, *thermo.dat*, and *thermo.com.v8.r6+.dat* (The Geochemist's Workbench); *llnl.dat*, *minteq.dat*, *phreeqc.dat*, and *wateq4f.dat* (Phreeqc). In general, thermodynamic databases incorporate the Debye-Hückel theory or the Pitzer formalism for activity coefficient calculation. The databases using the Pitzer formalism calculate valid activity coefficients for high ionic strength waters (Pitzer and Mayorga, 1974;

Table 3.1

Equilibrium constants as log_K_{eq}'s of the CO_2(aq) conversion to CO_3^{2-}, calcite, anorthite dissolution (Equations 3.1–3.3) at 25 °C and 60 °C of the applied thermodynamic databases.

Code	Database	CO_2(aq)		Calcite		Anorthite	
		25 °C	60 °C	25 °C	60 °C	25 °C	60 °C
PHREEQC	*phreeqc.dat*	−16.681	−16.443	−8.480	−8.757	−20.314	−24.716
	wateq4f.dat	−16.681	−16.443	−8.480	−8.757	−20.314	−24.716
	minteq.dat	−16.681	−16.530	−8.475	−8.819	−17.810	−19.179
	llnl.dat	−16.673	−16.448	−8.480	−8.819	−19.342	−24.945
THE GOCHEMIST'S WORKBENCH	*thermo_phreeqc.dat*	−16.680	−16.443	−8.480	−8.759	−20.380	−23.464
	thermo_wateq.dat	−16.681	−16.443	−8.480	−8.759	−20.380	−23.464
	thermo.dat	−16.709	−16.542	−8.631	−8.996	−18.750	−21.788
	thermo.com.v8.r6+.dat	−16.674	−16.542	−8.480	−8.797	−19.340	−25.111
	log_K_{eq} range	0.03	0.10	0.16	0.24	2.57	5.93

Pitzer, 1973) commonly occuring in deep formations suitable for CO_2 storage. However, the main mineral phases used for this study are not included in the Pitzer databases (chalcedony, kaolinite, and anorthite).

$$CO_2(aq) + H_2O \rightleftarrows CO_3^{-2} + H^+ \tag{3.1}$$

$$CaCO_3 \rightleftarrows CO_3^{-2} + Ca^{+2} \tag{3.2}$$

$$\underset{\text{Anorthite}}{CaAlSi_3O_8} + 8H_2O \rightleftarrows Ca^{+2} + 2Al(OH)_4^- + 2H_4SiO_4 \tag{3.3}$$

Thermodynamic databases differ in data such as the equilibrium constants K_{eq} for CO_2(aq) conversion into CO_3^{-2} (Equation 3.1), as well as calcite (Equation 3.2) and anorthite dissolution reactions (Equation 3.3). The range (min/max) of the equilibrium constants of CO_2(aq) conversion into CO_3^{-2} is 0.03 and 0.10 at 25 °C and 60 °C, respectively, and the range of the equilibrium constants of the calcite reaction is 0.16 and 0.24 at 25 °C and 60 °C, respectively. The range of the equilibrium constants for anorthite dissolution is between 2.57 and 5.93 at 25 °C and 60 °C, respectively (Table 3.1).

Beyond equilibrium constant variations, the thermodynamic databases differ in type and number of species and elements, activity models (mainly activity equations), Debye-Hückel parameters (a_0 and b_0), and ΔH_r^0 for the Van't Hoff equation or different empirical relations for temperature correction of equilibrium constants. This study did not comprise pressure impact on equilibrium constants, as the pressure only subordinately influenced simulation results of CO_2 storage i. e. using Keuper formation waters (Dethlefsen et al., 2012).

3.2.2 Model setup and Formation waters

The scenarios consisted of four different formation waters from Northern Germany as initial input solutions, but otherwise similar boundary conditions. The dissolution time length of anorthite was simulated by the geochemical codes applying the described thermodynamic databases (Section 3.2.1).

Table 3.2

Compositions of Buntsandstein, Keuper, Tertiary, and Quaternary formation waters. Concentrations are in molar units. Ionic strengths were calculated applying PHREEQC using *phreeqc.dat*. Water analyses are from [1]Kühn et al. (2002), [2]Seibt et al. (1997), [3]Peter et al. (2012), [4]Carlé (1975), n. a. = data not available.

	Storage formations		Transfer formation	Near-surface formation
		Retention formations		
Parameter	Middle Buntsandstein[1]	Upper Keuper[2] (Rhaetian)	Tertiary[4]	Quaternary[3]
Depth [m]	1520	1248	n. a.	15
pH	5.6	6.2	5.9	7.0
Temperature [°C]	58	54	15*	7
Ionic strength [mol/kgw]	6.49	2.98	1.40	0.086
Charge error [%]	1.09	0.00	0.00	0.00
Na^+	3.97	2.3	1.08	5.5×10^{-04}
K^+	0.017	0.005	0.0056	1.1×10^{-04}
Ca^{2+}	0.35	0.1	0.05	2.7×10^{-03}
Mg^{2+}	0.094	0.04	0.035	2.8×10^{-04}
Al^{3+}	n.a.	n.a.	n.a.	5.0×10^{-07}
Si	n.a.	n.a.	n.a.	n.a.
Cl^-	4.86	2.25	1.24	1.5×10^{-03}
HCO^{3-}	n.a.	9.31×10^{-04}	0.0042	n.a.
SO_4^{2-}	0.0039	0.0051	0.0013	1.3×10^{-03}

* Temperature was calculated according to the geothermal gradient of 3 °C/100 m

The different durations calculated for anorthite dissolution in the scenarios were understood as a range of dissolution time lengths. Formation water compositions were taken from potential storage formations (Middle Buntsandstein, Detfurth formation (Kühn et al., 2002) and Upper Keuper Rhaetian formation (Seibt et al., 1997), retention formations (Upper Keuper Rhaetian formation and Paleogene), transfer formations (Paleogene; Carlé, 1975) and near-surface formations (Pleistocene glacial sand, Peter et al. 2012) in Northern Germany (Table 3.2). In the following, these formations are referred to as Buntsandstein, Keuper, Tertiary, and Quaternary.

3.2.3 Model boundary conditions

The boundary conditions were similar for all scenarios, i. e. hydraulic properties for flow model, concentrations of CO_2 and anorthite. The hydraulic parameters represent a porous aquifer. The reactive model consisted of one cell at a length of 0.5 m (Figure 3.1). Cell dimensions could only be defined in The Geochemist's Workbench; cell width and length were set to 0.5 m and 0.01 m, respectively. The model cell comprised an initial solution consisting of one kilogram formation water. The flow

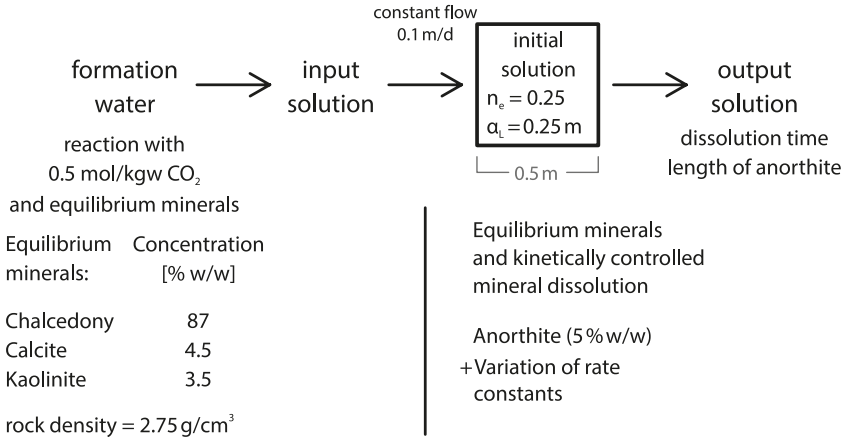

Figure 3.1

Set up of the one-dimensional reaction model, the used thermodynamically controlled mineral phases reacting instantaneously and anorthite dissolving by a kinetic expression.

velocity was constant at 0.1 m/d and the pore volume was set to n_e = 0.25. Longitudinal dispersivity was α_L = 0.25 m. The simulated comparison parameter is the simulated dissolution time length until anorthite is completely dissolved in the model cell.

Initially, the formation water reacted irreversibly with 0.5 molal aqueous CO_2 and the equilibrium mineral assemblage. The resulting solution was used as input solution for all scenarios (Figure 3.1). Compositions of the input solutions differ depending on the applied thermodynamic database and are given in Appendix B (Table B1–B4). Degassing of CO_2 was not possible; hence a gas phase could not develop. The fixed CO_2 concentration represented a closed system with respect to CO_2 describing a formation segment without an available CO_2 gas phase. Large scale models mainly apply closed systems with respect to CO_2 assessing the impact of CO_2 storage or leakage as the computation time is shorter applying CO_2 closed systems (Beyer et al., 2012; Kolditz et al., 2012).

The initial equilibration of the formation water with CO_2 and the specific mineral assemblage (Figure 3.1) resulted in eight different input solutions calculated by the code and database combinations (Appendix B). The same mineral assemblage was also present in the model cell. As equilibrium minerals kaolinite and chalcedony (chosen as a reactive SiO_2 phase) were selected, because of lacking Al and Si concentrations (Table 3.2) in the formation water analysis (Bazin et al., 1997; Pang et al., 1998). As calcite is present in the selected geologic formations the mineral assemblage consisted of calcite, chalcedony and kaolinite. The mineral concentrations are chosen according to mean values in North German sediments (Dethlefsen et al., 2014; Figure 3.1).

3.2.4 Kinetic reactions

For calculating the anorthite dissolution time length, also the rate law of Palandri and Kharaka (2004) was applied, which is based on Lasaga (1984; 1994; 1995). The surface area of anorthite is set to a fixed value of 1 m^2/g. The initial anorthite content is 2.0 molal corresponding to a modal concentration of 5.0 % w/w and a rock density of 2.75 g/cm^3 (Figure 3.1). Anorthite dissolution was the only kinetically controlled reaction, where the rate constants from Palandri & Kharaka (2004) were

Table 3.3

Rate constants k [mol m^{-2} s^{-1}] for anorthite dissolution compiled by Palandri and Kharaka (2004) for the base case and variations of the rate constants derived from the experiments of Berg and Banwart (2000) and Oelkers and Schott (1995). The rate constants were converted to 298.15 °K applying the rate law by Palandri and Kharaka (2004).

Mechanism of rate law	k for acid mechanism [mol m^{-2} s^{-1}]	k for neutral mechanism [mol m^{-2} s^{-1}]
	Base case	
k from Palandri & Kharaka 2004	3.16×10^{-04}	7.59×10^{-10}
Activation energy [kJ mol^{-1}]	16.6	17.8
	Variation of kinetic rate constants	
Experiment by	Oelkers and Schott (1995)	Berg and Banwart (2000)
Minimal value of k	9.55×10^{-05}	4.90×10^{-12}
Maximal value of k	6.31×10^{-04}	1.70×10^{-11}

used (Table 3.3). The rate law includes a temperature correction using the activation energies from Table 3.3 (Lasaga, 1981), but not a pressure correction of the rate constants. The input solutions including CO_2 and mineral equilibrium reactions are strongly undersaturated with respect to anorthite (Appendix B).

The dissolution time range caused by using different rate constants was investigated applying PHREEQC in combination with *phreeqc.dat*. The scenarios were simulated by using rate constants for anorthite from Oelkers and Schott (1995), Berg and Banwart (2000), and Amrhein and Suarez (1992) representing wide ranges of experimental data (Table 3.3).

3.2.5 Database synchronisation

Thermodynamic databases differ for instance in equilibrium constants for mineral reactions, the number and identity of aqueous species, and the activity coefficient calculation method of the aquatic species. A calculation matrix was developed in order to investigate the impact of each of these single database parameters on the simulation results. Based on this matrix, the parameters of two thermodynamic databases were assimilated step by step, a procedure referred to as »synchronisation«.

In this approach, two different thermodynamic databases from PHREEQC (*phreeqc.dat*) and The Geochemist's Workbench (*thermo.com.v8.r6+.dat*) were synchronized by a stepwise assimilation of the databases' constituents: At first, similar equilibrium constants were used for mineral reactions (1). Secondly, the aqueous species of both databases were reduced with the result that the databases contain similar aqueous species (2). In the following step the activity coefficient calculation of main aquatic species of both databases was adjusted (3). Furthermore, the activity coefficient calculation of the aquatic species from *thermo.com.v8.r6+.dat* was applied to both databases (4). In the next step, the calculation method for the activity coefficient of aquatic CO_2 from *phreeqc.dat* was used (5). Finally, similar equilibrium constants were applied for the aquatic species (6). These synchronisation steps were combined in different orders, referred to as »pathways« (Figure 3.4).

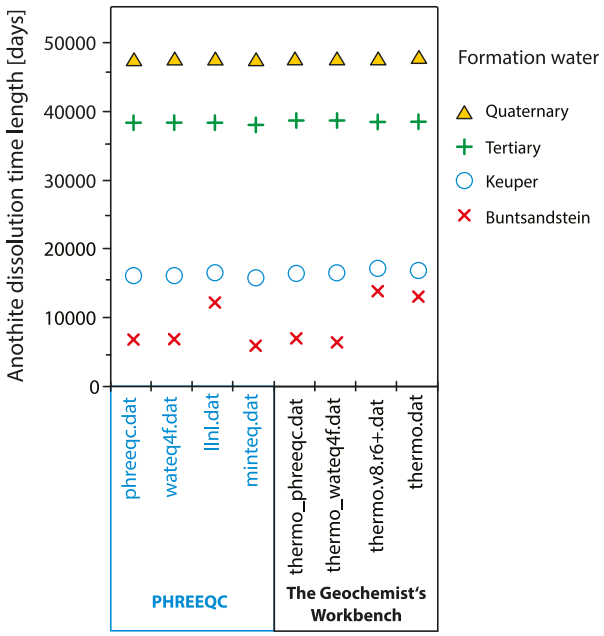

Figure 3.2
Anorthite dissolution times calculated using PHREEQC and THE GEOCHEMIST'S WORKBENCH codes and using different thermodynamic databases for four different formation waters.

The impact of the thermodynamic database parameters was investigated using formation specific water from the Buntsandstein formation for the calculation matrix. In preceding step, synthetic formation waters were used at ionic strengths of 0.1 and 4.0 mol/kgw. The initial difference in the anorthite dissolution time length is maximal 6 % between applying *phreeqc.dat* and *thermo.com.v8.r6+.dat*. After synchronizing the databases the difference was less than 1 % (Details in Appendix A, Table A1).

3.3 Results

3.3.1 Variations caused by thermodynamic databases

For each scenario, a different anorthite dissolution time length was calculated in the model cell using dissolution kinetics. The anorthite dissolution time length increased from 5,880 to 47,984 days using different formation waters from Buntsandstein to Quaternary formations (Figure 3.2). The dissolution time lengths showed not only high variations comparing different formation waters, but also high variations in the time length simulating the anorthite dissolution within one formation water. Using one single formation water, the variation rose due to the use of different codes and thermodynamic databases. Using the Buntsandstein formation water produced the highest variation, whereby the anorthite dissolution time length reached from 5,880 to 13,875 days corresponding to a variation of 88 % compared to the arithmetic mean (x = 9,026 days, Figure 3.2). Applying the database from PHREEQC to the Buntsandstein formation water resulted in the fastest dissolution, while applying the *thermo.dat* and *thermo.com.v8.r6+.dat* databases from THE GEOCHEMIST'S WORKBENCH resulted in the slowest dissolution. Using the Quaternary formation water provided the smallest variation in the dissolution time, i. e. the time varies between 47,685 and 47,984 days corresponding to a relative variation of 0.6 % compared to the arithmetic mean (x = 47,881 days, Figure 3.2)

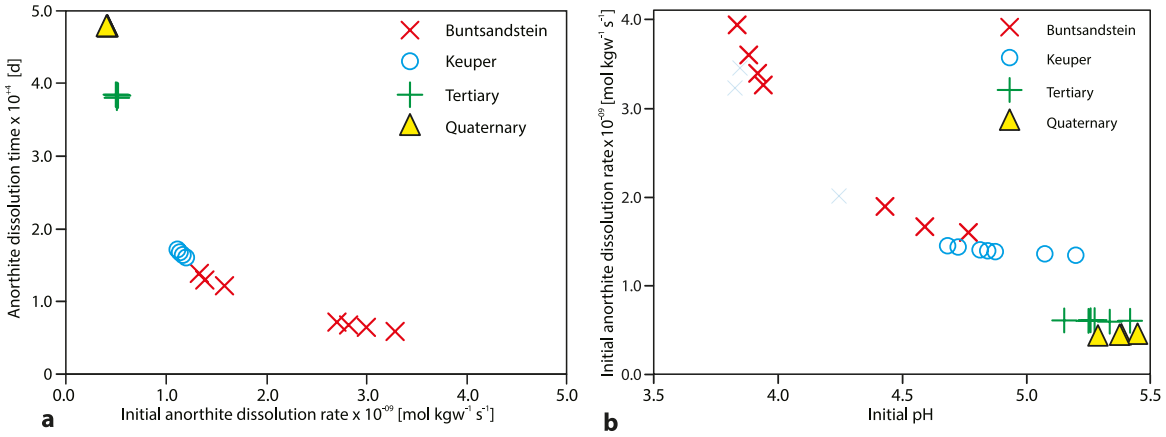

Figure 3.3 a and b

a) Initial dissolution rates decreasing exponentially with the dissolution time length of anorthite (b) pH values decreasing exponentially with the initial dissolution rates calculated by the different model codes and thermodynamic databases for the formations waters. Differences in dissolution rates in formation waters at equal pH are due to the temperature effect on dissolution kinetics.

The anorthite dissolution was calculated in the model cell for strongly undersaturated systems in all scenarios. The resulting saturation indices were between −7.9 and −9.6 for the Buntsandstein formation water due to the preceding CO_2 dissolution (Appendix B, Table B4) indicating that more sophisticated rate laws for calculating the slow dissolution approaching anorthite saturation are not required (Blum and Lasaga, 1988; Blum and Lasaga, 1991). The initial dissolution rates calculated by using the rate law of Palandri and Kharaka (2004) correlate well with the simulated dissolution time lengths (Figure 3.3 a), indicating that the initial dissolution rate is the major controlling factor for the kinetics of anorthite dissolution in all scenarios. The variation of the initial dissolution rates amounted to a similar factor as the variation in the dissolution time lengths calculated for a specific formation water (i. e. factor 2.47 compared to factor 2.36 for the Buntsandstein formation water). The initial dissolution rates and dissolution time lengths varied in similar factors of 1.08 for the Keuper and of 1.01 for the Tertiary and Quaternary formation water, respectively.

Furthermore, the initial dissolution rates showed a strong relationship with the initial pH calculated for each scenario (Figure 3.3 b). For example, the *llnl.dat* database calculated a pH for the Buntsandstein formation which is higher by factor 1.13 than the pH calculated by the *phreeqc.dat* or *wateq4f.dat* databases. Consequently, the *llnl.dat* database calculated a longer anorthite dissolution time compared to other databases (ca. 12,220 days compared to ca. 6,840 days, Figure 3.2). The higher rate coefficient of the acid mechanism in the rate law used is responsible for the strong pH effect on the initial dissolution rates in the scenarios, when the pH is smaller than approximately 5.0. At pH 5.0 the acid mechanism contributes less than 1 % to the total dissolution rate, whereas at pH 4.0 the acid mechanism controls ca. 40 % of the total dissolution rate.

A simple interrelation between the equilibrium constants for mineral reactions or speciation reactions and dissolution times or initial pH values is not appropriate. The equilibrium constants for anorthite dissolution differ in larger factors (Table 3.1), compared to the variances in the dissolution time lengths. Thus more complex reasons must explain the observations.

3.3.2 Results of database synchronisation

The initial difference of the dissolution time length of anorthite was 6,365 days for the Buntsandstein formation water using the original databases *phreeqc.dat* and *thermo.com.v8.r6+.dat*. Reducing the aquatic species of the thermodynamic databases at first (pathway 2), the difference in the dissolution time length of anorthite decreased to 4,730 days. The impact of this parameter was 26 % (Figure 3.4). Including the calculation method for the CO_2 activity coefficients from *phreeqc.dat* for both databases resulted in a reduction of the dissolution time difference to 2,721 days (corresponding to an impact of 32 %). Additionally, equivalent usages of the activity coefficients of the main species lead to a decrease in the difference in the dissolution time length of 317 days. The calculation of the main species activity coefficients is therefore attributed an impact of 38 %. The smallest impact along this pathway had the calculation of the activity coefficient of aquatic species, which was only 0.6 %. Using the same equilibrium constants for aquatic species reduced the dissolution time length to a difference of 116 days, corresponding to 2 %. The remaining difference in the dissolution time is caused by differences in equilibrium constants of the mineral phases, numerical codes, and Debye-Hückel parameters. Different pH values are calculated by the databases due to different activity coefficient calculation methods for the main aqueous species and due to different activity parameters for H^+.

However, if the synchronization steps are performed in a different order (pathway 1 to 4, Figure 3.4) the impact on reducing the dissolution time was different. Synchronizing the equilibrium minerals in pathway 4 resulted in a larger dissolution time difference, whereby this pathway was not further pursued. In general, the ratio of the impact of the database parameters therefore depended on the order within a single pathway. It is not possible to assign an exact ratio to one parameter's influence, because the parameters mutually interfere. In general, an order of the parameter's influence could be provided by using the calculation matrix. The influence of the activity coefficient calculation of the main species is most important for simulating the anorthite dissolution time (38 %–55 %). Second most important is the activity calculation method of aquatic CO_2 (16 %–32 %) and third most important is the reduction of aqueous species to the lowest common number (0.1 %–16 %, Figure 3.4).

The strong impact of the activity coefficient calculation of the main species was caused by different calculation methods incorporated in the thermodynamic databases. The WATEQ Debye-Hückel, Debye-Hückel, Davies, or Setschenow equation is used by the databases. Furthermore, partially different parameters (a_0 and b_0) for the WATEQ Debye-Hückel and Debye-Hückel equation are included in the databases. Using different equations results in different activity coefficients, especially for uncharged species such as CO_2(aq) or $CaCO_3$(aq), but also for charged species such as $CaOH^+$(aq). The *thermo.com.v8.r6+.dat* (such as all the databases of The Geochemist's Workbench) database contains a similar value for the B-dot parameter ($b_0 = 0.041$ at 25 °C), whereas the B-dot parameter of *phreeqc.dat* depends on the specific species. Furthermore, the calculation method for the activity coefficient of CO_2(aq) differs between the two databases. The *phreeqc.dat* database uses the Setschenow equation for the activity coefficient calculation of uncharged species such as CO_2(aq). The *thermo.com.v8.r6+.dat* database can use three different equations to calculate the CO_2(aq) activity coefficient, which are 1) a temperature dependent expression for calculating the CO_2(aq) activity in pure NaCl solutions; 2) the activity is equal to unity; and 3) the Setschenow equation ($\gamma_i = b_o \times I$) (Cleverley & Bastrakov, 2005).

Figure 3.3 b shows, that the temperature effect is a further factor for calculating variable dissolution time lengths of anorthite. In general, higher temperatures resulted in faster dissolution times due to

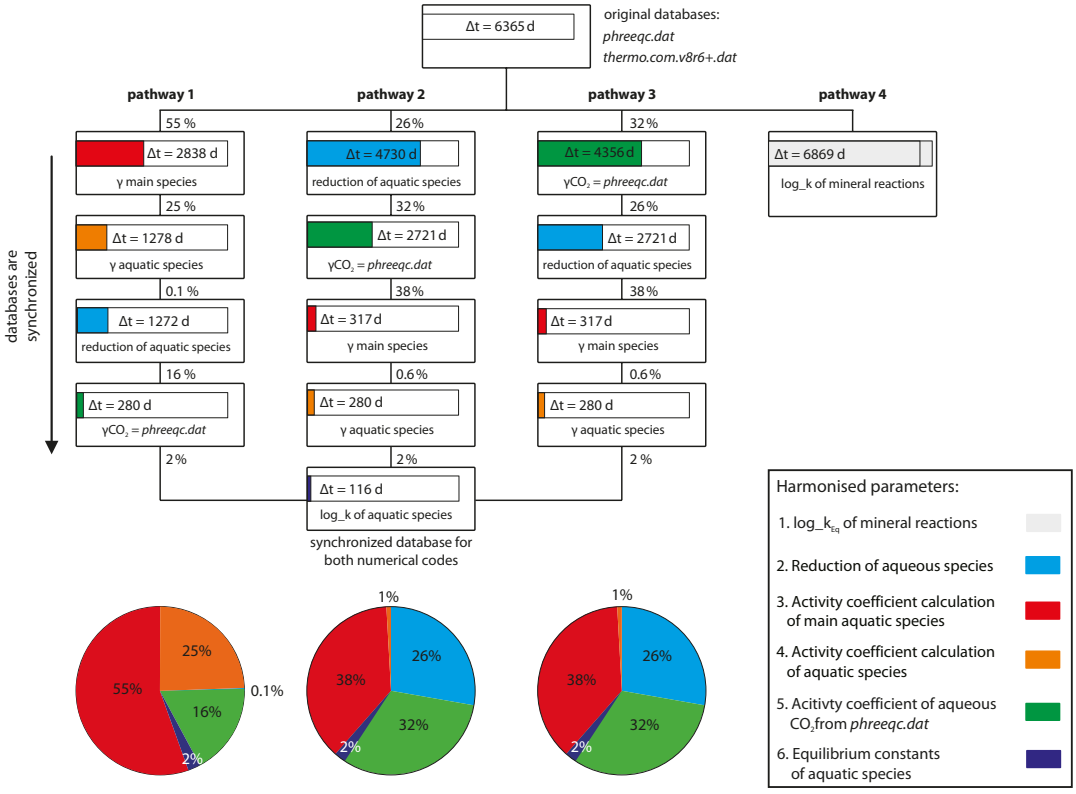

Figure 3.4

Flow chart and pie charts of the calculation matrix identifying an order of the single database parameter's influence on anorthite dissolution time length using the Buntsandstein formation water. For synchronizing the databases, the parameters were combined in four different orders (pathway 1-4).

temperature correction used in the rate law. The temperature influence is shown, since different dissolution time lengths are calculated at equal initial pH conditions using different formation waters (Figure 3.3 b).

In general, the calculation of the initial pH becomes crucial, because the CO_2 system buffered the pH between 4.0 and 5.5 in this study, which is the pH range where the dominant dissolution mechanism of anorthite switches from the slower neutral mechanism to the faster acid mechanism at undersaturated conditions (Palandri and Kharaka, 2004). Different pH values are mainly calculated due to variances in the activity coefficient calculation method for the main aqueous species. The exact percentage for each parameter's influence could not be evaluated as a differing combination order changes the percentage ratio. The precise magnitude for the uncertainty resulting from the thermodynamic model used, which is expected for CO_2 storage scenario modelling at high NaCl concentrations and high temperatures of the formation waters, was specified. However, when geochemical codes are used, it is not possible quantifying the exact parameter's influence.

3.3.3 Variation of kinetic rate constants

The range of the dissolution time length of anorthite increased by varying the rate constants compared to the range of dissolution time lengths calculated by all thermodynamic databases. PHREEQC with

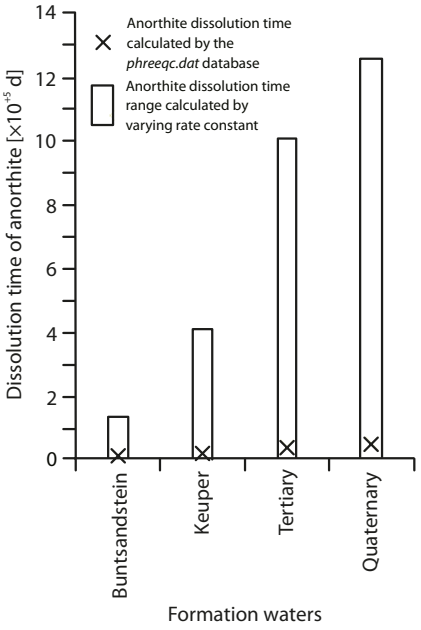

Figure 3.5

Range of anorthite dissolution time length simulated for different formation waters with variation of kinetic rate coefficients using PHREEQC with phreeqc.dat compared to simulated dissolution times using the rate coefficients of Palandri and Kharaka (2004) (crosses).

only *phreeqc.dat* was previously applied with the rate constants of Palandri and Kharaka (2004) for the base case (Results in Figure 3.2, identical with crosses in Figure 3.5). The dissolution time lengths decreased in factors of between 13 and 62 in all formation waters compared to the basic scenario when using the maximal rate coefficients ($k_{acid} = 6.3 \times 10^{-4}$ and $k_{neutral} = 9.5 \times 10^{-9}$ mol m^{-2} s^{-1}) and increased in factors of between 15 and 26 when using the minimal rate coefficients instead ($k_{acid} = 2.0 \times 10^{-5}$ and $k_{neutral} = 5.0 \times 10^{-13}$ mol m^{-2} s^{-1}). On an absolute scale, the range of the anorthite dissolution time was smallest for the Buntsandstein formation water ($1.3 \times 10+5$ days) and largest for the Quaternary formation water ($1.3 \times 10^{+6}$ days, Figure 3.5).

3.4. Discussion

In this study, the relative model uncertainty of the anorthite dissolution time length determined by varying the thermodynamic database is 88 % and corresponds well to relative uncertainties quantified by Dethlefsen et al. (2012), Gaus et al. (2008), and Haase et al. (2013). Nordstrom et al. (1979) demonstrated that the thermodynamic databases, number of ion pairs and complexes, and the form of activity coefficients were prominent factors influencing the simulated results. Beyond the scope of previous studies, this study also quantified the sources influencing the dissolution time length of anorthite using a calculation matrix, whereby the influence of individual database parameters was analysed.

The negligible influence of using different numerical codes (in this study smaller than 1 %) was also acknowledged by studies of INTERA (1983) and Brown et al. (2000). These authors compared simulation results of different geochemical codes (i. e. PHREEQC, EQ3/6, and HYDROGEOCHEM)

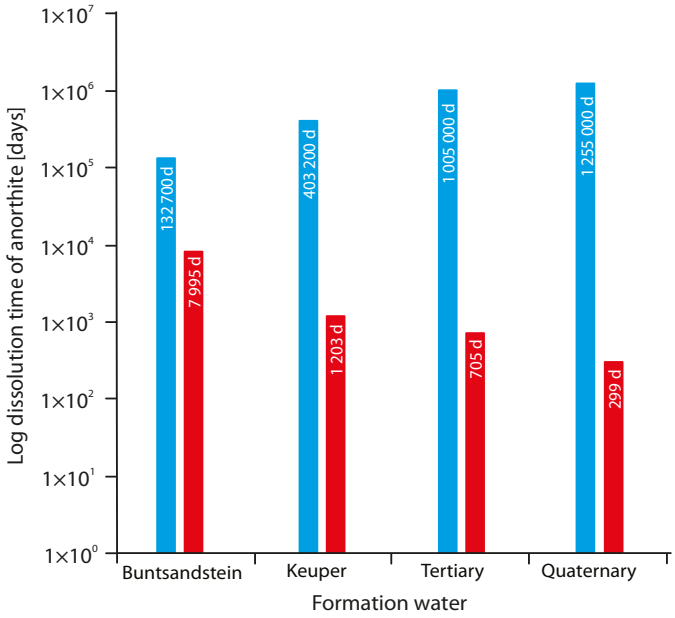

Figure 3.6

Comparison of the range of the anorthite dissolution time lengths caused by varying numerical codes and thermodynamic databases (red bars) and by varying the kinetic rate coefficients using different formation waters (blue bars). Note that the vertical axis is in logarithmic scale.

using similar databases resulting in nearly identical results. However, Benbow et al. (2008) calculated differing results at high ionic strength converting a Pitzer database from EQ3/6 for the use with PHREEQC. Benbow et al. (2008) attributed the differences to numerical methods, conversion of activities and concentrations, and activity coefficient calculations, which also have a high impact on simulation results in the presented study. The results furthermore showed that the percentage ratio for the parameters' influence varies depending on the combination order of varying the database parameters, because the parameters are code dependent. However, a classification of parameters influencing the results of geochemical codes was evaluated in this study revealing that the activity calculation of main aquatic species has the strongest influence on the simulation results.

The Pitzer databases (Pitzer, 1973) were not applied in this study as the application of Pitzer databases is not possible for the defined geochemical problem. Nevertheless, the pH of the Buntsandstein formation water calculated by applying *pitzer.dat* with PHREEQC neglecting Al and Si mineral phases differs in only 0.1 from the pH calculated by using the *phreeqc.dat* database. Therefore, the pH calculated by *pitzer.dat* is in the range of the pH values calculated by the other databases applied in this study. The application of the *pitzer.dat* database calculating the anorthite dissolution time length, had Al and Si been included, would probably deliver similar results compared to the calculation using the *phreeqc.dat* database as the pH controls the initial dissolution rates controlling the dissolution velocity in our model system. Consequently, it is supposed that the differences to the results of this study will be small for modelling CO_2 storage scenarios applying Pitzer databases.

For the simulation of site-specific reactive transport models, further sources for uncertainties may arise, i. e. different mineralogical and hydrogeological parameters for the formation, different kinetic parameters (i. e. rate constants, activation energy, and surface area; i. e. Balashov et al., 2013; Wald-

mann et al., 2014; Arvidsson et al., 2003; Black et al., 2014), an open or closed system with respect to CO_2, different boundary conditions, and finally different model scales. Examples for parameters characterizing the formation are the plagioclase content, which varies in possible storage formations such as the Middle Buntsandstein in Northern Germany between 0.5 and 14.0 wt-% (Dethlefsen et al., 2014). Simulating dissolution kinetics, the rate constants have a broad range determined by experiments (Black et al., 2014; Arvidsson et al., 2003)—especially at high temperatures and high salinities dissolution rates are unknown—and can lead to large uncertainties in simulation results as shown by this study in comparison to the influence of selecting thermodynamic databases (Figure 3.6). Calculating the solubility of CO_2 applying an open system—different to the presented study—can incorporate significant uncertainties in model predictions for solubilities and concentrations (Gundogan et al., 2011; Haase et al., 2013; Kervévan et al., 2005; Thomas et al., 2012). The hydrodynamic parameters and their heterogeneities in the geologic subsoil can further influence the prediction of reactive transport models (i. e. Bauer et al., 2006; Carrera 1993; Walker et al. 2003; Ambrose et al., 2007; Watanabe et al., 2010; Atchley et al., 2014; Refsgaard et al., 2012). The investigated uncertainties influence the prognosis of processes such as the pH buffer capacity of near-surface formations, reaction front positions, and mineral trapping in CO_2 storage formations. For predicting uncertainties of reactive transport models, the variations in mineralogical and also in hydraulic parameters are also important, but quantifying these uncertainties to general values is not possible, since they could only be quantified for certain field scale models. Despite the large parameter uncertainties, the relative model uncertainty due to using different model codes and thermodynamic databases will persist for every setting—independently from additional uncertainties—and add up on the simulation uncertainty. It is in the modeller's responsibility to choose a thermodynamic database to the best knowledge and to be aware of resulting uncertainties.

In this study, the model uncertainty was largest using the Buntsandstein formation water and using different thermodynamic databases. The Buntsandstein formation could be a potential CO_2 storage formation where mineral trapping is one of the most efficient CO_2 trapping mechanisms, if sufficiently high anorthite concentrations are present in the formation. Therefore, the investigated uncertainties arising by selecting a thermodynamic database strongly affect the prediction of mineral trapping for CO_2 storage formation.

3.5. Conclusions

This study contributes to the assessment of predicting uncertainties of geochemical models using thermodynamic databases applied for CO_2 storage and leakage scenarios. In CO_2 storage formations, mineral trapping is one of the most important processes for the safe storage of CO_2 (Bachu et al., 2007; Matter and Kelemen, 2009) and the accurate prediction of stored CO_2 is of greatest importance, but exactly this prediction comprises the largest uncertainties (ca. 90 %) caused by combinations of geochemical codes and thermodynamic databases. Additionally, the parameter uncertainty affects the prediction accuracy of geochemical codes resulting from variations of rate constants. However, for near-surface formations the uncertainty is limited to 1 % arising by the selection of code and database combinations, which is negligible compared to the much greater parameter uncertainty from issues investigating heterogeneous sites. For near-surface formations, only the kinetic rate variation has a significant impact on the prediction accuracy. Being aware of these uncertainties, geochemical modellers will have a better assessment of their simulated model results.

Especially in CO_2 storage formations such as in the Buntsandstein and Keuper reservoirs, the model uncertainty originating from choosing combinations of geochemical codes and thermodynamic databases is significant because of the pH dependence in anorthite dissolution. In this study, the pH was calculated to range from ca. 4.0 to 5.5 due to CO_2 dissolution in formation waters. In this pH range, the dissolution mechanism of anorthite switches from the slow neutral mechanism to the faster acid mechanism. The pH variation increases when anorthite dissolution is simulated in formation waters with high NaCl concentrations and at high temperatures existing in deep saline formations suitable as CO_2 repositories. The investigated model uncertainties can also be important for dissolution of other silicate minerals, because the rate laws for minerals such as biotite, k-feldspar, or kaolinite also include pH dependent dissolution mechanisms. The rate constants for the dissolution mechanisms for these minerals also vary in some orders of magnitude. In this study, large differences of dissolution time lengths were simulated exemplarily for anorthite, but the consequences of calculating pH variations by different thermodynamic databases can also cause large uncertainties of the dissolution time length for the above mentioned mineral phases in CCS.

Although applying numerical models leads to uncertainties in the simulation results, the models are state-of-the-art and are applied for the prognosis of the impact of CO_2 on geologic formations. The main sources for these uncertainties were identified by developing a calculation matrix to investigate the influence of database parameters. When thermodynamic databases are used for geochemical codes it is not possible to establish exact values for a database parameters' influence. The ratio can vary depending on the order implementing parameters in the calculation matrix. When the impact of database parameters is needed to be quantified for geochemical models, a calculation matrix according to the scheme developed in this study has to be established; otherwise it is not possible to quantify values for the uncertainty sources.

For complex systems such as geochemical systems of near-surface or storage formations, a calibration of numerical codes and thermodynamic databases is not possible. Until now, thermodynamic databases are calibrated to experiments, mostly consisting of simple reaction systems. However, it is not possible to validate a thermodynamic database due to the large number of chemical and physical processes proceeding in complex geological systems. Reaction transport models simulating complex geological systems for i. e. CO_2 storage incorporate uncertainties due to using thermodynamic databases. Validating a thermodynamic database to complex geological systems is not possible because it diverges from limited experimental systems. The quantification of uncertainties according to this study is essential for assessing the reliability of model predictions. For specifying uncertainties caused by thermodynamic databases the modeller is encouraged to incorporate a routine in the simulation setup to quantify the uncertainties especially for the constructed model scenario.

Acknowledgements

This study was funded by the German Federal Ministry of Education and Research (BMBF), EnBW Energie Baden-Württemberg AG, E.ON Energie AG, E.ON Gas Storage AG, RWE Dea AG, Vattenfall Europe Technology Research GmbH, Wintershall Holding AG and Stadtwerke Kiel AG as part of the CO_2-MoPa joint project in the framework of the Special Program GEOTECHNOLOGIEN.

Appendix A

Calculation matrix using synthetic formation water

A calculation matrix was developed in order to compare the parameter's influence of thermodynamic databases using simplified zero- and one-dimensional scenarios (Table A1). The scenarios were established at a temperature range from 25 °C to 60 °C and a NaCl concentration range from 0.1 to 4.0 molar. Additionally, CO_2 was added as irreversible reaction.

In general, the thermodynamic databases differ in a large number of parameters (Section 3.2.1). Large differences in prediction results were originated between applying *themo.com.v8.r6+.dat* and *phreeqc.dat* for the Buntsandstein formation water and were selected for the use in the calculation matrix. The two databases were synchronized by steps 2–5 (Table A1). The dissolution time difference of anorthite was calculated in steps 1–5. The steps are: (1) using the original databases (2 a) the calculation method for the CO_2 activity coefficient of the *phreeqc.dat* database was used for both databases (2 b) the mineral's equilibrium constants of the *thermo.com.v8.r6+.dat* database were applied for both databases (3) additionally to the identical CO_2 activity coefficient calculation method, the aquatic species were reduced to the same number out of both databases (4) additionally to step (3), the activity coefficient calculation of the main aquatic species was similar (5) Synchronized databases were used.

Table A1

Calculation matrix for database synchronization using a synthetic formation water. Numbers are the percentage differences in relation to the arithmetic mean between applying *phreeqc.dat* and *thermo.com.v8r6+.dat* synchronizing the databases by parameter synchronization (steps 1–5).

		without CO_2				0.5 mol CO_2/kgw				Kinetic controlled reaction	Equilibrium reaction
NaCl concentration		0.1 mol/kgw		4.0 mol/kgw		0.1 mol/kgw		4.0 mol/kgw			
Temperature [°C]		25	60	25	60	25	60	25	60	–	–
zero dimensional scenarios (comparison parameters: difference of H^+-activity/anorthite solubility)											
similar databases	H^+	0.04	1.06	0.06	0.99	0.05	0.02	0.06	0.02	–	–
	Δ Anorthite	18.8	30.2	30.2	45.3	0.28	0.32	0.43	0.34	–	Anorthite
one dimensional scenarios (comparison parameter: difference of dissolution time length [%])											
1. original databases		–	–	–	–	0.53	0.73	4.63	6.16	Anorthite	Calcite, chalcedony, kaolinite
2 a. γCO_2 = *phreeqc.dat*		–	–	–	–	0.49	0.68	2.56	3.44	Anorthite	Calcite, chalcedony, kaolinite
2 b. Log_k_{eq}(min)		–	–	–	–	0.54	0.88	4.63	6.61	Anorthite	Calcite, chalcedony, kaolinite
3. γCO_2 = *phreeqc.dat*, species reduced		–	–	–	–	0.03	0.53	2.20	1.84	Anorthite	Calcite, chalcedony, kaolinite
4. γCO_2 = *phreeqc.dat*, species reduced, $\gamma_{Species}$ = *thermo.com.v8.r6+.dat*		–	–	–	–	0.02	0.46	0.83	0.52	Anorthite	Calcite, chalcedony, kaolinite
5. synchronised databases		–	–	–	–	0.37	0.09	0.34	0.52	Anorthite	Calcite, chalcedony, kaolinite

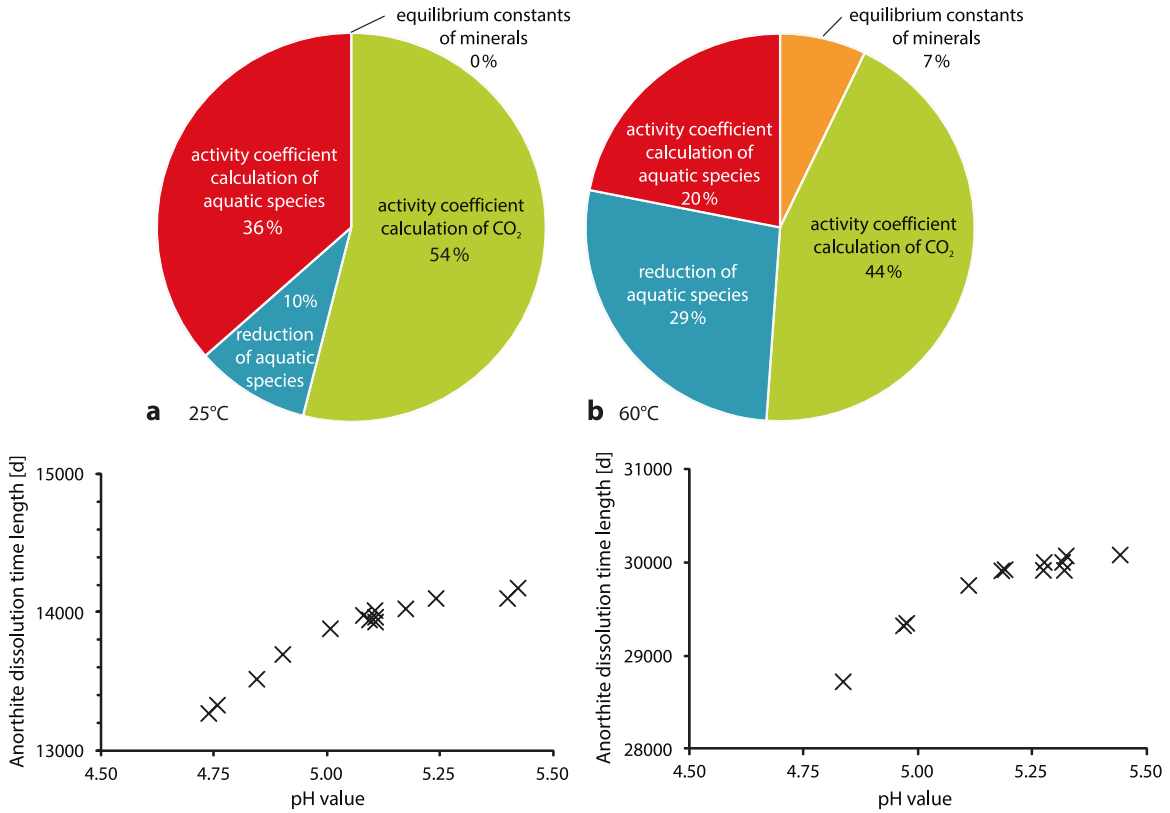

Figure A1a and A1b

Database parameters influencing the simulated results for simplified scenarios using the calculation matrix for scenarios at 25 °C (a) and at 60 °C (b). Pie charts are only shown for a concentration of 4.0 molar NaCl. The dependence of the anorthite dissolution time on the pH values is shown for both temperatures in the diagrams below.

At first the results of the zero-dimensional scenarios with equilibrium minerals were compared using similar thermodynamic databases in order to compare the numerical methods of the codes. Comparing the simulation results without mineral reactions revealed that the codes calculated nearly identical results for the H^+ activity (max. relative variation 1 %, Table A1). Including the anorthite equilibrium phase reaching the state of equilibrium thermodynamically, the relative variation of the anorthite solubility increased to ca. 45 % in the scenarios without CO_2, because the anorthite solubility was very small at these conditions (ca. $2.0–3.0 \times 10^{-07}$ mol/kgw, Table A1). At these small dimensions the impact on the simulation result by the numerical codes used is strong. Including the irreversible CO_2 reaction (0.5 molal CO_2) the variation of the anorthite solubility between the codes was smaller than 1 %. The reasons for the variations applying the different codes are diverging calculation methods for the water activity, variations in the Debye-Hückel parameters (A and B), hard-coded in PHREEQC, and different numerical methods.

Kinetically controlled anorthite dissolution is simulated in more complex one-dimensional scenarios including three equilibrium mineral phases. The relative variation in the dissolution time of anorthite in relation to the arithmetic mean is 4.63 % at 25 °C using *phreeqc.dat* and *thermo.com.v8.r6+.dat* (step (1), Table A1). Using the calculation method of the CO_2 activity coefficient from *phreeqc.dat* for

both databases yields a relative variation of 2.56 % (step (2 a)). The application of the equilibrium constants from *thermo.com.v8r6+.dat* for the instantaneously reacting minerals yields a relative variation of 4.63 % (step (2 a)). The reduction of the aquatic species generates a smaller relative variation of 2.20 % (step (3)). In step (4), the activity calculation of the aquatic species from *thermo.com.v8.r6+.dat* was applied, whereby the relative variation further reduces to 0.83 % (Table A1).

Summarizing the calculation matrix results, the calculation of the CO_2 activity coefficient influenced the simulated results strongest at 25 °C (54 %), followed by the calculation of the activity coefficients of aquatic species (36 %; Figure A1). The reduction of aquatic species had a minor impact on the model results (10 %). Using similar equilibrium constants for the mineral reactions had negligible influence on model results at 25 °C. The application of higher temperatures to the calculation matrix changed the ratios for the influence of the thermodynamic parameters. For example, the ratio of the percentage influence of the included aquatic species increased from 10 % at 25 °C to 29 % at 60 °C (Figure A1 a). Using the calculation matrix, the pH values also correlated well with the anorthite dissolution times up to a pH of 5.4 (Figure A1 b).

Appendix B

Input solutions for calculation matrix calculated by the eight thermodynamic databases for formation waters.

Table B1

Input solutions calculated for Quaternary formation water (Concentrations are in mol/kgw). Species with concentrations < 1.0×10^{-08} are not displayed.

	phreeqc.dat	*wateq4f.dat*	*minteq.dat*	*llnl.dat*	*thermo_ phreeqc.dat*	*thermo_ wateq4f.dat*	*thermo.dat*	*thermo.com. v8.r6+.dat*
pH	5.45	5.45	5.45	5.45	5.44	5.44	5.44	5.44
T [°C]	7.0	7.0	7.0	7.0	7.0	7.0	7.0	7.0
I [mol/kgw]	0.086	0.085	0.085	0.086	0.086	0.086	0.085	0.085
Al^{+3}	4.84×10^{-08}	4.82×10^{-08}	2.08×10^{-08}	5.05×10^{-08}	5.21×10^{-08}	8.11×10^{-08}	5.19×10^{-08}	5.19×10^{-08}
$AlOH^{+2}$	1.90×10^{-08}	1.90×10^{-08}	5.25×10^{-09}	2.22×10^{-08}	2.07×10^{-08}	2.07×10^{-08}	2.27×10^{-08}	2.27×10^{-08}
$Al(OH)_2^{+}$	3.7×10^{-09}	3.72×10^{-09}	1.41×10^{-08}	2.02×10^{-09}	$< 1.0\times10^{-08}$	$< 1.0\times10^{-08}$	$< 1.0\times10^{-08}$	$< 1.0\times10^{-08}$
Ca^{+2}	0.026	0.026	0.032	0.026	0.026	0.026	0.025	0.025
$CaCl^{+}$	n. a.	n. a.	n. a.	8.06×10^{-06}	n. a.	n. a.	3.34×10^{-06}	3.34×10^{-06}
$CaCl_2$	n. a.	n. a.	n. a.	2.62×10^{-08}	n. a.	n. a.	n. a.	$< 1\times10^{-08}$
$CaCO_3$	5.26×10^{-06}	5.26×10^{-06}	4.15×10^{-06}	5.78×10^{-06}	5.26×10^{-06}	5.25×10^{-06}	5.85×10^{-06}	5.85×10^{-06}
$CaOH^{+}$	6.43×10^{-10}	6.43×10^{-10}	1.69×10^{-10}	5.44×10^{-10}	$< 1\times10^{-08}$	$< 1\times10^{-08}$	$< 1\times10^{-08}$	$< 1\times10^{-08}$
$CaCO_3^{+}$	0.0050	0.0049	0.0052	0.0069	0.0051	0.0052	0.0071	0.0071
$CaHSO_4^{+}$	1.26×10^{-08}	1.27×10^{-08}	n. a.	n. a.	1.25×10^{-08}	< 1×10–8	n. a.	n. a.
$CaSO_4$	5.26×10^{-04}	5.28×10^{-04}	5.92×10^{-04}	4.46×10^{-04}	5.49×10^{-04}	5.49×10^{-04}	4.35×10^{-04}	4.35×10^{-04}
Cl^{-}	0.0037	0.0037	0.0037	0.0037	0.0015	0.0015	0.0015	0.0015
CO_2/H_2CO_3	0.47	0.047	0.47	0.47	0.5	0.50	0.50	0.50
CO_3^{-2}	8.75×10^{-07}	8.70×10^{-07}	7.55×10^{-07}	8.99×10^{-07}	8.80×10^{-07}	8.80×10^{-07}	9.10×10^{-07}	9.10×10^{-07}
H^{+}	4.24×10^{-06}	4.24×10^{-06}	6.22×10^{-06}	4.24×10^{-06}	4.35×10^{-06}	4.35×10^{-06}	4.30×10^{-06}	4.30×10^{-06}
H_4SiO_4/SiO_2	1.62×10^{-04}	1.62×10^{-04}	1.74×10^{-04}	7.21×10^{-05}	1.62×10^{-04}	1.62×10^{-04}	7.16×10^{-05}	7.16×10^{-05}
HCl	n. a.	n. a.	n. a.	2.16×10^{-09}	n. a.	n. a.	$< 1\times10^{-08}$	$< 1\times10^{-08}$
HCO_3^{-}	0.053	0.053	0.065	0.054	0.0555	0.056	0.055	0.055
HSO_4^{-}	9.55×10^{-08}	9.56×10^{-08}	1.03×10^{-07}	9.11×10^{-08}	9.51×10^{-08}	9.51×10^{-08}	9.40×10^{-08}	9.40×10^{-08}
K^{+}	1.12×10^{-04}	1.12×10^{-04}	1.13×10^{-04}	1.12×10^{-04}	1.12×10^{-04}	1.12×10^{-04}	1.12×10^{-04}	1.12×10^{-04}
KCl	n. a.	n. a.	n. a.	5.61×10^{-09}	n. a.	n. a.	$< 1.0\times10^{-8}$	$< 1.0\times10^{-08}$
KSO_4^{-}	1.73×10^{-07}	1.74×10^{-07}	1.41×10^{-07}	2.73×10^{-07}	1.70×10^{-07}	1.70×10^{-07}	2.77×10^{-07}	2.77×10^{-07}
Mg^{+2}	2.23×10^{-04}	2.23×10^{-04}	2.22×10^{-04}	2.18×10^{-04}	2.22×10^{-04}	2.22×10^{-04}	2.16×10^{-04}	2.16×10^{-04}
$MgCO_3$	2.47×10^{-08}	2.47×10^{-08}	2.04×10^{-08}	2.93×10^{-08}	2.48×10^{-08}	2.48×10^{-08}	2.94×10^{-08}	2.94×10^{-08}
$MgCO_3^{+}$	5.92×10^{-05}	5.92×10^{-05}	6.28×10^{-05}	6.25×10^{-05}	6.02×10^{-05}	6.02×10^{-05}	6.42×10^{-05}	6.42×10^{-05}
$Mg_2CO_3^{+2}$	n. a.	n. a.	n. a.	n. a.	n. a.	n. a.	$< 1.0\times10^{-08}$	n. a.
$MgSO_4$	4.27×10^{-06}	4.29×10^{-06}	3.77×10^{-06}	5.60×10^{-06}	4.14×10^{-06}	4.14×10^{-06}	5.58×10^{-06}	5.58×10^{-06}
$MgCl^{+}$	n. a.	n. a.	n. a.	3.01×10^{-07}	n. a.	n. a.	1.25×10^{-07}	1.25×10^{-07}
Na^{+}	5.45×10^{-04}	5.45×10^{-04}	5.54×10^{-04}	5.21×10^{-04}	5.46×10^{-04}	5.46×10^{-04}	5.19×10^{-04}	0.00052
$NaCO_3^{-}$	1.40×10^{-09}	1.40×10^{-09}	1.15×10^{-09}	9.97×10^{-10}	$< 1.0\times10^{-08}$	$< 1.0\times10^{-08}$	$< 1.0\times10^{-08}$	$< 1.0\times10^{-08}$
$NaCO_3$	1.15×10^{-05}	1.15×10^{-05}	7.80×10^{-06}	3.55×10^{-05}	1.07×10^{-05}	1.07×10^{-05}	3.68×10^{-05}	3.68×10^{-05}
NaCl	n. a.	n. a.	n. a.	1.79×10^{-07}	n. a.	n. a.	7.41×10^{-08}	7.41×10^{-08}
$NaSO_4^{-}$	7.62×10^{-07}	7.63×10^{-07}	6.34×10^{-07}	1.14×10^{-06}	7.46×10^{-07}	7.46×10^{-07}	1.15×10^{-06}	1.15×10^{-06}
$NaHSiO_3$	n. a.	n. a.	n. a.	3.37×10^{-11}	n. a.	n. a.	$< 1.0\times10^{-08}$	$< 1.0\times10^{-08}$
SO_4^{-2}	7.90×10^{-04}	7.88×10^{-04}	7.35×10^{-04}	8.68×10^{-04}	7.66×10^{-04}	7.66×10^{-04}	8.78×10^{-04}	8.78×10^{-04}
$SI_{Anorthite}$	–11.04	–11.04	–12.66	–12.52	–11.06	–11.06	–12.54	–12.54

Table B2

Input solutions calculated for Tertiary formation water (Concentrations are in mol/kgw). Species with concentrations < 1.0×10^{-08} are not displayed.

	phreeqc.dat	*wateq4f.dat*	*minteq.dat*	*llnl.dat*	*thermo_ phreeqc.dat*	*thermo_ wateq4f.dat*	*thermo.dat*	*thermo.com. v8.r6+.dat*
pH	5.27	5.27	5.272	5.29	5.26	5.25	5.42	5.34
T [°C]	15	15	15	15	15	15	15	15
I [mol/kgw]	1.40	1.40	1.40	1.31	1.40	1.40	1.31	1.30
Al^{+3}	1.87×10^{-07}	1.85×10^{-07}	5.41×10^{-08}	1.28×10^{-07}	2.06×10^{-07}	4.82×10^{-08}	9.55×10^{-08}	8.86×10^{-08}
$AlOH^{+2}$	6.39×10^{-08}	6.34×10^{-08}	1.41×10^{-08}	6.19×10^{-08}	2.04×10^{-08}	2.08×10^{-08}	5.99×10^{-08}	4.86×10^{-08}
$Al(OH)_2^{+}$	n. a.	n. a.	7.93×10^{-09}	3.13×10^{-09}	$< 1.0\times10^{-08}$	$< 1.0\times10^{-08}$	1.61×10^{-08}	$< 1.0\times10^{-08}$
Ca^{+2}	0.047	0.046	0.048	0.055	0.046	0.0469	0.0269	0.053
$CaCl^{+}$	n. a.	n. a.	n. a.	0.0026	n. a.	n. a.	0.039	0.0025
$CaCl_2$	n. a.	n. a.	n. a.	0.0016	n. a.	n. a.	n. a.	0.0015
$CaCO_3$	3.85×10^{-06}	3.84×10^{-06}	3.20×10^{-06}	6.32×10^{-06}	3.85×10^{-06}	3.84×10^{-06}	3.65×10^{-06}	6.38×10^{-06}
$CaOH^{+}$	4.19×10^{-10}	5.47×10^{-10}	3.46×10^{-10}	4.72×10^{-10}	$< 1.0\times10^{-08}$	$< 1.0\times10^{-08}$	$< 1.0\times10^{-08}$	$< 1.0\times10^{-08}$
$CaHCO_3^{+}$	0.0085	0.0084	0.0081	0.0088	0.0090	0.0067	0.0059	0.0079
$CaHSO_4^{+}$	6.02×10^{-09}	5.96×10^{-09}	n. a.	n. a.	$< 1.0\times10^{-08}$	$< 1.0\times10^{-08}$	n. a.	n. a.
$CaSO_4$	1.23×10^{-04}	1.34×10^{-04}	1.50×10^{-04}	1.27×10^{-04}	1.48×10^{-04}	1.50×10^{-04}	1.06×10^{-04}	1.14×10^{-04}
Cl^{-}	1.25	1.25	1.264	1.16	1.25	1.25	1.19	1.16
CO_2/H_2CO_3	0.46	0.46	0.46	0.45	0.50	0.50	0.50	0.50
CO_3^{-2}	1.76×10^{-06}	1.78×10^{-06}	1.42×10^{-06}	1.84×10^{-06}	1.79×10^{-06}	1.76×10^{-06}	2.89×10^{-06}	2.00×10^{-06}
H^{+}	7.25×10^{-06}	7.22×10^{-06}	9.45×10^{-06}	6.24×10^{-06}	7.49×10^{-06}	7.55×10^{-06}	4.66×10^{-06}	5.52×10^{-06}
H_4SiO_4/SiO_2	1.39×10^{-04}	1.39×10^{-04}	1.49×10^{-04}	1.10×10^{-04}	1.39×10^{-04}	0.00014	8.89×10^{-05}	0.00011
HCl	n. a.	n. a.	n. a.	8.02×10^{-07}	n. a.	n. a.	$< 1.0\times10^{-08}$	6.75×10^{-07}
HCO_3^{-}	0.067	0.067	0.070	0.060	0.070	0.070	0.069	0.059
HSO_4^{-}	n. a.	5.78×10^{-08}	6.01×10^{-08}	4.71×10^{-08}	4.63×10^{-08}	4.66×10^{-08}	3.98×10^{-08}	4.12×10^{-08}
K^{+}	0.0060	0.0060	0.0061	0.0060	0.0060	0.0060	0.005968	0.0060
KSO_4^{-}	2.70×10^{-06}	2.70×10^{-06}	2.19×10^{-06}	3.31×10^{-06}	2.21×10^{-06}	2.20×10^{-06}	$< 1\times10^{-08}$	$< 1\times10^{-08}$
KCl	n. a.	n. a.	n. a.	6.87×10^{-05}	n. a.	n. a.	5.50×10^{-05}	6.65×10^{-05}
Mg^{+2}	0.029	0.029	0.028	0.026	0.031	0.031	0.022	0.026
$MgCO_3$	1.74×10^{-06}	1.75×10^{-06}	1.63×10^{-06}	2.01×10^{-06}	1.89×10^{-06}	1.86×10^{-06}	1.88×10^{-06}	2.12×10^{-06}
$MgHCO_3^{+}$	0.0081	0.0082	0.0095	0.0054	0.0061	0.0061	0.0045	0.0051
$Mg_2CO_3^{+2}$	n. a.	n. a.	n. a.	n. a.	n. a.	n. a.	2.89×10^{-07}	n.a.
$MgSO_4$	1.06×10^{-04}	1.06×10^{-04}	9.60×10^{-05}	1.24×10^{-04}	0.00013	0.00013	9.38×10^{-05}	1.24×10^{-04}
$MgCl^{+}$	n. a.	n. a.	n. a.	0.0064	n. a.	n. a.	0.011	0.0064
Na^{+}	1.15	1.15	1.16	1.04	1.15	1.15	1.10	1.04
$NaCO_3^{-}$	3.36×10^{-06}	4.45×10^{-06}	3.58×10^{-06}	1.34×10^{-06}	3.31×10^{-06}	3.25×10^{-06}	2.02×10^{-06}	1.42×10^{-06}
$NaHCO_3$	0.016	0.015	0.013	0.049	0.016	0.016	0.055	0.047
NaCl	n. a.	n. a.	n. a.	0.078	n. a.	n. a.	0.010	0.077
$NaSO_4^{-}$	5.35×10^{-04}	5.22×10^{-04}	4.48×10^{-04}	5.38×10^{-04}	4.26×10^{-04}	4.25×10^{-04}	4.76×10^{-04}	5.47×10^{-04}
$NaHSiO_3$	n. a.	n. a.	n. a.	6.38×10^{-08}	n. a.	n. a.	$< 1.0\times10^{-08}$	7.20×10^{-08}
SO_4^{-2}	6.11×10^{-04}	6.13×10^{-04}	6.93×10^{-04}	5.86×10^{-04}	6.76×10^{-04}	6.75×10^{-04}	6.98×10^{-04}	5.89×10^{-04}
$SI_{Anorthite}$	−10.49	−10.49	−12.07	−12.00	−10.52	−10.52	−11.92	−11.93

Table B3

Input solutions calculated for Keuper formation water (Concentrations are in mol/kgw). Species with concentrations < 1.0×10^{-08} are not displayed.

	phreeqc.dat	*wateq4f.dat*	*minteq.dat*	*llnl.dat*	*thermo_ phreeqc.dat*	*thermo_ wateq4f.dat*	*thermo.dat*	*thermo.com. v8.r6+.dat*
pH	4.73	4.73	4.68	4.87	4.84	4.81	5.20	5.07
T [°C]	50	50	50	50	50	50	50	50
I [mol/kgw]	2.98	2.98	2.99	2.50	2.88	2.89	2.66	2.42
Al^{+3}	1.93×10^{-07}	1.94×10^{-07}	3.54×10^{-08}	2.46×10^{-08}	8.62×10^{-08}	$< 1.0\times10^{-08}$	$< 1.0\times10^{-08}$	$< 1.0\times10^{-08}$
$AlOH^{++}$	$< 1.0\times10^{-08}$	1.54×10^{-07}	2.63×10^{-08}	4.31×10^{-08}	$< 1.0\times10^{-08}$	$< 1.0\times10^{-08}$	1.75×10^{-08}	1.67×10^{-08}
$Al(OH)_2^{+}$	7.98×10^{-08}	7.99×10^{-08}	3.91×10^{-10}	5.62×10^{-09}	2.73×10^{-08}	2.92×10^{-08}	1.71×10^{-08}	$< 1.0\times10^{-08}$
$Al(OH)_3$	$< 1.0\times10^{-08}$	7.93×10^{-10}	6.32×10^{-12}	n.a.	$< 1.0\times10^{-08}$	$< 1.0\times10^{-08}$	1.10×10^{-08}	n.a.
$AlSO_4^{+}$	1.89×10^{-08}	1.94×10^{-08}	1.01×10^{-09}	8.70×10^{-10}	$<1.0\times10^{-08}$	$<1.0\times10^{-08}$	$< 1.0\times10^{-08}$	$< 1.0\times10^{-8}$
Ca^{+2}	0.077	0.078	0.072	0.075	0.045	0.051	0.021	0.045
$CaCl^{+}$	n.a.	n.a.	n.a.	0.0074	n.a.	n.a.	0.033	0.0037
$CaCl_2$	n.a.	n.a.	n.a.	0.0069	n.a.	n.a.	n.a.	0.0042
$CaCO_3$	7.52×10^{-06}	3.56×10^{-06}	3.10×10^{-06}	3.57×10^{-06}	3.65×10^{-06}	3.63×10^{-06}	3.33×10^{-06}	7.63×10^{-06}
$CaOH^{+}$	1.53×10^{-10}	3.42×10^{-10}	3.89×10^{-09}	2.05×10^{-10}	$< 1.0\times10^{-08}$	$< 1.0\times10^{-08}$	$< 1.0\times10^{-08}$	$< 1.0\times10^{-08}$
$CaHCO_3^{+}$	0.016	0.016	0.022	0.0077	0.013	0.0060	0.0037	0.0049
$CaHSO_4^{+}$	2.17×10^{-07}	2.22×10^{-07}	n.a	n.a	1.52×10^{-07}	$<1\times10^{-8}$	n.a.	n.a.
$CaSO_4$	0.00080	0.00096	0.0010	0.0011	0.00085	0.0010	0.00052	0.00059
Cl^{-}	2.82	2.82	2.85	2.35	2.74	2.75	2.56	2.30
$CO_2.H_2CO_3$	0.47	0.46	0.47	0.46	0.50	0.50	0.50	0.50
CO_3^{-2}	6.48×10^{-07}	6.45×10^{-07}	4.77×10^{-07}	1.01×10^{-06}	1.14×10^{-06}	9.96×10^{-07}	2.49×10^{-06}	1.82×10^{-06}
H^{+}	2.65×10^{-05}	2.65×10^{-05}	2.94×10^{-05}	1.48×10^{-05}	2.03×10^{-05}	2.18×10^{-05}	6.74×10^{-06}	9.40×10^{-06}
H_4SiO_4/SiO_2	0.00021	0.00021	0.00022	0.00022	0.00022	0.00022	0.00024	0.00045
HCl	n.a.	n.a.	n.a.	4.23×10^{-06}	n.a.	n.a.	$< 1.0\times10^{-8}$	2.40×10^{-06}
HCO_3^{-}	0.038	0.038	0.031	0.038	0.052	0.049	0.047	0.043
HSO_4^{-}	1.72×10^{-06}	6.76×10^{-07}	1.92×10^{-06}	1.62×10^{-06}	8.44×10^{-07}	8.92×10^{-07}	9.01×10^{-07}	1.03×10^{-06}
$HSiO_3^{-}$	n.a.	n.a.	n.a.	1.09×10^{-08}	n.a.	n.a.	n.a.	1.81×10^{-08}
$H3SiO_4^{-}$	1.32×10^{-08}	1.31×10^{-08}	1.41×10^{-08}	n.a.	$< 1.0\times10^{-8}$	$< 1.0\times10^{-8}$	2.32×10^{-08}	n.a.
K^{+}	0.0058	0.006	0.006	0.0055	0.006	0.0058	0.0056	0.0055
KCl	n.a.	n.a.	n.a.	2.49×10	n.a.	n.a.	0.00020	0.00023
KSO_4^{-}	1.58×10^{-05}	n.a.	1.33×10^{-05}	1.79×10^{-05}	1.11×10^{-05}	1.09×10^{-05}	1.84×10^{-05}	1.80×10^{-05}
Mg^{+2}	0.022	0.022	0.023	0.018	0.025	0.025	0.015	0.018
$MgCO_3$	6.59×10^{-07}	6.56×10^{-07}	6.44×10^{-07}	9.42×10^{-07}	1.28×10^{-06}	1.13×10^{-06}	1.70×10^{-06}	1.60×10^{-06}
$MgHCO_3^{+}$	0.0069	0.0069	0.0067	0.0026	0.0040	0.0037	0.0027	0.0028
$Mg_2CO_3^{++}$	n.a.	n.a.	n.a.	n.a.	n.a.	n.a.	1.78×10^{-07}	n.a.
$MgOH^{+}$	2.50×10^{-08}	2.49×10^{-08}	1.30×10^{-08}	n.a.	1.66×10^{-08}	1.56×10^{-08}	1.20×10^{-08}	n.a.
$MgSO_4$	6.91×10	9.05×10	4.16×10	0.0010	0.0012	0.0012	0.00043	0.0011
$MgCl^{+}$	n.a.	n.a.	n.a.	1.75×10^{-03}	n.a.	n.a.	0.012	0.0083
Na^{+}	2.65	2.65	2.67	2.18	2.64	2.64	2.49	2.20
$NaCO_3^{-}$	8.68×10^{-06}	1.89×10^{-05}	1.40×10^{-05}	4.51×10^{-07}	1.49×10^{-05}	1.29×10^{-05}	1.35×10^{-06}	7.84×10^{-07}
$NaHCO_3$	0.036	0.015	0.018	0.014	0.021	0.019	0.053	0.040
NaCl	n.a.	n.a.	n.a.	0.45	n.a.	n.a.	0.12	0.42
$NaSO_4^{-}$	0.0068	0.0065	0.0058	0.0057	0.0044	0.0044	0.0064	0.0060
$NaHSiO_3$	n.a.	n.a.	n.a.	3.41×10^{-07}	n.a.	n.a.	n.a.	5.47×10^{-07}
NaH_3SiO_4	n.a.	n.a.	n.a.	n.a.	n.a.	n.a.	3.62×10^{-07}	n.a.
SO_4^{-2}	0.0033	0.0034	0.0044	0.0038	0.0051	0.0051	0.0043	0.0039
$SI_{Anorthite}$	-8.16	-8.16	-9.76	-9.75	-8.18	-8.18	-9.53	-9.59

Table B4

Input solutions calculated for Buntsandstein formation water (Concentrations are in mol/kgw). Species with concentrations < 1.0×10^{-08} are not displayed.

	phreeqc.dat	*wateq4f.dat*	*minteq.dat*	*llnl.dat*	*thermo_ phreeqc.dat*	*thermo_ wateq4f.dat*	*thermo.dat*	*thermo.com. v8.r6+.dat*
pH	3.92	3.92	3.83	4.43	3.94	3.88	4.75	4.60
T [°C]	58	58	58	58	58	58	58	58
I [mol/kgw]	6.49	6.49	6.51	4.45	6.33	6.48	5.04	4.44
Al^{+3}	3.70×10^{-05}	3.70×10^{-05}	8.73×10^{-06}	2.34×10^{-07}	3.11×10^{-05}	1.81×10^{-07}	6.05×10^{-08}	6.91×10^{-08}
$AlOH^{+2}$	6.42×10^{-06}	6.42×10^{-06}	n.a.	2.30×10^{-07}	n.a.	n.a.	8.39×10^{-08}	1.02×10^{-07}
$Al(OH)_2^{+}$	6.43×10^{-07}	6.43×10^{-07}	n.a.	1.34×10^{-08}	7.83×10^{-08}	8.46×10^{-08}	3.44×10^{-08}	9.01×10^{-09}
$Al(OH)_3$	$<1.0\times10^{-08}$	$<1.0\times10^{-08}$	n.a.	n.a.	n.a.	n.a.	1.46×10^{-08}	n.a.
$AlSO_4^{+}$	3.77×10^{-07}	3.89×10^{-07}	2.72×10^{-08}	1.56×10^{-09}	7.15×10^{-08}	9.35×10^{-08}	$< 1.0\times10^{-08}$	5.02×10^{-09}
Ca^{+2}	0.46	0.46	0.43	0.32	0.39	0.46	0.12	0.30
$CaCl^{+}$	n.a.	n.a.	n.a.	0.059	n.a.	n.a.	0.35	0.055
$CaCl_2$	n.a.	n.a.	n.a.	0.12	n.a.	n.a.	n.a.	0.11
$CaCO_3$	1.72×10^{-06}	1.71×10^{-06}	1.53×10^{-06}	7.52×10^{-06}	1.78×10^{-06}	1.72×10^{-06}	3.12×10^{-06}	7.65×10^{-06}
$CaOH^{+}$	$< 1.0\times10^{-08}$	$< 1.0\times10^{-08}$	1.67×10^{-08}	$< 1.0\times10^{-08}$	$< 1.0\times10^{-08}$	$< 1.0\times10^{-08}$	$< 1.0\times10^{-08}$	$< 1.0\times10^{-08}$
$CaHCO_3^{+}$	0.088	0.088	0.16	0.015	0.087	0.012	0.0072	0.010
$CaHSO_4^{+}$	1.01×10^{-06}	1.04×10^{-06}	n.a.	n.a.	1.55×10^{-06}	n.a.	n.a.	n.a.
$CaSO_4$	0.00074	0.00091	0.0011	0.0011	0.0014	0.0016	8.01×10^{-04}	9.54×10^{-04}
Cl^{-}	5.94	5.94	5.99	4.06	5.82	5.90	4.86	4.06
CO_2	0.43	0.43	0.40	0.47	0.5	0.5	0.5	0.5
CO_3^{-2}	3.74×10^{-08}	3.74×10^{-08}	2.51×10^{-08}	1.95×10^{-07}	4.63×10^{-08}	3.70×10^{-08}	3.15×10^{-07}	2.16×10^{-07}
H^{+}	1.75×10^{-04}	1.75×10^{-04}	2.12×10^{-04}	3.39×10^{-05}	1.66×10^{-04}	1.89×10^{-04}	1.50×10^{-05}	2.32×10^{-05}
$H_4SiO_4.SiO_2$	8.90×10^{-05}	8.90×10^{-05}	9.26×10^{-05}	5.57×10^{-04}	9.29×10^{-05}	8.95×10^{-05}	2.01×10^{-04}	5.67×10^{-04}
HCl	n.a.	n.a.	n.a.	2.21×10^{-05}	n.a.	n.a.	n.a.	1.43×10^{-05}
HCO_3^{-}	0.012	0.012	0.0093	0.016	0.014	0.012	0.013	0.012
HSO_4^{-}	n.a.	n.a.	n.a.	1.03×10^{-06}	3.37×10^{-07}	3.38×10^{-07}	6.34×10^{-07}	6.98×10^{-07}
$HSiO_3^{-}$	n.a.	n.a.	n.a.	$< 1.0\times10^{-08}$	n.a.	n.a.	n.a.	$< 1.0\times10^{-08}$
$H_3SiO_4^{-}$	$< 1.0\times10^{-08}$	$< 1.0\times10^{-08}$	$< 1.0\times10^{-08}$	n.a	$< 1.0\times10^{-08}$	$< 1.0\times10^{-08}$	$< 1.0\times10^{-08}$	n.a.
K^{+}	0.021	0.021	0.021	0.019	0.021	0.021	0.019	0.019
KCl	n.a.	n.a.	n.a.	2.06×10^{-03}	n.a.	n.a.	0.0019	0.0020
KSO_4^{-}	n.a.	n.a.	n.a.	1.31×10^{-05}	1.85×10^{-06}	1.63×10^{-06}	1.44×10^{-05}	1.29×10^{-05}
Mg^{+2}	0.079	0.079	0.083	0.054	0.11	0.11	0.042	0.056
$MgCO_3$	2.25×10^{-07}	2.25×10^{-07}	2.13×10^{-07}	6.83×10^{-07}	3.63×10^{-07}	2.99×10^{-07}	7.88×10^{-07}	7.30×10^{-07}
$MgHCO_3^{+}$	0.033	0.033	0.030	0.0040	0.0054	0.0050	0.0026	0.0029
$Mg_2CO_3^{++}$	n.a.	n.a.	n.a.	n.a.	n.a.	n.a.	2.64×10^{-07}	n.a.
$MgOH^{+}$	9.44×10^{-08}	9.44×10^{-08}	4.78×10^{-08}	n.a	1.74×10^{-08}	1.55×10^{-08}	2.03×10^{-08}	n.a.
$MgSO_4$	5.82×10^{-04}	6.01×10^{-04}	3.47×10^{-04}	9.27×10^{-04}	0.0014	0.0014	3.39×10^{-04}	9.66×10^{-04}
$MgCl^{+}$	n.a.	n.a.	n.a.	0.053	n.a.	n.a.	0.067	0.053
Na^{+}	4.74	4.74	4.78	3.19	4.73	4.73	4.11	3.22
$NaCO_3^{-}$	5.42×10^{-07}	3.98×10^{-06}	2.68×10^{-06}	9.55×10^{-08}	6.20×10^{-07}	4.79×10^{-07}	2.33×10^{-07}	1.03×10^{-07}
$NaHCO_3$	0.0055	0.0058	0.0072	0.025	0.0069	0.0062	0.032	0.019
NaCl	n.a.	n.a.	n.a.	1.53	n.a.	n.a.	0.60	1.50
$NaSO_4^{-}$	0.0026	0.0024	0.0022	0.0018	0.00056	0.00051	0.0025	0.0018
$NaHSiO_3$	n.a.	n.a.	n.a.	2.71×10^{-07}	n.a.	n.a.	n.a.	4.03×10^{-07}
NaH_3SiO_4	n.a.	n.a.	n.a.	n.a.	n.a.	n.a.	3.11×10^{-07}	4.11×10^{-07}
SO_4^{-2}	6.41×10^{-04}	6.62×10^{-04}	9.71×10^{-04}	8.48×10^{-04}	0.0012	0.0011	9.69×10^{-04}	8.61×10^{-04}
$SI_{Anorthite}$	−7.89	−7.89	−9.56	−9.34	−7.94	−7.85	−9.04	−9.05

References

Ambrose W. A., Lakshminarasimhan S., Holtz M. H. Holtz, M. H., Núñez-López, V., Hovorka, S. D. & Duncan, I. 2007. Geologic factors controlling CO_2 storage capacity and permanence: case studies based on experience with heterogeneity in oil and gas reservoirs applied to CO_2 storage. Environmental Geology 54(8), 1619–1633. *doi:10.1007/s00254-007-0940-2*

Amrhein, A. & Suarez, D. L. 1988. The use of a surface complexation model to describe the kinetics of ligand-promoted dissolution of anorthite. Geochimica et Cosmochimica Acta 52(12), 2785–2793. *doi: 10.1016/0016-7037(88)90146-9*

Amrhein, C. & Suarez, D. L., 1992. Some factors affecting the dissolution kinetics of anorthite at 25 °C. Geochimica et Cosmochimica Acta 56(5), 1815–1826. *doi:10.1016/0016-7037(92)90312-7*

Arvidson, R. S., Ertan, I. E., Amonette, J. E. & Luttge, A. 2003. Variation in calcite dissolution rates, Geochimica et Cosmochimica Acta 67(9), 1623–1634. *doi: 10.1016/S0016-7037(02)01177-8*

Audigane, P., Gaus, I., Pruess, K. & Xu, T. 2006. A long term 2D vertical modelling study of CO_2 Storage at Sleipner (North Sea) using TOUGHREACT, in: Proceedings, TOUGH Symposium 2006. Lawrence Berkeley National Laboratory, Berkeley, California, USA, p. 8.

Atchley, A. L., Navarre-Sitchler, A. K. & Maxwell, R. M. 2014. The Effects of Physical and Geochemical Heterogeneity on Hydro-geochemical Transport and Effective Reaction Rates. Journal of Contaminant Hydrology. 165(2014), 53–64. *doi:10.1016/j.jconhyd.2014.07.008*

Bachu, S., Bonijoly, D., Bradshaw, J., Burruss, R., Holloway, S., Christensen, N. P. & Mathiassen, O. M. 2007. CO_2 storage capacity estimation: Methodology and gaps. International Journal of Greenhouse Gas Control 1(4), 430–443. *doi:10.1016/S1750-5836(07)00086-2*

Bachu, S., Gunter, W. D. & Perkins, E. H., 1994. Aquifer disposal of CO_2: Hydrodynamic and mineral trapping. Energy Conversion and Management 35(4), 269–279. *doi:10.1016/0196-8904(94)90060-4*

Balashov, V. N., Guthrie, G. D., Hakala, J. A., Lopano, C. L., Rimstidt, J. D. & Brantley, S. L. 2013. Predictive modeling of CO_2 sequestration in deep saline sandstone reservoirs: Impacts of geochemical kinetics. Applied Geochemistry 30(March 2013), 41-56. *doi:10.1016/j.apgeochem.2012.08.016*

Bauer, S., Beyer, C. & Kolditz, O. 2006. Assessing measurement uncertainty of first-order degradation rates in heterogeneous aquifers. Water Resources Research 42(1–2), 1–14. *doi:10.1016/j.jconhyd.2006.04.006*

Bazin, B., Brosse, É. & Sommer, F. 1997. Chemistry of oil-field brines in relation to diagenesis of reservoirs: 2. Reconstruction of palaeo-water composition for modelling illite diagenesis in the Greater Alwyn area (North Sea). Marine and Petroleum Geology 14(5), 497–511. *doi:10.1016/S0264-8172(97)00005-6*

Benbow, S., Metcalfe, R. & Wilson, J. 2008. Pitzer databases for use in thermodynamic modeling. Technical Memorandum, Quintessa.

Berg, A. & Banwart, S. A. 2000. Carbon dioxide mediated dissolution of Ca-feldspar: Implications for silicate weathering. Chemical Geology 163(1–4), 25–42. *doi:10.1016/S0009-2541(99)00132-1*

Berger, P. M., Roy, W. R. & Mehnert, E. 2009. Geochemical Modeling of Carbon Sequestration, MMV, and EOR in the Illinois Basin. Energy Procedia 1(1), 3437–3444. *doi:10.1016/j.egypro.2009.02.134*

Berner, R. A. & Morse, J. W. 1974. Dissolution kinetics of calcium carbonate in seawater: IV. Theory of calcite dissolution. American Journal of Science 274(2), 108–134. *doi:10.2475/ajs.274.2.108*

Bethke, C. M. & Yeakel, S. 2012. The Geochemist's Workbench Release 9.0.

Bethke, C. M. 2008. Geochemical and Biogeochemical Reaction Modeling. Cambridge University Press, Cambridge.

Beyer, C., Li, D., Lucia, M. D., Kühn, M. & Bauer, S. 2012. Modelling CO_2-induced fluid-rock interactions in the Altensalzwedel gas reservoir. Part II: Coupled reactive transport simulation. Environmental Earth Sciences 67(2), 573–588. *doi:10.1007/s12665-012-1684-1*

Black, J. R., Carroll, S. A. & Haese, R. R. (2015). Rates of mineral dissolution under CO_2 storage conditions. Chemical Geology 399(2 April 2015), 134–144. *doi:10.1016/j.chemgeo.2014.09.020*

Blum, A. E. 1994. Feldspars in Weathering, in: Parsons, I. (Ed.), Feldspars and Their Reactions. Kluwer Academic Publishers, Dordrecht, The Netherlands, p. 665.

Blum, A. E. & Lasaga, A. C. 1988. Role of surface speciation in the low-temperature dissolution of minerals. Nature 331(4), 431–433. *doi:10.1038/33143140*

Blum, A. E. & Lasaga, A. C. 1991. The role of surface speciation in the dissolution of albite. Geochimica et Cosmochimica Acta 55(8), 2193–2201. *doi:10.1016/0016-7037(91)90096-N*

Busenberg, E. & Clemency, C. V. 1976. The dissolution kinetics of feldspars at 25 °C and 1 atm CO_2 partial pressure. Geochimica et Cosmochimica Acta 40(1), 41–49. *doi:10.1016/0016-7037(76)90192-7*

Brendler, V., Richter, A. & Gester, S. 2009. The THEREDA-Thermodynamic Reference Database for nuclear waste disposal in Germany. WM2009 Conference. p. 7.

Brown, J. G., Bassett, R. L. & Glynn, P. D. 2000. Reactive transport of metal contaminants in alluvium-model comparison and column simulation. Applied Geochemistry 15(1), 35–49. *doi:10.1016/S0883-2927(99)00004-9*

Cantucci, B., Montegrossi, G., Vaselli, O., Tassi, F., Quattrocchi, F. & Perkins, E. H. 2009. Geochemical modeling of CO_2 storage in deep reservoirs: The Weyburn Project (Canada) case study. Chemical Geology 265, 181–197. *doi:10.1016/j.chemgeo.2008.12.029*

Carlé, W., 1975. Die Mineral- und Thermalwässer von Mitteleuropa: Geologie, Chemismus, Genese. Wissenschaftliche Verlagsgesellschaft, Stuttgart.

Carrera, J. 1993. An overview of uncertainties in modelling groundwater solute transport. Journal of Contaminant Hydrology 13(1–4), 23–48. *doi:10.1016/0169-7722(93)90049-X*

Carroll, S., Hao, Y. & Aines, R. 2009. Geochemical detection of carbon dioxide in dilute aquifers. Geochemical Transactions 10(4), 18. *doi:10.1186/1467-4866-10-4*

Casey, W. H., Westrich, H. R. & Holdren, G. R., 1991. Dissolution rates of plagioclase at pH = 2 and 3. American Mineralogist 76(1–2), 211–217.

Chou, L. & Wollast, R., 1985. Steady-state kinetics and dissolution mechanisms of albite. American Journal of Science 285(10), 963–993. *doi:10.2475/ajs.285.10.963*

Compton, R. G. & Daly, P. J., 1987. The dissolution/precipitation kinetics of calcium carbonate: An assessment of various kinetic equations using a rotating disk method. Journal of Colloid and Interface Science 115,(2) 493–498. *doi:10.1016/0021-9797(87)90066-x*

Cleverley, J. S. & Bastrakov, E. N. (2005). K2GWB: Utility for generating thermodynamic data files for The Geochemist's Workbench® at 0-1000 °C and 1-5000bar from UT2K and the UNITHERM database. Computers & Geosciences, 31(6), 756–767. *doi:10.1016/j.cageo.2005.01.007*

Dethlefsen, F., Ebert, M. & Dahmke, A. 2014. A Geological Database for Parameterization in Numerical Modeling of Subsurface Storage in Northern Germany. Environmental Earth Sciences 71(5), 2227-2244. *doi:10.1007/s12665-013-2627-1*

Dethlefsen, F., Haase, C., Ebert, M. & Dahmke, A. 2012. Uncertainties of geochemical modeling during CO_2 sequestration applying batch equilibrium calculations. Environmental Earth Sciences 65(4), 1105–1117. *doi:10.1007/s12665-011-1360-x*

Dethlefsen, F., Köber, R., Schäfer, D., al Hagrey, S. A., Hornbruch, G., Ebert, M., Beyer, M., Großmann, J. & Dahmke, A. 2013. Monitoring Approaches for Detecting and Evaluating CO_2 and Formation Water Leakages into Near-surface Aquifers. Energy Procedia 37, 4886–4893. *doi:10.1016/j.egypro.2013.06.399*

Gaus, I., Audigane, P., André, L., Lions, J., Jacquemet, N., Durst, P., Czernichowski-Lauriol, I. & Azaroual, M. 2008. Geochemical and solute transport modelling for CO_2 storage, what to expect from it? International Journal of Greenhouse Gas Control 2(4), 605–625. *doi:10.1016/j.ijggc.2008.02.011*

Gaus, I., Azaroual, M. & Czernichowski-Lauriol, I. 2005. Reactive transport modelling of the impact of CO_2 injection on the clayey cap rock at Sleipner (North Sea). Chemical Geology 217(3–4), 319–337. *doi:10.1016/j.chemgeo.2004.12.016*

Gherardi, F., Xu, T. & Pruess, K. 2007. Numerical modeling of self-limiting and self-enhancing caprock alteration induced by CO_2 storage in a depleted gas reservoir. Chemical Geology 244(1–2), 103–129. *doi:10.1016/j.chemgeo.2007.06.009*

Gilfillan, S. M. V, Lollar, B. S., Holland, G., Blagburn, D., Stevens, S., Schoell, M., Cassidy, M., Ding, Z., Zhou, Z., Lacrampe-couloume, G. & Ballentine, C. J. 2009. Solubility trapping in formation water as dominant CO_2 sink in natural gas fields. Nature 458(7238), 614–618. *doi:10.1038/nature07852*

Großmann, J., Naue, G., Schreck, A., Woiwode, R., Bauer, S., Dahmke, A., Ebert, M., Schäfer, D., Reinicke, K. M., Schilling, F. & Krawczyk, C. 2011. Sicherheit und Umweltverträglichkeit der CO_2-Speicherung. Report for the German Federal Environmental Agency. Dessau-Roßlau.

Gundogan, O., Mackay, E. & Todd, A. 2011. Comparison of numerical codes for geochemical modelling of CO_2 storage in target sandstone reservoirs. Chemical Engineering Research and Design 89(9), 1805–1816. *doi:10.1016/j.cherd.2010.09.008*

Gunter, W. D., Perkins, E. H. & McCann, T. J. 1993. Aquifer disposal of CO_2-rich gases: Reaction design for added capacity. Energy Conversion and Management 34(9–11), 941–948. *doi:10.1016/0196-8904(93)90040-H*

Haase, C., Dethlefsen, F., Ebert, M. & Dahmke, A. 2013. Uncertainty in geochemical modelling of CO_2 and calcite dissolution in NaCl solutions due to different modelling codes and thermodynamic databases. Applied Geochemistry 33(2013), 306–317. *doi:10.1016/j.apgeochem.2013.03.001*

Haase, C., Dahmke, A., Schäfer, D. & Dethlefsen, F. 2014. Suitability of existing numerical model codes and thermodynamic databases for the prognosis of calcite dissolution processes in near-surface sediments due to a CO_2 leakage investigated by column experiments. Aquatic Geochemistry 20(6), 639–661. *doi:10.1007/s10498-014-9240-0*

Helgeson, H. C. 1969. Thermodynamics of hydrothermal systems at elevated temperatures and pressures. American Journal of Science 267(7), 729–804. *doi:10.2475/ajs.267.7.729*

Hellevang, H., Aagaard, P., Oelkers, E. H. & Kvamme, B. 2005. Can dawsonite permanently trap CO_2? Environmental Science & Technology 39(21), 8281–8287. *doi:10.1021/es0504791*

Hellevang, H., Pham, V. T. H. & Aagaard, P. 2013. Kinetic modelling of CO_2-water-rock interactions. International Journal of Greenhouse Gas Control 15(July 2013), 3–15. *doi:10.1016/j.ijggc.2013.01.027*

Hellmann, R. 1994. The albite-water system: Part I. The kinetics of dissolution as a function of pH at 100, 200, and 300 °C. Geochimica et Cosmochimica Acta 58(2), 595–611. *doi:10.1016/0016-7037(94)90491-X*

Hellmann, R. 1995. The albite-water system: Part II. The time-evolution of the stoichiometry of dissolution as a function of pH at 100, 200, and 300 °C. Geochimica et Cosmochimica Acta 59(9), 1669–1697. *doi:10.1016/0016-7037(95)00075-B*

Holdren, G. R. & Speyer, P. M. 1987. Reaction rate-surface area relationships during the early stages of weathering. II. Data on eight additional feldspars. Geochimica et Cosmochimica Acta 51(9), 2311–2318.

INTERA, 1983. Geochemical models suitable for performance assessment of nuclear waste storage: Comparison of PHREEQE and EQ3/EQ6. INTERA Environmental Consultants Inc. Technical Report ONWI-473, 114.

Johnson, J. W., Nitao, J. J., Steefel, C. I. & Knauss, K. G. 2001. Reactive transport modeling of geologic CO_2 sequestration in saline aquifers: The influence of intra-aquifer shales, in: Proceedings of the 1st National Conference on Carbon Sequestration. p. 60.

Huertas, F. J., Chou, L. & Wollast, R. 1999. Mechanism of kaolinite dissolution at room temperature and pressure Part II: kinetic study. Geochimica et Cosmochimica Acta 63(19–20), 3261–3275. *doi:10.1016/S0016-7037-(99)00249-5*

Johnson, J. W., Nitao, J. J. & Knauss, K. G. 2004. Reactive transport modeling of CO_2 storage in saline aquifers to elucidate fundamental processes, trapping mechanisms and sequestration partitioning. Technical report UCRL-JRNL-205627. Lawrence Livermore National Laboratory (LLNL). Livermore, California. Geological Society of Lonon Special Publication on Carbon Sequestration Technologies. p. 45.

Kervévan, C., Azaroual, M. & Durst, P. 2005. Improvement of the Calculation Accuracy of Acid Gas Solubility in Deep Reservoir Brines: Application to the Geological Storage of CO_2. Oil & Gas Science and Technology 60(2), 357–379. *doi:10.2516/ogst:2005022*

Knauss, K. G. & Wolery, T. J. 1986. Dependence of albite dissolution kinetics on pH and time at 25 °C and 70 °C. Geochimica et Cosmochimica Acta 50(11), 2481–2497. *doi:10.1016/0016-7037(86)90031-1*

Kolditz, O., Bauer, S., Beyer, C., Böttcher, N., Dietrich, P., Görke, U.-J., Kalbacher, T., Park, C.-H., Sauer, U., Schütze, C., Shao, H., Singh, A., Taron, J., Wang, W. & Watanabe, N. 2012. A systematic benchmarking approach for geologic CO_2 injection and storage. Environmental Earth Sciences 67(2), 613-632. *doi:10.1007/s12665-012-1656-5*

Kühn, M., Bartel, J. & Iffland, J. 2002. Predicting reservoir property trends under heat exploitation: interaction between flow, heat transfer, transport, and chemical reactions in a deep aquifer at Stralsund, Germany. Geothermics 31(6), 725–749. doi:10.1016/S0375-6505(02)00033-0

Lasaga, A. C. 1981. Rate laws of chemical reactions. Reviews in Mineralogy and Geochemistry 8(3), 1–68.

Lasaga, A. C. 1984. Chemical Kinetics of Water-Rock. Journal of Geophysical Research 89(B6), 4009–4025. *doi:10.1029/JB089iB06p04009*

Lasaga, A. C. 1995. Fundamental approaches in describing mineral dissolution and precipitation rates. Reviews in Mineralogy and Geochemistry 31(1), 23–86.

Lasaga, A. C., Soler, J. M., Ganor, J., Burch, T. E. & Nagy, K. L. 1994. Chemical weathering rate laws and global geochemical cycles. Geochimica et Cosmochimica Acta 58(10), 2361–2386. *doi:10.1016/0016-7037(94)90016-7*

Lu, J., Partin, J. W., Hovorka, S. D., Wong, C. 2010. Potential risks to freshwater resources as a result of leakage from CO_2 geological storage: A batch-reaction experiment. Environmental Earth Sciences 60(2), 335–348. *doi:10.1007/s12665-009-0382-0*

Matter, J. M. & Kelemen, P. B., 2009. Permanent storage of carbon dioxide in geological reservoirs by mineral carbonation. Nature Geoscience 2(12), 837–841. *doi:10.1038/ngeo683*

Metz, B., Davidson, O., Coninck, H.D., Loos, M. & Meyer, L. 2005. IPCC special report on carbon dioxide capture and storage. Geneva, Switzerland.

Moore, J., Adams, M., Allis, R., Lutz, S., Rauzi, S., 2005. Mineralogical and geochemical consequences of the long-term presence of CO_2 in natural reservoirs: An example from the Springerville-St. Johns Field, Arizona, and New Mexico, U.S.A. Chemical Geology 217(3–4), 365–385. *doi:10.1016/j.chemgeo.2004.12.019*

Nordstrom D. K., Plummer L. N., Wigley T. M. L., Wolery, T. J., Ball, J. W., Jenne, E. A., Bassett, R. L., Crear, D. A., Florence, T. M., Fritz, B., Hoffman, M., Holdren, G. R., Lafon, G. M., Mattigod, S. V., McDuff, R. E., Morel, F., Reddy, M. M., Sposito, G. & Thrailkill, J. 1979. A Comparison of Computerized Chemical Models for Equilibrium Calculations in Aqueous Systems. In: Jenne, E. A. (ed) Chemical Modeling in Aqueous Systems–Speciation, Sorption, Solubility, Kinetics. American Chemical Society, Washington, D. C., pp. 857–892. *doi:10.1021/bk-1979-0093*

Oelkers, E. H. & Schott, J. 1995. Experimental study of anorthite dissolution and the relative mechanism of feldspar hydrolysis. Geochimica et Cosmochimica Acta 59(24), 5039–5053. *doi:10.1016/0016-7037(95)00326-6*

Palandri, J. L. & Kharaka, Y. K. 2004. A compilation of rate parameters of water-mineral interaction kinetics for application to geochemical modeling. U. S. Geological Survey Open file Report 2004-1068, 71.

Pang, L. S. K., George, S. C. & Quezada, R. A. 1998. A study of the gross compositions of oil-bearing fluid inclusions using high performance liquid chromatography. Organic Geochemistry 29(5–7), 1149-1161.

Pang, Z.-H. & Reed, M., 1998. Theoretical Chemical Thermometry on Geothermal Waters: Problems and Methods. Geochimica et Cosmochimica Acta 62(6), 1083–1091. *doi:10.1016/S0016-7037(98)00037-4*

Parkhurst, D. L., Appelo, C. A. J. 1999. User's Guide to PHREEQC (Version 2): A Computer Program for Speciation, Batch-Reaction, One-Dimensional Transport, and Inverse Geochemical Calculations, Water-Resources Investigations Report 99-4259. Denver, Colorado, USA.

Peter, A., Lamert, H., Beyer, M., Hornbruch, G., Heinrich, B., Schulz, A., Geistlinger, H., Schreiber, B., Dietrich, P., Werban, U., Vogt, C., Richnow, H.-H., Großmann, J. & Dahmke, A. 2012. Investigation of the geochemical impact of CO_2 on shallow groundwater: Design and implementation of a CO_2 injection test in Northeast Germany. Environmental Earth Sciences 67(2), 335–349. *doi:10.1007/s12665-012-1700-5*

Pitzer, K. S. 1973. Thermodynamics of electrolytes. I. Theoretical basis and general equations. The Journal of Physical Chemistry 77(7), 268–277. *doi:10.1007/BF00648138*

Pitzer, K. S. & Mayorga, G., 1973. Thermodynamics of Electrolytes. II. Activity and Osmotic Coefficients for strong electrolytes with one or both ions univalent. The Journal of Physical Chemistry 77, 2300-2308. *doi:10.1021/j100638a009*

Pitzer, K. S. & Mayorga, G. 1974. Thermodynamics of electrolytes. III. Activity and Osmotic Coefficients for 2-2 Electrolytes. Journal of Solution Chemistry 3(7), 539–546. *doi:10.1007/BF00648138*

Plummer, L. N., Wigley, T. M. L., Parkhurst, D. L., 1978. The kinetics of calcite dissolution in CO_2-water systems at 5 to 60 °C and 0.0 to 1.0 atm CO_2. American Journal of Science 278(2), 179–216. *doi:10.2475/ajs.278.2.179*

Pruess, K., Xu, T., Apps, J. & Garci, J. 2003. Numerical modeling of aquifer disposal of CO_2. Society of Petroleum Engineers Journal 8(1), 12. *doi:10.2118/83695-PA*

Reddy, M. M., Plummer, L. N. & Busenberg, E. 1981. Crystal growth of calcite from calcium bicarbonate solutions at constant pCO_2 and 25 °C: A test of the calcite dissolution model. Geochimica et Cosmochimica Acta 45(8), 1281–1291. *doi:10.1016/0016-7037(81)90222-2*

Refsgaard, J. C., Christensen, S., Sonnenborg, T. O., Seifert, D., Højberg, A. L. & Troldborg, L. 2012. Review of strategies for handling geological uncertainty in groundwater flow and transport modeling. Advances in Water Resources. 36(2012), 36–50. *doi:10.1016/j.advwatres.2011.04.006*

Seibt, A., Kellner, T. & Hoth, P. 1997. Geowissenschaftliche Bewertungsgrundlagen zur Nutzung hydrogeothermaler Ressourcen in Norddeutschland. Scientific Technical Report 97/15 of the German Research Centre for Geosciences (GFZ). Potsdam.

Svensson, U. & Dreybrodt, W. 1992. Dissolution kinetics of natural calcite minerals in CO_2-water systems approaching calcite equilibrium. Chemical Geology 100(1–2), 129–145. *doi:10.1016/0009-2541(92)90106-F*

Sverdrup, H. U., 1990. The kinetics of base cation release due to chemical weathering. Lund University Press, Lund, Sweden.

Thomas, M. W., Stewart, M., Trotz, M. & Cunningham, J. A. 2012. Geochemical modeling of CO_2 sequestration in deep, saline, dolomitic-limestone aquifers: Critical evaluation of thermodynamic sub-models. Chemical Geology 306–307(4 May 2012), 29–39. *doi:10.1016/0009-2541(92)90106-F*

Truesdell, A. H. & Jones, B. F., 1974. WATEQ, a computer program for calculating chemical equilibria of natural waters. Lawrence Livermore National Laboratory. Livermore, California.

Trautz, R. C., Pugh, J. D., Varadharajan, C., Zheng, L., Bianchi, M., Nico, P. S., Spycher, N. F., Newell, D. L., Esposito, R. A., Wu, Y., Dafflon, B., Hubbard, S. S. & Birkholzer, J. T. 2013. Effect of dissolved CO_2 on a shallow groundwater system: a controlled release field experiment. Environmental Science & Technology 47(1), 298–305. *doi:10.1021/es301280t*

Waldmann, S., Busch, A., van Ojik, K. & Gaupp, R. 2014. Importance of mineral surface areas in Rotliegend sandstones for modeling CO_2-water-rock interactions. Chemical Geology 378-379(15 June 2014), 89–109. *doi:10.1016/j.chemgeo.2014.03.014*

Walker, W. E., Harremoës, P., Rotmans, J., van der Sluijs, J. P., van Asselt, M. B. A., Janssen, P. & Krayer von Krauss, M. P. 2003. Defining Uncertainty: A Conceptual Basis for Uncertainty Management in Model-Based Decision Support. Integrated Assessment 4(1), 5–17. *doi:10.1076/iaij.4.1.5.16466*

Wang, S. & Jaffe, P. R. 2004. Dissolution of a mineral phase in potable aquifers due to CO_2 releases from deep formations; Effect of dissolution kinetics. Energy Conversion and Management 45(18), 2833–2848. *doi:10.1016/j.enconman.2004.01.002*

Watanabe, N., Wang, W., McDermott, C. I., Taniguchi, T. & Kolditz, O. 2010. Uncertainty analysis of thermo-hydro-mechanical coupled processes in heterogeneous porous media. Computational Mechanics 45(4), 263–280. *doi:10.1007/s00466-009-0445-9*

White, S. P., Allis, R. G., Moore, J., Chidsey, T., Morgan, C., Gwynn, W. & Adams, M. 2005. Simulation of reactive transport of injected CO_2 on the Colorado Plateau, Utah, USA. Chemical Geology 217(3–4), 387–405. *doi:10.1016/j.chemgeo.2004.12.020*

Xiao, Y., Xu, T. & Pruess, K. 2009. The effects of gas-fluid-rock interactions on CO_2 injection and storage: Insights from reactive transport modeling. Energy Procedia 7(1), 1783–1790. *doi:10.1016/j.egypro.2009.01.233*

Xu T., Apps J. A. & Pruess K. 2003. Reactive geochemical transport simulation to study mineral trapping for CO_2 disposal in deep arenaceous formations. Journal of Geophysical Research 108(B2), 1–13. *doi:10.1029/2002JB001979*

Xu, T., Apps, J. A. & Pruess, K. 2005. Mineral sequestration of carbon dioxide in a sandstone-shale system. Chemical Geology 217(3–4), 295–318. *doi:10.1016/j.chemgeo.2004.12.015*

Xu, T., Yue, G., Wang, F. & Liu, N. 2014. Using Natural CO_2 Reservoir to Constrain Geochemical Models for CO_2 Geological Sequestration. Applied Geochemistry 43(April 2014), 22–34. *doi:10.1016/j.apgeochem.2014.01.009*

Zheng, L., Apps, J. A., Zhang, Y., Xu, T. & Birkholzer, J. T. 2009 a. Reactive transport simulations to study groundwater quality changes in response to CO_2 leakage from deep geological storage. Energy Procedia 1(1), 1887–1894. *doi:10.1016/j.egypro.2009.01.246*

Zheng, L., Apps, J. A., Zhang, Y., Xu, T. & Birkholzer, J. T. 2009 b. On mobilization of lead and arsenic in groundwater in response to CO_2 leakage from deep geological storage. Chemical Geology 268(3–4), 281–297. *doi:10.1016/j.chemgeo.2009.09.007*

4. Suitability of existing numerical model codes and thermodynamic databases for the prognosis of calcite dissolution processes in near-surface sediments due to a CO_2 leakage investigated by column experiments

Christoph Haase*[1], Andreas Dahmke[1], Markus Ebert[1], Dirk Schäfer[1], Frank Dethlefsen[1]

[1]Kiel University, Institute of Geosciences, Ludewig-Meyn-Straße 10, 24118 Kiel, Germany

Published in Aquatic Geochemistry (Editor: R. Arvidsson) *doi:10.1007/s10498-014-9240-0*
Article history: Received 10 November 2013, Accepted 12 August 2014

Abstract

Among the risks of CO_2 storage is the potential of CO_2 leakage into overlaying formations and near-surface potable aquifers. Through a leakage, the CO_2 can intrude into protected groundwater resources, which can lead to groundwater acidification followed by potential mobilisation of heavy metals and other trace metals through mineral dissolution or ion exchange processes. The prediction of pH buffer reactions in the formations overlaying a CO_2 storage site is essential for assessing the impact of CO_2 leakages in terms of trace metal mobilisation. For buffering the pH-value, calcite dissolution is one of the most important mechanisms. Although calcite dissolution has been studied for decades, experiments conducted under elevated CO_2 partial pressures are rare. Here, the first study for column experiments is presented applying CO_2 partial pressures from 6 to 43 bars and realising a near-natural flow regime. Geochemical calculations of calcite dissolution kinetics were conducted using PHREEQC together with different thermodynamic databases. Applying calcite surface areas, which were previously acquired by N_2-BET or calculated based on grain diameters, respectively, to the rate laws according to Plummer et al. (Am J Sci 278:179–216, doi:10.2475/ajs.278.2.179, 1978) or Palandri and Kharaka (US Geol Surv Open file Rep 2004-1068:71, 2004) in the numerical simulations led to an overestimation of the calcite dissolution rate by up to three orders of magnitude compared to the results of the column experiments. Only reduction of the calcite surface area in the simulations as a fitting procedure allowed reproducing the experimental results. A reason may be that the diffusion boundary layer (DBL), which depends on the groundwater flow velocity and develops at the calcite grain surface separating it from the bulk of the solution, has to be regarded: The DBL leads to a decrease in the calcite dissolution rate under natural laminar flow conditions compared to turbulent mixing in traditional batch experiments. However, varying the rate constants by three orders of magnitudes in a field scale PHREEQC model simulating a CO_2 leakage produced minor variations in the pH buffering through calcite dissolution. This justifies the use of equilibrium models when calculating the calcite dissolution in CO_2 leakage scenarios for porous aquifers and slow or moderate groundwater flow velocities. However, the selection of the thermodynamic database has an impact on the dissolved calcium concentration, leading to an uncertainty in the simulation results. The resulting uncertainty, which applies also to the calculated propagation of an aquifer zone depleted in calcite through dissolution, seems negligible for shallow aquifers of approximately 60 m depth, but amounts to 35 % of the calcium concentration for aquifers at a depth of approximately 400 m.

*corresponding author

4.1 Introduction

The geological storage of CO_2 is a technology to reduce the CO_2 emissions from power plants into the atmosphere and to counteract the climate change. A risk of the CO_2 storage in deep geological formations is a potential leakage of CO_2 into overlaying potable aquifers (Lemieux, 2011), which reach a depth of maximal 400 m in Northern Germany (Gabriel et al., 2003). The groundwater in these aquifers can be acidified by the intrusion of CO_2 (i. e. Peter et al., 2012; Trautz et al., 2013). As the dissolution of some minerals is sensitive to changes in CO_2 partial pressure due to decreases in pH, larger amounts of hazardous trace metals like lead, arsenic or zinc can be released into the groundwater (Birkholzer et al., 2008; Zheng et al., 2009 a). Birkholzer et al. (2008) stated that zinc and arsenic concentrations increased strongly at elevated CO_2 partial pressures and due to a pH decrease in calcite depleted sections. The important processes for increasing concentrations are desorption and dissolution of minerals phases such as galena, arsenopyrite, or sphalerite at acidic conditions (Wang and Jaffe, 2004; Zheng et al., 2009 b). Thereby, the quality of the produced potable water can be endangered. However, mineral dissolution can act as a buffer mechanism to keep the pH at near-neutral levels. An example is calcite, which is a fast-reacting mineral being present in 1–5 wt% in near-surface aquifers overlaying potential CO_2 storage sites in Northern Germany (Ohse, 1983). Through the calcite dissolution, the groundwater pH can be buffered, whereby the potable water quality could be sustained. Until now, the ability to reliably predict the calcite buffer reaction in the context of CO_2 leakage in aquifers reaching depths of 400 m applying numerical models was not investigated.

Calcite is abundant in many sedimentary rocks and is important for many geologic topics. Therefore, numerous zero-dimensional batch experiments were conducted in the past to determine the kinetics of calcite dissolution, such as by Berner and Morse (1974), Buhmann and Dreybrodt (1985 a, b), Busenberg and Plummer (1986), Compton and Daly (1987), Plummer et al. (1978), Reddy et al. (1981), and Svensson and Dreybrodt (1992). In the last decade, dissolution experiments were also conducted at high CO_2 pressures of up to approximately 50 bars and ionic strengths of up to 1 mol/l (Finneran and Morse, 2009; Pokrovsky et al., 2005). However, column experiments investigating the kinetics of calcite dissolution were conducted rarely in the past and were conducted at low CO_2 partial pressures (Schulz, 1988) or observed a dependency of the dissolution rate with the flow velocity (Gong et al., 2010). It is well known that dissolution rates produced in different laboratories differ in the order of up to two orders of magnitude (Kump et al., 2000; Arvidson et al., 2003). In addition to the problematic role of surface areas of minerals (Klotz, 1991; Gaus et al., 2008; Fischer et al., 2012) and mineral-fluid ratio (Casey et al., 1993) in rate determinations, a major influencing factor is the hydrodynamic condition chosen for the laboratory experiment. In zero-dimensional batch experiments, the stirring rate and in rotating disc experiments the rotating rate, respectively, influence the dissolution rate, as it has already been intensely discussed by Morse and Arvidson (2002), Plummer et al. (1978), Pokrovsky et al. (2005) and Sjöberg and Rickard (1984). Consequently, a dependence of the calcite dissolution rates from the groundwater flow velocity in porous aquifers can also be expected (Schulz, 1988; Dreybrodt and Buhmann, 1991; Liu and Dreybrodt, 1997; Gong et al., 2010), especially in the acidic regime induced by equilibria with high CO_2 partial pressures.

The model code PHREEQC (Parkhurst and Appelo, 1999) can be applied using several available thermodynamic databases and two different rate laws (Plummer et al., 1978; Palandri and Kharaka, 2004). The selection of the thermodynamic databases yielding variations in the model results for calcite dissolution under the influence of CO_2 was discussed in Haase et al. (2013). Additionally, the parameterisation

of the rate laws suffers from unambiguous results of laboratory experiments resulting from different experimental set-ups, stirring rates, or assigned surface areas. The latter has to be seen in connection with the slow mass transport of the species towards the mineral surface and from the surface into the solution which can limit the dissolution rate (Dreybrodt and Buhmann, 1991; Dreybrodt et al., 1996). Furthermore, the rate laws only describe the calcite surface reaction, but the dissolution can also be restricted by the slow reaction of CO_2 with the groundwater to form hydrogen carbonate HCO_3^- (Dreybrodt et al., 1996). Including these three mechanisms, (1) reaction at the calcite surface, (2) conversion of CO_2 to HCO_3^-, and (3) mass transport of species a kinetic model for calcite dissolution was developed by Buhmann and Dreybrodt (1985 a, b). On the basis of this theoretical background, a method was developed by Schulz (1988) to calculate the rate constant of calcite dissolution experiments by using the length of the mass transfer zone. However, for this method, column experiments have to be conducted to determine the specific rate of calcite dissolution for a field site. The kinetic models of Buhmann and Dreybrodt (1985 a, b) and Schulz (1988) were not applied in this study, because this study focused only on the application of commonly applied rate laws for calcite dissolution.

This is the first presentation of flow-through column experiments to investigate the calcite dissolution kinetics at CO_2 partial pressures of up to 43 bars. The experimental set-up as well as the development of the sampling method is described. The other aim of this study was to test in what way the geochemical model PHREEQC using various thermodynamic databases and standard rate laws can be used to calculate the calcite dissolution determined in the column experiments under the influence of high CO_2 partial pressures. Furthermore, the impact of the application of different thermodynamic databases on the calcite solubility leading to a prediction of the calcite dissolution front in field scale models was determined. The differences in the calculated solubilities of CO_2 and calcite can influence the resulting electric conductivity of the groundwater of near-surface formations resulting from dissolved CO_2 and solids. The electric conductivity is a promising monitoring parameter for potential CO_2 leakages (Dethlefsen et al., 2013).

4.2 Methods

Using the commonly applied geochemical model PHREEQC version 2 (Parkhurst and Appelo, 1999), the calcite dissolution rates were calculated at different partial pressures of CO_2 as a base scenario. To reproduce the experimental results, the surface areas in the rate law were adapted and different thermodynamic databases were tested as the standard database did not represent the concentrations determined by the experiments accurately. The impact of the application of different thermodynamic databases was investigated applying field scale scenario analyses using simplified reactive transport models. The models were used to calculate the reaction front position in carbonate-bearing formations.

4.2.1 Experimental set-up

The main components of the overall experimental set-up consisted of a mixing cell and an experimental column, which was filled with the porous medium under evaluation (Figure 4.1). A 0.1 M NaCl solution was used in order to maintain a relatively constant ionic strength during the experiments. The solution was equilibrated with CO_2 in the mixing cell before it percolated through the experimental column from the bottom to the top. Capillary tubes were connected to the column at distances of 5, 15, 25, and 35 cm from the inflow as sampling ports. In this way, fluid samples could not only be gained from the inflow and the outflow of the column, but also along the flow path.

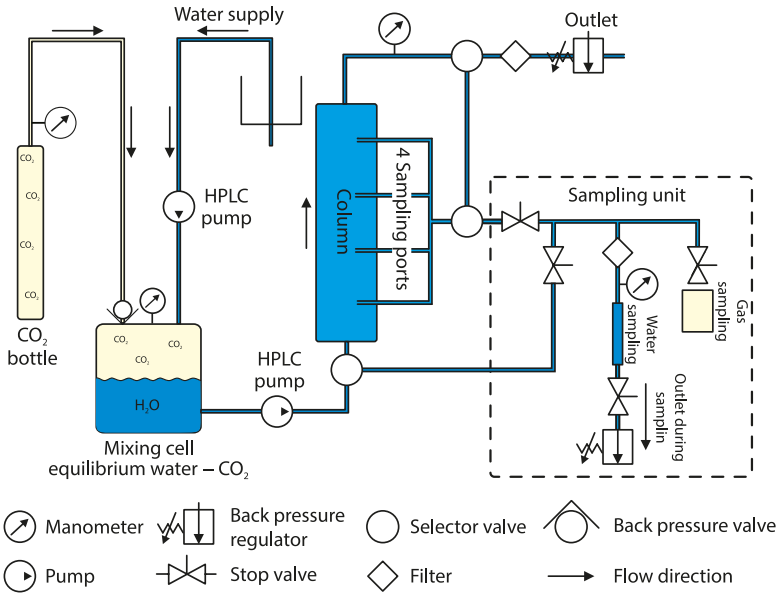

Figure 4.1

Set-up of the column experiment and the sampling unit to determine the calcite dissolution rate.

The experiment was pressurised by two HPLC K-1001 pumps (Knauer GmbH, Germany), while back pressureregulators at the end of the flow line sustained the pressure within the set-up. The experiment was conducted at different partial pressures of CO_2. At 6 bars CO_2 partial pressure and a flow velocity of 8.4 m/s, the experiment was conducted three times at the same conditions without changing the filling of the experimental column.

The inflow, the outflow, and the sampling ports could be connected to the sampling unit of the experimental set-up (Figure 4.1). This unit consisted of a pressure cylinder of 25 cm^3 which was percolated with the pressurised fluid for sampling. When beginning the sampling, the pressure cylinder was separated from the remaining system and the overpressure was then released, whereby the fluid was degassed. The developed CO_2 gas phase was measured by connecting the sampling unit to an aluminium bag where the gas phase was captured. The volume was quantified after disconnecting the bag from the sampling unit by repeatedly extracting gas with a 60-ml syringe. After this procedure, the fluid in the sampling unit was at atmospheric pressure. Fluid samples for analysing the total inorganic carbon (TIC) content were then extracted by a glass syringe through a septum in the sampling unit and directly injected into the TIC analyser. For cation analyses, the remaining volume of the sampling unit was rinsed and acidified with diluted nitric acid to prevent minerals from precipitating. The Ca_{tot}^{2+} concentration was measured using ICP-AES. The dilution of the sample due to the acid was corrected when the Ca_{tot}^{2+} concentrations were calculated.

The hydrodynamic properties of the column experiment were measured by performing a tracer test using a 1 mM lithium bromide solution. The effective porosity and the longitudinal dispersivity of the sedimentary column filling were determined. The evaluation of the tracer test was done by applying the analytic solution of the transport equation in one-dimensional flow and by applying a one-dimensional transport model using the model code PHREEQC (Parkhurst and Appelo, 1999). The calculation of the effective porosity using the analytic solution resulted in 35 % and using PHREEQC the porosity was 34 %. The longitudinal dispersivity was 1.1 mm using the analytic solution and 2.4 mm applying PHREEQC.

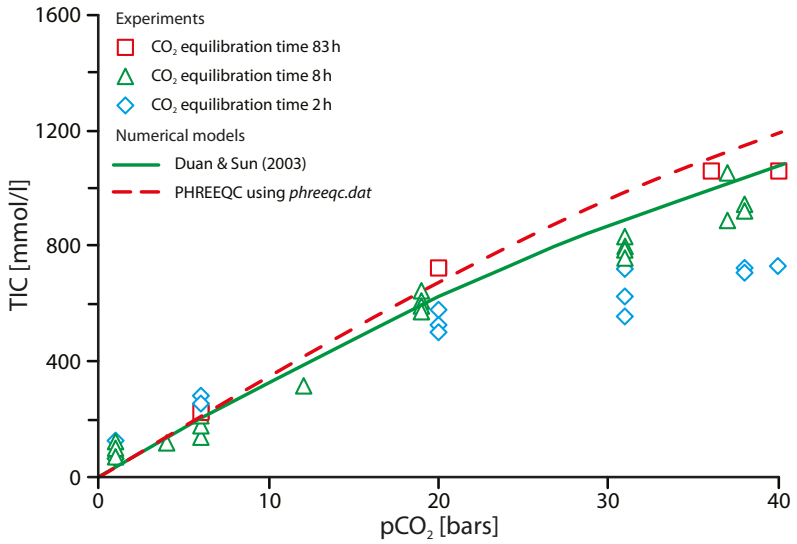

Figure 4.2

Measured and calculated TIC concentrations in the system H_2O–CO_2 at CO_2 partial pressures of up to 40 bars.

Calcite minerals were washed using distilled water and dried. Then, they were ground to sand size and sieved to a spectrum from 0.063 to 0.5 mm. The purity of calcite was determined by X-ray diffractometry. The N_2-BET surface area (Brunauer et al., 1938) was approximately 800 cm^2/g determined by using the Areameter II (Fa. Ströhlein). The experimental column was filled with the porous medium, which consisted of a mixture of 30 % calcite by weight and 70 % quartz by weight. According to Plummer et al. (1978), spherical grains were assumed and the calcite surface area was additionally calculated using the minimum and maximum grain diameters. For the parameterisation of the rate laws applied, the calcite surface area in contact with one litre of water at an effective porosity of 34 % was calculated. The calculation resulted in surface areas of 5,550 and 700 dm^2/dm^3 (Table 4.1).

4.2.2 Preliminary experiments

Preliminary experiments were conducted to determine the time needed for saturating the solution with CO_2 in the mixing cell. Thereby, potential limits with respect to the flow velocity in the subsequently conducted column experiments were quantified, since the experimental set-up requires the saturation of the solution with respect to CO_2. In preliminary experiments, the solution was equilibrated with the CO_2 gas phase in a mixing cell at various CO_2 pressures ranging from 6 to 43 bars whereby the solution was stirred. Fluid samples were retrieved and analysed as described above, using non-circulating, deionised water as reactant solution. For this set-up, the experimental column was not percolated by the fluid. A batch model for calculating the CO_2 solubility was set up in PHREEQC (Parkhurst and Appelo, 1999) using a 0.1 molar NaCl solution. In the simulation, the solution was equilibrated with the CO_2 gas phase at the fugacities corresponding to the preliminary experiments. The applicable equilibration time of CO_2 was determined by the increasing discrepancy between the concentration of total inorganic carbon (TIC) in the preliminary experiments and the calculated TIC concentration using PHREEQC and the method of Duan and Sun (2003) (Figure 4.2).

The results showed that the TIC concentrations increased proportionally to the CO_2 partial pressure (Figure 4.2). The measured TIC concentrations differed depending on the equilibration time of the

Table 4.1
Minimum and maximum surface areas using the range of grain diameters assuming spherical grains of calcite calculated according to Equation 4.1.

	Minimal values of grain diameter	Maximum values of grain diameter	BET surface area
Diameter of grains [mm]	0.063	0.5	0.063-0.5
Surface area of spherical grains [cm^2/g]	353	44	ca. 800
Surface area in contact with 1 l water [dm^2/dm^3]	ca. 5,550	ca. 700	

solution with CO_2 at high partial pressures. The two model approaches applied, which are PHREEQC using the *phreeqc.dat* database and the model of Duan and Sun (2003), calculated consistent TIC concentrations (Figure 4.2). Comparing the model results with the TIC analyses of samples retrieved from the CO_2 mixing cell revealed the best conformity for the CO_2 equilibration times of 83 and 8 h, especially according to the Duan and Sun (2003) model. However, the TIC concentration of the CO_2 equilibration time of 2 h showed an incomplete CO_2 equilibration at pressures higher than 20 bars and a poor agreement with the calculated concentrations. Consequently, calcite dissolution experiments using these boundary conditions were not carried out. The scattering in the TIC analyses amounts to a range of approximately 100–200 mmol/l with a minor increase in the range related to the increasing CO_2 partial pressure. This scattering likely reflects an incomplete degassing of the sample when depressurising the fluid sample.

4.2.3 Model code and implemented rate laws

In this part of the study, the model code PHREEQC (Parkhurst and Appelo, 1999) was applied using the databases *phreeqc.dat*, *wateq4f.dat*, *minteq.dat*, *minteq.v4.dat*, and *llnl.dat* including the ion-dissociation approach and *sit.dat* and *pitzer.dat* including the ion-association approach for calculating the species activities. The databases using the ion-dissociation theory incorporate the Davies, Debye-Hückel and extended Debye-Hückel equations to calculate the aquatic species activities. The ion-association model is either represented by the Pitzer theory or by the Specific ion Interaction Theory (SIT) both using ion–ion interaction parameters. Additionally, the *thereda.dat* database was applied (Brendler et al., 2011), which is based on the Pitzer approach. The range of the validity of the *sit.dat*, *pitzer.dat* and *thereda.dat* databases reaches up to an ionic strength of 6 mol/l (Pitzer and Kim, 1974). However, the equations calculating the activity coefficients like the extended Debye-Hückel or the Davies equation, which are included in the databases based on the ion-dissociation theory, are valid up to an ionic strength of only 0.1 mol/kg. Only the WATEQ Debye-Hückel equation can be valid up to a higher ionic strength. Merkel and Planer-Friedrich (2008) state a range of validity for the Cl, SO_4 and Ca ion up to an ionic strength of 3.0 mol/kg. Therefore, all of the databases are valid at the ionic strength of the solution used in the column experiment, which was I = 0.1 mol/l. Beyond that, the thermodynamic databases differ in the equilibrium constants of the mineral and species reactions.

Two different rate laws were applied to calculate the calcite dissolution rate. The first rate law applied in this study was developed for calcite dissolution by Plummer et al. (1978), which is included in the database *phreeqc.dat* (Equation 4.1). dm/dt is the rate and k_1, k_2 and k_3 are the rate constants for the

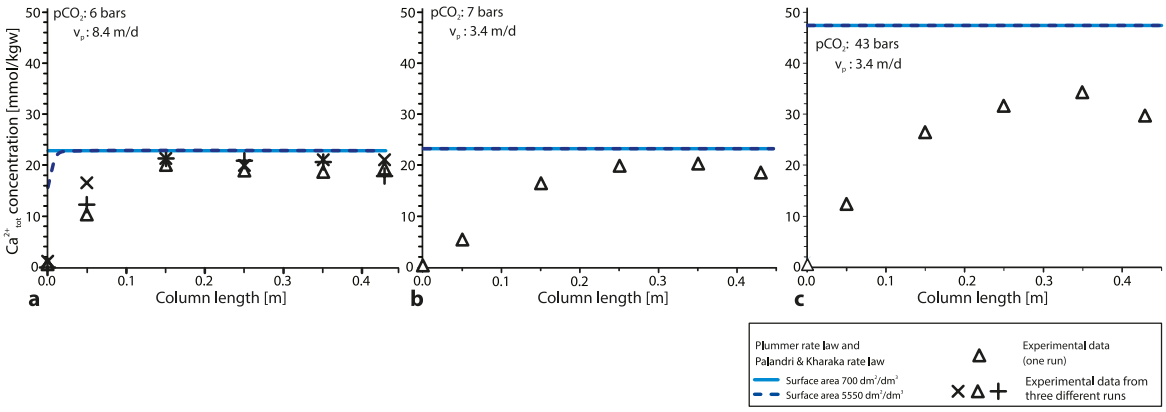

Figure 4.3 a, b, c

Concentration of calcite for experiments and simulations at CO_2 partial pressure of 6 bars and a flow velocity of 8.4 m/day as well as 7 and 43 bars pCO_2 and a flow velocity of 3.4 m/day. The concentrations were calculated applying PHREEQC using the *phreeqc.dat* database and the rate laws of Palandri and Kharaka (2004) and Plummer et al. (1978). The equilibrium is approached instantaneously by using the surface areas from Table 4.1 almost at all model conditions.

forward reaction mechanisms of the semi-empirical rate equation and a is the activity of the respective species (indices H^+, $H_2CO_3{}^*$ and H_2O in Equation 4.1). k_4 is the rate constant for the backward reaction (Equation 4.1). The rate constants include temperature correction terms (Table 4.2).The activation energies were estimated by Plummer et al. (1978) (Table 4.2). According to Plummer et al. (1978), n and p were set to 1.

$$\frac{dm}{dt} = k_1 \times a_{H^+}^{n} + k_2 \times a_{H_2O} - k_4 \times a_{Ca^{2+}} \times a_{HCO_3^-} \qquad (4.1)$$

The second applied rate law was developed by Lasaga (1984) and was parameterised by Palandri and Kharaka (2004) (Equation 4.2). The rate law was selected because it can serve as a general rate law (non mineral-specific) for reactive transport models, i. e. applied by Mitiku et al. (2013). The calcite rate constants for the law of Palandri and Kharaka (2004) were derived from the experimental studies of Plummer et al. (1978) and Talman et al. (1990) (Table 4.2). The mechanisms of the rate equation for calcite dissolution were the neutral mechanism in pure H_2O and the mechanisms catalysed by the activity of H^+ and CO_2 (acid and carbonate mechanisms, Equation 4.2).

$$\frac{\delta m}{\delta t} = -SA \begin{array}{l} k_{acid} \times e^{\frac{-E_{acid}}{R}\left(\frac{}{T}\right)} \times a_{H^+}^{n_1} (1-\Omega^{p_1})^{q_1} \\ +k_{neut} \times e^{\frac{-E_{neut}}{R}\left(\frac{}{T}\right)} \times (1-\Omega^{p_2})^{q_2} \\ +k_{carb} \times e^{\frac{-Ecarb}{R}\left(\frac{}{T}\right)} \times a_{CO_2}^{n_3} (1-\Omega^{p_3})^{q_3} \end{array} \qquad (4.2)$$

The rate $\delta m/\delta t$ is in the unit mol/l/s. SA is the surface area of calcite in m^2. The three rate constants k_{mech} are specified for the three reaction mechanisms of the rate law, which are the acidic, neutral, and carbonatic mechanisms, respectively. The temperature dependency is expressed through the Arrhenius equation, where T is the temperature in Kelvin, E is the Arrhenius activation energy in kJ/mol, and R is the gas constant of 8.314×10^{-3} kJ/mol/K (Equation 4.2). The acid and the carbonate mechanism include the activity a of the species H^+ and CO_2, which are calculated by the model code. The activities have reaction orders n_1 and n_3, which are equal to one for calcite (Palandri and Kharaka, 2004).

Table 4.2
Parameters for the kinetic rate law of calcite of Palandri and Kharaka (2004) and Plummer et al. (1978).

Rate law	Mechanism	Kinetic rate constant k [mol/l s^{-1}]	Kinetic rate constant k at 25 °C [mol/l s^{-1}]	Activation energy E [kJ/mol]
Palandri and Kharaka (2004)	Acid	0.5	0.5	14.4
	Neutral	1.5×10^{-6}	1.5×10^{-6}	23.5
	Carbonate	3.3×10^{-4}	3.3×10^{-4}	35.4
Plummer et al. (1978)	k_1		0.051	≈ 8.4
	k_2		3.3×10^{-5}	≈ 41.2
	k_3		1.18×10^{-7}	≈ 33.1

The chemical affinity parameters p_i an q_i were only quantified for some minerals, but as the parameters are not available for calcite they are set to unity (Palandri and Kharaka, 2004). The mineral saturation $\Omega = Q/K_{eq}$ is calculated by the model code, where Q is the activity product and K_{eq} is the equilibrium constant.

4.2.4 Numerical Model Set-up

The experimental scale models were set up on a small scale and represent the experimental set-up. The models were calculated applying PHREEQC and consisted of a one-dimensional model with 120 cells having a length of 0.0036 m each to avoid numerical dispersion at the flow velocities from Table 4.3. The total length of the model column resulted in 0.43 m. The dispersivity was set to a value of 0.0024 m according to the tracer test results. The molecular diffusion coefficient was set to 0.3×10^{-9} m^2/s, which is the standard value of PHREEQC. The diffusion coefficient for major ions in groundwater ranges from 1.0×10^{-9} to 2.0×10^{-9} m^2/s (Robinson and Stokes, 1959). Boving and Grathwohl (2001) measured effective diffusion coefficients between 6.8×10^{-11} and 2.9×10^{-10} m^2/s for iodide in limestone samples. A 0.1 molar NaCl solution was equilibrated with CO_2 at different pressures (Table 4.3), but at constant temperature of 22 °C. The partial pressure of CO_2 was converted to fugacity applying the model of Duan and Sun (2003) for the input in PHREEQC, which uses Henry's Law. The solution saturated with CO_2 flowed through the model column at two different flow velocities reacting with calcite (Table 4.3).

At first, the calcite dissolution was simulated applying the rate law of Plummer et al. (1978) and Palandri and Kharaka (2004) applying the surface areas calculated using the minimal and maximal calcite grain diameters (Table 4.1). In the next step, the surface areas, being of considerable uncertainty in their determination, were fitted in a way that the experimental results were represented adequately. The surface area was therefore the only fitting parameter to achieve matching between experimental and simulation results. For the fitting procedure, only the rate law of Palandri and Kharaka (2004) was applied, because the results applying both rate laws were similar (Figure 4.3).

The field scale models have larger dimensions and represent the conditions of near-surface aquifers. The models were one-dimensional aquifer models of a length of 10 m set up in PHREEQC applying the thermodynamic databases *pitzer.dat* and *phreeqc.dat*, where the calcite dissolution rate was calculated applying the rate law of Palandri and Kharaka (2004) using the fitted surface areas in the rate law.

Table 4.3

Parameters used in one-dimensional transport models set up in PHREEQC for experimental scale. The pressure ranges for the experimental data reflect observed pressure variations during the experiment.

Flow velocity [m/day]	CO_2 Pressure in experiments [bars]	Fugacity applied in model [bars]	Simulation time [min]
8.4	6 (to 7)	5.8	148
3.4	(6 to) 7	6.8	368
3.4	43	34.9	368

The model column was divided into 100 cells of a length of 0.1 m each and the longitudinal dispersivity was set to 0.05 m. The dispersivity was defined differently compared to the model in experimental scale, because the flow path is longer and the dispersivity scales with the length of the flow path (Pickens and Grisak, 1981; Beims, 1983; Gelhar et al., 1992). The flow velocity was set to v = 1.0 m/d and the simulation time was 200 days in total, interim results were retrieved after 100 days. The calcite concentration was defined as 1.3 wt% of the solid phase mass being in the range of low calcite content of near-surface sedimentary formations in northern Germany (Ohse, 1983). The porosity was set to be 34 % according to the experimental set-up. The CO_2 partial pressure was set to 6 and 43 bars in two different simulation runs representing a CO_2 intrusion in a near-surface aquifer and also a deeper situated aquifer at a depth of about 400 m.

4.3 Results and Discussion

4.3.1 Experimental Results of Calcium Concentrations

The experimental results for the dissolved calcium concentration (Ca_{tot}^{2+}) in the column reflect the calcite solubility, since the input solution did not contain any dissolved calcium and other processes such as cation exchange are negligible. The Ca_{tot}^{2+} concentration increased significantly during percolating the column (Figure 4.3; symbols). The saturation concentration was defined to be the maximum of the achieved concentrations for Ca_{tot}^{2+} at the respective temperature and CO_2 pressure conditions. While the experiments carried out at 6 bars pCO_2 and the fast flow velocity (8.4 m/day) reached the calcium saturation concentration at approximately 0.15 m of the column (Figure 4.3 a), the saturation concentration was reached at approximately 0.25 m of the column applying the slow flow velocity of 3.4 m/day (Figure 4.3 b). This indicates that the higher flow rate allows for a faster transport of dissolved ions from the calcite surface into the bulk solution resulting in a higher local undersaturation of calcite at the grain surface. For the experiment carried out at 43 bars CO_2, the calcite saturation concentration was reached in a length of 0.35 m. Note that the Ca_{tot}^{2+} concentrations analysed in the samples taken after 0.05 m of the column length in the experiments at 6 bars and a flow velocity of 8.4 m/day decreased in the same order as the experiments have been carried out (Figure 4.3 a). This indicates decreasing reaction kinetics with the experimental run time and could stem from the decrease in the surface area due to the dissolution of calcite grains. In all experiments, the Ca_{tot}^{2+} concentration decreased slightly at the end of the experimental column, probably due to the precipitation of calcite in a quartz filter section at the end of the column. Furthermore, a faster flow velocity allowed faster calcite dissolution at the same CO_2 pressure (compare Figure 4.3 a with b). At 43 bars pCO_2, the equilibrium concentration reached 35 mmol/kgw and was therewith 1.5 times higher than the concentration at 6–7 bars pCO_2 due to the lower pH caused by the higher partial pressure of CO_2 (Figure 4.3 c).

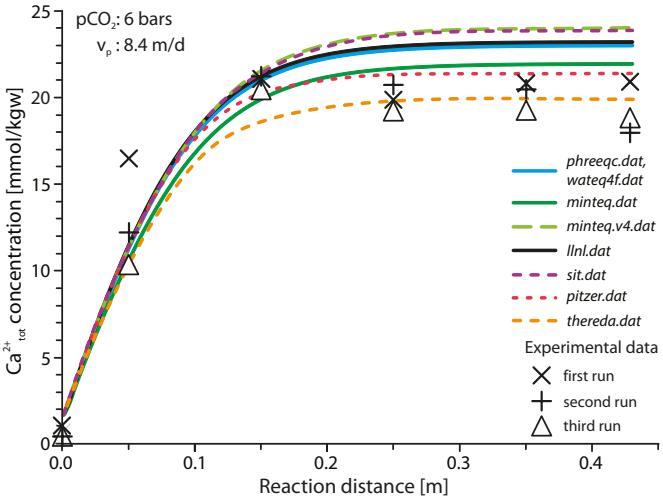

Figure 4.4

Calculated concentrations of Ca_{tot}^{2+} using PHREEQC applying different thermodynamic database and applying a surface area of 30 dm^2/dm^3 in comparison with the Ca_{tot}^{2+} concentrations provided by the experiments at 6 bars pCO_2 and a flow velocity of 8.4 m/day.

4.3.2 Application of Calculated Surface Areas

The prognosis capability of a geochemical model for calcite dissolution kinetics was tested applying a model calculated by PHREEQC using the *phreeqc.dat* database and the rate laws of Palandri and Kharaka (2004) and also of Plummer et al. (1978). In this first step, the surface areas of 5,550 and 700 dm^2/dm^3 calculated from the minimal and maximal grain diameters were applied to both rate laws (Table 4.1). Applying the surface area of 5,550 dm^2/dm^3, the equilibrium of the solution with respect to calcite, which was defined to be at 100 % of the Ca_{tot}^{2+} concentration (in the following „calcite equilibrium"), was reached quasi instantaneously (Figure 4.3 a, b, c; lines). When the lower surface area of 700 dm2/dm3, a CO_2 partial pressure of 6 bars, and the fast flow velocity (8.4 m/day) were applied, the calcite equilibrium was reached at a distance of 0.03 m, corresponding to a reaction time of < 5 min (Figure 4.3 a, dashed line). When the slow flow velocity (3.4 m/day) and CO_2 pressures of 7 and 43 bars, respectively, were applied, the increase in the calculated Ca_{tot}^{2+} concentrations applying both rate laws was still faster than the Ca_{tot}^{2+} concentrations of the column experiments (Figure 4.3 b, c). The calculated equilibrium concentrations were equal applying both rate laws, because the concentration only depends on the thermodynamic database used, which was *phreeqc.dat* in all cases here. However, the calculated concentrations of Ca_{tot}^{2+} using *phreeqc.dat* were higher compared to the results of the column experiments. Especially, at a CO_2 pressure of 43 bars PHREEQC calculated a concentration of Ca_{tot}^{2+}, which was 40 % higher compared to the experimentally determined concentrations (Figure 4.3 c).

Table 4.4

Summary of fitted surface areas at the different flow velocities and CO_2 pressures using PHREEQC.

Flow velocity v_p [m/day]	8.4	3.4	3.4
CO_2 pressure in experiment [bars]	6 (to 7)	(6 to) 7	43.0
Fitted surface area [dm^2/dm^3]	30.0	6.5	2.0

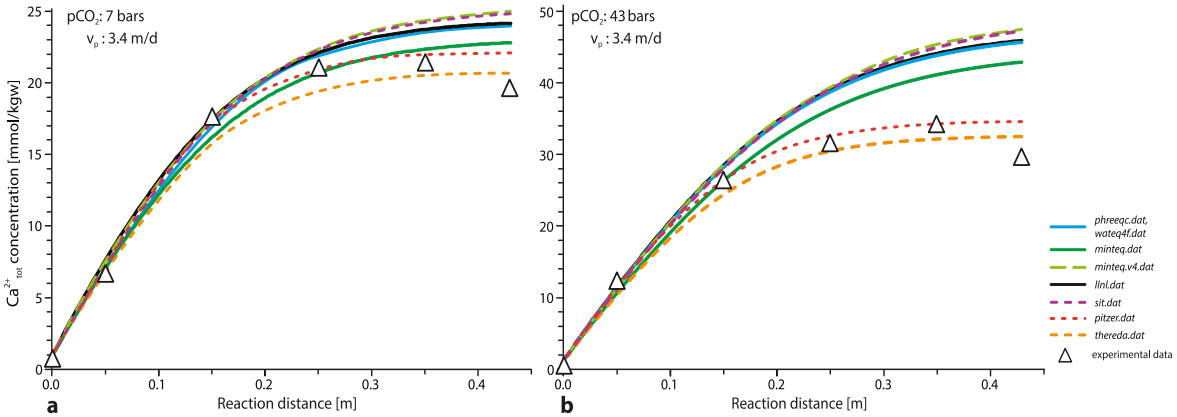

Figure 4.5 a und b

Calculated concentrations of Ca_{tot}^{2+} using PHREEQC applying different thermodynamic databases and applying a surface area of 6.5 and 2.0 dm^2/dm^3 in comparison to the Ca_{tot}^{2+} concentrations provided by the experiments at a flow velocity of 3.4 m/d and 7 bars and 43 bars pCO_2.

4.3.3 Application of Fitted Surface Areas

The accordance of the model results using the standard thermodynamic database of PHREEQC and using calcite surface areas of 5,550 and 700 dm^2/dm^3, respectively, for the rate laws with the experimental results was poor, especially at 43 bars pCO_2 (Figure 4.3c). Therefore, in the next step, all available thermodynamic from PHREEQC were applied. Likewise, the rate was decreased by reduction of the calcite surface area in the model in order to reproduce the experimentally determined concentrations. The surface area was fitted using the flow velocities of 8.4 and 3.4 m/day and applying the rate law of Palandri and Kharaka (2004). The model represented the increase in the experimentally determined Ca_{tot}^{2+} concentrations at 6 bars by using a fitted surface area of 30 dm^2/dm^3 applying the fast flow velocity of 8.4 m/day (Figure 4.4).

At a CO_2 partial pressure of 7 bars and a flow velocity of 3.4 m/day, the fitting resulted in a surface area of 6.5 dm^2/dm^3. The experimental values were represented at a CO_2 pressure of 43 bars by the rate law applying a fitted surface area of 2.0 dm^2/dm^3 (Figure 4.5b). The fitted surface areas of 6.5 and 2.0 dm^2/dm^3 at the slower flow velocity were smaller compared to the surface area fitted at the fast flow velocity (30 dm^2/dm^3, Table 4.4). In general, the fitted surface areas were decreased by one to three orders of magnitudes compared to the surface areas calculated by the grain diameters from Table 4.1, which could be explained by two interconnected approaches: First, the difference in concentrations at different velocities can be explained by faster removal of the reaction product from the bulk solution near the calcite grains via flow, a decrease of local concentration and consequently an increase of the local dissolution rate with further accumulation of the reaction products in the solvent while passing through the column. The second explanation is that the diffusion boundary layer (DBL) is responsible for the differences in the calcite concentrations (Liu and Dreybrodt, 1997). The calcite dissolution is not only limited by the surface controlled reaction process, but it is also limited by transport, which is controlled by molecular diffusion. Ca^{2+} ions are transported into the solution and H^+ ions are transported to the calcite surface. The DBL can develop around the calcite grains and can be responsible for the slowing down of dissolution. The slowing down is especially significant at pH values lower than 5.5 and at the applied high flow velocities (Plummer et al., 1978; Sjöberg and Rickard, 1984; Dreybrodt and Buhmann, 1991).

The Ca_{tot}^{2+} concentration near calcite equilibrium calculated by PHREEQC was only influenced by the chosen database, among which the application of the Pitzer databases agreed best with the experimentally determined concentrations. The remaining databases including *phreeqc.dat* calculated Ca_{tot}^{2+} concentrations, which were higher in 14 mmol/kgw compared to the experimental data at 43 bars pCO_2. The equilibrium concentrations of Ca_{tot}^{2+} calculated by the different databases at 7 bars pCO_2 differed in only 7 mmol/kgw. The saturation with respect to calcite calculated by the *pitzer.dat* and *thereda.dat* database is closer to equilibrium at a CO_2 pressure of 43 bars and a flow distance of up to at least 43 cm compared to the saturation calculated by the remaining databases resulting in lower calcite rates (Figure 4.6). Therefore, lower Ca_{tot}^{2+} concentrations are calculated by using the *pitzer.dat* and *thereda.dat* databases. Both of these databases show a higher equilibrium constant (log_K) of the calcite dissolution reaction (Equation 4.3), which are −8.41 for the *pitzer.dat* compared to −8.48 for the *phreeqc.dat* database (Table 4.5).

$$CaCO_3 \rightleftarrows CO_3^{-2} + Ca^{+2} \qquad (4.3)$$

$$CO_3^{-2} + 2H^+ \rightleftarrows CO_2(aq) + H_2O \qquad (4.4)$$

The difference between the log_K_{eq} for the calcite dissolution is 18 % and the difference between the log_K_{eq} of the CO_2(aq) dissolution (Equation 4.4) is <1 %. The small differences between the log_K_{eq} of calcite and CO_2 are therefore probably not the reason for the variances in the calculated calcite equilibrium concentrations. The *pitzer.dat* and *thereda.dat* databases include a different activity model compared to the remaining databases, which is based on the Pitzer approach. These two databases are also valid at the low applied ionic strength of 0.1 mol/l and include only one aqueous complex, in contrast to the remaining databases, which include 5–7 aqueous complexes (Table 4.5). However, the calculated ionic strength differs in only 9 % (data not shown), whereby the aqueous complexes are not the main reason for the differences, as the complexes influence the ionic strength due to their

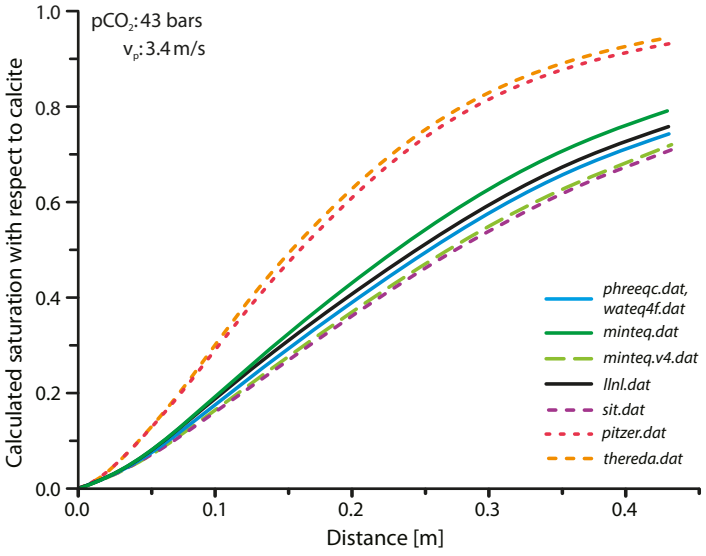

Figure 4.6

Calculated saturation with respect to calcite at a CO_2 pressure of 43 bars using PHREEQC and applying different thermodynamic databases.

lower charge. However, the activity coefficient of Ca^{2+} calculated by the *pitzer.dat* database was larger by a factor of 1.7 compared to the activity coefficients calculated by databases such as *phreeqc.dat* (Table 4.5), which is also valid for the Ca^{2+} activities. Consequently, the calculated equilibrium concentration of Ca_{tot}^{2+} is smaller using these two Pitzer databases (Figure 4.5). However, at the low partial pressure of CO_2, the activities of Ca^{2+} calculated by *phreeqc.dat* and *pitzer.dat* were equal. In contrast, at higher partial pressures of CO_2, the *pitzer.dat* database calculated larger activities of Ca^{2+} than the *phreeqc.dat* database, because the interaction between Ca^{2+} and CO_2 is considered in the Pitzer model. In general, several database parameters influence the calculated Ca^{2+} concentrations though the calcite saturation state used by the rate law. The largest influence was attributed to the activity calculation method at 43 bars CO_2 partial pressure especially when using the Pitzer model.

4.3.4 Impact of Databases Using a Field Scale Model

Closed systems with respect to CO_2 are commonly applied in reactive transport models representing possible CO_2 storage formations, and the concentration of CO_2 in the solution is an input parameter for the model (i. e. Beyer et al., 2012). Since the selection of the thermodynamic databases influenced the calculated equilibrium concentration of Ca_{tot}^{2+} significantly in the experimental scale models presented in this study, a large-scale model was calculated at the conditions of a depth of 400 m. The field scale model column set up in PHREEQC has a length of 10 m (Figure 4.7). This model was at first calculated using a closed system regarding CO_2 and secondly using an open system regarding CO_2 to investigate the differences in the proceeding reaction fronts (Figure 4.7). The left boundary of the PHREEQC model represented a point source of water in equilibrium with CO_2 (open system) or with a fixed concentration of CO_2 (closed system), which leaked into a near-surface aquifer. Through the intrusion of CO_2, the available calcite content dissolved completely in a section of the model. The region of active calcite dissolution is termed a reaction front. Reaction fronts developed between the sections where calcite was not present any more and where calcite was still present (Figures 4.8, 4.9).

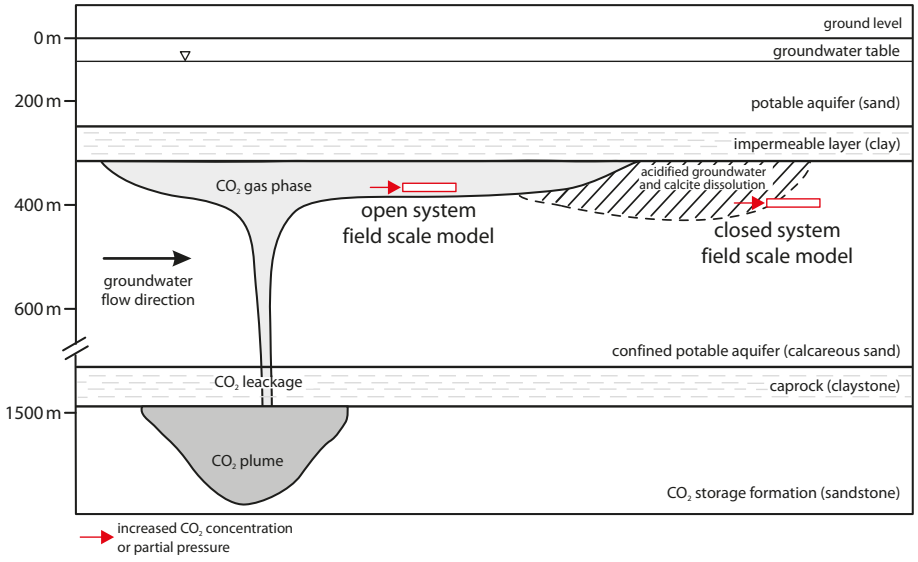

Figure 4.7

Conceptual sketch of the position of the field scale models with open and closed systems regarding CO_2 in the geologic environment.

For the field scale model, the databases *pitzer.dat* and *phreeqc.dat* were selected as the *pitzer.dat* database calculated Ca_{tot}^{2+} concentrations being in good agreement with the experimental results at the fugacity of 43 bars (Figure 4.5 b). By contrast, using the *phreeqc.dat* database, which is frequently applied by others (Wigley et al., 2012; Fahrner et al., 2012), resulted in the calculated concentrations deviating strongest from the experimental results. The field scale model calculated different positions of the reaction front with respect to the distance from the CO_2 source showing the impact of the selection of different thermodynamic databases (Figure 4.8). The presence of calcite, which still can be dissolved and can contribute to raise the groundwater electric conductivity, is of interest for using the electric conductivity as a monitoring parameter (Dethlefsen et al., 2013).

The closed system model was calculated with a concentration of CO_2 of 1.0 mol/kgw in the 0.1 molar NaCl solution. This concentration represents the solubility of CO_2 in aquifers at 40 bars and at 22 °C (Duan and Li, 2008). When the closed system was applied to the model the calculated distance, at which calcite was completely dissolved, was 6.15 m using the *pitzer.dat* database and 8.05 m using the *phreeqc.dat* database after a simulation time of 200 days (Figure 4.8). The pH values coincided using the databases *pitzer.dat* and *phreeqc.dat*.

The reaction front positions calculated by applying the open system regarding CO_2 are comparable to the results of applying the closed system model when the model is calculated at the same temperature and pressure conditions. The difference between the distances of the reaction fronts from the left model boundary was subordinate, because the concentrations of CO_2(aq) were similar. The variation of the equilibrium concentration of Ca_{tot}^{2+} calculated applying a closed system model was similar to the Ca_{tot}^{2+} concentration applying an open system model at the corresponding CO_2 partial pressure.

When the inflowing water was in equilibrium with the CO_2 partial pressure of 43 bars, the open system model results showed that calcite was completely dissolved in a distance of 8.75 m from the left model boundary applying *phreeqc.dat* after a simulation time of 200 days (Figure 4.9 b). Using *pitzer.dat*, calcite was dissolved in a distance of 6.50 m from the left boundary. The pH values were 3.1 calculated by using both databases when calcite was dissolved. However, in the region where calcite was still present the pH values calculated by the different databases were 5.0, using both databases.

Table 4.5

Equilibrium constants of the calcite and CO_2 dissolution of the different thermodynamic databases of PHREEQC and pH, activity of calcium and CO_2(aq) at a CO_2 pressure of 43 bars in the last model cell.

Database	log_K calcite	log_K CO_2	Aqueous complexes with one of the components Na, Cl, Ca, C	pH value	Activity of Ca^{2+}	Activity coefficient γ of Ca^{2+}	Activity of CO_2(aq)
phreeqc.dat	−8.480	16.681	5	5.040	0.011	0.32	1.280
wateq4f.dat	−8.480	16.681	5	5.040	0.011	0.32	1.280
llnl.dat	−8.480	16.674	7	5.025	0.012	0.33	1.296
minteq.dat	−8.475	16.681	5	5.028	0.012	0.35	1.152
minteq.v4.dat	−8.480	16.681	5	5.051	0.010	0.31	1.215
sit.dat	−8.480	16.680	5	5.057	0.010	0.29	1.238
pitzer.dat	-8.410	16.677	1	4.973	0.019	0.56	1.274
thereda.dat	-8.405	16.683	1	4.985	0.018	0.54	1.160

Consequently, at a pressure of 43 bars, the application of the *pitzer.dat* thermodynamic database resulted in a slower progress of the calculated calcite dissolution front compared to applying the *phreeqc.dat* database. However, at a CO_2 partial pressure of 6 bars, calcite was completely dissolved in a distance of 3.95 m from the left model boundary when PHREEQC was applied with the *pitzer.dat* database after the simulated reaction time of 200 days (Figure 4.9 a). In contrast, applying the *phreeqc.dat* database resulted in a distance from the left boundary of 4.35 m in which calcite was dissolved.

The model code PHREEQC calculated a sharp increase in the Ca_{tot}^{2+} concentration for the field scale model, even when the fitted surface areas (6.5 and 2.0 dm^2/dm^3 at 6 and 43 bars) were applied to the field scale models. The sharp increase at the calculated reaction fronts and the quasi instantaneous achievement of the Ca_{tot}^{2+} saturation concentration using the rate law justifies the application of a calcite equilibrium phase, which implies the instantaneous achievement of the saturation state, in this scenario simulation. Consequently, the calculation of the field scale model in this study applying a calcite equilibrium phase in PHREEQC led to the same results compared to using calcite kinetics (not shown). However, the justification for using an equilibrium phase for calcite instead of kinetically limited calcite dissolution depends on the model cell size and on the groundwater flow velocity. In this study, the model cells were very small (0.1 m) and thereby much smaller than in commonly applied models to simulate a CO_2 leakage at a large scale, which usually have cell sizes in the range of several metres. Therefore, it can be assumed that also the retention time of the groundwater in a cell of such large-scale models is much longer compared to the retention time per model cell simulated in this study. Consequently, a calcite equilibrium phase only using a thermodynamic reaction can be applied to calculate the calcite dissolution with sufficient precision. Applying reaction kinetics for calculating the calcite dissolution is not regarded as important for the application to field scale models simulating CO_2 leakage in calcareous porous aquifers with up to moderate groundwater flow velocities (1.0 m/day for the simulated field scale models). However, this conclusion has to be questioned in case of high groundwater flow velocities in porous media as well as in fractured media such as karst aquifers.

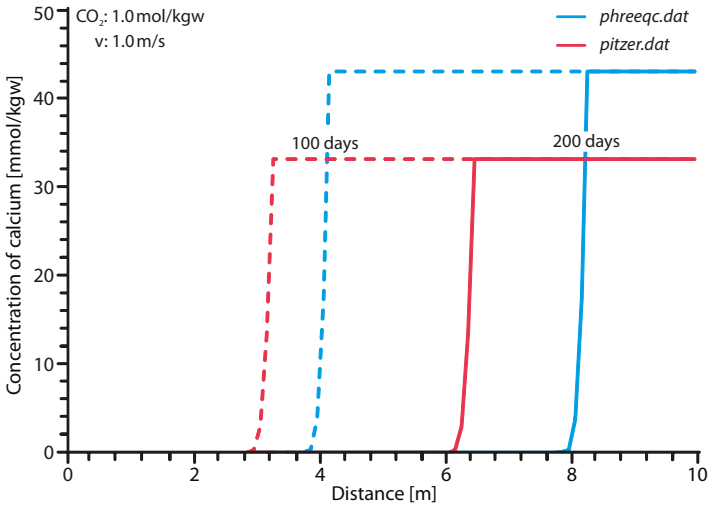

Figure 4.8

Calculated concentration of Ca_{tot}^{2+} applying PHREEQC using the databases *phreeqc.dat* and *pitzer.dat* using a closed system regarding CO_2 after a simulation time of 100 and 200 days. The concentration of CO_2 in the solution was set to 1.0 mol/kgw and the flow velocity was set to 1.0 m/s.

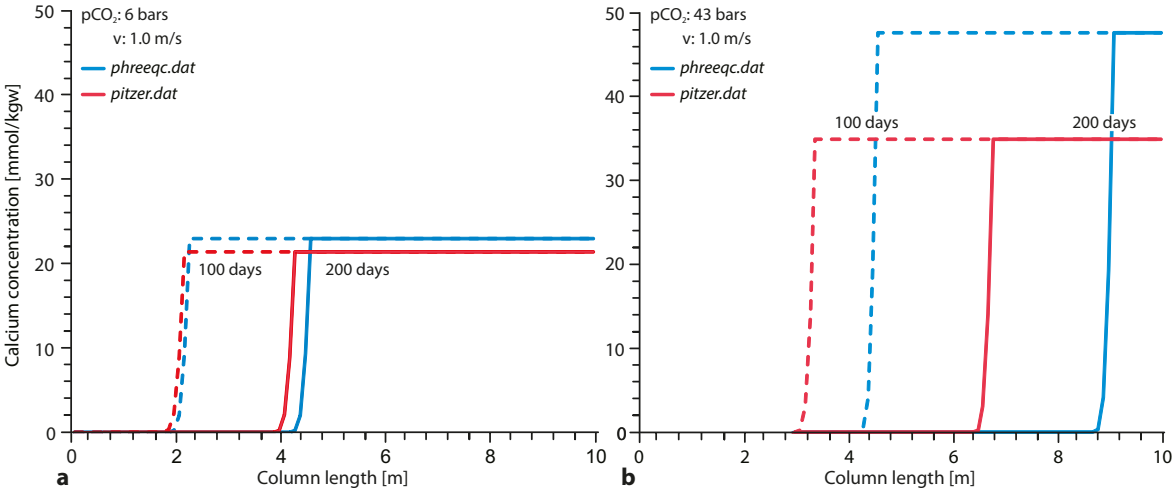

Figure 4.9 a und b

Calculated concentration of Ca_{tot}^{2+} applying PHREEQC and the databases *phreeqc.dat* and *pitzer.dat* in the field scale model with an open system regarding CO_2 after a simulation time of 100 and 200 days. The results applying a CO_2 partial pressure of 6 bars are at the left side and at 43 bars on the right side.

4.4 Conclusion

4.4.1 Calcite Dissolution Kinetics

Applying PHREEQC with the standard thermodynamic database and using the standard parameterisation for the rate laws did not reproduce the experimental results adequately. Only by fitting the surface area used in the model, the model results coincided with the calcium concentrations determined by the conducted column experiments. The necessity for this fitting procedure implies two main issues.

First, maintaining the rate constants from Plummer et al. (1978) or from Palandri and Kharaka (2004) required an overall decrease in the a priori measured and calculated physical calcite surface areas by one to three orders of magnitude, covering the discrepancy range between physical surface area and its reactive portion deducted by White and Peterson (1990). This discrepancy could perhaps be explained by the intrinsic variation of energy spectra between different calcite grains (Fischer et al., 2012). Therefore, Fischer and co-workers proposed abandoning the approach of relating mineral dissolution to surface areas, starting to define »surface energy spectra« and applying a probabilistic approach to regard the numerous possible energy spectra of mineral grains. In this way, crystal faces in different orientations and surface roughnesses can be regarded. Although thoroughly acknowledging Fischer's findings for demonstrating mineral dissolution mechanisms on a microscopic scale, we emphasise the practical applicability of the mineral dissolution kinetics on larger scales, like in column or field studies. In our presented study, numerous calcite grains probably showing different crystal faces and surface roughness were used, thus already implementing an intrinsic but nature-like probabilistic approach. Studies comparing an energy spectrum density function of naturally occurring mineral grains of a geological structure with larger scale dissolution experiments using the same material might be able to close the gap between Fischer's approach and the traditional relation of mineral surface areas to dissolution rates.

Second, the dissolution rate in the presented experiments was influenced by the applied water flow velocity, which we attribute to a variation in the thickness of the diffusion boundary layer (DBL) especially at the applied high flow velocities (Dreybrodt and Buhmann, 1991). Grathwohl (1998) defined the thickness of the DBL (d) by dividing the average grain size diameter (d_{50}) by the Sherwood number (S_h) (Equation 4.5). Including the Sherwood model of (Cussler, 2009), the thickness of the DBL is:

$$\delta = \frac{d_{50}}{\frac{6 \times \nu \times d_{50}}{\pi \times D}0.5} \tag{4.5}$$

with d in [m], d_{50} in [m], the water flow velocity v [m/s] and the diffusion constant for Ca^{2+} of 7.1×10^{-10} m^2/s (Aeschbach-Hertig, 2005). Applying an exemplary calcite grain size diameter of d_{50} of 5.0×10^{-04} m, DBL thicknesses of 4.4×10^{-06} m and 6.9×10^{-06} m were calculated for the flow velocities of 8.4 and 3.4 m/day, respectively, used in the presented laboratory experiment. This discrepancy might be decisive for the observed discrepancies of the calcite dissolution kinetics varying the flow velocity. However, the presented laboratory results in this study are too few to support a more general statement leaving this issue to be subject of current and future work.

4.4.2 Impact of Thermodynamic Databases on Calculated Calcium Equilibrium Concentrations

The uncertainty in the calcite solubility arising by the application of different thermodynamic databases was 150 % as it was determined by Haase et al. (2013). This uncertainty is larger compared to the results of this study and resulted from the application of a larger number of thermodynamic databases and a broader range of CO_2 partial pressures and temperatures. In our study, the Ca_{tot}^{2+} equilibrium concentrations differ most using the *pitzer.dat* database since the calculated Ca_{tot}^{2+} concentrations were in best agreement with the experimental values at 43 bars in contrast to using the *phreeqc.dat* database. The main reasons for the differences were the different activity models calculating varying calcite saturation states. As the equilibrium concentration of Ca_{tot}^{2+} was equal using a closed or an open system with respect to CO_2, the calculation method for the CO_2 solubility can be ruled out as a reason for the calculated differences in the Ca_{tot}^{2+} concentration. In this study, the pressure effect on the equilibrium constants (log_k) of calcite, CO_2 and the aquatic species was not considered, because Fahrner et al. (2012) and Dethlefsen et al. (2012) determined the influence of the pressure on the equilibrium constants as a minor factor.

In the presented study, the impact of the thermodynamic databases was only remarkable at CO_2 partial pressures of 43 bars. Independently, Haase et al. (2013) concluded that the application of the *pitzer.dat* database does not improve the results of the calcite and CO_2 solubility. The authors recommended to use the *phreeqc.dat* database to calculate the calcite dissolution due to CO_2 leakage into formations at a maximal depth of 400 m, as the regarded chemical system probably includes Si- or Al-components, which are not available in Pitzer databases (Pitzer, 1973). Maybe for this reason, the *pitzer.dat* database has not yet been applied for modelling the effects of CO_2 leakage. However, the presented study raises the question whether using the *pitzer.dat* can provide a more precise calculation of the calcite dissolution.

4.4.3 Insights for a Field Site Model

For field scale models simulating CO_2 leakages, the application of calcite dissolution kinetics is not absolutely necessary. The reason is, on the one hand, the fast calcite dissolution rate determined by the column experiments and, on the other hand, the application of a calcite equilibrium phase resulting in the same results compared to the application of calcite dissolution kinetics.

The increase in the dissolved Ca_{tot}^{2+} concentration is fast in the simulated field scale models using the fitted parameterisation based on the column experiment's results. The selection of the thermodynamic database is of minor relevance for the predictions made by a field scale model simulating a CO_2 leakage at the conditions of a near-surface formation (60 m). However, at larger depth (400 m) and consequently at higher pressures, the selection of the databases led to more significant differences. In general, the reaction front position varies in a small length compared to the regarded spatial dimension of a potential CO_2 leakage area.

The uncertainty in the extent of a decalcified aquifer zone due to the simulated CO_2 leakage in this study was approximately 2.5 m, depending on the thermodynamic database used. Consequently, pH values in this region cannot be calculated reliably. Other sources for site specific variations in the resulting pH-value can be varying mineral (i. e. calcite) content or the variability of the hydraulic parameters of the aquifer. The predicted extent of a decalcified aquifer zone can vary by an additional factor of 5 if the calcite content varies between 1 and 5 wt% in near-surface formations as it is described in Ohse (1983). Therefore, the mineral content variation can have a larger impact on the uncertainty of the model prediction than the variation caused by the choice of the suitable thermodynamic database if no further site investigation with respect to the calcite content is provided. Furthermore, real geologic formations include heterogeneities of the geochemical and hydraulic parameters, which can presumably increase the uncertainties.

Acknowledgements

This study was funded by the German Federal Ministry of Education and Research (BMBF), EnBW Energie Baden-Württemberg AG, E.ON Energie AG, E.ON Gas Storage AG, RWE Dea AG, Vattenfall Europe Technology Research GmbH, Wintershall Holding AG and Stadtwerke Kiel AG as part of the CO_2–MoPa joint project in the framework of the Special Program GEOTECHNOLOGIEN. We would like to acknowledge the associate editor Dr. Rolf S. Arvidson and an anonymous reviewer whose thorough reviews helped to considerably improve the quality of this manuscript.

References

Aeschbach-Hertig W. 2005. Physikalische Eigenschaften des Wassers, Heidelberg

Arvidson, R. S., Ertan, I. E., Amonette, J. E. & Luttge, A. 2003. Variation in calcite dissolution rates. Geochimica et Cosmochimica Acta 67(9), 1623–1634. *doi:10.1016/S0016-7037(02)01177-8*

Beims, U. 1983. Planung, Durchführung und Auswertung von Gütepumpversuchen. Zeitschrift für Angewandte Geologie 29(10), 482–490.

Berner, R. A. & Morse, J. W. 1974. Dissolution kinetics of calcium carbonate in seawater: IV. Theory of calcite dissolution. American Journal of Science 274(2), 108–134. *doi:10.2475/ajs.274.2.108*

Beyer, C., Li, D., Lucia M. D., Kühn, M. & Bauer, S. 2012. Modelling CO_2-induced fluid-rock interactions in the Altensalzwedel gas reservoir. Part II: coupled reactive transport simulation. Environmental Earth Sciences 67(2), 573–588. *doi:10.1007/s12665-012-1684-1*

Birkholzer, J., Apps, J., Zheng, L., Zhang, Y., Xu, T. & Tsang, C.-F. 2008. Research project on CO_2 geological storage and groundwater resources: Water quality effects caused by CO_2 intrusion into shallow groundwater, Technical Report, October 2008. pp. 472.

Boving, T. B. & Grathwohl, P. 2001. Tracer diffusion coefficients in sedimentary rocks: correlation to porosity and hydraulic conductivity. Journal of Contaminant Hydrology 53(1–2), 85–100. *doi:10.1016/S0169-7722 (01)00138-3*

Brendler, V., Richter, A. & Wilhelm, S. 2011. Thermodynamische Referenzdatenbasis. 1–16.

Brunauer S., Emmett P. H. & Teller, E. 1938. Adsorption of gases in multimolecular layers. Journal of the American Chemical Society 60(2), 309–319. *doi:10.1021/ja01269a023*

Buhmann, D. & Dreybrodt, W. 1985 a. The kinetics of calcite dissolution and precipitation in geologically relevant situations of karst areas, 1 Open System. Chemical Geology 48(1–2), 189–211. *doi:10.1016/0009-2541(85)90046-4*

Buhmann, D. & Dreybrodt, W. 1985 b. The kinetics of calcite dissolution and precipitation in geologically relevant situations of karst areas, 2 Closed System. Chemical Geology 53(3–4), 109–124. *doi:10.1016/0009-2541(85)90024-5*

Busenberg, E. & Plummer, L. N. 1986. A comparative study of the dissolution and crystal growth kinetics of calcite and aragonite. Studies in Diagenesis 1578:139–168

Casey, W. H., Banfield, J. F., Westrich, H. R. & Mclaughlin, L. 1993. What do dissolution experiments tell us about natural weathering? Chemical Geology 105(1–3), 1–15. *doi:10.1016/0009-2541(93)90115-Y*

Compton, R. G. & Daly, P. J. 1987. The dissolution/precipitation kinetics of calcium carbonate: an assessment of various kinetic equations using a rotating disk method. Journal of Colloid and Interface Science 115(2), 493–498. *doi:10.1016/0021-9797(87)90066-x*

Cussler, E. L. 2009. Diffusion: mass transfer in fluid systems. Cambridge University Press, p 631.

Dethlefsen, F., Haase, C., Ebert, M. & Dahmke, A. 2012. Uncertainties of geochemical modeling during CO_2 sequestration applying batch equilibrium calculations. Environmental Earth Sciences 65(4), 1105–1117. *doi:10.1007/s12665-011-1360-x*

Dethlefsen, F., Köber, R., Schäfer, D., al Hagrey, S. A., Hornbruch, G., Ebert, M., Beyer, M., Großmann, J. & Dahmke, A. 2013. Monitoring approaches for detecting and evaluating CO_2 and formation water leakages in near-surface aquifers. Energy Procedia 37:4886–4893. *doi:10.1016/j.egypro.2013.06.399*

Dreybrodt, W. & Buhmann, D. 1991. A mass transfer model for dissolution and precipitation of calcite from solutions in turbulent motion. Chemical Geology 90(1–2), 107–122. *doi:10.1016/0009-2541(91)90037-R*

Dreybrodt, W., Lauckner, J., Zaihua, L., Svensson, U. & Buhmann, D. 1996. The kinetics of the reaction $CO_2 + H_2O \rightarrow H^+ + HCO_3^-$, as one of the rate limiting steps for the dissolution of calcite in the system H_2O–CO_2–$CaCO_3$. Geochimica et Cosmochimica Acta 60(18), 3375–3381. *doi:10.1016/0016-7037(96)00181-0*

Duan, Z. & Li, D. 2008. Coupled phase and aqueous species equilibrium of the H_2O–CO_2–NaCl–$CaCO_3$ system from 0 to 250 °C, 1 to 1,000 bar with NaCl concentrations up to saturation of halite. Geochimica et Cosmochimica Acta 72:5128–5145. *doi:10.1016/j.gca.2008.07.025*

Duan, Z. & Sun, R. 2003. An improved model calculating CO_2 solubility in pure water and aqueous NaCl solutions from 273 to 533 K and from 0 to 2,000 bar. Chemical Geology 193(3–4), 257–271. *doi:10.1016/S0009-2541(02)00263-2*

Fahrner, S., Schäfer, D., Dethlefsen, F. & Dahmke, A. 2012. Reactive modelling of CO_2 intrusion into freshwater aquifers: current requirements, approaches and limitations to account for temperature and pressure effects. Environmental Earth Science 67(8), 2269–2283. *doi:10.1007/s12665-012-1673-4*

Finneran, D. W. & Morse, J. W. 2009. Calcite dissolution kinetics in saline waters. Chemical Geology 268(1–2), 137–146. *doi:10.1016/j.chemgeo.2009.08.006*

Fischer, C., Arvidson, R. S. & Lüttge, A. 2012. How predictable are dissolution rates of crystalline material? Geochimica et Cosmochimica Acta 98(1 December 2012), 177–185. *doi:10.1016/j.gca.2012.09.011*

Gabriel, G., Kirsch, R., Siemon, B. & Wiederhold, H. 2003. Geophysical investigation of buried Pleistocene subglacial valleys in Northern Germany. Journal of Applied Geophysics 53(4), 159–180. *doi:10.1016/j.jappgeo.2003.08.005*

Gaus, I., Audigane, P., André, L., Lions, J., Jacquemet, N., Durst, P., Czernichowski-Lauriol, I., Azaroual, M. 2008. Geochemical and solute transport modelling for CO_2 storage, what to expect from it? International Journal of Greenhouse Gas Control 2(4), 605–625. *doi:10.1016/j.ijggc.2008.02.011*

Gelhar, L. W., Welty, C., Rehfeldt, K. R. 1992. A critical review of data on field-scale dispersion in aquifers. Water Resources Research 28(7), 1955–1974. *doi:10.1029/92WR00607*

Gong, Q., Deng, J., Wang, Q., Yang, L., She, M. 2010. Experimental determination of calcite dissolution rates and equilibrium concentrations in deionized water approaching calcite equilibrium. Journal of Earth Science 21(4), 402–411. *doi:10.1007/s12583-010-0103-3*

Grathwohl, P. 1998. Diffusion in Natural Porous Media: contaminant transport, sorption/desorption and dissolution kinetics. 207

Haase, C., Dethlefsen, F., Ebert, M. & Dahmke, A. 2013. Uncertainty in geochemical modelling of CO_2 and calcite dissolution in NaCl solutions due to different modelling codes and thermodynamic databases. Applied Geochemistry 33(June 2013), 306–317. *doi:10.1016/j.apgeochem.2013.03.001*

Klotz, D. 1991. Erfahrung mit Säulenversuchen zur Bestimmung der Schadstoffmigration. Neuherberg.

Kump, L. R., Brantley, S. L. & Arthur, M. A. 2000. Chemical weathering, atmospheric CO_2, and climate. Annu Rev Earth Planet Science 28(1), 611–667. *doi:10.1146/annurev.earth.28.1.611*

Lasaga, A. C. 1984. Chemical kinetics of water-rock. Journal of Geophysical Research 89(B6), 4009–4025. *doi:10.1029/JB089iB06p04009*

Lemieux, J.-M. 2011. Review: the potential impact of underground geological storage of carbon dioxide in deep saline aquifers on shallow groundwater resources. Hydrogeology Journal 19(4), 757–778. *doi:10.1007/s10040-011-0715-4*

Liu, Z., Dreybrodt, W. 1997. Dissolution kinetics of calcium carbonate minerals in H_2O–CO_2 solutions in turbulent flow: the role of the diffusion boundary layer and the slow reaction $H_2O + CO_2 = H^+ + HCO_3^-$. Geochimica et Cosmochimica Acta 61(14), 2879–2889. *doi:10.1016/S0016-7037(97)00143-9*

Merkel, B., Planer-Friedrich, B. 2008. Groundwater geochemistry: a practical guide to modeling of natural and contaminated aquatic systems. pp. 242.

Mitiku, A.B., Li, D., Bauer, S. & Beyer, C. 2013. Geochemical modelling of CO_2-water-rock interactions in a potential storage formation of the North German sedimentary basin. Applied Geochemistry 36(September 2013), 169–186. *doi:10.1016/j.apgeochem.2013.06.008*

Morse, J. W., Arvidson, R. S. 2002. The dissolution kinetics of major sedimentary carbonate minerals. Earth-Science Reviews 58(1–2), 51–84. *doi:10.1016/S0012-8252(01)00083-6*

Ohse, W. 1983. Lösungs- und Fällungserscheinungen im System oberflächennanhes unterirdisches Wasser, gesteinsbildende Minerale -eine Untersuchung auf der Grundlage der chemischen Gleichgewichtsthermodynamik. Dissertation, Christian-Albrechts-Universität zu Kiel.

Palandri, J. L. & Kharaka, Y. K. 2004. A compilation of rate parameters of water–mineral interaction kinetics for application to geochemical modeling. U. S. Geological Survey Open file Report 2004–1068:71

Parkhurst, D. L. & Appelo, C. A. J. 1999. User's Guide to PHREEQC (Version 2): a computer program for speciation, batch-reaction, one-dimensional transport, and inverse geochemical calculations. U. S. Geological Survey. Water-Resources Investigation Report 99–4259:312

Peter, A., Lamert, H., Beyer, M., Hornbruch, G., Heinrich, B., Schulz, A., Geistlinger, H., Schreiber, B., Dietrich, P., Werban, U., Vogt, C., Richnow, H.-H., Großmann, J. & Dahmke, A. 2012. Investigation of the geochemical impact of CO_2 on shallow groundwater: design and implementation of a CO_2 injection test in Northeast Germany. Environmental Earth Sciences 67(2), 335–349. *doi:10.1007/s12665-012-1700-5*

Pickens, J. F. & Grisak, G. E. 1981. Scale-dependent dispersion in a stratified granular aquifer. Water Resour Res 17:(4), 191–1211. *doi:10.1029/WR017i004p01191*

Pitzer, K. S. 1973. Thermodynamics of electrolytes. I. Theoretical basis and general equations. The Journal of Physical Chemistry 77(2), 268–277. *doi:10.1021/j100621a026*

Pitzer, K. S., Kim J. J. 1974. Thermodynamics of electrolytes. IV. activity and osmotic coefficients for mixed electrolytes. Journal of the American Chemical Society 1426(4), 5701–5707. *doi:10.1021/ja00825a004*

Plummer, L. N., Wigley, T. M. L & Parkhurst, D. L. 1978. The kinetics of calcite dissolution in CO_2-water systems at 5–60 °C and 0.0–1.0 atm CO_2. American Journal of Science 278(2), 179–216. *doi:10.2475/ajs.278.2.179*

Pokrovsky, O. S., Golubev, S. V. & Schott, J. 2005. Dissolution kinetics of calcite, dolomite and magnesite at 25 °C and 0–50 atm pCO_2. Chemical Geology 217(3–4), 239–255. *doi:10.1016/j.chemgeo.2004.12.012*

Reddy, M. M., Plummer, L. N. & Busenberg, E. 1981. Crystal growth of calcite from calcium bicarbonate solutions at constant pCO_2 and 25 °C: a test of the calcite dissolution model. Geochimica et Cosmochimica Acta 45(8), 1281–1291. *doi:10.1016/0016-7037(81)90222-2*

Robinson, R. & Stokes, R. 1959. Electrolyte solutions: The Measurement and Interpretation of Conductance. Chemical Potential and Diffusion in Solutions of Simple Electrolytes, Butterworths. pp 559.

Schulz, H. D. 1988. Labormessung der Sättigungslänge als Maß für die Lösungskinetik von Karbonaten im Grundwasser. Geochim Cosmochim Acta 52(11), 2651–2657

Sjöberg, E. L. & Rickard, D. T. 1984. Temperature dependence of calcite dissolution kinetics between 1 and 62 °C at pH 2.7–8.4 in aqueous solutions. Geochimica et Cosmochimica Acta 48(3), 485–493. *doi:10.1016/0016-7037(84)90276-X*

Svensson, U. & Dreybrodt, W. 1992. Dissolution kinetics of natural calcite minerals in CO_2-water systems approaching calcite equilibrium. Chemical Geology 100(1–2), 129–145. *doi:10.1016/0009-2541(92)90106-F*

Talman, S. J., Wiwchar, B. & Gunter, W. D. 1990. Dissolution kinetics of calcite in the H2O-CO2 system along the steam saturation curve to 210 °C. In: Spencer, R. J. & Chou, I.-M. (eds) Fluid-Mineral Interactions. A Tribute to H. P. Eugster. Lancaster Press Inc, San Antonio, pp 41–55.

Trautz, R. C., Pugh J. D., Varadharajan, C., Zheng, L., Bianchi, M., Nico, P. S., Spycher, N. F., Newell, D. L., Esposito, R. A., Wu, Y., Dafflon, B., Hubbard, S. S. & Birkholzer, J. T. 2013. Effect of dissolved CO_2 on a shallow groundwater system: a controlled release field experiment. Environmental Science & Technology 47(1), 298–305. *doi:10.1021/es301280t*

Wang, S. & Jaffe, P. R. 2004. Dissolution of a mineral phase in potable aquifers due to CO_2 releases from deep formations; effect of dissolution kinetics. Energy Conversion and Management 45(18), 2833–2848. *doi:10.1016/j.enconman.2004.01.002*

White, A. F. & Peterson, M. L. 1990. Role of Reactive-Surface-Area Characterization in Geochemical Kinetic Models. In: Melchior, D. C. & Bassett, R. L. (eds). Chemical Modeling of Aqueous Systems II. American Chemical Society, Washington, DC. pp 461–475.

Wigley, M., Kampman, N., Dubacq, B. & Bickle, M. 2012. Fluid-mineral reactions and trace metal mobilization in an exhumed natural CO_2 reservoir, Green River, Utah. Geology 40(6), 555–558. *doi:10.1130/G32946.1*

Zheng, L., Apps, J. A., Zhang, Y., Xu, T. & Birkholzer, J. T. 2009 a. On mobilization of lead and arsenic in groundwater in response to CO_2 leakage from deep geological storage. Chemical Geology 268(3–4), 281–297. *doi:10.1016/j.chemgeo.2009.09.007*

Zheng, L., Apps, J. A., Zhang, Y., Xu, T. & Birkholzer, J. T. 2009 b. Reactive transport simulations to study groundwater quality changes in response to CO_2 leakage from deep geological storage. Energy Procedia 1:1887–1894. *doi:10.1016/j.egypro.2009.01.246*

5. Schlussfolgerungen & Ausblick

Unsicherheiten der geochemischen Codes und Datenbanken

Die Ergebnisse der Modellierung der Reaktion von CO_2 mit Calcit und Formationswasser in einem null-dimensionalen Modell weist bei variation der thermodynamischen Datenbanken maximale Unsicherheiten von 100 % auf. Die Unsicherheiten nehmen von kleinen Ionenstärken zu hohen Ionenstärken zu. Daher hat die Wahl der thermodynamischen Datenbanken besonders für Modelle von Speicherformationen einen signifikanten Einfluss auf die resultierende Unsicherheit. In reaktiven eindimensionalen Transportmodellen führt die Variation der thermodynamischen Datenbanken bei der Modellierung von Speicher- und Leckageszenarien von CO_2 für die Auflösung von Anorthit ebenfalls zu Unsicherheiten von ca. 100 %. Besonders in CO_2-Speicherformationen wie dem Rotliegend, Buntsandstein und dem Keuper, in denen die Mineralausfällung zur Festlegung von CO_2 der wichtigste Prozess für die langzeitspeicherung von CO_2 ist, ist die in dieser Arbeit bestimmte Unsicherheit am größten. In oberflächennahen Formationen ergibt sich bei Variation der Datenbanken eine viel geringere Unsicherheit. Die Vorhersageunsicherheit ist jedoch hauptsächlich abhängig von dem gewählten kinetischen Ratengesetz und den Ratenkonstanten.

Zur Bestimmung der Datenbank, die die besten Ergebnisse für CO_2-Leckagemodelle liefert, können die simulierten Daten mit experimentell erhobenen Daten verglichen werden. Da es bisher jedoch nur eine kleine Anzahl geeigneter Daten für die Calcitlösung bei höheren CO_2-Partialdrücken als 1 bar gibt, war es bisher nicht möglich die Ergebnisse von geochemischen Codes und deren thermodynamischen Datenbanken mit experimentellen Ergebnissen zu vergleichen. Daher wurden in dieser Arbeit Säulenversuche durchgeführt und deren Ergebnisse mit denen eines geochemischen Modellprogramms verglichen. Für kleinskalige Modelle wurde die Eignung der *pitzer.dat* Datenbank von PHREEQC für die Berechnung einer CO_2-Leckage in einen Aquifer in einer Tiefe von 400 m mit einem Formationswasser geringer Ionenstärke ermittelt. Die Modellunsicherheiten bei höheren Partialdrücken von 40 bar betragen bei Anwendung verschiedener thermodynamischer Datenbanken ca. 30 %. In einem eindimensionalen Feldskalamodell wurden Unterschiede in der Position der Reaktionsfront für Calcit ca. 20 % zwischen der Verwendung der *pitzer.dat* und *phreeqc.dat* Datenbank.

Durch die Verwendung der experimentell ermittelten Rate in einem ein-dimensionalen Transportmodell kann zudem nachgewiesen werden, dass die Auflösung von Calcit unter Verwendung einer Gleichgewichtsreaktion berechnet werden kann, ohne dass dadurch ein Fehler in der Berechnung der Calcitlösung gemacht wird. Die experimentell ermittelte Gleichgewichtseinstellung ist schnell genug, so dass in einer Modellzelle von großskaligen reaktiven Transportmodellen der Gleichgewichtszustand während der Aufenthaltszeit des Formationswassers in dieser Zelle erreicht wird.

Jedoch wurde in den Experimenten nur die CO_2- und Calcitlösung für ein Leckageszenario untersucht. Daher fehlen Vergleiche von Modellergebnissen mit Daten von Experimenten bei hohen Ionenstärken., Temperaturen und Drücken, wie sie in den Formationswässern möglicher Speicherformationen auftreten. Ebenso kann ein Vergleich der Modellergebnisse mit den experimentellen Daten für andere

Mineralphasen und andere Hauptkationen und -anionen in der Lösung, die Eignung einer anderen Datenbank zeigen.

Generell können die Unsicherheiten reduziert werden, wenn die CO_2-Lösung mit einer Zustandsgleichung berechnet wird, da CO_2 kein ideales Gas ist, aber die verwendeten Modellprogramme CO_2 als ideales Gas berechnen. Diese Studie zeigt, dass die Berechnung der CO_2-Löslichkeit ein einflussreicher Faktor für die Größe der Unsicherheiten ist. Für CO_2 können z. B. die Zustandsgleichungen von Redlich-Kwong, Redlich-Kwong-Soave, Peng-Robinson oder Duan et al. (1992) angewendet werden. Die Zustandsgleichungen müssten daher in den Modellcode implementiert werden. Nach Erscheinen des ersten Artikels (Kapitel 2) wurde die Zustandsgleichung von Peng-Robinson in die Version 3 von PHREEQC integriert (Parkhurst et al., 2013, Appelo et al., 2014).

Erkenntnisse für die Modellierung der CO_2-Speicherung

Die Unsicherheiten bei der Modellierung der Reaktion zwischen CO_2, dem Formationswasser und den Mineralen der Formation im Rahmen der CCS-Technologie können sich auf die Genauigkeit der Vorhersage der hydrodynamischen Speicherung von CO_2, der Festlegung von CO_2 in Mineralphasen oder der Entwicklung von Reaktionsfronten infolge von Minerallösungen auswirken. Dadurch kann die Vorhersage der gespeicherten CO_2-Menge eine große Spannweite aufweisen oder ein auf den Modellergebnissen basierendes Monitoringkonzept kann keine exakten Ergebnisse liefern. Dadurch kann eine CO_2-Leckage möglicherweise zu spät entdeckt werden. Ebenfalls können im Fall einer CO_2-Leckage die berechneten pH-Werte variieren und die Berechnung der Schwermetallfreisetzung durch Sorptions- oder Minerallösungsprozesse kann unterschiedliche Ergebnisse liefern. Durch diese Unsicherheiten kann eine Risikoabschätzung ungenau bleiben, so dass der Schutz der Trinkwasserqualität nicht ausreichend gesichert ist.

Die Unsicherheiten der Ergebnisse eines reaktiven Transportmodells werden zum einen durch das geochemische Modell und zum anderen durch das hydraulische Modell bestimmt. Welcher Reaktionsprozess überhaupt berechnet werden kann, wird durch das geochemische Teilmodell festgelegt. Wenn dem Programm Mineralphasen als Eingabeparameter und in der thermodynamischen Datenbank zur Verfügung stehen, können diese Reaktionen berechnet werde. Daher beeinflussen die Unsicherheiten in der Bestimmung der Mineralarten und -konzentrationen sowie die Wahl der zu verwendenden thermodynamischen Datenbank die möglichen zu berechnenden Prozesse. Die räumliche Position der ablaufenden Prozesse wird im Simulationsverlauf durch die Spannweiten der Eingabeparameter und daraus folgende Ergebnisunsicherheiten des hydraulischen Modells bestimmt. Diese Parameter können die hydraulische Durchlässigkeit, die Porosität oder das Strömungsfeld sein. In tiefen Formationen oder Aquiferen, die für die CO_2-Speicherung geeignet sind, ist besonders das Strömungsfeld, d. h. die Strömungsrichtung und -geschwindigkeit, unbekannt. Da das Strömungsfeld den Transport der im Wasser gelösten Stoffe wahrscheinlich am stärksten beeinflusst, ist der Einfluss der übrigen hydraulischen Parameter auf die Position von z. B. Reaktionsfronten als geringer einzustufen.

Die Bestimmung der reaktiven Oberfläche eines Minerals wird für kinetische Reaktionen nicht für jedes Szenariomodell eines CO_2-Speicherkomplexes experimentell bestimmt. Meist werden Literaturwerte für die reaktiven Mineraloberflächen verwendet. Daher sind die Oberflächen für das Standortmodell nicht genau bekannt. Weiterhin ist es nicht möglich die Mineraloberflächen für das gesamte Modellgebiet zu bestimmen. Daher kann die Variation der Oberflächen im Modellgebiet nicht ermittelt werden, wodurch weitere Ergebnisunsicherheiten auftreten können.

Zusätzlich zu den Spannbreiten der Parameter, die in das Transportmodell eingehen, ist natürlich die räumliche Verteilung der hydraulischen Parameter, also die Heterogenität der Formation, nicht hinreichend genau bekannt. Die räumliche Verteilung der Mineralarten und der -konzentrationen der Formation ist für Speicherformationen oder potentielle Leckageformationen ebenso weitgehend unbekannt. Eine Quantifizierung der Unsicherheiten verursacht durch Heterogenitäten ist im Allgemeinen nicht möglich und kann nur für jedes einzelne Szenariomodell eines Speicherstandortes vorgenommen werden.

Wenn ein Modell für eine CO_2-Speicherformation erstellt wird, sind neben den Unsicherheiten des geochemischen und hydraulischen Modells auch die Unsicherheiten des Mehrphasenströmungsmodells wichtig. Dabei weisen die intrinsischen Permeabilitäten, relativen Permeabilitäten und der Kapillardruck Spannbreiten auf, die zu einer ungenauen Prognose der Ausbreitung der CO_2-Gasphase in der Speicherformation führen können. Diese Unsicherheiten können die vorgenannten Unsicherheiten überlagern und damit wesentlich wichtiger sein.

Die Anwendung reaktiver Transportmodelle für die CO_2-Speicherung sollte angesichts der Größenordnung der in dieser Arbeit bestimmten Unsicherheiten immer von einer Unsicherheitsanalyse begleitet werden. Besonderes Augenmerk sollte dabei auf den Unsicherheiten des geochemischen Teilmodells liegen. Wenn es möglich ist, sollte die Anwendung verschiedener thermodynamischer Datenbanken getestet werden, um die Modellunsicherheiten zu bestimmen. Bei der Anwendung kinetischer Reaktionen sollten ebenso die kinetischen Ratenkonstanten innerhalb der bekannten experimentellen Spannweiten variiert werden. Mit dieser Vorgehensweise kann der Einfluss der verschiedenen Eingabeparameter des geochemischen Modells auf die Modellvorhersage quantifiziert werden. Damit kann die Prognosesicherheit in einen bestimmten Rahmen bewertet werden.

Ausblick

Die Simulation geochemischer Prozesse in tiefen geologischen Formationen bei hohen CO_2-Partialdrücken ist eine Herausforderung für die bisher bestehenden Codes und thermodynamischen Datenbanken. Zur Verbesserung der Simulation geochemischer Prozesse werden Erweiterungen der thermodynamischen Datenbanken im Hinblick auf Pitzer-Parameter bei hohen Temperaturen, dabei besonders für Aluminium und Silizium, die Berechnung der CO_2-Löslichkeit und kinetische Minerallösungs- und -fällungsraten benötigt.

Die geochemischen Codes und ihre Datenbanken können anhand von experimentellen Daten kalibriert werden. Experimentelle Daten sind bisher für wichtige gesteinsbildende Mineralphasen und Sekundärminerale gerade bei den Randbedingungen einer CO_2-Speicherformation nicht verfügbar. Zum Beispiel wurde die Calcit-Löslichkeit bei CO_2-Partialdrücken von maximal 50 bar bestimmt. Daher sind besonders für diese Randbedingengen experimentelle Daten notwendig.

Bei der Berechnung komplexer geochemischer Systeme ist es fraglich, ob die Kalibrierung geochemischer Modelle mit Hilfe von experimentellen Daten die Modellvorhersage verbessert. Die thermodynamischen Datenbanken können durch Experimente für spezielle geochemische Systeme (Reaktionsszenarien) kalibriert werden. Die Reaktionsparameter können jedoch am Standort des CO_2-Speichers von den experimentellen Randbedingungen abweichen. Zum Beispiel können am Speicherstandort andere Reaktionen ablaufen oder die Randbedingen von denen der Experimente abweichen. Für diesen Fall ist die Kalibrierung der geochemischen Modelle nicht mehr gegeben. Um zumindest die Spannwei-

ten der Modellergebnisse zu bestimmen ist es notwendig Unsicherheitsanalysen – wie in dieser Arbeit gezeigt – durchzuführen.

Generell eignen sich geochemische Codes und ihrer thermodynamischen Datenbanken um geochemische Reaktionen in CO_2-Speicherformationen und in oberflächennahen Formationen vorherzusagen. Allerdings sind die Vorhersagen besonders in tiefen Speicherformationen mit großen Unsicherheiten behaftet. Die Ergebnisspannweiten können in diesem Fall – auch für reaktive Transportmodelle – nur durch Unsicherheitsanalysen ermittelt werden.

Referenzen

Appelo, C. A. J., Parkhurst, D. L. & Post, V. E. A. 2014. Equations for calculating hydrogeochemical reactions of minerals and gases such as CO_2 at high pressures and temperatures. Geochimica et Cosmochimica Acta, 125 (15), 49–67. *doi:10.1016/j.gca.2013.10.003*

Palandri, J. L., & Kharaka, Y. K. 2004. A compilation of rate parameters of water-mineral interaction kinetics for application to geochemical modeling. U. S. Geological Survey Open File Report 2004-1068 (Vol. 1068). Retrieved from http://www.dtic.mil/cgi-bin/GetTRDoc?Location=U2&doc=GetTRDoc.pdf&AD=ADA440035

Parkhurst, D. L. & Appelo, C. A. J. 2013. PHREEQC (Version 3)–A Computer Program for Speciation, Batch-Reaction, One-Dimensional Transport, and Inverse Geochemical Calculations. Modeling Techniques, Book 6. U. S. Department of the Interior, U. S. Geological Survey. Retrieved from http://pubs.usgs.gov/tm/06/a43/

Eigenständigkeitserklärung

Hiermit versichere ich, dass ich die vorliegende Arbeit — abgesehen von der Beratung durch den Betreuer — selbstständig und nur mit den angegebenen Hilfsmitteln verfasst habe. Die Arbeit wurde keinen anderen Stellen im Rahmen eines Prüfungsverfahrens zur Promotion vorgelegt.

Weiterhin wurde die Arbeit unter der Einhaltung der Regeln guter wissenschaftlicher Praxis der Deutschen Forschungsgemeinschaft (DFG) erstellt.

Kiel, 05. November 2015 Christoph Haase

Danksagung

An erster Stelle gilt mein herzlicher Dank PD Dr. Markus Ebert, der erst diese Arbeit ermöglichte und mich bei der Erstellung der Arbeit betreute. PD Dr. Markus Ebert danke ich für die intensiven Korrekturen meiner Publikationen, für viele Anregungen und Ratschläge, die er mir für diese Arbeit gab, und für interessante fachliche Diskussionen .

Für die Übernahme des zweiten Gutachters gilt mein Dank Prof. Dr. Romain Bousquet.

Die Säulenversuche für das fünfte Kapitel und für die Publikation wurden von Dr. Frank Dethlefsen, seinen Diplomanden und Bachelor-Studenten durchgeführt. Dr. Frank Dethlefsen hat die Publikationen, aus denen diese Arbeit besteht, intensiv korrektur gelesen und mit zahlreichen und hilfreichen Anmerkungen versehen. Er stand immer für Diskussionen bereit und beantwortete gerne viele meiner Fragen. Dafür bedanke ich mich sehr herzlich bei ihm.

Dem Arbeitsgruppenleiter der »Angewandten Geologie« Prof. Dr. Andreas Dahmke gilt mein Dank für zahlreiche kritische Kommentare, die zur Verbesserung meiner Manuskripte beigetragen haben.

Ein herzliches Dankeschön geht an meine Kollegen Dr. Christof Beyer, Dr. Katharina Erning, Dr. Sven Fahrner, Dr. Anna Jeßusek und Dr. Ralf Köber, die Teile meiner Publikationen gelesen oder mir Ratschläge gegeben haben und immer für Diskussionen bereitstanden.

Meinen Eltern danke ich für das Korrekturlesen der Einleitung und für die Unterstützung während der gesamten Zeit meiner Doktorarbeit.

Wissenschaftlicher Lebenslauf

Christoph Haase

Stellinger Weg 51
20255 Hamburg

0175 62 91 27 1
haase02@gmail.com

*30. Januar 1982 in Wolfenbüttel

Berufliche Praxis

04/2014 – heute	Projektleiter, Ingenieurgesellschaft Dr. Schmidt mbH
	Hydrogeologische Gutachten und Stellungnahmen zur Grundwasserennahme Hydrogeologische Stellungnahmen zur Grundwasserbeschaffenheit Beprobung und Bewertung von Böden Betreuung und Auswertung geologischer und hydrogeologischer Bohrungen Anwendung numerischer Grundwasserstömungsmodelle für die Berechnung von Absenkungsbereichen, Einzugsgebieten und für Bahnlinienanalysen
01/2009 – 11/2015	Promotion, Christian-Albrechts-Universität zu Kiel
06/2013 – 08/2013	wissenschaftlicher Mitarbeiter, Christian-Albrechts-Universität zu Kiel
	Projekt: Auswirkungen der Nutzung des geologischen Untergrundes als thermischer, elektrischer oder stofflicher Speicher im Kontext der Energiewende (ANGUS+)
	Qualitätsanalyse von Wasseranalysen aus tiefen geologischen Formationen Deutschlands
01/2009 – 06/2012	wissenschaftlicher Mitarbeiter, Christian-Albrechts-Universität zu Kiel
	Projekt: Modellierung und Parametrisierung von CO_2-Speicherung in tiefen, salinen Formationen für Dimensionierungs- und Risikoanalysen (CO_2-MoPa), Verbundvorhaben im Rahmen des deutschen Forschungsprogrammes GEOTECHNOLOGIEN
	Bestimmung der Unsicherheiten bei der geochemischen Modellierung der CO_2-Speicherung und CO_2-Leckage Einfluss der Datenvarianz thermodynamischer Datenbanken auf die Berechnung von Gas-Wasser-Gesteins-Wechselwirkungen Vergleich von Modellergebnissen mit experimentellen Ergebnissen von Säulenversuchen der Calcitlösung

Studium

10/2002 – 10/2008	Studium der Geologie, Technische Universität Clausthal
	Schwerpunkte: Hydrogeologie, Petrologie/Geochemie Abschluss: Diplom
	Diplomarbeit in Zusammenarbeit mit dem Hessischen Landesamt für Umwelt und Geologie (HLUG): »Auswertung von Thermal- und Mineralwasseranalysen aus dem Raum Frankfurt am Main« Ausgezeichnet mit dem Förderpreis der Wolfgang-Helms-Stiftung 2009
	Diplomkartierung: »Strukturgeologische Kartierung des westlichen Kullabergs (Schonen, SW-Schweden)«
	Exkursionen u. a. in den Harz und das Harzvorland, in die Alpen und nach Südafrika Kartierkurse u.a. im Harz und Harzvorland und in den Alpen
10/2001 – 09/2002	Studium des Bauingenieurwesens, Technische Universität Carolo-Wilhelmina Braunschweig

Kiel, 05. November 2015

Anhang A

Anhang A

Eingabedateien für PHREEQC, EQ3/6 und THE GEOCHEMIST'S WORKBENCH zu Kapitel 4 (»Uncertainty in geochemical modelling of CO_2 and calcite dissolution in NaCl solutions due to different modelling codes and thermodynamic databases«).

Die Eingabedateien von FactSage sind nicht dargestellt, da die einzelnen Eingabedateien nicht abgespeichert werden können.

A.1 Eingabedateien für PhreeqC

Die Datenbanken können bei PHREEQC über die Benutzeroberfläche oder über die Eingabe des Keywords DATABASE variiert werde.

A.1.1 Calcitauflösung

A.1.1.1 offenes System bei einer Fugazität von 1 bar

```
TITLE open system; 1bar CO2 fugacity; T 25°C, 50°C, 75°C; calcite dissolution

SOLUTION 1
-units mol/kgw
-temp   25              # 50    # 75
-pH     7.0
Ca              0.002
Alkalinity      0.004
END

USE SOLUTION 1
EQUILIBRIUM_PHASES 1
CO2(g)          0.0     # Logarithm of 1bar CO2 fugacity
Calcite         0.0

REACTION 1
NaCl    4.0
1 in 51 steps
END
```

A.1.1.2 offenes System bei einer Fugazität von 10 bar

```
TITLE open system; 10bars CO2 fugacity; T 25°C, 50°C, 75°C; calcite dissolution

SOLUTION 1
-units mol/kgw
-temp   25              # 50    # 75
-pH     7.0
Ca              0.002
Alkalinity      0.004
END

USE SOLUTION 1
EQUILIBRIUM_PHASES 1
CO2(g)          1.0     # Logarithm of 10bars CO2 fugacity
Calcite         0.0

REACTION 1
NaCl    4.0
1 in 51 steps
END
```

A.1.1.3 offenes System bei einer Fugazität von 50 bar

```
TITLE open system, 50bars CO2 fugacity; T 25°C, 50°C, 75°C; calcite dissolution

SOLUTION 1
-units mol/kgw
-temp   25              # 50 # 75
-pH     7.0
Ca              0.002
Alkalinity      0.004
END

USE SOLUTION 1
EQUILIBRIUM_PHASES 1
```

```
CO2(g)          1.69    # Logarithm of 50bars CO2 fugacity
Calcite         0.0
SAVE SOLUTION 2

REACTION 1
NaCl    4.0
1 in 51 steps
END
```

A.1.1.4 offenes System bei einer Fugazität von 100 bar

```
TITLE open system; 100bars CO2 fugacity; T 25°C, 50°C, 75°C; calcite dissolution

SOLUTION 1
-units mol/kgw
-temp   25              # 50    # 75
-pH     7.0
Ca              0.002
Alkalinity      0.004
END

USE SOLUTION 1
EQUILIBRIUM_PHASES 1
CO2(g)          2.0     # Logarithm of 100 bars CO2 fugacity
Calcite         0.0

REACTION 1
NaCl    4.0
1 in 51 steps
END
```

A.1.1.5 geoschlossenes System bei einer Konzentration von 0.5 mol/kgw

```
TITLE closed system; concentration 0.5mol CO2/kgw; T 25°C, 50°C, 75°C; calcite dissolution

SOLUTION 1
-units mol/kgw
-temp   25              # 50    # 75
-pH     7.0
Ca              0.002
Alkalinity      0.004
END

USE SOLUTION 1
REACTION 1
CO2(g)          0.5
EQUILIBRIUM_PHASES 1
Calcite         0.0

REACTION 1
NaCl    4.0
1 in 51 steps
END
```

A.1.1.6 geoschlossenes System bei einer Konzentration von 1.0 mol/kgw

```
TITLE closed system; concentration 1.0mol CO2/kgw; T 25°C, 50°C, 75°C; calcite dissolution

SOLUTION 1
-units mol/kgw
-temp   25              # 50    # 75
-pH     7.0
Ca              0.002
Alkalinity      0.004
END
```

```
USE SOLUTION 1
REACTION 1
CO2(g)          1.0
EQUILIBRIUM_PHASES 1
Calcite         0.0

REACTION 2
NaCl    4.0
1 in 51 steps
END
```

A.1.2 Calcitauflösung mit der Ausfällung von Halit

A.1.2.1 offenes System bei einer Fugazität von 1 bar, Ausfällung von Halit

```
TITLE open System, 1bar CO2 fugacity; T 25°C, 50°C, 75°C; Calcite dissolution; Halite
equilibrium

SOLUTION 1
-units mol/kgw
-temp   25              # 50    # 75
-pH     7.0
Ca              0.002
Alkalinity      0.004
END

USE SOLUTION 1
EQUILIBRIUM_PHASES 1
CO2(g)          0.0     # Logarithm of 1bar CO2 fugacity
Calcite         0.0
Halite          0.0

REACTION 1
NaCl    4.0
1 in 51 steps
END
```

A.1.2.2 offenes System bei einer Fugazität von 10 bar, Ausfällung von Halit

```
TITLE open System, 10bar CO2 fugacity; T 25°C, 50°C, 75°C; Calcite dissolution; Halite
equilibrium
SOLUTION 1
-units mol/kgw
-temp   25              # 50    # 75
-pH     7.0
Ca              0.002
Alkalinity      0.004
END

USE SOLUTION 1
EQUILIBRIUM_PHASES 1
CO2(g)          1.0     # Logarithm of 10bar CO2 fugacity
Calcite         0.0
Halite          0.0

REACTION 1
NaCl    4.0
1 in 51 steps
END
```

A.1.2.3 offenes System bei einer Fugazität von 50 bar, Ausfällung von Halit

```
TITLE open System, 50bar CO2 fugacity; T 25°C, 50°C, 75°C; Calcite dissolution; Halite
equilibrium
```

```
SOLUTION 1
-units mol/kgw
-temp   25              # 50    # 75
-pH     7.0
Ca              0.002
Alkalinity      0.004
END

USE SOLUTION 1
EQUILIBRIUM_PHASES 1
CO2(g)          1.69    # Logarithm of 50bars CO2 fugacity
Calcite         0.0
Halite          0.0

REACTION 1
NaCl    4.0
1 in 51 steps
END
```

A.1.2.4 offenes System bei einer Fugazität von 100 bar, Ausfällung von Halit

```
TITLE open System, 100bar CO2 fugacity; T 25°C, 50°C, 75°C; Calcite dissolution; Halite
equilibrium

SOLUTION 1
-units mol/kgw
-temp   25              # 50    # 75
-pH     7.0
Ca              0.002
Alkalinity      0.004
END

USE SOLUTION 1
EQUILIBRIUM_PHASES 1
CO2(g)          2.0     # Logarithm of 100bars CO2 fugacity
Calcite         0.0
Halite          0.0

REACTION 1
NaCl    4.0
1 in 51 steps
END
```

A.1.2.5 geschlossenes System bei einer Konzentration von 0.5 mol/kgw

```
TITLE closed system; concentration 0.5 mol CO2/kgw; T 25°C, 50°C, 75°C; calcite dissolution

SOLUTION 1
-units mol/kgw
-temp   25              # 50    # 75
-pH     7.0
Ca              0.002
Alkalinity      0.004
END

USE SOLUTION 1
REACTION 1
CO2(g)  0.5
EQUILIBRIUM_PHASES 1
Calcite         0.0
Halite          0.0

REACTION 1
NaCl    4.0
```

```
1 in 51 steps
END
```

A.1.2.6 geoschlossenes System bei einer Konzentration von 1.0 mol/kgw

```
TITLE closed system; concentration 1.0 mol CO2/kgw; T 25 °C, 50 °C, 75 °C; calcite dissolu-
tion; Halite equilibrium

SOLUTION 1
-units mol/kgw
-temp   25              # 50    # 75
-pH     7.0
Ca              0.002
Alkalinity      0.004
END

USE SOLUTION 1
REACTION 1
CO2(g)  1.0
EQUILIBRIUM_PHASES 1
Calcite         0.0
Halite          0.0

REACTION 1
NaCl    4.0
1 in 51 steps
END
```

A.2. Eingabedateien für The Geochemist's Workbench

Für höhere Temperaturen `temperature = 25` durch `50` oder `75` ersetzen.
Für höhere Fugazitäten `CO2(g) = 1.0 fugacity` durch `10`, `50` oder `100` ersetzten.

A.2.1 offenes System

A.2.1.1 thermo_phreeqc.dat, thermo_wateq4f.dat

```
# React script, saved Thu Jan 13 2011 by C.Haase
data = C:\Programme\Gwb\Gtdata\thermo_phreeqc.dat verify
temperature = 25
H2O     = 1.0 free kg
Na+     = 1.0E-20 mmolal
Cl-     = 1.0E-20 mmolal
Ca++    = 2.0 mmolal
swap CO2(g) for H+
CO2(g)  = 1.0 fugacity
swap Calcite for CO3--
Calcite = 1.0 free mol
balance on Ca++
react 4.0 mol of Na+
react 4.0 mol of Cl-
fix fugacity of CO2(g)
printout alphabetical  species = long minerals = long       basis = long
plot    = character
delxi   = 0.5 linear
dxplot  = 0.1
dxprint = 0.01
itmax   = 200
```

A.2.1.2 thermo_minteq.dat

```
# React script, saved Thu Jan 13 2011 by C.Haase
data = C:\Programme\Gwb\Gtdata\thermo_minteq.dat verify
temperature = 25
H2O     = 1.0 free kg
Na+     = 1.0E-20 mmolal
```

```
Cl-     = 1.0E-20 mmolal
Ca++    = 2.0 mmolal
swap „CO2 (g)“ for H+
„CO2 (g)“ = 1.0 fugacity
swap Calcite for CO3--
Calcite = 1.0 free mol
balance on Ca++
react 4.0 mol of Na+
react 4.0 mol of Cl-
fix fugacity of „CO2 (g)“
printout alphabetical  species = long minerals = long       basis = long
plot    = character
delxi   = 0.01 linear
dxplot  = 0.01
dxprint = 0.01
itmax   = 200
```

A.2.1.3 thermo.dat, thermo.com.v8.r6+.dat, thermo_hdata.dat, thermo_hmw.dat, thermo_phrqpitz.dat

```
# React script, saved Thu Jan 13 2011 by C.Haase
data = C:\Programme\Gwb\Gtdata\thermo.dat verify
temperature = 25
H2O     = 1.0 free kg
Na+     = 1.0E-20 mmolal
Cl-     = 1.0E-20 mmolal
Ca++    = 2.0 mmolal
swap CO2(g) for H+
CO2(g)  = 1.0 fugacity
swap Calcite for HCO3-
Calcite = 1.0 free mol
balance on Ca++
react 4.0 mol of Na+
react 4.0 mol of Cl-
fix fugacity of CO2(g)
printout alphabetical  species = long minerals = long       basis = long
plot    = character
delxi   = 0.01 linear
dxplot  = 0.01
dxprint = 0.01
simax   = 4
timax   = 4
```

A.2.2 geschlossenes System

A.2.2.1 thermo_wateq4f.dat, thermo_phreeqc.dat

```
# React script, saved Thu Jan 20 2011 by C.Haase
data = C:\Programme\Gwb\Gtdata\thermo_phreeqc.dat verify
temperature = 25
H2O     = 1.0 free kg
Na+     = 1.0E-20 mmolal
Cl-     = 1.0E-20 mmolal
Ca++    = 2.0 mmolal
swap CO2 for H+
CO2     = 1.0 mol
swap Calcite for CO3--
Calcite = 1.0 free mol
balance on Ca++
react 4.0 mol of Cl-
react 4.0 mol of Na+
printout  basis = long
delxi   = 0.01 linear
dxplot  = 0.01
dxprint = 0.01
```

```
simax   = 4
timax   = 4
```

A.2.2.2 thermo_minteq.dat

```
# React script, saved Thu Jan 20 2011 by C.Haase
data = C:\Programme\Gwb\Gtdata\thermo_minteq.dat verify
temperature = 25
H2O     = 1.0 free kg
Na+     = 1.0E-20 mmolal
Cl-     = 1.0E-20 mmolal
Ca++    = 2.0 mmolal
swap „CO2 (aq)“ for H+
„CO2 (aq)“ = 1.0 mol
swap Calcite for CO3--
Calcite = 1.0 free mol
balance on Ca++
react 4.0 mol of Cl-
react 4.0 mol of Na+
printout  basis = long
delxi   = 0.01 linear
dxplot  = 0.01
dxprint = 0.01
simax   = 4
timax   = 4
```

A.2.2.3 thermo.dat, thermo.com.v8.r6+.dat

```
# React script, saved Tue Jun 08 2010 by C.Haase
data = C:\Programme\Gwb\Gtdata\thermo.dat verify
temperature = 25
H2O     = 1.0 free kg
Na+     = 1.0E-20 mmolal
Cl-     = 1.0E-20 mmolal
Ca++    = 2.0 mmolal
swap CO2(aq) for H+
CO2(aq) = 0.5 mol
swap Calcite for HCO3-
Calcite = 1.0 free mol
balance on Ca++
react   4.0 mol of Cl-
react   4.0 mol of Na+
delxi   = 0.01 linear
dxplot  = 0.01
dxprint = 0.01
simax   = 4
timax   = 4
```

A.3 Eingabedateien für EQ3/6

Im Anhang wird beispielhaft nur eine Eingabedatei je Szenario für EQ3 und EQ6 dargestellt. Die Eingabedateien für alle Datenbanken befinden sich auf beiliegender CD.

A.3.1 Calcitauflösung

A.3.1.1 EQ3 Eingabedatei, data0.cmp (offenes System)

```
|-------------------------------------------------------------------------------|
| Title                  | (utitl(n))                                           |
|-------------------------------------------------------------------------------|
|EQ3NR input file name= NaCl_offen.3i                                           |
|Description=„Calcite dissolution in NaCl solution"                             |
|Version level= 8.0                                                             |
|Revised 12/10/2010    Revisor= C.Haase                                         |
|                                                                               |
|Szenario NaCl; T= 25 °C, fCO2= 1 bar                                           |
|Input für Nacl_offen.6i                                                        |
|Ca= 2.0 mmol; CO3= 4.0 mmol                                                    |
|Database data0.cmp                                                             |
|                                                                               |
|-------------------------------------------------------------------------------|
|Special Basis Switches (for model definition only)       | (nsbswt)            |
|-------------------------------------------------------------------------------|
|Replace |None                                            | (usbsw(1,n))        |
|   with |None                                            | (usbsw(2,n))        |
|-------------------------------------------------------------------------------|
|Temperature (C)         | 2.50000E+01| (tempc)                                 |
|-------------------------------------------------------------------------------|
|Pressure option (jpres3):                                                      |
|  [ ] ( 0) Data file reference curve value                                     |
|  [x] ( 1) 1.013-bar/steam-saturation curve value                              |
|  [ ] ( 2) Value (bars) | 0.00000E+00| (press)                                 |
|-------------------------------------------------------------------------------|
|Density (g/cm3)         | 1.00000E+00| (rho)                                   |
|-------------------------------------------------------------------------------|
|Total dissolved solutes option (itdsf3):                                       |
|  [x] ( 0) Value (mg/kg.sol) | 0.00000E+00| (tdspkg)                         |
|  [ ] ( 1) Value (mg/L)      | 0.00000E+00| (tdspl)                          |
|-------------------------------------------------------------------------------|
|Electrical balancing option (iebal3):                                          |
|  [x] ( 0) No balancing is done                                                |
|  [ ] ( 1) Balance on species |Cl-                      | (uebal)              |
|-------------------------------------------------------------------------------|
|Default redox constraint (irdxc3):                                             |
|  [ ] (-3) Use O2(g) line in the aqueous basis species block                   |
|  [x] (-2) pe (pe units)      | 4.00000E+00| (pei)                             |
|  [ ] (-1) Eh (volts)         | 5.00000E-01| (ehi)                             |
|  [ ] ( 0) Log fO2 (log bars) | 0.00000E+00| (fo2lgi)                          |
|  [ ] ( 1) Couple (aux. sp.)  |None                     | (uredox)             |
|-------------------------------------------------------------------------------|
|Aqueous Basis Species/Constraint Species        |Conc., etc. |Units/Constraint|
| (uspeci(n)/ucospi(n))                          | (covali(n))|(ujf3(jflgi(n)))|
|-------------------------------------------------------------------------------|
|H+                                              |7.00000E+00|pH                 |
|Ca++                                            |2.00000E-03|Molality           |
|HCO3-                                           |4.00000E-03|Molality           |
|Na+                                             |1.00000E-20|Molality           |
|Cl-                                             |1.00000E-20|Molality           |
|-------------------------------------------------------------------------------|
|Create Ion Exchangers  | (net)                                                 |
|-------------------------------------------------------------------------------|
|Advisory: no exchanger creation blocks follow on this file.                    |
```

```
|Option: on further processing (writing a PICKUP file or running XCON3 on the  |
|present file), force the inclusion of at least one such block (qgexsh):       |
|  [ ] (.true.)                                                                |
|------------------------------------------------------------------------------|
|Ion Exchanger Compositions      | (neti)                                      |
|------------------------------------------------------------------------------|
|Exchanger phase |None                    | (ugexpi(n))                        |
|------------------------------------------------------------------------------|
|->|Moles/kg.H2O    |  0.0000    | (cgexpi(n))                                |
|------------------------------------------------------------------------------|
|->|Exchange site   |None    | (ugexji(j,n))                                  |
|------------------------------------------------------------------------------|
|--->|Exchange species        |Eq. frac.   | (this is a table header)          |
|------------------------------------------------------------------------------|
|--->|None                    | 0.00000E+00| (ugexsi(i,j,n), egexsi(i,j,n))    |
|------------------------------------------------------------------------------|
|Solid Solution Compositions     | (nxti)                                      |
|------------------------------------------------------------------------------|
|Solid Solution          |None                    | (usoli(n))                 |
|------------------------------------------------------------------------------|
|->|Component               |Mole frac.  | (this is a table header)            |
|------------------------------------------------------------------------------|
|->|None                    | 0.00000E+00| (umemi(i,n), xbari(i,n))            |
|------------------------------------------------------------------------------|
|Alter/Suppress Options  | (nxmod)                                             |
|------------------------------------------------------------------------------|
|Species                                        |Option          |Alter value |
|  (uxmod(n))                                   |(ukxm(kxmod(n)))| (xlkmod(n))|
|------------------------------------------------------------------------------|
|None                                           |Suppress        | 0.00000E+00|
|------------------------------------------------------------------------------|
|Iopt Model Option Switches („( 0)“ marks default choices)                     |
|------------------------------------------------------------------------------|
|iopt(4) - Solid Solutions:                                                    |
|  [x] ( 0) Ignore                                                             |
|  [ ] ( 1) Permit                                                             |
|------------------------------------------------------------------------------|
|iopt(11) - Auto Basis Switching in pre-N-R Optimization:                      |
|  [x] ( 0) Turn off                                                           |
|  [ ] ( 1) Turn on                                                            |
|------------------------------------------------------------------------------|
|iopt(17) - PICKUP File Options:                                               |
|  [ ] (-1) Don‘t write a PICKUP file                                          |
|  [x] ( 0) Write a PICKUP file                                                |
|------------------------------------------------------------------------------|
|iopt(19) - Advanced EQ3NR PICKUP File Options:                                |
|  [x] ( 0) Write a normal EQ3NR PICKUP file                                   |
|  [ ] ( 1) Write an EQ6 INPUT file with Quartz dissolving, relative rate law  |
|  [ ] ( 2) Write an EQ6 INPUT file with Albite dissolving, TST rate law       |
|  [ ] ( 3) Write an EQ6 INPUT file with Fluid 1 set up for fluid mixing       |
|------------------------------------------------------------------------------|
|Iopg Activity Coefficient Option Switches („( 0)“ marks default choices)      |
|------------------------------------------------------------------------------|
|iopg(1) - Aqueous Species Activity Coefficient Model:                         |
|  [ ] (-1) The Davies equation                                                |
|  [x] ( 0) The B-dot equation                                                 |
|  [ ] ( 1) Pitzer‘s equations                                                 |
|  [ ] ( 2) HC + DH equations                                                  |
|------------------------------------------------------------------------------|
|iopg(2) - Choice of pH Scale (Rescales Activity Coefficients):                |
|  [ ] (-1) „Internal“ pH scale (no rescaling)                                 |
|  [x] ( 0) NBS pH scale (uses the Bates-Guggenheim equation)                  |
```

```
|   [ ] ( 1) Mesmer pH scale (numerically, pH = -log m(H+))                    |
|------------------------------------------------------------------------------|
|Iopr Print Option Switches („( 0)" marks default choices)                     |
|------------------------------------------------------------------------------|
|iopr(1) - Print All Species Read from the Data File:                          |
|   [x] ( 0) Don't print                                                       |
|   [ ] ( 1) Print                                                             |
|------------------------------------------------------------------------------|
|iopr(2) - Print All Reactions:                                                |
|   [x] ( 0) Don't print                                                       |
|   [ ] ( 1) Print the reactions                                               |
|   [ ] ( 2) Print the reactions and log K values                              |
|   [ ] ( 3) Print the reactions, log K values, and associated data            |
|------------------------------------------------------------------------------|
|iopr(3) - Print the Aqueous Species Hard Core Diameters:                      |
|   [x] ( 0) Don't print                                                       |
|   [ ] ( 1) Print                                                             |
|------------------------------------------------------------------------------|
|iopr(4) - Print a Table of Aqueous Species Concentrations, Activities, etc.:  |
|   [x] (-3) Omit species with molalities < 1.e-8                              |
|   [ ] (-2) Omit species with molalities < 1.e-12                             |
|   [ ] (-1) Omit species with molalities < 1.e-20                             |
|   [ ] ( 0) Omit species with molalities < 1.e-100                            |
|   [ ] ( 1) Include all species                                               |
|------------------------------------------------------------------------------|
|iopr(5) - Print a Table of Aqueous Species/H+ Activity Ratios:                |
|   [x] ( 0) Don't print                                                       |
|   [ ] ( 1) Print cation/H+ activity ratios only                              |
|   [ ] ( 2) Print cation/H+ and anion/H+ activity ratios                      |
|   [ ] ( 3) Print ion/H+ activity ratios and neutral species activities       |
|------------------------------------------------------------------------------|
|iopr(6) - Print a Table of Aqueous Mass Balance Percentages:                  |
|   [x] (-1) Don't print                                                       |
|   [ ] ( 0) Print those species comprising at least 99% of each mass balance  |
|   [ ] ( 1) Print all contributing species                                    |
|------------------------------------------------------------------------------|
|iopr(7) - Print Tables of Saturation Indices and Affinities:                  |
|   [ ] (-1) Don't print                                                       |
|   [x] ( 0) Print, omitting those phases undersaturated by more than 10 kcal  |
|   [ ] ( 1) Print for all phases                                              |
|------------------------------------------------------------------------------|
|iopr(8) - Print a Table of Fugacities:                                        |
|   [ ] (-1) Don't print                                                       |
|   [x] ( 0) Print                                                             |
|------------------------------------------------------------------------------|
|iopr(9) - Print a Table of Mean Molal Activity Coefficients:                  |
|   [x] ( 0) Don't print                                                       |
|   [ ] ( 1) Print                                                             |
|------------------------------------------------------------------------------|
|iopr(10) - Print a Tabulation of the Pitzer Interaction Coefficients:         |
|   [x] ( 0) Don't print                                                       |
|   [ ] ( 1) Print a summary tabulation                                        |
|   [ ] ( 2) Print a more detailed tabulation                                  |
|------------------------------------------------------------------------------|
|iopr(17) - PICKUP file format („W" or „D"):                                   |
|   [x] ( 0) Use the format of the INPUT file                                  |
|   [ ] ( 1) Use „W" format                                                    |
|   [ ] ( 2) Use „D" format                                                    |
|------------------------------------------------------------------------------|
|Iodb Debugging Print Option Switches („( 0)" marks default choices)           |
|------------------------------------------------------------------------------|
|iodb(1) - Print General Diagnostic Messages:                                  |
```

```
|  [x] ( 0) Don't print                                                          |
|  [ ] ( 1) Print Level 1 diagnostic messages                                    |
|  [ ] ( 2) Print Level 1 and Level 2 diagnostic messages                        |
|--------------------------------------------------------------------------------|
|iodb(3) - Print Pre-Newton-Raphson Optimization Information:                    |
|  [x] ( 0) Don't print                                                          |
|  [ ] ( 1) Print summary information                                            |
|  [ ] ( 2) Print detailed information (including the beta and del vectors)     |
|  [ ] ( 3) Print more detailed information (including matrix equations)        |
|  [ ] ( 4) Print most detailed information (including activity coefficients)   |
|--------------------------------------------------------------------------------|
|iodb(4) - Print Newton-Raphson Iteration Information:                           |
|  [x] ( 0) Don't print                                                          |
|  [ ] ( 1) Print summary information                                            |
|  [ ] ( 2) Print detailed information (including the beta and del vectors)     |
|  [ ] ( 3) Print more detailed information (including the Jacobian)            |
|  [ ] ( 4) Print most detailed information (including activity coefficients)   |
|--------------------------------------------------------------------------------|
|iodb(6) - Print Details of Hypothetical Affinity Calculations:                  |
|  [x] ( 0) Don't print                                                          |
|  [ ] ( 1) Print summary information                                            |
|  [ ] ( 2) Print detailed information                                           |
|--------------------------------------------------------------------------------|
|Numerical Parameters                                                            |
|--------------------------------------------------------------------------------|
| Beta convergence tolerance      | 0.00000E+00| (tolbt)                         |
| Del convergence tolerance       | 0.00000E+00| (toldl)                         |
| Max. Number of N-R Iterations   |   0        | (itermx)                        |
|--------------------------------------------------------------------------------|
|Ordinary Basis Switches (for numerical purposes only)    | (nobswt)             |
|--------------------------------------------------------------------------------|
|Replace |None                                              | (uobsw(1,n))         |
|   with |None                                              | (uobsw(2,n))         |
|--------------------------------------------------------------------------------|
|Sat. flag tolerance     | 0.00000E+00| (tolspf)                                 |
|--------------------------------------------------------------------------------|
|Aq. Phase Scale Factor  | 1.00000E+00| (scamas)                                 |
|--------------------------------------------------------------------------------|
|End of problem                                                                  |
|--------------------------------------------------------------------------------|
```

A.3.1.2 Eingabedatei für EQ6, data0.cmp (offenes System)

```
|--------------------------------------------------------------------------------|
| Main Title             | (utitl1(n))                                           |
|--------------------------------------------------------------------------------|
|EQ6 input file name= NaCl_offen.6i                                              |
|Description= „Calcite dissolution in NaCl solution"                            |
|Version level= 8.0                                                              |
|Revised 12/10/2010    Revisor= C.Haase                                          |
|                                                                                |
|Szenario NaCl; T= 25 °C, fCO2= 1 bar                                            |
|                                                                                |
|                                                                                |
|Database data0.cmp                                                              |
|                                                                                |
|--------------------------------------------------------------------------------|
|Temperature option (jtemp):                                                     |
|  [x] ( 0) Constant temperature:                                                |
|             Value (C)          | 2.50000E+01| (tempcb)                       |
|  [ ] ( 1) Linear tracking in Xi:                                               |
|             Base Value (C)     | 0.00000E+00| (tempcb)                       |
|             Derivative         | 0.00000E+00| (ttk(1))                       |
```

```
|  [ ] ( 2) Linear tracking in time:                                          |
|             Base Value (C)    | 0.00000E+00| (tempcb)                     |
|             Derivative        | 0.00000E+00| (ttk(1))                     |
|  [ ] ( 3) Fluid mixing tracking (fluid 2 = special reactant):               |
|             T of fluid 1 (C)  | 0.00000E+00| (tempcb)                     |
|             T of fluid 2 (C)  | 0.00000E+00| (ttk(2))                     |
|             Mass ratio factor | 0.00000E+00| (ttk(1))                     |
|-----------------------------------------------------------------------------|
|Pressure option (jpress):                                                    |
|  [ ] ( 0) Follow the data file reference pressure curve                     |
|  [x] ( 1) Follow the 1.013-bar/steam-saturation curve                       |
|  [ ] ( 2) Constant pressure:                                                |
|             Value (bars)      | 0.00000E+00| (pressb)                     |
|  [ ] ( 3) Linear tracking in Xi:                                            |
|             Base Value (bars) | 0.00000E+00| (pressb)                     |
|             Derivative        | 0.00000E+00| (ptk(1))                     |
|  [ ] ( 4) Linear tracking in time:                                          |
|             Base Value (bars) | 0.00000E+00| (pressb)                     |
|             Derivative        | 0.00000E+00| (ptk(1))                     |
|-----------------------------------------------------------------------------|
|Reactants (Irreversible Reactions) | (nrct)                                  |
|-----------------------------------------------------------------------------|
|Reactant        |Calcite                | (ureac(n))                         |
|-----------------------------------------------------------------------------|
|->|Type         |Pure mineral           | (urcjco(jcode(n)))                 |
|-----------------------------------------------------------------------------|
|->|Status       |Saturated, reacting    | (urcjre(jreac(n)))                 |
|-----------------------------------------------------------------------------|
|->|Amount remaining (moles) | 1.00000E+01| (morr(n))                        |
|-----------------------------------------------------------------------------|
|->|Amount destroyed (moles) | 0.00000E+00| (modr(n))                        |
|-----------------------------------------------------------------------------|
|->|Surface area option (nsk(n)):                                            |
|->|  [x] ( 0) Constant surface area:                                        |
|->|             Value (cm2)       | 1.00000E+01| (sfcar(n))                 |
|->|  [ ] ( 1) Constant specific surface area:                               |
|->|             Value (cm2/g)     | 0.00000E+00| (ssfcar(n))                |
|->|  [ ] ( 2) n**2/3 growth law- current surface area:                      |
|->|             Value (cm2)       | 0.00000E+00| (sfcar(n))                 |
|-----------------------------------------------------------------------------|
|->|Surface area factor      | 1.00000E+01| (fkrc(n))                        |
|-----------------------------------------------------------------------------|
|->|Forward rate law          |Relative rate equation  | (urcnrk(nrk(1,n)))     |
|-----------------------------------------------------------------------------|
|--->|dXi(n)/dXi (mol/mol)      | 1.00000E+00| (rkb(1,1,n))                    |
|-----------------------------------------------------------------------------|
|--->|d2Xi(n)/dXi2 (mol/mol2)   | 0.00000E+00| (rkb(2,1,n))                    |
|-----------------------------------------------------------------------------|
|--->|d3Xi(n)/dXi3 (mol/mol3)   | 0.00000E+00| (rkb(3,1,n))                    |
|-----------------------------------------------------------------------------|
|->|Backward rate law         |Partial equilibrium     | (urcnrk(nrk(2,n)))     |
|-----------------------------------------------------------------------------|
|Reactant        |NaCl                   | (ureac(n))                         |
|-----------------------------------------------------------------------------|
|->|Type         |Special reactant       | (urcjco(jcode(n)))                 |
|-----------------------------------------------------------------------------|
|->|Status       |Reacting               | (urcjre(jreac(n)))                 |
|-----------------------------------------------------------------------------|
|->|Amount remaining (moles) | 4.00000E+00| (morr(n))                        |
|-----------------------------------------------------------------------------|
|->|Amount destroyed (moles) | 0.00000E+00| (modr(n))                        |
|-----------------------------------------------------------------------------|
```

```
|->|Molar volume (cm3/mol)   | 0.00000E+00| (vreac(n))                          |
|-------------------------------------------------------------------------------|
|->|Composition                                                                 |
|-------------------------------------------------------------------------------|
|--->|Element |Stoich. Number        | (this is a table header)                  |
|-------------------------------------------------------------------------------|
|--->|Na      | 1.0000000000000000+00| (uesri(i,n), cesri(i,n))                  |
|--->|Cl      | 1.0000000000000000+00| (uesri(i,n), cesri(i,n))                  |
|-------------------------------------------------------------------------------|
|->|Reaction                                                                    |
|-------------------------------------------------------------------------------|
|--->|Species                 |Reaction Coefficient  | (this is a table header)|
|-------------------------------------------------------------------------------|
|--->|NaCl                    |-1.000000000000000E+00| (ubsri(i,n), cbsri(i,n))|
|--->|Na+                     | 4.000000000000000E+00| (ubsri(i,n), cbsri(i,n))|
|--->|Cl-                     | 4.000000000000000E+00| (ubsri(i,n), cbsri(i,n))|
|-------------------------------------------------------------------------------|
|->|Surface area option (nsk(n)):                                              |
|->|  [x] ( 0) Constant surface area:                                          |
|->|             Value (cm2)       | 1.00000E+01| (sfcar(n))                   |
|->|  [ ] ( 1) Constant specific surface area:                                 |
|->|             Value (cm2/g)     | 0.00000E+00| (ssfcar(n))                  |
|->|  [ ] ( 2) n**2/3 growth law- current surface area:                        |
|->|             Value (cm2)       | 0.00000E+00| (sfcar(n))                   |
|-------------------------------------------------------------------------------|
|->|Surface area factor      | 1.00000E+00| (fkrc(n))                          |
|-------------------------------------------------------------------------------|
|->|Forward rate law           |Relative rate equation | (urcnrk(nrk(1,n)))    |
|-------------------------------------------------------------------------------|
|--->|dXi(n)/dXi (mol/mol)      | 1.00000E+00| (rkb(1,1,n))                     |
|-------------------------------------------------------------------------------|
|--->|d2Xi(n)/dXi2 (mol/mol2)   | 0.00000E-00| (rkb(2,1,n))                     |
|-------------------------------------------------------------------------------|
|--->|d3Xi(n)/dXi3 (mol/mol3)   | 0.00000E-00| (rkb(3,1,n))                     |
|-------------------------------------------------------------------------------|
|->|Backward rate law         |Partial equilibrium     | (urcnrk(nrk(2,n)))    |
|-------------------------------------------------------------------------------|
|Starting, minimum, and maximum values of key run parameters.                   |
|-------------------------------------------------------------------------------|
|Starting Xi value        | 1.00000E-01| (xistti)                               |
|-------------------------------------------------------------------------------|
|Maximum Xi value         | 1.10000E+00| (ximaxi)                               |
|-------------------------------------------------------------------------------|
|Starting time (seconds)  | 0.00000E+00| (tistti)                               |
|-------------------------------------------------------------------------------|
|Maximum time (seconds)   | 1.00000E+38| (timmxi)                               |
|-------------------------------------------------------------------------------|
|Minimum value of pH      | 1.00000E-00| (phmini)                               |
|-------------------------------------------------------------------------------|
|Maximum value of pH      | 1.00000E+10| (phmaxi)                               |
|-------------------------------------------------------------------------------|
|Minimum value of Eh (v)  |-1.00000E+38| (ehmini)                               |
|-------------------------------------------------------------------------------|
|Maximum value of Eh (v)  | 1.00000E+38| (ehmaxi)                               |
|-------------------------------------------------------------------------------|
|Minimum value of log fO2 |-1.00000E+38| (o2mini)                               |
|-------------------------------------------------------------------------------|
|Maximum value of log fO2 | 1.00000E+38| (o2maxi)                               |
|-------------------------------------------------------------------------------|
|Minimum value of aw      |-1.00000E+38| (awmini)                               |
|-------------------------------------------------------------------------------|
|Maximum value of aw      | 1.00000E+38| (awmaxi)                               |
```

```
|-------------------------------------------------------------------------------|
|Maximum number of steps  |         400| (kstpmx)                               |
|-------------------------------------------------------------------------------|
|Print interval parameters.                                                     |
|-------------------------------------------------------------------------------|
|Xi print interval        | 2.00000E-02| (dlxprn)                               |
|-------------------------------------------------------------------------------|
|Log Xi print interval    | 5.00000E-01| (dlxprl)                               |
|-------------------------------------------------------------------------------|
|Time print interval      | 1.00000E+38| (dltprn)                               |
|-------------------------------------------------------------------------------|
|Log time print interval  | 1.00000E+38| (dltprl)                               |
|-------------------------------------------------------------------------------|
|pH print interval        | 1.00000E+38| (dlhprn)                               |
|-------------------------------------------------------------------------------|
|Eh (v) print interval    | 1.00000E+38| (dleprn)                               |
|-------------------------------------------------------------------------------|
|Log fO2 print interval   | 1.00000E+38| (dloprn)                               |
|-------------------------------------------------------------------------------|
|aw print interval        | 1.00000E+38| (dlaprn)                               |
|-------------------------------------------------------------------------------|
|Steps print interval     |         0.1| (ksppmx)                               |
|-------------------------------------------------------------------------------|
|Plot interval parameters.                                                      |
|-------------------------------------------------------------------------------|
|Xi plot interval         | 2.00000E-01| (dlxplo)                               |
|-------------------------------------------------------------------------------|
|Log Xi plot interval     | 2.00000E-01| (dlxpll)                               |
|-------------------------------------------------------------------------------|
|Time plot interval       | 1.00000E+38| (dltplo)                               |
|-------------------------------------------------------------------------------|
|Log time plot interval   | 1.00000E+38| (dltpll)                               |
|-------------------------------------------------------------------------------|
|pH plot interval         | 2.00000E-01| (dlhplo)                               |
|-------------------------------------------------------------------------------|
|Eh (v) plot interval     | 2.00000E-01| (dleplo)                               |
|-------------------------------------------------------------------------------|
|Log fO2 plot interval    | 1.00000E+38| (dloplo)                               |
|-------------------------------------------------------------------------------|
|aw plot interval         | 2.00000E-01| (dlaplo)                               |
|-------------------------------------------------------------------------------|
|Steps plot interval      |         100| (ksplmx)                               |
|-------------------------------------------------------------------------------|
|Iopt Model Option Switches („( 0)" marks default choices)                      |
|-------------------------------------------------------------------------------|
|iopt(1) - Physical System Model Selection:                                     |
|  [x] ( 0) Closed system                                                       |
|  [ ] ( 1) Titration system                                                    |
|  [ ] ( 2) Fluid-centered flow-through open system                             |
|-------------------------------------------------------------------------------|
|iopt(2) - Kinetic Mode Selection:                                              |
|  [x] ( 0) Reaction progress mode (arbitrary kinetics)                         |
|  [ ] ( 1) Reaction progress/time mode (true kinetics)                         |
|-------------------------------------------------------------------------------|
|iopt(3) - Phase Boundary Searches:                                             |
|  [x] ( 0) Search for phase boundaries and constrain the step size to match    |
|  [ ] ( 1) Search for phase boundaries and print their locations               |
|  [ ] ( 2) Don't search for phase boundaries                                   |
|-------------------------------------------------------------------------------|
|iopt(4) - Solid Solutions:                                                     |
|  [x] ( 0) Ignore                                                              |
|  [ ] ( 1) Permit                                                              |
```

```
|-------------------------------------------------------------------------------|
|iopt(5) - Clear the ES Solids Read from the INPUT File:                        |
|   [x] ( 0) Don't do it                                                        |
|   [ ] ( 1) Do it                                                              |
|-------------------------------------------------------------------------------|
|iopt(6) - Clear the ES Solids at the Initial Value of Reaction Progress:       |
|   [x] ( 0) Don't do it                                                        |
|   [ ] ( 1) Do it                                                              |
|-------------------------------------------------------------------------------|
|iopt(7) - Clear the ES Solids at the End of the Run:                           |
|   [x] ( 0) Don't do it                                                        |
|   [ ] ( 1) Do it                                                              |
|-------------------------------------------------------------------------------|
|iopt(9) - Clear the PRS Solids Read from the INPUT file:                       |
|   [x] ( 0) Don't do it                                                        |
|   [ ] ( 1) Do it                                                              |
|-------------------------------------------------------------------------------|
|iopt(10) - Clear the PRS Solids at the End of the Run:                         |
|   [x] ( 0) Don't do it                                                        |
|   [ ] ( 1) Do it, unless numerical problems cause early termination           |
|-------------------------------------------------------------------------------|
|iopt(11) - Auto Basis Switching in pre-N-R Optimization:                       |
|   [x] ( 0) Turn off                                                           |
|   [ ] ( 1) Turn on                                                            |
|-------------------------------------------------------------------------------|
|iopt(12) - Auto Basis Switching after Newton-Raphson Iteration:                |
|   [x] ( 0) Turn off                                                           |
|   [ ] ( 1) Turn on                                                            |
|-------------------------------------------------------------------------------|
|iopt(13) - Calculational Mode Selection:                                       |
|   [x] ( 0) Normal path tracing                                                |
|   [ ] ( 1) Economy mode (if permissible)                                      |
|   [ ] ( 2) Super economy mode (if permissible)                                |
|-------------------------------------------------------------------------------|
|iopt(14) - ODE Integrator Corrector Mode Selection:                            |
|   [x] ( 0) Allow Stiff and Simple Correctors                                  |
|   [ ] ( 1) Allow Only the Simple Corrector                                    |
|   [ ] ( 2) Allow Only the Stiff Corrector                                     |
|   [ ] ( 3) Allow No Correctors                                                |
|-------------------------------------------------------------------------------|
|iopt(15) - Force the Suppression of All Redox Reactions:                       |
|   [x] ( 0) Don't do it                                                        |
|   [ ] ( 1) Do it                                                              |
|-------------------------------------------------------------------------------|
|iopt(16) - BACKUP File Options:                                                |
|   [ ] (-1) Don't write a BACKUP file                                          |
|   [x] ( 0) Write BACKUP files                                                 |
|   [ ] ( 1) Write a sequential BACKUP file                                     |
|-------------------------------------------------------------------------------|
|iopt(17) - PICKUP File Options:                                                |
|   [ ] (-1) Don't write a PICKUP file                                          |
|   [x] ( 0) Write a PICKUP file                                                |
|-------------------------------------------------------------------------------|
|iopt(18) - TAB File Options:                                                   |
|   [ ] (-1) Don't write a TAB file                                             |
|   [x] ( 0) Write a TAB file                                                   |
|   [ ] ( 1) Write a TAB file, prepending TABX file data from a previous run    |
|-------------------------------------------------------------------------------|
|iopt(20) - Advanced EQ6 PICKUP File Options:                                   |
|   [x] ( 0) Write a normal EQ6 PICKUP file                                     |
|   [ ] ( 1) Write an EQ6 INPUT file with Fluid 1 set up for fluid mixing       |
|-------------------------------------------------------------------------------|
```

```
|Iopr Print Option Switches („( 0)" marks default choices)                      |
|-------------------------------------------------------------------------------|
|iopr(1) - Print All Species Read from the Data File:                           |
|   [x] ( 0) Don't print                                                        |
|   [ ] ( 1) Print                                                              |
|-------------------------------------------------------------------------------|
|iopr(2) - Print All Reactions:                                                 |
|   [x] ( 0) Don't print                                                        |
|   [ ] ( 1) Print the reactions                                                |
|   [ ] ( 2) Print the reactions and log K values                               |
|   [ ] ( 3) Print the reactions, log K values, and associated data             |
|-------------------------------------------------------------------------------|
|iopr(3) - Print the Aqueous Species Hard Core Diameters:                       |
|   [x] ( 0) Don't print                                                        |
|   [ ] ( 1) Print                                                              |
|-------------------------------------------------------------------------------|
|iopr(4) - Print a Table of Aqueous Species Concentrations, Activities, etc.:   |
|   [ ] (-3) Omit species with molalities < 1.e-8                               |
|   [ ] (-2) Omit species with molalities < 1.e-12                              |
|   [ ] (-1) Omit species with molalities < 1.e-20                              |
|   [x] ( 0) Omit species with molalities < 1.e-100                             |
|   [ ] ( 1) Include all species                                                |
|-------------------------------------------------------------------------------|
|iopr(5) - Print a Table of Aqueous Species/H+ Activity Ratios:                 |
|   [x] ( 0) Don't print                                                        |
|   [ ] ( 1) Print cation/H+ activity ratios only                               |
|   [ ] ( 2) Print cation/H+ and anion/H+ activity ratios                       |
|   [ ] ( 3) Print ion/H+ activity ratios and neutral species activities        |
|-------------------------------------------------------------------------------|
|iopr(6) - Print a Table of Aqueous Mass Balance Percentages:                   |
|   [ ] (-1) Don't print                                                        |
|   [x] ( 0) Print those species comprising at least 99% of each mass balance   |
|   [ ] ( 1) Print all contributing species                                     |
|-------------------------------------------------------------------------------|
|iopr(7) - Print Tables of Saturation Indices and Affinities:                   |
|   [ ] (-1) Don't print                                                        |
|   [x] ( 0) Print, omitting those phases undersaturated by more than 10 kcal   |
|   [ ] ( 1) Print for all phases                                               |
|-------------------------------------------------------------------------------|
|iopr(8) - Print a Table of Fugacities:                                         |
|   [ ] (-1) Don't print                                                        |
|   [x] ( 0) Print                                                              |
|-------------------------------------------------------------------------------|
|iopr(9) - Print a Table of Mean Molal Activity Coefficients:                   |
|   [ ] ( 0) Don't print                                                        |
|   [x] ( 1) Print                                                              |
|-------------------------------------------------------------------------------|
|iopr(10) - Print a Tabulation of the Pitzer Interaction Coefficients:          |
|   [x] ( 0) Don't print                                                        |
|   [ ] ( 1) Print a summary tabulation                                         |
|   [ ] ( 2) Print a more detailed tabulation                                   |
|-------------------------------------------------------------------------------|
|iopr(17) - PICKUP file format („W" or „D"):                                    |
|   [x] ( 0) Use the format of the INPUT file                                   |
|   [ ] ( 1) Use „W" format                                                     |
|   [ ] ( 2) Use „D" format                                                     |
|-------------------------------------------------------------------------------|
|Iodb Debugging Print Option Switches („( 0)" marks default choices)            |
|-------------------------------------------------------------------------------|
|iodb(1) - Print General Diagnostic Messages:                                   |
|   [x] ( 0) Don't print                                                        |
|   [ ] ( 1) Print Level 1 diagnostic messages                                  |
```

```
|  [ ] ( 2) Print Level 1 and Level 2 diagnostic messages                      |
|------------------------------------------------------------------------------|
|iodb(2) - Kinetics Related Diagnostic Messages:                               |
|  [x] ( 0) Don't print                                                        |
|  [ ] ( 1) Print Level 1 kinetics diagnostic messages                         |
|  [ ] ( 2) Print Level 1 and Level 2 kinetics diagnostic messages             |
|------------------------------------------------------------------------------|
|iodb(3) - Print Pre-Newton-Raphson Optimization Information:                  |
|  [x] ( 0) Don't print                                                        |
|  [ ] ( 1) Print summary information                                          |
|  [ ] ( 2) Print detailed information (including the beta and del vectors)    |
|  [ ] ( 3) Print more detailed information (including matrix equations)       |
|  [ ] ( 4) Print most detailed information (including activity coefficients)  |
|------------------------------------------------------------------------------|
|iodb(4) - Print Newton-Raphson Iteration Information:                         |
|  [x] ( 0) Don't print                                                        |
|  [ ] ( 1) Print summary information                                          |
|  [ ] ( 2) Print detailed information (including the beta and del vectors)    |
|  [ ] ( 3) Print more detailed information (including the Jacobian)           |
|  [ ] ( 4) Print most detailed information (including activity coefficients)  |
|------------------------------------------------------------------------------|
|iodb(5) - Print Step-Size and Order Selection:                                |
|  [x] ( 0) Don't print                                                        |
|  [ ] ( 1) Print summary information                                          |
|  [ ] ( 2) Print detailed information                                         |
|------------------------------------------------------------------------------|
|iodb(6) - Print Details of Hypothetical Affinity Calculations:                |
|  [x] ( 0) Don't print                                                        |
|  [ ] ( 1) Print summary information                                          |
|  [ ] ( 2) Print detailed information                                         |
|------------------------------------------------------------------------------|
|iodb(7) - Print General Search (e.g., for a phase boundary) Information:      |
|  [x] ( 0) Don't print                                                        |
|  [ ] ( 1) Print summary information                                          |
|------------------------------------------------------------------------------|
|iodb(8) - Print ODE Corrector Iteration Information:                          |
|  [x] ( 0) Don't print                                                        |
|  [ ] ( 1) Print summary information                                          |
|  [ ] ( 2) Print detailed information (including the betar and delvcr vectors)|
|------------------------------------------------------------------------------|
|Mineral Sub-Set Selection Suppression Options | (nxopt)                       |
|------------------------------------------------------------------------------|
|Option  |Sub-Set Defining Species| (this is a table header)                   |
|------------------------------------------------------------------------------|
|All     |                        | (uxopt(n), uxcat(n))                      |
|------------------------------------------------------------------------------|
|Exceptions to the Mineral Sub-Set Selection Suppression Options | (nxopex)    |
|------------------------------------------------------------------------------|
|Mineral                 | (this is a table header)                            |
|------------------------------------------------------------------------------|
|Calcite                 | (uxopex(n))                                         |
|------------------------------------------------------------------------------|
|Fixed Fugacity Options | (nffg)                                               |
|------------------------------------------------------------------------------|
|Gas                     |Moles to Add |Log Fugacity | --                      |
| (uffg(n))              | (moffg(n))  | (xlkffg(n)) | --                      |
|------------------------------------------------------------------------------|
|CO2(g)                  |  1.00000E+01| 0.000000E+00| --                      |
|------------------------------------------------------------------------------|
|Numerical Parameters                                                          |
|------------------------------------------------------------------------------|
|Max. finite-difference order              |   6        | (nordmx)             |
```

```
|Beta convergence tolerance                | 0.00000E+00| (tolbt)             |
|Del convergence tolerance                 | 0.00000E+00| (toldl)             |
|Max. No. of N-R iterations                |   0        | (itermx)            |
|Search/find convergence tolerance         | 0.00000E+00| (tolxsf)            |
|Saturation tolerance                      | 0.00000E+00| (tolsat)            |
|Max. No. of Phase Assemblage Tries        |   0        | (ntrymx)            |
|Zero order step size (in Xi)              | 0.00000E+00| (dlxmx0)            |
|Max. interval in Xi between PRS transfers | 0.00000E+00| (dlxdmp)            |
|-------------------------------------------------------------------------------|
* Start of the bottom half of the input file                                    *
*-------------------------------------------------------------------------------*
| Secondary Title        | (utitl2(n))                                          |
|-------------------------------------------------------------------------------|
|EQ3NR input file name= NaCl_offen.3i                                           |
|Description=„Calcite dissolution in NaCl solution“                             |
|Version level= 8.0                                                             |
|Revised 12/10/2010    Revisor= C.Haase                                         |
|                                                                               |
|Szenario NaCl; T= 25°C, fCO2= 1 bar                                            |
|Input für Nacl_offen.6i                                                        |
|Ca= 2.0 mmol; CO3= 4.0 mmol                                                    |
|Database data0.cmp                                                             |
|                                                                               |
|-------------------------------------------------------------------------------|
|Special Basis Switches (for model definition only)       | (nsbswt)            |
|-------------------------------------------------------------------------------|
|Replace |None                                            | (usbsw(1,n))        |
|   with |None                                            | (usbsw(2,n))        |
|-------------------------------------------------------------------------------|
|Original temperature (C) | 2.50000E+01| (tempci)                               |
|-------------------------------------------------------------------------------|
|Original pressure (bars) | 1.01320E+00| (pressi)                               |
|-------------------------------------------------------------------------------|
|Create Ion Exchangers  | (net)                                                 |
|-------------------------------------------------------------------------------|
|Advisory: no exchanger creation blocks follow on this file.                    |
|Option: on further processing (writing a pickup file or running XCON6 on the   |
|present file), force the inclusion of at least one such block (qgexsh):        |
|  [ ] (.true.)                                                                 |
|-------------------------------------------------------------------------------|
|Alter/Suppress Options  | (nxmod)                                              |
|-------------------------------------------------------------------------------|
|Species                                        |Option          |Alter value |
| (uxmod(n))                                    |(ukxm(kxmod(n)))| (xlkmod(n))|
|-------------------------------------------------------------------------------|
|None                                           |None            | 0.00000E+00|
|-------------------------------------------------------------------------------|
|Iopg Activity Coefficient Option Switches („( 0)“ marks default choices)       |
|-------------------------------------------------------------------------------|
|iopg(1) - Aqueous Species Activity Coefficient Model:                          |
|  [ ] (-1) The Davies equation                                                 |
|  [x] ( 0) The B-dot equation                                                  |
|  [ ] ( 1) Pitzer‘s equations                                                  |
|  [ ] ( 2) HC + DH equations                                                   |
|-------------------------------------------------------------------------------|
|iopg(2) - Choice of pH Scale (Rescales Activity Coefficients):                 |
|  [ ] (-1) „Internal“ pH scale (no rescaling)                                  |
|  [x] ( 0) NBS pH scale (uses the Bates-Guggenheim equation)                   |
|  [ ] ( 1) Mesmer pH scale (numerically, pH = -log m(H+))                      |
|-------------------------------------------------------------------------------|
|Matrix Index Limits                                                            |
|-------------------------------------------------------------------------------|
```

No. of chem. elements	6	(kct)	
No. of basis species	9	(kbt)	
Index of last pure min.	9	(kmt)	
Index of last sol-sol.	9	(kxt)	
Matrix size	9	(kdim)	
PRS data flag	0	(kprs)	

Mass Balance Species (Matrix Row Variables) (ubmtbi(n))		Units/Constraint (ujf6(jflgi(n)))	--
H2O	Aqueous solution	Moles	--
Ca++	Aqueous solution	Moles	--
Cl-	Aqueous solution	Moles	--
H+	Aqueous solution	Moles	--
HCO3-	Aqueous solution	Moles	--
Na+	Aqueous solution	Moles	--
O2(g)	Aqueous solution	Moles	--
H2(aq)	Aqueous solution	Make non-basis	--
O2(aq)	Aqueous solution	Make non-basis	--

Mass Balance Totals (moles)

Basis species (info. only) (ubmtbi(n))		Equilibrium System (mtbi(n))	Aqueous Solution (mtbaqi(n))
H2O	Aqueous	5.550776599863284E+01	5.550776599863284E+01
Ca++	Aqueous	2.000000000012504E-03	2.000000000012504E-03
Cl-	Aqueous	1.000000000000066E-20	1.000000000000066E-20
H+	Aqueous	6.629300314760190E-04	6.629300314760190E-04
HCO3-	Aqueous	4.000000000085537E-03	4.000000000085537E-03
Na+	Aqueous	1.000000000000475E-20	1.000000000000475E-20
O2(g)	Aqueous	-2.673346963152712E-25	-2.673346963152712E-25
H2(aq)	Aqueous	7.840862442287172E-26	7.840862442287172E-26
O2(aq)	Aqueous	9.911176217668912E-43	9.911176217668912E-43
Electrical imbalance		6.629300314154904E-04	6.629300314154904E-04

Ordinary Basis Switches (for numerical purposes only)	(nobswt)
Replace None	(uobsw(1,n))
with None	(uobsw(2,n))

Matrix Column Variables and Values

Basis species (uzveci(n))		Log moles (zvclgi(n))	--
H2O	Aqueous solution	1.744358983526984E+00	--
Ca++	Aqueous solution	-2.711411211913575E+00	--
Cl-	Aqueous solution	-2.000012510504641E+01	--
H+	Aqueous solution	-6.968009027850386E+00	--
HCO3-	Aqueous solution	-2.485132672373344E+00	--
Na+	Aqueous solution	-2.000172755723271E+01	--
O2(g)	Aqueous solution	-3.910498863696397E+01	--
H2(aq)	Aqueous solution	-2.510563616520762E+01	--
O2(aq)	Aqueous solution	-4.200387480217158E+01	--

Phases and Species in the PRS

Phase	None	(uprphi(n))	
->No. of Moles	0.000000000000000E+00	(mprphi(n))	

--->Species	No. of Moles	--

```
|--->| (uprspi(i,n))          | (mprspi(i,n))        | --                    |
|-------------------------------------------------------------------------------|
|--->|None                    | 0.000000000000000E+00| --                    |
|-------------------------------------------------------------------------------|
|End of problem                                                                 |
|-------------------------------------------------------------------------------|
```

A.3.1.3 Eingabedatei für EQ3, data0.cmp (geschlossenes System, 0.5 mol CO_2)

```
|-------------------------------------------------------------------------------|
| Title                  | (utitl(n))                                           |
|-------------------------------------------------------------------------------|
|EQ3NR input file name= NaCl_geschlossen.3i                                     |
|Description= „Calcite dissolution in NaCl solution"                           |
|Version level= 8.0                                                            |
|Revised 12/10/2010    Revisor= C.Haase                                        |
|                                                                               |
|Szenario NaCl: T= 25°C, CO2= 0.5 mol                                          |
|Input für NaCl_geschlossen.6i                                                 |
|Ca= 2.0 mmol; CO3= 4.0 mmol                                                   |
|Database data0.cmp                                                            |
|                                                                               |
|-------------------------------------------------------------------------------|
|Special Basis Switches (for model definition only)       | (nsbswt)            |
|-------------------------------------------------------------------------------|
|Replace |None                                            | (usbsw(1,n))        |
|   with |None                                            | (usbsw(2,n))        |
|-------------------------------------------------------------------------------|
|Temperature (C)         | 2.50000E+01| (tempc)                                 |
|-------------------------------------------------------------------------------|
|Pressure option (jpres3):                                                      |
|  [ ] ( 0) Data file reference curve value                                     |
|  [x] ( 1) 1.013-bar/steam-saturation curve value                              |
|  [ ] ( 2) Value (bars) | 0.00000E+00| (press)                                 |
|-------------------------------------------------------------------------------|
|Density (g/cm3)         | 1.00000E+00| (rho)                                   |
|-------------------------------------------------------------------------------|
|Total dissolved solutes option (itdsf3):                                       |
|  [x] ( 0) Value (mg/kg.sol) | 0.00000E+00| (tdspkg)                         |
|  [ ] ( 1) Value (mg/L)      | 0.00000E+00| (tdspl)                          |
|-------------------------------------------------------------------------------|
|Electrical balancing option (iebal3):                                          |
|  [x] ( 0) No balancing is done                                                |
|  [ ] ( 1) Balance on species |Cl-                    | (uebal)              |
|-------------------------------------------------------------------------------|
|Default redox constraint (irdxc3):                                             |
|  [ ] (-3) Use O2(g) line in the aqueous basis species block                   |
|  [x] (-2) pe (pe units)      | 4.00000E+00| (pei)                             |
|  [ ] (-1) Eh (volts)         | 5.00000E-01| (ehi)                             |
|  [ ] ( 0) Log fO2 (log bars) | 0.00000E+00| (fo2lgi)                          |
|  [ ] ( 1) Couple (aux. sp.)  |None                | (uredox)                 |
|-------------------------------------------------------------------------------|
|Aqueous Basis Species/Constraint Species        |Conc., etc. |Units/Constraint|
| (uspeci(n)/ucospi(n))                          | (covali(n))|(ujf3(jflgi(n)))|
|-------------------------------------------------------------------------------|
|H+                                              |7.00000E+00|pH                 |
|Ca++                                            |2.00000E-03|Molality           |
|HCO3-                                           |1.00000E-00|Hetero. equil.     |
|->|Calcite                                          | (ucospi(n))          |
|Na+                                             |1.00000E-20|Molality           |
|Cl-                                             |1.00000E-20|Molality           |
|CO2(aq)                                         |5.00000E-01|Molality           |
|-------------------------------------------------------------------------------|
```

```
|Create Ion Exchangers  | (net)                                                    |
|-------------------------------------------------------------------------------|
|Advisory: no exchanger creation blocks follow on this file.                    |
|Option: on further processing (writing a PICKUP file or running XCON3 on the   |
|present file), force the inclusion of at least one such block (qgexsh):        |
|  [ ] (.true.)                                                                 |
|-------------------------------------------------------------------------------|
|Ion Exchanger Compositions      | (neti)                                       |
|-------------------------------------------------------------------------------|
|Exchanger phase |None                    | (ugexpi(n))                         |
|-------------------------------------------------------------------------------|
|->|Moles/kg.H2O    |  0.0000    | (cgexpi(n))                                 |
|-------------------------------------------------------------------------------|
|->|Exchange site   |None    | (ugexji(j,n))                                   |
|-------------------------------------------------------------------------------|
|--->|Exchange species        |Eq. frac.   | (this is a table header)          |
|-------------------------------------------------------------------------------|
|--->|None                    | 0.00000E+00| (ugexsi(i,j,n), egexsi(i,j,n))    |
|-------------------------------------------------------------------------------|
|Solid Solution Compositions     | (nxti)                                       |
|-------------------------------------------------------------------------------|
|Solid Solution          |None                     | (usoli(n))                 |
|-------------------------------------------------------------------------------|
|->|Component               |Mole frac.  | (this is a table header)             |
|-------------------------------------------------------------------------------|
|->|None                    | 0.00000E+00| (umemi(i,n), xbari(i,n))             |
|-------------------------------------------------------------------------------|
|Alter/Suppress Options  | (nxmod)                                              |
|-------------------------------------------------------------------------------|
|Species                                          |Option          |Alter value |
| (uxmod(n))                                      |(ukxm(kxmod(n)))| (xlkmod(n))|
|-------------------------------------------------------------------------------|
|None                                             |Suppress        | 0.00000E+00|
|-------------------------------------------------------------------------------|
|Iopt Model Option Switches („( 0)" marks default choices)                      |
|-------------------------------------------------------------------------------|
|iopt(4) - Solid Solutions:                                                     |
|  [x] ( 0) Ignore                                                              |
|  [ ] ( 1) Permit                                                              |
|-------------------------------------------------------------------------------|
|iopt(11) - Auto Basis Switching in pre-N-R Optimization:                       |
|  [x] ( 0) Turn off                                                            |
|  [ ] ( 1) Turn on                                                             |
|-------------------------------------------------------------------------------|
|iopt(17) - PICKUP File Options:                                                |
|  [ ] (-1) Don't write a PICKUP file                                           |
|  [x] ( 0) Write a PICKUP file                                                 |
|-------------------------------------------------------------------------------|
|iopt(19) - Advanced EQ3NR PICKUP File Options:                                 |
|  [x] ( 0) Write a normal EQ3NR PICKUP file                                    |
|  [ ] ( 1) Write an EQ6 INPUT file with Quartz dissolving, relative rate law   |
|  [ ] ( 2) Write an EQ6 INPUT file with Albite dissolving, TST rate law        |
|  [ ] ( 3) Write an EQ6 INPUT file with Fluid 1 set up for fluid mixing        |
|-------------------------------------------------------------------------------|
|Iopg Activity Coefficient Option Switches („( 0)" marks default choices)       |
|-------------------------------------------------------------------------------|
|iopg(1) - Aqueous Species Activity Coefficient Model:                          |
|  [ ] (-1) The Davies equation                                                 |
|  [x] ( 0) The B-dot equation                                                  |
|  [ ] ( 1) Pitzer's equations                                                  |
|  [ ] ( 2) HC + DH equations                                                   |
|-------------------------------------------------------------------------------|
```

```
|iopg(2) - Choice of pH Scale (Rescales Activity Coefficients):                 |
|   [ ] (-1) „Internal" pH scale (no rescaling)                                  |
|   [x] ( 0) NBS pH scale (uses the Bates-Guggenheim equation)                   |
|   [ ] ( 1) Mesmer pH scale (numerically, pH = -log m(H+))                      |
|--------------------------------------------------------------------------------|
|Iopr Print Option Switches („( 0)" marks default choices)                       |
|--------------------------------------------------------------------------------|
|iopr(1) - Print All Species Read from the Data File:                            |
|   [x] ( 0) Don't print                                                         |
|   [ ] ( 1) Print                                                               |
|--------------------------------------------------------------------------------|
|iopr(2) - Print All Reactions:                                                  |
|   [x] ( 0) Don't print                                                         |
|   [ ] ( 1) Print the reactions                                                 |
|   [ ] ( 2) Print the reactions and log K values                                |
|   [ ] ( 3) Print the reactions, log K values, and associated data              |
|--------------------------------------------------------------------------------|
|iopr(3) - Print the Aqueous Species Hard Core Diameters:                        |
|   [x] ( 0) Don't print                                                         |
|   [ ] ( 1) Print                                                               |
|--------------------------------------------------------------------------------|
|iopr(4) - Print a Table of Aqueous Species Concentrations, Activities, etc.:    |
|   [x] (-3) Omit species with molalities < 1.e-8                                |
|   [ ] (-2) Omit species with molalities < 1.e-12                               |
|   [ ] (-1) Omit species with molalities < 1.e-20                               |
|   [ ] ( 0) Omit species with molalities < 1.e-100                              |
|   [ ] ( 1) Include all species                                                 |
|--------------------------------------------------------------------------------|
|iopr(5) - Print a Table of Aqueous Species/H+ Activity Ratios:                  |
|   [x] ( 0) Don't print                                                         |
|   [ ] ( 1) Print cation/H+ activity ratios only                                |
|   [ ] ( 2) Print cation/H+ and anion/H+ activity ratios                        |
|   [ ] ( 3) Print ion/H+ activity ratios and neutral species activities         |
|--------------------------------------------------------------------------------|
|iopr(6) - Print a Table of Aqueous Mass Balance Percentages:                    |
|   [x] (-1) Don't print                                                         |
|   [ ] ( 0) Print those species comprising at least 99% of each mass balance    |
|   [ ] ( 1) Print all contributing species                                      |
|--------------------------------------------------------------------------------|
|iopr(7) - Print Tables of Saturation Indices and Affinities:                    |
|   [ ] (-1) Don't print                                                         |
|   [x] ( 0) Print, omitting those phases undersaturated by more than 10 kcal    |
|   [ ] ( 1) Print for all phases                                                |
|--------------------------------------------------------------------------------|
|iopr(8) - Print a Table of Fugacities:                                          |
|   [ ] (-1) Don't print                                                         |
|   [x] ( 0) Print                                                               |
|--------------------------------------------------------------------------------|
|iopr(9) - Print a Table of Mean Molal Activity Coefficients:                    |
|   [x] ( 0) Don't print                                                         |
|   [ ] ( 1) Print                                                               |
|--------------------------------------------------------------------------------|
|iopr(10) - Print a Tabulation of the Pitzer Interaction Coefficients:           |
|   [x] ( 0) Don't print                                                         |
|   [ ] ( 1) Print a summary tabulation                                          |
|   [ ] ( 2) Print a more detailed tabulation                                    |
|--------------------------------------------------------------------------------|
|iopr(17) - PICKUP file format („W" or „D"):                                     |
|   [x] ( 0) Use the format of the INPUT file                                    |
|   [ ] ( 1) Use „W" format                                                      |
|   [ ] ( 2) Use „D" format                                                      |
|--------------------------------------------------------------------------------|
```

```
|Iodb Debugging Print Option Switches („( 0)" marks default choices)           |
|------------------------------------------------------------------------------|
|iodb(1) - Print General Diagnostic Messages:                                  |
|  [x] ( 0) Don't print                                                        |
|  [ ] ( 1) Print Level 1 diagnostic messages                                  |
|  [ ] ( 2) Print Level 1 and Level 2 diagnostic messages                      |
|------------------------------------------------------------------------------|
|iodb(3) - Print Pre-Newton-Raphson Optimization Information:                  |
|  [x] ( 0) Don't print                                                        |
|  [ ] ( 1) Print summary information                                          |
|  [ ] ( 2) Print detailed information (including the beta and del vectors)    |
|  [ ] ( 3) Print more detailed information (including matrix equations)       |
|  [ ] ( 4) Print most detailed information (including activity coefficients)  |
|------------------------------------------------------------------------------|
|iodb(4) - Print Newton-Raphson Iteration Information:                         |
|  [x] ( 0) Don't print                                                        |
|  [ ] ( 1) Print summary information                                          |
|  [ ] ( 2) Print detailed information (including the beta and del vectors)    |
|  [ ] ( 3) Print more detailed information (including the Jacobian)           |
|  [ ] ( 4) Print most detailed information (including activity coefficients)  |
|------------------------------------------------------------------------------|
|iodb(6) - Print Details of Hypothetical Affinity Calculations:                |
|  [x] ( 0) Don't print                                                        |
|  [ ] ( 1) Print summary information                                          |
|  [ ] ( 2) Print detailed information                                         |
|------------------------------------------------------------------------------|
|Numerical Parameters                                                          |
|------------------------------------------------------------------------------|
| Beta convergence tolerance      | 0.00000E+00| (tolbt)                       |
| Del convergence tolerance       | 0.00000E+00| (toldl)                       |
| Max. Number of N-R Iterations   |   0        | (itermx)                      |
|------------------------------------------------------------------------------|
|Ordinary Basis Switches (for numerical purposes only)    | (nobswt)           |
|------------------------------------------------------------------------------|
|Replace |None                                            | (uobsw(1,n))       |
|   with |None                                            | (uobsw(2,n))       |
|------------------------------------------------------------------------------|
|Sat. flag tolerance     | 0.00000E+00| (tolspf)                               |
|------------------------------------------------------------------------------|
|Aq. Phase Scale Factor  | 1.00000E+00| (scamas)                               |
|------------------------------------------------------------------------------|
|End of problem                                                                |
|------------------------------------------------------------------------------|
```

A.3.1.4 Eingabedatei für EQ6, data0.cmp (geschlossenes System, 0.5 mol CO_2)

```
|------------------------------------------------------------------------------|
| Main Title             | (utitl1(n))                                         |
|------------------------------------------------------------------------------|
|EQ6 input file name= NaCl_geschlossen.6i                                      |
|Description= „Calcite dissolution in NaCl solution"                          |
|Version level= 8.0                                                            |
|Revised 12/10/2010    Revisor= C.Haase                                        |
|                                                                              |
|Szenario NaCl: T= 25 °C, CO2= 0.5 mol                                         |
|                                                                              |
|                                                                              |
|Database data0.cmp                                                            |
|                                                                              |
|------------------------------------------------------------------------------|
|Temperature option (jtemp):                                                   |
|  [x] ( 0) Constant temperature:                                              |
|             Value (C)         | 2.50000E+01| (tempcb)                        |
```

```
|  [ ] ( 1) Linear tracking in Xi:                                                |
|             Base Value (C)    | 0.00000E+00| (tempcb)                        |
|             Derivative        | 0.00000E+00| (ttk(1))                        |
|  [ ] ( 2) Linear tracking in time:                                              |
|             Base Value (C)    | 0.00000E+00| (tempcb)                        |
|             Derivative        | 0.00000E+00| (ttk(1))                        |
|  [ ] ( 3) Fluid mixing tracking (fluid 2 = special reactant):                   |
|             T of fluid 1 (C)  | 0.00000E+00| (tempcb)                        |
|             T of fluid 2 (C)  | 0.00000E+00| (ttk(2))                        |
|             Mass ratio factor | 0.00000E+00| (ttk(1))                        |
|---------------------------------------------------------------------------------|
|Pressure option (jpress):                                                        |
|  [ ] ( 0) Follow the data file reference pressure curve                         |
|  [x] ( 1) Follow the 1.013-bar/steam-saturation curve                           |
|  [ ] ( 2) Constant pressure:                                                    |
|             Value (bars)      | 0.00000E+00| (pressb)                        |
|  [ ] ( 3) Linear tracking in Xi:                                                |
|             Base Value (bars) | 0.00000E+00| (pressb)                        |
|             Derivative        | 0.00000E+00| (ptk(1))                        |
|  [ ] ( 4) Linear tracking in time:                                              |
|             Base Value (bars) | 0.00000E+00| (pressb)                        |
|             Derivative        | 0.00000E+00| (ptk(1))                        |
|---------------------------------------------------------------------------------|
|Reactants (Irreversible Reactions) | (nrct)                                      |
|---------------------------------------------------------------------------------|
|Reactant        |Calcite                | (ureac(n))                             |
|---------------------------------------------------------------------------------|
|->|Type         |Pure mineral           | (urcjco(jcode(n)))                     |
|---------------------------------------------------------------------------------|
|->|Status       |Saturated, reacting    | (urcjre(jreac(n)))                     |
|---------------------------------------------------------------------------------|
|->|Amount remaining (moles) | 1.00000E+01| (morr(n))                          |
|---------------------------------------------------------------------------------|
|->|Amount destroyed (moles) | 0.00000E+00| (modr(n))                          |
|---------------------------------------------------------------------------------|
|->|Surface area option (nsk(n)):                                                 |
|->|  [x] ( 0) Constant surface area:                                             |
|->|             Value (cm2)       | 1.00000E+01| (sfcar(n))                     |
|->|  [ ] ( 1) Constant specific surface area:                                    |
|->|             Value (cm2/g)     | 0.00000E+00| (ssfcar(n))                    |
|->|  [ ] ( 2) n**2/3 growth law- current surface area:                           |
|->|             Value (cm2)       | 0.00000E+00| (sfcar(n))                     |
|---------------------------------------------------------------------------------|
|->|Surface area factor      | 1.00000E+01| (fkrc(n))                        |
|---------------------------------------------------------------------------------|
|->|Forward rate law          |Relative rate equation  | (urcnrk(nrk(1,n)))     |
|---------------------------------------------------------------------------------|
|--->|dXi(n)/dXi (mol/mol)      | 1.00000E+00| (rkb(1,1,n))                    |
|---------------------------------------------------------------------------------|
|--->|d2Xi(n)/dXi2 (mol/mol2)   | 0.00000E+00| (rkb(2,1,n))                    |
|---------------------------------------------------------------------------------|
|--->|d3Xi(n)/dXi3 (mol/mol3)   | 0.00000E+00| (rkb(3,1,n))                    |
|---------------------------------------------------------------------------------|
|->|Backward rate law         |Partial equilibrium     | (urcnrk(nrk(2,n)))     |
|---------------------------------------------------------------------------------|
|Reactant        |NaCl                   | (ureac(n))                             |
|---------------------------------------------------------------------------------|
|->|Type         |Special reactant       | (urcjco(jcode(n)))                     |
|---------------------------------------------------------------------------------|
|->|Status       |Reacting               | (urcjre(jreac(n)))                     |
|---------------------------------------------------------------------------------|
|->|Amount remaining (moles) | 4.00000E+00| (morr(n))                          |
```

```
|-------------------------------------------------------------------------------|
|->|Amount destroyed (moles) | 0.00000E+00| (modr(n))                          |
|-------------------------------------------------------------------------------|
|->|Molar volume (cm3/mol)   | 0.00000E+00| (vreac(n))                         |
|-------------------------------------------------------------------------------|
|->|Composition                                                                 |
|-------------------------------------------------------------------------------|
|--->|Element |Stoich. Number        | (this is a table header)                 |
|-------------------------------------------------------------------------------|
|--->|Na      | 1.00000000000000+00| (uesri(i,n), cesri(i,n))                  |
|--->|Cl      | 1.00000000000000+00| (uesri(i,n), cesri(i,n))                  |
|-------------------------------------------------------------------------------|
|->|Reaction                                                                    |
|-------------------------------------------------------------------------------|
|--->|Species                |Reaction Coefficient  | (this is a table header)|
|-------------------------------------------------------------------------------|
|--->|NaCl                   |-1.000000000000000E+00| (ubsri(i,n), cbsri(i,n))|
|--->|Na+                    | 4.000000000000000E+00| (ubsri(i,n), cbsri(i,n))|
|--->|Cl-                    | 4.000000000000000E+00| (ubsri(i,n), cbsri(i,n))|
|-------------------------------------------------------------------------------|
|->|Surface area option (nsk(n)):                                               |
|->|  [x] ( 0) Constant surface area:                                           |
|->|             Value (cm2)       | 1.00000E+01| (sfcar(n))                   |
|->|  [ ] ( 1) Constant specific surface area:                                  |
|->|             Value (cm2/g)     | 0.00000E+00| (ssfcar(n))                  |
|->|  [ ] ( 2) n**2/3 growth law- current surface area:                         |
|->|             Value (cm2)       | 0.00000E+00| (sfcar(n))                   |
|-------------------------------------------------------------------------------|
|->|Surface area factor      | 1.00000E+00| (fkrc(n))                          |
|-------------------------------------------------------------------------------|
|->|Forward rate law           |Relative rate equation | (urcnrk(nrk(1,n)))    |
|-------------------------------------------------------------------------------|
|--->|dXi(n)/dXi (mol/mol)      | 1.00000E+00| (rkb(1,1,n))                     |
|-------------------------------------------------------------------------------|
|--->|d2Xi(n)/dXi2 (mol/mol2)   | 0.00000E-00| (rkb(2,1,n))                     |
|-------------------------------------------------------------------------------|
|--->|d3Xi(n)/dXi3 (mol/mol3)   | 0.00000E-00| (rkb(3,1,n))                     |
|-------------------------------------------------------------------------------|
|->|Backward rate law         |Partial equilibrium     | (urcnrk(nrk(2,n)))    |
|-------------------------------------------------------------------------------|
|Starting, minimum, and maximum values of key run parameters.                   |
|-------------------------------------------------------------------------------|
|Starting Xi value        | 1.00000E-01| (xistti)                               |
|-------------------------------------------------------------------------------|
|Maximum Xi value         | 1.10000E+00| (ximaxi)                               |
|-------------------------------------------------------------------------------|
|Starting time (seconds)  | 0.00000E+00| (tistti)                               |
|-------------------------------------------------------------------------------|
|Maximum time (seconds)   | 1.00000E+38| (timmxi)                               |
|-------------------------------------------------------------------------------|
|Minimum value of pH      | 1.00000E-00| (phmini)                               |
|-------------------------------------------------------------------------------|
|Maximum value of pH      | 1.00000E+10| (phmaxi)                               |
|-------------------------------------------------------------------------------|
|Minimum value of Eh (v)  |-1.00000E+38| (ehmini)                               |
|-------------------------------------------------------------------------------|
|Maximum value of Eh (v)  | 1.00000E+38| (ehmaxi)                               |
|-------------------------------------------------------------------------------|
|Minimum value of log fO2 |-1.00000E+38| (o2mini)                               |
|-------------------------------------------------------------------------------|
|Maximum value of log fO2 | 1.00000E+38| (o2maxi)                               |
|-------------------------------------------------------------------------------|
```

```
|Minimum value of aw      |-1.00000E+38| (awmini)                                |
|-------------------------------------------------------------------------------|
|Maximum value of aw      | 1.00000E+38| (awmaxi)                                |
|-------------------------------------------------------------------------------|
|Maximum number of steps  |         400| (kstpmx)                                |
|-------------------------------------------------------------------------------|
|Print interval parameters.                                                     |
|-------------------------------------------------------------------------------|
|Xi print interval        | 2.00000E-02| (dlxprn)                                |
|-------------------------------------------------------------------------------|
|Log Xi print interval    | 5.00000E-01| (dlxprl)                                |
|-------------------------------------------------------------------------------|
|Time print interval      | 1.00000E+38| (dltprn)                                |
|-------------------------------------------------------------------------------|
|Log time print interval  | 1.00000E+38| (dltprl)                                |
|-------------------------------------------------------------------------------|
|pH print interval        | 1.00000E+38| (dlhprn)                                |
|-------------------------------------------------------------------------------|
|Eh (v) print interval    | 1.00000E+38| (dleprn)                                |
|-------------------------------------------------------------------------------|
|Log fO2 print interval   | 1.00000E+38| (dloprn)                                |
|-------------------------------------------------------------------------------|
|aw print interval        | 1.00000E+38| (dlaprn)                                |
|-------------------------------------------------------------------------------|
|Steps print interval     |         0.1| (ksppmx)                                |
|-------------------------------------------------------------------------------|
|Plot interval parameters.                                                      |
|-------------------------------------------------------------------------------|
|Xi plot interval         | 2.00000E-01| (dlxplo)                                |
|-------------------------------------------------------------------------------|
|Log Xi plot interval     | 2.00000E-01| (dlxpll)                                |
|-------------------------------------------------------------------------------|
|Time plot interval       | 1.00000E+38| (dltplo)                                |
|-------------------------------------------------------------------------------|
|Log time plot interval   | 1.00000E+38| (dltpll)                                |
|-------------------------------------------------------------------------------|
|pH plot interval         | 2.00000E-01| (dlhplo)                                |
|-------------------------------------------------------------------------------|
|Eh (v) plot interval     | 2.00000E-01| (dleplo)                                |
|-------------------------------------------------------------------------------|
|Log fO2 plot interval    | 1.00000E+38| (dloplo)                                |
|-------------------------------------------------------------------------------|
|aw plot interval         | 2.00000E-01| (dlaplo)                                |
|-------------------------------------------------------------------------------|
|Steps plot interval      |         100| (ksplmx)                                |
|-------------------------------------------------------------------------------|
|Iopt Model Option Switches („( 0)" marks default choices)                      |
|-------------------------------------------------------------------------------|
|iopt(1) - Physical System Model Selection:                                     |
|  [x] ( 0) Closed system                                                       |
|  [ ] ( 1) Titration system                                                    |
|  [ ] ( 2) Fluid-centered flow-through open system                             |
|-------------------------------------------------------------------------------|
|iopt(2) - Kinetic Mode Selection:                                              |
|  [x] ( 0) Reaction progress mode (arbitrary kinetics)                         |
|  [ ] ( 1) Reaction progress/time mode (true kinetics)                         |
|-------------------------------------------------------------------------------|
|iopt(3) - Phase Boundary Searches:                                             |
|  [x] ( 0) Search for phase boundaries and constrain the step size to match    |
|  [ ] ( 1) Search for phase boundaries and print their locations               |
|  [ ] ( 2) Don't search for phase boundaries                                   |
|-------------------------------------------------------------------------------|
```

```
|iopt(4) - Solid Solutions:                                                    |
|  [x] ( 0) Ignore                                                             |
|  [ ] ( 1) Permit                                                             |
|------------------------------------------------------------------------------|
|iopt(5) - Clear the ES Solids Read from the INPUT File:                       |
|  [x] ( 0) Don't do it                                                        |
|  [ ] ( 1) Do it                                                              |
|------------------------------------------------------------------------------|
|iopt(6) - Clear the ES Solids at the Initial Value of Reaction Progress:      |
|  [x] ( 0) Don't do it                                                        |
|  [ ] ( 1) Do it                                                              |
|------------------------------------------------------------------------------|
|iopt(7) - Clear the ES Solids at the End of the Run:                          |
|  [x] ( 0) Don't do it                                                        |
|  [ ] ( 1) Do it                                                              |
|------------------------------------------------------------------------------|
|iopt(9) - Clear the PRS Solids Read from the INPUT file:                      |
|  [x] ( 0) Don't do it                                                        |
|  [ ] ( 1) Do it                                                              |
|------------------------------------------------------------------------------|
|iopt(10) - Clear the PRS Solids at the End of the Run:                        |
|  [x] ( 0) Don't do it                                                        |
|  [ ] ( 1) Do it, unless numerical problems cause early termination           |
|------------------------------------------------------------------------------|
|iopt(11) - Auto Basis Switching in pre-N-R Optimization:                      |
|  [x] ( 0) Turn off                                                           |
|  [ ] ( 1) Turn on                                                            |
|------------------------------------------------------------------------------|
|iopt(12) - Auto Basis Switching after Newton-Raphson Iteration:               |
|  [x] ( 0) Turn off                                                           |
|  [ ] ( 1) Turn on                                                            |
|------------------------------------------------------------------------------|
|iopt(13) - Calculational Mode Selection:                                      |
|  [x] ( 0) Normal path tracing                                                |
|  [ ] ( 1) Economy mode (if permissible)                                      |
|  [ ] ( 2) Super economy mode (if permissible)                                |
|------------------------------------------------------------------------------|
|iopt(14) - ODE Integrator Corrector Mode Selection:                           |
|  [x] ( 0) Allow Stiff and Simple Correctors                                  |
|  [ ] ( 1) Allow Only the Simple Corrector                                    |
|  [ ] ( 2) Allow Only the Stiff Corrector                                     |
|  [ ] ( 3) Allow No Correctors                                                |
|------------------------------------------------------------------------------|
|iopt(15) - Force the Suppression of All Redox Reactions:                      |
|  [x] ( 0) Don't do it                                                        |
|  [ ] ( 1) Do it                                                              |
|------------------------------------------------------------------------------|
|iopt(16) - BACKUP File Options:                                               |
|  [ ] (-1) Don't write a BACKUP file                                          |
|  [x] ( 0) Write BACKUP files                                                 |
|  [ ] ( 1) Write a sequential BACKUP file                                     |
|------------------------------------------------------------------------------|
|iopt(17) - PICKUP File Options:                                               |
|  [ ] (-1) Don't write a PICKUP file                                          |
|  [x] ( 0) Write a PICKUP file                                                |
|------------------------------------------------------------------------------|
|iopt(18) - TAB File Options:                                                  |
|  [ ] (-1) Don't write a TAB file                                             |
|  [x] ( 0) Write a TAB file                                                   |
|  [ ] ( 1) Write a TAB file, prepending TABX file data from a previous run    |
|------------------------------------------------------------------------------|
|iopt(20) - Advanced EQ6 PICKUP File Options:                                  |
```

```
|   [x] ( 0) Write a normal EQ6 PICKUP file                                    |
|   [ ] ( 1) Write an EQ6 INPUT file with Fluid 1 set up for fluid mixing      |
|------------------------------------------------------------------------------|
|Iopr Print Option Switches („( 0)" marks default choices)                     |
|------------------------------------------------------------------------------|
|iopr(1) - Print All Species Read from the Data File:                          |
|   [x] ( 0) Don't print                                                       |
|   [ ] ( 1) Print                                                             |
|------------------------------------------------------------------------------|
|iopr(2) - Print All Reactions:                                                |
|   [x] ( 0) Don't print                                                       |
|   [ ] ( 1) Print the reactions                                               |
|   [ ] ( 2) Print the reactions and log K values                              |
|   [ ] ( 3) Print the reactions, log K values, and associated data            |
|------------------------------------------------------------------------------|
|iopr(3) - Print the Aqueous Species Hard Core Diameters:                      |
|   [x] ( 0) Don't print                                                       |
|   [ ] ( 1) Print                                                             |
|------------------------------------------------------------------------------|
|iopr(4) - Print a Table of Aqueous Species Concentrations, Activities, etc.:  |
|   [ ] (-3) Omit species with molalities < 1.e-8                              |
|   [ ] (-2) Omit species with molalities < 1.e-12                             |
|   [ ] (-1) Omit species with molalities < 1.e-20                             |
|   [x] ( 0) Omit species with molalities < 1.e-100                            |
|   [ ] ( 1) Include all species                                               |
|------------------------------------------------------------------------------|
|iopr(5) - Print a Table of Aqueous Species/H+ Activity Ratios:                |
|   [x] ( 0) Don't print                                                       |
|   [ ] ( 1) Print cation/H+ activity ratios only                              |
|   [ ] ( 2) Print cation/H+ and anion/H+ activity ratios                      |
|   [ ] ( 3) Print ion/H+ activity ratios and neutral species activities       |
|------------------------------------------------------------------------------|
|iopr(6) - Print a Table of Aqueous Mass Balance Percentages:                  |
|   [ ] (-1) Don't print                                                       |
|   [x] ( 0) Print those species comprising at least 99% of each mass balance  |
|   [ ] ( 1) Print all contributing species                                    |
|------------------------------------------------------------------------------|
|iopr(7) - Print Tables of Saturation Indices and Affinities:                  |
|   [ ] (-1) Don't print                                                       |
|   [x] ( 0) Print, omitting those phases undersaturated by more than 10 kcal  |
|   [ ] ( 1) Print for all phases                                              |
|------------------------------------------------------------------------------|
|iopr(8) - Print a Table of Fugacities:                                        |
|   [ ] (-1) Don't print                                                       |
|   [x] ( 0) Print                                                             |
|------------------------------------------------------------------------------|
|iopr(9) - Print a Table of Mean Molal Activity Coefficients:                  |
|   [ ] ( 0) Don't print                                                       |
|   [x] ( 1) Print                                                             |
|------------------------------------------------------------------------------|
|iopr(10) - Print a Tabulation of the Pitzer Interaction Coefficients:         |
|   [x] ( 0) Don't print                                                       |
|   [ ] ( 1) Print a summary tabulation                                        |
|   [ ] ( 2) Print a more detailed tabulation                                  |
|------------------------------------------------------------------------------|
|iopr(17) - PICKUP file format („W" or „D"):                                   |
|   [x] ( 0) Use the format of the INPUT file                                  |
|   [ ] ( 1) Use „W" format                                                    |
|   [ ] ( 2) Use „D" format                                                    |
|------------------------------------------------------------------------------|
|Iodb Debugging Print Option Switches („( 0)" marks default choices)           |
|------------------------------------------------------------------------------|
```

```
|iodb(1) - Print General Diagnostic Messages:                                  |
|  [x] ( 0) Don't print                                                        |
|  [ ] ( 1) Print Level 1 diagnostic messages                                  |
|  [ ] ( 2) Print Level 1 and Level 2 diagnostic messages                      |
|------------------------------------------------------------------------------|
|iodb(2) - Kinetics Related Diagnostic Messages:                               |
|  [x] ( 0) Don't print                                                        |
|  [ ] ( 1) Print Level 1 kinetics diagnostic messages                         |
|  [ ] ( 2) Print Level 1 and Level 2 kinetics diagnostic messages             |
|------------------------------------------------------------------------------|
|iodb(3) - Print Pre-Newton-Raphson Optimization Information:                  |
|  [x] ( 0) Don't print                                                        |
|  [ ] ( 1) Print summary information                                          |
|  [ ] ( 2) Print detailed information (including the beta and del vectors)    |
|  [ ] ( 3) Print more detailed information (including matrix equations)       |
|  [ ] ( 4) Print most detailed information (including activity coefficients)  |
|------------------------------------------------------------------------------|
|iodb(4) - Print Newton-Raphson Iteration Information:                         |
|  [x] ( 0) Don't print                                                        |
|  [ ] ( 1) Print summary information                                          |
|  [ ] ( 2) Print detailed information (including the beta and del vectors)    |
|  [ ] ( 3) Print more detailed information (including the Jacobian)           |
|  [ ] ( 4) Print most detailed information (including activity coefficients)  |
|------------------------------------------------------------------------------|
|iodb(5) - Print Step-Size and Order Selection:                                |
|  [x] ( 0) Don't print                                                        |
|  [ ] ( 1) Print summary information                                          |
|  [ ] ( 2) Print detailed information                                         |
|------------------------------------------------------------------------------|
|iodb(6) - Print Details of Hypothetical Affinity Calculations:                |
|  [x] ( 0) Don't print                                                        |
|  [ ] ( 1) Print summary information                                          |
|  [ ] ( 2) Print detailed information                                         |
|------------------------------------------------------------------------------|
|iodb(7) - Print General Search (e.g., for a phase boundary) Information:      |
|  [x] ( 0) Don't print                                                        |
|  [ ] ( 1) Print summary information                                          |
|------------------------------------------------------------------------------|
|iodb(8) - Print ODE Corrector Iteration Information:                          |
|  [x] ( 0) Don't print                                                        |
|  [ ] ( 1) Print summary information                                          |
|  [ ] ( 2) Print detailed information (including the betar and delvcr vectors)|
|------------------------------------------------------------------------------|
|Mineral Sub-Set Selection Suppression Options | (nxopt)                       |
|------------------------------------------------------------------------------|
|Option  |Sub-Set Defining Species| (this is a table header)                   |
|------------------------------------------------------------------------------|
|All     |                        | (uxopt(n), uxcat(n))                      |
|------------------------------------------------------------------------------|
|Exceptions to the Mineral Sub-Set Selection Suppression Options | (nxopex)    |
|------------------------------------------------------------------------------|
|Mineral                 | (this is a table header)                            |
|------------------------------------------------------------------------------|
|Calcite                 | (uxopex(n))                                         |
|------------------------------------------------------------------------------|
|Fixed Fugacity Options  | (nffg)                                              |
|------------------------------------------------------------------------------|
|Gas                     |Moles to Add |Log Fugacity | --                      |
| (uffg(n))              | (moffg(n))  | (xlkffg(n)) | --                      |
|------------------------------------------------------------------------------|
|None                    |  1.00000E+01| 0.000000E+00| --                      |
|------------------------------------------------------------------------------|
```

```
|Numerical Parameters                                                          |
|------------------------------------------------------------------------------|
|Max. finite-difference order               |   6        | (nordmx)            |
|Beta convergence tolerance                 | 0.00000E+00| (tolbt)             |
|Del convergence tolerance                  | 0.00000E+00| (toldl)             |
|Max. No. of N-R iterations                 | 0          | (itermx)            |
|Search/find convergence tolerance          | 0.00000E+00| (tolxsf)            |
|Saturation tolerance                       | 0.00000E+00| (tolsat)            |
|Max. No. of Phase Assemblage Tries         | 0          | (ntrymx)            |
|Zero order step size (in Xi)               | 0.00000E+00| (dlxmx0)            |
|Max. interval in Xi between PRS transfers  | 0.00000E+00| (dlxdmp)            |
|------------------------------------------------------------------------------|
* Start of the bottom half of the input file                                   *
*------------------------------------------------------------------------------*
| Secondary Title        | (utitl2(n))                                         |
|------------------------------------------------------------------------------|
|EQ3NR input file name= NaCl_geschlossen.3i                                    |
|Description= „Calcite dissolution in NaCl solution"                          |
|Version level= 8.0                                                           |
|Revised 12/10/2010    Revisor= C.Haase                                       |
|                                                                              |
|Szenario NaCl: T= 25°C, CO2= 0.5 mol                                         |
|Input für NaCl_geschlossen.6i                                                |
|Ca= 2.0 mmol; CO3= 4.0 mmol                                                  |
|Database data0.cmp                                                           |
|                                                                              |
|------------------------------------------------------------------------------|
|Special Basis Switches (for model definition only)       | (nsbswt)           |
|------------------------------------------------------------------------------|
|Replace |None                                            | (usbsw(1,n))       |
|   with |None                                            | (usbsw(2,n))       |
|------------------------------------------------------------------------------|
|Original temperature (C) | 2.50000E+01| (tempci)                              |
|------------------------------------------------------------------------------|
|Original pressure (bars) | 1.01320E+00| (pressi)                              |
|------------------------------------------------------------------------------|
|Create Ion Exchangers    | (net)                                              |
|------------------------------------------------------------------------------|
|Advisory: no exchanger creation blocks follow on this file.                   |
|Option: on further processing (writing a pickup file or running XCON6 on the  |
|present file), force the inclusion of at least one such block (qgexsh):       |
|  [ ] (.true.)                                                                |
|------------------------------------------------------------------------------|
|Alter/Suppress Options  | (nxmod)                                             |
|------------------------------------------------------------------------------|
|Species                                        |Option          |Alter value |
| (uxmod(n))                                    |(ukxm(kxmod(n)))| (xlkmod(n))|
|------------------------------------------------------------------------------|
|None                                           |None            | 0.00000E+00|
|------------------------------------------------------------------------------|
|Iopg Activity Coefficient Option Switches („( 0)" marks default choices)      |
|------------------------------------------------------------------------------|
|iopg(1) - Aqueous Species Activity Coefficient Model:                         |
|  [ ] (-1) The Davies equation                                                |
|  [x] ( 0) The B-dot equation                                                 |
|  [ ] ( 1) Pitzer's equations                                                 |
|  [ ] ( 2) HC + DH equations                                                  |
|------------------------------------------------------------------------------|
|iopg(2) - Choice of pH Scale (Rescales Activity Coefficients):                |
|  [ ] (-1) „Internal" pH scale (no rescaling)                                 |
|  [x] ( 0) NBS pH scale (uses the Bates-Guggenheim equation)                  |
|  [ ] ( 1) Mesmer pH scale (numerically, pH = -log m(H+))                     |
```

Matrix Index Limits		
No. of chem. elements	6	(kct)
No. of basis species	10	(kbt)
Index of last pure min.	10	(kmt)
Index of last sol-sol.	10	(kxt)
Matrix size	10	(kdim)
PRS data flag	0	(kprs)

Mass Balance Species (Matrix Row Variables) (ubmtbi(n))		Units/Constraint (ujf6(jflgi(n)))	--
H2O	Aqueous solution	Moles	--
Ca++	Aqueous solution	Moles	--
Cl-	Aqueous solution	Moles	--
H+	Aqueous solution	Moles	--
HCO3-	Aqueous solution	Moles	--
Na+	Aqueous solution	Moles	--
O2(g)	Aqueous solution	Moles	--
H2(aq)	Aqueous solution	Make non-basis	--
O2(aq)	Aqueous solution	Make non-basis	--
CO2(aq)	Aqueous solution	Make non-basis	--

Mass Balance Totals (moles)			
Basis species (info. only) (ubmtbi(n))		Equilibrium System (mtbi(n))	Aqueous Solution (mtbaqi(n))
H2O	Aqueous	5.550843517294234E+01	5.550843517294234E+01
Ca++	Aqueous	2.000000004567650E-03	2.000000004567650E-03
Cl-	Aqueous	1.000000000013663E-20	1.000000000013663E-20
H+	Aqueous	-1.043859538452722E-05	-1.043859538452722E-05
HCO3-	Aqueous	5.728535851048820E-03	5.728535851048820E-03
Na+	Aqueous	1.000000000178489E-20	1.000000000178489E-20
O2(g)	Aqueous	-4.636168198045946E-25	-4.636168198045946E-25
H2(aq)	Aqueous	7.838717489141694E-26	7.838717489141694E-26
O2(aq)	Aqueous	9.730995588502664E-43	9.730995588502664E-43
CO2(aq)	Aqueous	5.000000000000000E-01	5.000000000000000E-01
Electrical imbalance		-1.738974437298047E-03	-1.738974437298047E-03

Ordinary Basis Switches (for numerical purposes only)	(nobswt)
Replace None	(uobsw(1,n))
with None	(uobsw(2,n))

Matrix Column Variables and Values			
Basis species (uzveci(n))		Log moles (zvclgi(n))	--
H2O	Aqueous solution	1.744358983526984E+00	--
Ca++	Aqueous solution	-2.719636084494143E+00	--
Cl-	Aqueous solution	-2.000011964066534E+01	--
H+	Aqueous solution	-6.965444153944126E+00	--
HCO3-	Aqueous solution	-2.249322626609868E+00	--
Na+	Aqueous solution	-2.000292867438012E+01	--
O2(g)	Aqueous solution	-3.911283773692741E+01	--
H2(aq)	Aqueous solution	-2.510575498743690E+01	--
O2(aq)	Aqueous solution	-4.201184272432840E+01	--
CO2(aq)	Aqueous solution	-3.010299956639812E-01	--

Phases and Species in the PRS

```
|-------------------------------------------------------------------------------|
|Phase           |None                    | (uprphi(n))                         |
|-------------------------------------------------------------------------------|
|->|No. of Moles    | 0.000000000000000E+00| (mprphi(n))                       |
|-------------------------------------------------------------------------------|
|--->|Species                 |No. of Moles          | --                       |
|--->| (uprspi(i,n))          | (mprspi(i,n))        | --                       |
|-------------------------------------------------------------------------------|
|--->|None                    | 0.000000000000000E+00| --                       |
|-------------------------------------------------------------------------------|
|End of problem                                                                 |
|-------------------------------------------------------------------------------|
```

A.3.1.5 Eingabedatei für EQ3, offenes System, Gleichgewicht mit Halit (data0.cmp)

```
|-------------------------------------------------------------------------------|
| Title                  | (utitl(n))                                           |
|-------------------------------------------------------------------------------|
|EQ3NR input file name= NaCl_offen_Halit.3i                                      |
|Description= „Calcite dissolution in NaCl solution and                         |
|              precipitation of Halite possible"                                |
|Version level= 8.0                                                             |
|Revised 12/10/10    Revisor= C. Haase                                          |
|                                                                               |
|                                                                               |
|Szenario NaCl: T= 25 °C, pCO2= 1 bar                                           |
|Input für NaCl_offen_Halit.6i                                                  |
|Ca= 2.0 mmol und CO3= 4.0 mmol                                                 |
|                                                                               |
|-------------------------------------------------------------------------------|
|Special Basis Switches (for model definition only)       | (nsbswt)            |
|-------------------------------------------------------------------------------|
|Replace |None                                            | (usbsw(1,n))        |
|   with |None                                            | (usbsw(2,n))        |
|-------------------------------------------------------------------------------|
|Temperature (C)         | 2.50000E+01| (tempc)                                 |
|-------------------------------------------------------------------------------|
|Pressure option (jpres3):                                                      |
|  [ ] ( 0) Data file reference curve value                                     |
|  [x] ( 1) 1.013-bar/steam-saturation curve value                              |
|  [ ] ( 2) Value (bars) | 0.00000E+00| (press)                                 |
|-------------------------------------------------------------------------------|
|Density (g/cm3)         | 1.00000E+00| (rho)                                   |
|-------------------------------------------------------------------------------|
|Total dissolved solutes option (itdsf3):                                       |
|  [x] ( 0) Value (mg/kg.sol) | 0.00000E+00| (tdspkg)                         |
|  [ ] ( 1) Value (mg/L)      | 0.00000E+00| (tdspl)                          |
|-------------------------------------------------------------------------------|
|Electrical balancing option (iebal3):                                          |
|  [x] ( 0) No balancing is done                                                |
|  [ ] ( 1) Balance on species |Cl-                     | (uebal)              |
|-------------------------------------------------------------------------------|
|Default redox constraint (irdxc3):                                             |
|  [ ] (-3) Use O2(g) line in the aqueous basis species block                   |
|  [x] (-2) pe (pe units)      | 4.00000E+00| (pei)                             |
|  [ ] (-1) Eh (volts)         | 5.00000E-01| (ehi)                             |
|  [ ] ( 0) Log fO2 (log bars) | 0.00000E+00| (fo2lgi)                          |
|  [ ] ( 1) Couple (aux. sp.)  |None                    | (uredox)             |
|-------------------------------------------------------------------------------|
|Aqueous Basis Species/Constraint Species        |Conc., etc. |Units/Constraint|
| (uspeci(n)/ucospi(n))                          | (covali(n))|(ujf3(jflgi(n)))|
|-------------------------------------------------------------------------------|
|H+                                              |1.00000E+00|Hetero. equil.   |
```

```
|->|CO2(g)                                          |(ucospi(n))              |
|Ca++                                             |2.00000E-03|Molality         |
|HCO3-                                            |1.00000E-00|Hetero. equil.   |
|->|Calcite                                          | (ucospi(n))             |
|Na+                                              |1.00000E-20|Molality         |
|Cl-                                              |1.00000E-20|Molality         |
|-------------------------------------------------------------------------------|
|Create Ion Exchangers  | (net)                                                 |
|-------------------------------------------------------------------------------|
|Advisory: no exchanger creation blocks follow on this file.                    |
|Option: on further processing (writing a PICKUP file or running XCON3 on the   |
|present file), force the inclusion of at least one such block (qgexsh):        |
|  [ ] (.true.)                                                                 |
|-------------------------------------------------------------------------------|
|Ion Exchanger Compositions      | (neti)                                       |
|-------------------------------------------------------------------------------|
|Exchanger phase |None                    | (ugexpi(n))                         |
|-------------------------------------------------------------------------------|
|->|Moles/kg.H2O    |  0.0000    | (cgexpi(n))                                 |
|-------------------------------------------------------------------------------|
|->|Exchange site   |None     | (ugexji(j,n))                                  |
|-------------------------------------------------------------------------------|
|--->|Exchange species        |Eq. frac.   | (this is a table header)          |
|-------------------------------------------------------------------------------|
|--->|None                    | 0.00000E+00| (ugexsi(i,j,n), egexsi(i,j,n))    |
|-------------------------------------------------------------------------------|
|Solid Solution Compositions     | (nxti)                                       |
|-------------------------------------------------------------------------------|
|Solid Solution          |None                   | (usoli(n))                   |
|-------------------------------------------------------------------------------|
|->|Component               |Mole frac.  | (this is a table header)          |
|-------------------------------------------------------------------------------|
|->|None                    | 0.00000E+00| (umemi(i,n), xbari(i,n))          |
|-------------------------------------------------------------------------------|
|Alter/Suppress Options  | (nxmod)                                              |
|-------------------------------------------------------------------------------|
|Species                                          |Option          |Alter value |
|  (uxmod(n))                                     |(ukxm(kxmod(n)))| (xlkmod(n))|
|-------------------------------------------------------------------------------|
|None                                             |Suppress        | 0.00000E+00|
|-------------------------------------------------------------------------------|
|Iopt Model Option Switches („( 0)" marks default choices)                      |
|-------------------------------------------------------------------------------|
|iopt(4) - Solid Solutions:                                                     |
|  [x] ( 0) Ignore                                                              |
|  [ ] ( 1) Permit                                                              |
|-------------------------------------------------------------------------------|
|iopt(11) - Auto Basis Switching in pre-N-R Optimization:                       |
|  [x] ( 0) Turn off                                                            |
|  [ ] ( 1) Turn on                                                             |
|-------------------------------------------------------------------------------|
|iopt(17) - PICKUP File Options:                                                |
|  [ ] (-1) Don't write a PICKUP file                                           |
|  [x] ( 0) Write a PICKUP file                                                 |
|-------------------------------------------------------------------------------|
|iopt(19) - Advanced EQ3NR PICKUP File Options:                                 |
|  [x] ( 0) Write a normal EQ3NR PICKUP file                                    |
|  [ ] ( 1) Write an EQ6 INPUT file with Quartz dissolving, relative rate law   |
|  [ ] ( 2) Write an EQ6 INPUT file with Albite dissolving, TST rate law        |
|  [ ] ( 3) Write an EQ6 INPUT file with Fluid 1 set up for fluid mixing        |
|-------------------------------------------------------------------------------|
|Iopg Activity Coefficient Option Switches („( 0)" marks default choices)       |
```

```
|-------------------------------------------------------------------------------|
|iopg(1) - Aqueous Species Activity Coefficient Model:                          |
|   [ ] (-1) The Davies equation                                                |
|   [x] ( 0) The B-dot equation                                                 |
|   [ ] ( 1) Pitzer's equations                                                 |
|   [ ] ( 2) HC + DH equations                                                  |
|-------------------------------------------------------------------------------|
|iopg(2) - Choice of pH Scale (Rescales Activity Coefficients):                 |
|   [ ] (-1) „Internal" pH scale (no rescaling)                                 |
|   [x] ( 0) NBS pH scale (uses the Bates-Guggenheim equation)                  |
|   [ ] ( 1) Mesmer pH scale (numerically, pH = -log m(H+))                     |
|-------------------------------------------------------------------------------|
|Iopr Print Option Switches („( 0)" marks default choices)                      |
|-------------------------------------------------------------------------------|
|iopr(1) - Print All Species Read from the Data File:                           |
|   [x] ( 0) Don't print                                                        |
|   [ ] ( 1) Print                                                              |
|-------------------------------------------------------------------------------|
|iopr(2) - Print All Reactions:                                                 |
|   [x] ( 0) Don't print                                                        |
|   [ ] ( 1) Print the reactions                                                |
|   [ ] ( 2) Print the reactions and log K values                               |
|   [ ] ( 3) Print the reactions, log K values, and associated data             |
|-------------------------------------------------------------------------------|
|iopr(3) - Print the Aqueous Species Hard Core Diameters:                       |
|   [x] ( 0) Don't print                                                        |
|   [ ] ( 1) Print                                                              |
|-------------------------------------------------------------------------------|
|iopr(4) - Print a Table of Aqueous Species Concentrations, Activities, etc.:   |
|   [x] (-3) Omit species with molalities < 1.e-8                               |
|   [ ] (-2) Omit species with molalities < 1.e-12                              |
|   [ ] (-1) Omit species with molalities < 1.e-20                              |
|   [ ] ( 0) Omit species with molalities < 1.e-100                             |
|   [ ] ( 1) Include all species                                                |
|-------------------------------------------------------------------------------|
|iopr(5) - Print a Table of Aqueous Species/H+ Activity Ratios:                 |
|   [x] ( 0) Don't print                                                        |
|   [ ] ( 1) Print cation/H+ activity ratios only                               |
|   [ ] ( 2) Print cation/H+ and anion/H+ activity ratios                       |
|   [ ] ( 3) Print ion/H+ activity ratios and neutral species activities        |
|-------------------------------------------------------------------------------|
|iopr(6) - Print a Table of Aqueous Mass Balance Percentages:                   |
|   [x] (-1) Don't print                                                        |
|   [ ] ( 0) Print those species comprising at least 99% of each mass balance   |
|   [ ] ( 1) Print all contributing species                                     |
|-------------------------------------------------------------------------------|
|iopr(7) - Print Tables of Saturation Indices and Affinities:                   |
|   [ ] (-1) Don't print                                                        |
|   [x] ( 0) Print, omitting those phases undersaturated by more than 10 kcal   |
|   [ ] ( 1) Print for all phases                                               |
|-------------------------------------------------------------------------------|
|iopr(8) - Print a Table of Fugacities:                                         |
|   [ ] (-1) Don't print                                                        |
|   [x] ( 0) Print                                                              |
|-------------------------------------------------------------------------------|
|iopr(9) - Print a Table of Mean Molal Activity Coefficients:                   |
|   [x] ( 0) Don't print                                                        |
|   [ ] ( 1) Print                                                              |
|-------------------------------------------------------------------------------|
|iopr(10) - Print a Tabulation of the Pitzer Interaction Coefficients:          |
|   [x] ( 0) Don't print                                                        |
|   [ ] ( 1) Print a summary tabulation                                         |
```

```
|  [ ] ( 2) Print a more detailed tabulation                                    |
|-------------------------------------------------------------------------------|
|iopr(17) - PICKUP file format („W" or „D"):                                    |
|  [x] ( 0) Use the format of the INPUT file                                    |
|  [ ] ( 1) Use „W" format                                                      |
|  [ ] ( 2) Use „D" format                                                      |
|-------------------------------------------------------------------------------|
|Iodb Debugging Print Option Switches („( 0)" marks default choices)            |
|-------------------------------------------------------------------------------|
|iodb(1) - Print General Diagnostic Messages:                                   |
|  [x] ( 0) Don't print                                                         |
|  [ ] ( 1) Print Level 1 diagnostic messages                                   |
|  [ ] ( 2) Print Level 1 and Level 2 diagnostic messages                       |
|-------------------------------------------------------------------------------|
|iodb(3) - Print Pre-Newton-Raphson Optimization Information:                   |
|  [x] ( 0) Don't print                                                         |
|  [ ] ( 1) Print summary information                                           |
|  [ ] ( 2) Print detailed information (including the beta and del vectors)     |
|  [ ] ( 3) Print more detailed information (including matrix equations)       |
|  [ ] ( 4) Print most detailed information (including activity coefficients)  |
|-------------------------------------------------------------------------------|
|iodb(4) - Print Newton-Raphson Iteration Information:                          |
|  [x] ( 0) Don't print                                                         |
|  [ ] ( 1) Print summary information                                           |
|  [ ] ( 2) Print detailed information (including the beta and del vectors)     |
|  [ ] ( 3) Print more detailed information (including the Jacobian)            |
|  [ ] ( 4) Print most detailed information (including activity coefficients)  |
|-------------------------------------------------------------------------------|
|iodb(6) - Print Details of Hypothetical Affinity Calculations:                 |
|  [x] ( 0) Don't print                                                         |
|  [ ] ( 1) Print summary information                                           |
|  [ ] ( 2) Print detailed information                                          |
|-------------------------------------------------------------------------------|
|Numerical Parameters                                                           |
|-------------------------------------------------------------------------------|
| Beta convergence tolerance      | 0.00000E+00| (tolbt)                        |
| Del convergence tolerance       | 0.00000E+00| (toldl)                        |
| Max. Number of N-R Iterations   |   0        | (itermx)                       |
|-------------------------------------------------------------------------------|
|Ordinary Basis Switches (for numerical purposes only)    | (nobswt)          |
|-------------------------------------------------------------------------------|
|Replace |None                                            | (uobsw(1,n))      |
|   with |None                                            | (uobsw(2,n))      |
|-------------------------------------------------------------------------------|
|Sat. flag tolerance     | 0.00000E+00| (tolspf)                                |
|-------------------------------------------------------------------------------|
|Aq. Phase Scale Factor  | 1.00000E+00| (scamas)                                |
|-------------------------------------------------------------------------------|
|End of problem                                                                 |
|-------------------------------------------------------------------------------|
```

A.3.1.6 Eingabedatei für EQ6, offenes System, Gleichgewicht mit Halit (data0.cmp)

```
|-------------------------------------------------------------------------------|
| Main Title             | (utitl1(n))                                          |
|-------------------------------------------------------------------------------|
|EQ6 input file name= NaCl_offen_Halit.6i                                       |
|Description= „Calcite dissolution in NaCl and                                 |
|              precipitation of Halit possible"                                |
|Version level= 8.0                                                             |
|Revised 12/10/2010    Revisor= C.Haase                                         |
|                                                                               |
|Szenario NaCl: T= 25 °C, fCO2: 1 bar                                           |
```

```
|                                                                                |
|                                                                                |
|Database data0.cmp                                                              |
|                                                                                |
|--------------------------------------------------------------------------------|
|Temperature option (jtemp):                                                     |
|  [x] ( 0) Constant temperature:                                                |
|             Value (C)          | 2.50000E+01| (tempcb)                       |
|  [ ] ( 1) Linear tracking in Xi:                                               |
|             Base Value (C)     | 0.00000E+00| (tempcb)                       |
|             Derivative         | 0.00000E+00| (ttk(1))                       |
|  [ ] ( 2) Linear tracking in time:                                             |
|             Base Value (C)     | 0.00000E+00| (tempcb)                       |
|             Derivative         | 0.00000E+00| (ttk(1))                       |
|  [ ] ( 3) Fluid mixing tracking (fluid 2 = special reactant):                  |
|             T of fluid 1 (C)  | 0.00000E+00| (tempcb)                       |
|             T of fluid 2 (C)  | 0.00000E+00| (ttk(2))                       |
|             Mass ratio factor | 0.00000E+00| (ttk(1))                       |
|--------------------------------------------------------------------------------|
|Pressure option (jpress):                                                       |
|  [ ] ( 0) Follow the data file reference pressure curve                        |
|  [x] ( 1) Follow the 1.013-bar/steam-saturation curve                          |
|  [ ] ( 2) Constant pressure:                                                   |
|             Value (bars)       | 0.00000E+00| (pressb)                       |
|  [ ] ( 3) Linear tracking in Xi:                                               |
|             Base Value (bars) | 0.00000E+00| (pressb)                       |
|             Derivative         | 0.00000E+00| (ptk(1))                       |
|  [ ] ( 4) Linear tracking in time:                                             |
|             Base Value (bars) | 0.00000E+00| (pressb)                       |
|             Derivative         | 0.00000E+00| (ptk(1))                       |
|--------------------------------------------------------------------------------|
|Reactants (Irreversible Reactions) | (nrct)                                     |
|--------------------------------------------------------------------------------|
|Reactant        |Calcite                 | (ureac(n))                           |
|--------------------------------------------------------------------------------|
|->|Type         |Pure mineral            | (urcjco(jcode(n)))                   |
|--------------------------------------------------------------------------------|
|->|Status       |Saturated, reacting     | (urcjre(jreac(n)))                   |
|--------------------------------------------------------------------------------|
|->|Amount remaining (moles) | 1.00000E+01| (morr(n))                           |
|--------------------------------------------------------------------------------|
|->|Amount destroyed (moles) | 0.00000E+00| (modr(n))                           |
|--------------------------------------------------------------------------------|
|->|Surface area option (nsk(n)):                                               |
|->|  [x] ( 0) Constant surface area:                                           |
|->|             Value (cm2)       | 1.00000E+01| (sfcar(n))                     |
|->|  [ ] ( 1) Constant specific surface area:                                  |
|->|             Value (cm2/g)     | 0.00000E+00| (ssfcar(n))                    |
|->|  [ ] ( 2) n**2/3 growth law- current surface area:                         |
|->|             Value (cm2)       | 0.00000E+00| (sfcar(n))                     |
|--------------------------------------------------------------------------------|
|->|Surface area factor      | 1.00000E+01| (fkrc(n))                         |
|--------------------------------------------------------------------------------|
|->|Forward rate law          |Relative rate equation  | (urcnrk(nrk(1,n)))    |
|--------------------------------------------------------------------------------|
|--->|dXi(n)/dXi (mol/mol)      | 1.00000E+00| (rkb(1,1,n))                     |
|--------------------------------------------------------------------------------|
|--->|d2Xi(n)/dXi2 (mol/mol2)   | 0.00000E+00| (rkb(2,1,n))                     |
|--------------------------------------------------------------------------------|
|--->|d3Xi(n)/dXi3 (mol/mol3)   | 0.00000E+00| (rkb(3,1,n))                     |
|--------------------------------------------------------------------------------|
|->|Backward rate law         |Partial equilibrium     | (urcnrk(nrk(2,n)))    |
```

```
|-------------------------------------------------------------------------------|
|Reactant        |Halite                  | (ureac(n))                          |
|-------------------------------------------------------------------------------|
|->|Type         |Pure mineral            | (urcjco(jcode(n)))                  |
|-------------------------------------------------------------------------------|
|->|Status       |Saturated, reacting     | (urcjre(jreac(n)))                  |
|-------------------------------------------------------------------------------|
|->|Amount remaining (moles) | 0.00000E+00| (morr(n))                          |
|-------------------------------------------------------------------------------|
|->|Amount destroyed (moles) | 0.00000E+00| (modr(n))                          |
|-------------------------------------------------------------------------------|
|->|Surface area option (nsk(n)):                                               |
|->|  [x] ( 0) Constant surface area:                                           |
|->|             Value (cm2)       | 1.00000E+01| (sfcar(n))                   |
|->|  [ ] ( 1) Constant specific surface area:                                  |
|->|             Value (cm2/g)     | 0.00000E+00| (ssfcar(n))                  |
|->|  [ ] ( 2) n**2/3 growth law- current surface area:                         |
|->|             Value (cm2)       | 0.00000E+00| (sfcar(n))                   |
|-------------------------------------------------------------------------------|
|->|Surface area factor      | 1.00000E+01| (fkrc(n))                        |
|-------------------------------------------------------------------------------|
|->|Forward rate law          |Relative rate equation  | (urcnrk(nrk(1,n)))    |
|-------------------------------------------------------------------------------|
|--->|dXi(n)/dXi (mol/mol)      | 1.00000E+00| (rkb(1,1,n))                     |
|-------------------------------------------------------------------------------|
|--->|d2Xi(n)/dXi2 (mol/mol2)   | 0.00000E+00| (rkb(2,1,n))                     |
|-------------------------------------------------------------------------------|
|--->|d3Xi(n)/dXi3 (mol/mol3)   | 0.00000E+00| (rkb(3,1,n))                     |
|-------------------------------------------------------------------------------|
|->|Backward rate law         |Partial equilibrium     | (urcnrk(nrk(2,n)))    |
|-------------------------------------------------------------------------------|
|Reactant        |NaCl                    | (ureac(n))                          |
|-------------------------------------------------------------------------------|
|->|Type         |Special reactant        | (urcjco(jcode(n)))                  |
|-------------------------------------------------------------------------------|
|->|Status       |Reacting                | (urcjre(jreac(n)))                  |
|-------------------------------------------------------------------------------|
|->|Amount remaining (moles) | 4.00000E+00| (morr(n))                          |
|-------------------------------------------------------------------------------|
|->|Amount destroyed (moles) | 0.00000E+00| (modr(n))                          |
|-------------------------------------------------------------------------------|
|->|Molar volume (cm3/mol)   | 0.00000E+00| (vreac(n))                         |
|-------------------------------------------------------------------------------|
|->|Composition                                                                 |
|-------------------------------------------------------------------------------|
|--->|Element |Stoich. Number        | (this is a table header)                 |
|-------------------------------------------------------------------------------|
|--->|Na      | 1.0000000000000000+00| (uesri(i,n), cesri(i,n))                 |
|--->|Cl      | 1.0000000000000000+00| (uesri(i,n), cesri(i,n))                 |
|-------------------------------------------------------------------------------|
|->|Reaction                                                                    |
|-------------------------------------------------------------------------------|
|--->|Species                 |Reaction Coefficient  | (this is a table header)|
|-------------------------------------------------------------------------------|
|--->|NaCl                    |-1.000000000000000E+00| (ubsri(i,n), cbsri(i,n))|
|--->|Na+                     | 4.000000000000000E+00| (ubsri(i,n), cbsri(i,n))|
|--->|Cl-                     | 4.000000000000000E+00| (ubsri(i,n), cbsri(i,n))|
|-------------------------------------------------------------------------------|
|->|Surface area option (nsk(n)):                                               |
|->|  [x] ( 0) Constant surface area:                                           |
|->|             Value (cm2)       | 1.00000E+01| (sfcar(n))                   |
|->|  [ ] ( 1) Constant specific surface area:                                  |
```

```
|->|             Value (cm2/g)     | 0.00000E+00| (ssfcar(n))                  |
|->|  [ ] ( 2) n**2/3 growth law- current surface area:                          |
|->|             Value (cm2)       | 0.00000E+00| (sfcar(n))                   |
|-----------------------------------------------------------------------------|
|->|Surface area factor      | 1.00000E+00| (fkrc(n))                        |
|-----------------------------------------------------------------------------|
|->|Forward rate law            |Relative rate equation | (urcnrk(nrk(1,n)))   |
|-----------------------------------------------------------------------------|
|--->|dXi(n)/dXi (mol/mol)      | 1.00000E+00| (rkb(1,1,n))                     |
|-----------------------------------------------------------------------------|
|--->|d2Xi(n)/dXi2 (mol/mol2)   | 0.00000E-00| (rkb(2,1,n))                     |
|-----------------------------------------------------------------------------|
|--->|d3Xi(n)/dXi3 (mol/mol3)   | 0.00000E-00| (rkb(3,1,n))                     |
|-----------------------------------------------------------------------------|
|->|Backward rate law         |Partial equilibrium     | (urcnrk(nrk(2,n)))    |
|-----------------------------------------------------------------------------|
|Starting, minimum, and maximum values of key run parameters.                 |
|-----------------------------------------------------------------------------|
|Starting Xi value        | 1.00000E-01| (xistti)                             |
|-----------------------------------------------------------------------------|
|Maximum Xi value         | 1.10000E+00| (ximaxi)                             |
|-----------------------------------------------------------------------------|
|Starting time (seconds)  | 0.00000E+00| (tistti)                             |
|-----------------------------------------------------------------------------|
|Maximum time (seconds)   | 1.00000E+38| (timmxi)                             |
|-----------------------------------------------------------------------------|
|Minimum value of pH      | 1.00000E-00| (phmini)                             |
|-----------------------------------------------------------------------------|
|Maximum value of pH      | 1.00000E+10| (phmaxi)                             |
|-----------------------------------------------------------------------------|
|Minimum value of Eh (v)  |-1.00000E+38| (ehmini)                             |
|-----------------------------------------------------------------------------|
|Maximum value of Eh (v)  | 1.00000E+38| (ehmaxi)                             |
|-----------------------------------------------------------------------------|
|Minimum value of log fO2 |-1.00000E+38| (o2mini)                             |
|-----------------------------------------------------------------------------|
|Maximum value of log fO2 | 1.00000E+38| (o2maxi)                             |
|-----------------------------------------------------------------------------|
|Minimum value of aw      |-1.00000E+38| (awmini)                             |
|-----------------------------------------------------------------------------|
|Maximum value of aw      | 1.00000E+38| (awmaxi)                             |
|-----------------------------------------------------------------------------|
|Maximum number of steps  |         400| (kstpmx)                             |
|-----------------------------------------------------------------------------|
|Print interval parameters.                                                   |
|-----------------------------------------------------------------------------|
|Xi print interval        | 2.00000E-02| (dlxprn)                             |
|-----------------------------------------------------------------------------|
|Log Xi print interval    | 5.00000E-01| (dlxprl)                             |
|-----------------------------------------------------------------------------|
|Time print interval      | 1.00000E+38| (dltprn)                             |
|-----------------------------------------------------------------------------|
|Log time print interval  | 1.00000E+38| (dltprl)                             |
|-----------------------------------------------------------------------------|
|pH print interval        | 1.00000E+38| (dlhprn)                             |
|-----------------------------------------------------------------------------|
|Eh (v) print interval    | 1.00000E+38| (dleprn)                             |
|-----------------------------------------------------------------------------|
|Log fO2 print interval   | 1.00000E+38| (dloprn)                             |
|-----------------------------------------------------------------------------|
|aw print interval        | 1.00000E+38| (dlaprn)                             |
|-----------------------------------------------------------------------------|
```

```
|Steps print interval     |         0.1| (ksppmx)                                  |
|-------------------------------------------------------------------------------|
|Plot interval parameters.                                                      |
|-------------------------------------------------------------------------------|
|Xi plot interval         | 2.00000E-01| (dlxplo)                                 |
|-------------------------------------------------------------------------------|
|Log Xi plot interval     | 2.00000E-01| (dlxpll)                                 |
|-------------------------------------------------------------------------------|
|Time plot interval       | 1.00000E+38| (dltplo)                                 |
|-------------------------------------------------------------------------------|
|Log time plot interval   | 1.00000E+38| (dltpll)                                 |
|-------------------------------------------------------------------------------|
|pH plot interval         | 2.00000E-01| (dlhplo)                                 |
|-------------------------------------------------------------------------------|
|Eh (v) plot interval     | 2.00000E-01| (dleplo)                                 |
|-------------------------------------------------------------------------------|
|Log fO2 plot interval    | 1.00000E+38| (dloplo)                                 |
|-------------------------------------------------------------------------------|
|aw plot interval         | 2.00000E-01| (dlaplo)                                 |
|-------------------------------------------------------------------------------|
|Steps plot interval      |         100| (ksplmx)                                 |
|-------------------------------------------------------------------------------|
|Iopt Model Option Switches („( 0)" marks default choices)                      |
|-------------------------------------------------------------------------------|
|iopt(1) - Physical System Model Selection:                                     |
|  [x] ( 0) Closed system                                                       |
|  [ ] ( 1) Titration system                                                    |
|  [ ] ( 2) Fluid-centered flow-through open system                             |
|-------------------------------------------------------------------------------|
|iopt(2) - Kinetic Mode Selection:                                              |
|  [x] ( 0) Reaction progress mode (arbitrary kinetics)                         |
|  [ ] ( 1) Reaction progress/time mode (true kinetics)                         |
|-------------------------------------------------------------------------------|
|iopt(3) - Phase Boundary Searches:                                             |
|  [x] ( 0) Search for phase boundaries and constrain the step size to match    |
|  [ ] ( 1) Search for phase boundaries and print their locations               |
|  [ ] ( 2) Don't search for phase boundaries                                   |
|-------------------------------------------------------------------------------|
|iopt(4) - Solid Solutions:                                                     |
|  [x] ( 0) Ignore                                                              |
|  [ ] ( 1) Permit                                                              |
|-------------------------------------------------------------------------------|
|iopt(5) - Clear the ES Solids Read from the INPUT File:                        |
|  [x] ( 0) Don't do it                                                         |
|  [ ] ( 1) Do it                                                               |
|-------------------------------------------------------------------------------|
|iopt(6) - Clear the ES Solids at the Initial Value of Reaction Progress:       |
|  [x] ( 0) Don't do it                                                         |
|  [ ] ( 1) Do it                                                               |
|-------------------------------------------------------------------------------|
|iopt(7) - Clear the ES Solids at the End of the Run:                           |
|  [x] ( 0) Don't do it                                                         |
|  [ ] ( 1) Do it                                                               |
|-------------------------------------------------------------------------------|
|iopt(9) - Clear the PRS Solids Read from the INPUT file:                       |
|  [x] ( 0) Don't do it                                                         |
|  [ ] ( 1) Do it                                                               |
|-------------------------------------------------------------------------------|
|iopt(10) - Clear the PRS Solids at the End of the Run:                         |
|  [x] ( 0) Don't do it                                                         |
|  [ ] ( 1) Do it, unless numerical problems cause early termination            |
|-------------------------------------------------------------------------------|
```

```
|iopt(11) - Auto Basis Switching in pre-N-R Optimization:                      |
|  [x] ( 0) Turn off                                                           |
|  [ ] ( 1) Turn on                                                            |
|------------------------------------------------------------------------------|
|iopt(12) - Auto Basis Switching after Newton-Raphson Iteration:               |
|  [x] ( 0) Turn off                                                           |
|  [ ] ( 1) Turn on                                                            |
|------------------------------------------------------------------------------|
|iopt(13) - Calculational Mode Selection:                                      |
|  [x] ( 0) Normal path tracing                                                |
|  [ ] ( 1) Economy mode (if permissible)                                      |
|  [ ] ( 2) Super economy mode (if permissible)                                |
|------------------------------------------------------------------------------|
|iopt(14) - ODE Integrator Corrector Mode Selection:                           |
|  [x] ( 0) Allow Stiff and Simple Correctors                                  |
|  [ ] ( 1) Allow Only the Simple Corrector                                    |
|  [ ] ( 2) Allow Only the Stiff Corrector                                     |
|  [ ] ( 3) Allow No Correctors                                                |
|------------------------------------------------------------------------------|
|iopt(15) - Force the Suppression of All Redox Reactions:                      |
|  [x] ( 0) Don't do it                                                        |
|  [ ] ( 1) Do it                                                              |
|------------------------------------------------------------------------------|
|iopt(16) - BACKUP File Options:                                               |
|  [ ] (-1) Don't write a BACKUP file                                          |
|  [x] ( 0) Write BACKUP files                                                 |
|  [ ] ( 1) Write a sequential BACKUP file                                     |
|------------------------------------------------------------------------------|
|iopt(17) - PICKUP File Options:                                               |
|  [ ] (-1) Don't write a PICKUP file                                          |
|  [x] ( 0) Write a PICKUP file                                                |
|------------------------------------------------------------------------------|
|iopt(18) - TAB File Options:                                                  |
|  [ ] (-1) Don't write a TAB file                                             |
|  [x] ( 0) Write a TAB file                                                   |
|  [ ] ( 1) Write a TAB file, prepending TABX file data from a previous run    |
|------------------------------------------------------------------------------|
|iopt(20) - Advanced EQ6 PICKUP File Options:                                  |
|  [x] ( 0) Write a normal EQ6 PICKUP file                                     |
|  [ ] ( 1) Write an EQ6 INPUT file with Fluid 1 set up for fluid mixing       |
|------------------------------------------------------------------------------|
|Iopr Print Option Switches („( 0)" marks default choices)                     |
|------------------------------------------------------------------------------|
|iopr(1) - Print All Species Read from the Data File:                          |
|  [x] ( 0) Don't print                                                        |
|  [ ] ( 1) Print                                                              |
|------------------------------------------------------------------------------|
|iopr(2) - Print All Reactions:                                                |
|  [x] ( 0) Don't print                                                        |
|  [ ] ( 1) Print the reactions                                                |
|  [ ] ( 2) Print the reactions and log K values                               |
|  [ ] ( 3) Print the reactions, log K values, and associated data             |
|------------------------------------------------------------------------------|
|iopr(3) - Print the Aqueous Species Hard Core Diameters:                      |
|  [x] ( 0) Don't print                                                        |
|  [ ] ( 1) Print                                                              |
|------------------------------------------------------------------------------|
|iopr(4) - Print a Table of Aqueous Species Concentrations, Activities, etc.:  |
|  [ ] (-3) Omit species with molalities < 1.e-8                               |
|  [ ] (-2) Omit species with molalities < 1.e-12                              |
|  [ ] (-1) Omit species with molalities < 1.e-20                              |
|  [x] ( 0) Omit species with molalities < 1.e-100                             |
```

```
|   [ ] ( 1) Include all species                                                |
|-------------------------------------------------------------------------------|
|iopr(5) - Print a Table of Aqueous Species/H+ Activity Ratios:                 |
|   [x] ( 0) Don't print                                                        |
|   [ ] ( 1) Print cation/H+ activity ratios only                               |
|   [ ] ( 2) Print cation/H+ and anion/H+ activity ratios                       |
|   [ ] ( 3) Print ion/H+ activity ratios and neutral species activities        |
|-------------------------------------------------------------------------------|
|iopr(6) - Print a Table of Aqueous Mass Balance Percentages:                   |
|   [ ] (-1) Don't print                                                        |
|   [x] ( 0) Print those species comprising at least 99% of each mass balance   |
|   [ ] ( 1) Print all contributing species                                     |
|-------------------------------------------------------------------------------|
|iopr(7) - Print Tables of Saturation Indices and Affinities:                   |
|   [ ] (-1) Don't print                                                        |
|   [x] ( 0) Print, omitting those phases undersaturated by more than 10 kcal   |
|   [ ] ( 1) Print for all phases                                               |
|-------------------------------------------------------------------------------|
|iopr(8) - Print a Table of Fugacities:                                         |
|   [ ] (-1) Don't print                                                        |
|   [x] ( 0) Print                                                              |
|-------------------------------------------------------------------------------|
|iopr(9) - Print a Table of Mean Molal Activity Coefficients:                   |
|   [ ] ( 0) Don't print                                                        |
|   [x] ( 1) Print                                                              |
|-------------------------------------------------------------------------------|
|iopr(10) - Print a Tabulation of the Pitzer Interaction Coefficients:          |
|   [x] ( 0) Don't print                                                        |
|   [ ] ( 1) Print a summary tabulation                                         |
|   [ ] ( 2) Print a more detailed tabulation                                   |
|-------------------------------------------------------------------------------|
|iopr(17) - PICKUP file format („W" or „D"):                                    |
|   [x] ( 0) Use the format of the INPUT file                                   |
|   [ ] ( 1) Use „W" format                                                     |
|   [ ] ( 2) Use „D" format                                                     |
|-------------------------------------------------------------------------------|
|Iodb Debugging Print Option Switches („( 0)" marks default choices)            |
|-------------------------------------------------------------------------------|
|iodb(1) - Print General Diagnostic Messages:                                   |
|   [x] ( 0) Don't print                                                        |
|   [ ] ( 1) Print Level 1 diagnostic messages                                  |
|   [ ] ( 2) Print Level 1 and Level 2 diagnostic messages                      |
|-------------------------------------------------------------------------------|
|iodb(2) - Kinetics Related Diagnostic Messages:                                |
|   [x] ( 0) Don't print                                                        |
|   [ ] ( 1) Print Level 1 kinetics diagnostic messages                         |
|   [ ] ( 2) Print Level 1 and Level 2 kinetics diagnostic messages             |
|-------------------------------------------------------------------------------|
|iodb(3) - Print Pre-Newton-Raphson Optimization Information:                   |
|   [x] ( 0) Don't print                                                        |
|   [ ] ( 1) Print summary information                                          |
|   [ ] ( 2) Print detailed information (including the beta and del vectors)    |
|   [ ] ( 3) Print more detailed information (including matrix equations)       |
|   [ ] ( 4) Print most detailed information (including activity coefficients)  |
|-------------------------------------------------------------------------------|
|iodb(4) - Print Newton-Raphson Iteration Information:                          |
|   [x] ( 0) Don't print                                                        |
|   [ ] ( 1) Print summary information                                          |
|   [ ] ( 2) Print detailed information (including the beta and del vectors)    |
|   [ ] ( 3) Print more detailed information (including the Jacobian)           |
|   [ ] ( 4) Print most detailed information (including activity coefficients)  |
|-------------------------------------------------------------------------------|
```

```
|iodb(5) - Print Step-Size and Order Selection:                                |
|  [x] ( 0) Don't print                                                        |
|  [ ] ( 1) Print summary information                                          |
|  [ ] ( 2) Print detailed information                                         |
|------------------------------------------------------------------------------|
|iodb(6) - Print Details of Hypothetical Affinity Calculations:                |
|  [x] ( 0) Don't print                                                        |
|  [ ] ( 1) Print summary information                                          |
|  [ ] ( 2) Print detailed information                                         |
|------------------------------------------------------------------------------|
|iodb(7) - Print General Search (e.g., for a phase boundary) Information:      |
|  [x] ( 0) Don't print                                                        |
|  [ ] ( 1) Print summary information                                          |
|------------------------------------------------------------------------------|
|iodb(8) - Print ODE Corrector Iteration Information:                          |
|  [x] ( 0) Don't print                                                        |
|  [ ] ( 1) Print summary information                                          |
|  [ ] ( 2) Print detailed information (including the betar and delvcr vectors)|
|------------------------------------------------------------------------------|
|Mineral Sub-Set Selection Suppression Options | (nxopt)                       |
|------------------------------------------------------------------------------|
|Option  |Sub-Set Defining Species| (this is a table header)                   |
|------------------------------------------------------------------------------|
|All     |                        | (uxopt(n), uxcat(n))                      |
|------------------------------------------------------------------------------|
|Exceptions to the Mineral Sub-Set Selection Suppression Options | (nxopex)    |
|------------------------------------------------------------------------------|
|Mineral                 | (this is a table header)                            |
|------------------------------------------------------------------------------|
|Calcite                 | (uxopex(n))                                         |
|------------------------------------------------------------------------------|
|Fixed Fugacity Options | (nffg)                                               |
|------------------------------------------------------------------------------|
|Gas                     |Moles to Add |Log Fugacity | --                       |
| (uffg(n))              | (moffg(n))  | (xlkffg(n)) | --                       |
|------------------------------------------------------------------------------|
|CO2(g)                  |  1.00000E+01| 0.000000E+00| --                       |
|------------------------------------------------------------------------------|
|Numerical Parameters                                                          |
|------------------------------------------------------------------------------|
|Max. finite-difference order              | 6          | (nordmx)             |
|Beta convergence tolerance                | 0.00000E+00| (tolbt)              |
|Del convergence tolerance                 | 0.00000E+00| (toldl)              |
|Max. No. of N-R iterations                | 0          | (itermx)             |
|Search/find convergence tolerance         | 0.00000E+00| (tolxsf)             |
|Saturation tolerance                      | 0.00000E+00| (tolsat)             |
|Max. No. of Phase Assemblage Tries        | 0          | (ntrymx)             |
|Zero order step size (in Xi)              | 0.00000E+00| (dlxmx0)             |
|Max. interval in Xi between PRS transfers | 0.00000E+00| (dlxdmp)             |
|------------------------------------------------------------------------------|
* Start of the bottom half of the input file                                  *
*------------------------------------------------------------------------------*
| Secondary Title        | (utitl2(n))                                         |
|------------------------------------------------------------------------------|
|EQ3NR input file name= NaCl_offen_Halit.3i                                    |
|Description= „Calcite dissolution in NaCl solution and                       |
|              precipitation of Halite possible"                              |
|Version level= 8.0                                                           |
|Revised 12/10/10    Revisor= C. Haase                                        |
|                                                                             |
|                                                                             |
|Szenario NaCl: T= 25 °C, pCO2= 1 bar                                         |
```

```
|Input für NaCl_offen_Halit.6i                                                  |
|Ca= 2.0 mmol und CO3= 4.0 mmol                                                 |
|                                                                               |
|-------------------------------------------------------------------------------|
|Special Basis Switches (for model definition only)        | (nsbswt)           |
|-------------------------------------------------------------------------------|
|Replace |None                                             | (usbsw(1,n))       |
|   with |None                                             | (usbsw(2,n))       |
|-------------------------------------------------------------------------------|
|Original temperature (C) | 2.50000E+01| (tempci)                               |
|-------------------------------------------------------------------------------|
|Original pressure (bars) | 1.01320E+00| (pressi)                               |
|-------------------------------------------------------------------------------|
|Create Ion Exchangers  | (net)                                                 |
|-------------------------------------------------------------------------------|
|Advisory: no exchanger creation blocks follow on this file.                    |
|Option: on further processing (writing a pickup file or running XCON6 on the   |
|present file), force the inclusion of at least one such block (qgexsh):        |
|  [ ] (.true.)                                                                 |
|-------------------------------------------------------------------------------|
|Alter/Suppress Options  | (nxmod)                                              |
|-------------------------------------------------------------------------------|
|Species                                          |Option          |Alter value |
| (uxmod(n))                                      |(ukxm(kxmod(n)))| (xlkmod(n))|
|-------------------------------------------------------------------------------|
|None                                             |None            | 0.00000E+00|
|-------------------------------------------------------------------------------|
|Iopg Activity Coefficient Option Switches („( 0)“ marks default choices)       |
|-------------------------------------------------------------------------------|
|iopg(1) - Aqueous Species Activity Coefficient Model:                          |
|  [ ] (-1) The Davies equation                                                 |
|  [x] ( 0) The B-dot equation                                                  |
|  [ ] ( 1) Pitzer‘s equations                                                  |
|  [ ] ( 2) HC + DH equations                                                   |
|-------------------------------------------------------------------------------|
|iopg(2) - Choice of pH Scale (Rescales Activity Coefficients):                 |
|  [ ] (-1) „Internal“ pH scale (no rescaling)                                  |
|  [x] ( 0) NBS pH scale (uses the Bates-Guggenheim equation)                   |
|  [ ] ( 1) Mesmer pH scale (numerically, pH = -log m(H+))                      |
|-------------------------------------------------------------------------------|
|Matrix Index Limits                                                            |
|-------------------------------------------------------------------------------|
|No. of chem. elements   |    6| (kct)                                         |
|No. of basis species    |    9| (kbt)                                         |
|Index of last pure min. |    9| (kmt)                                         |
|Index of last sol-sol.  |    9| (kxt)                                         |
|Matrix size             |    9| (kdim)                                        |
|PRS data flag           |    0| (kprs)                                        |
|-------------------------------------------------------------------------------|
|Mass Balance Species (Matrix Row Variables)     |Units/Constraint| --          |
| (ubmtbi(n))                                    |(ujf6(jflgi(n)))| --          |
|-------------------------------------------------------------------------------|
|H2O                    Aqueous solution         |Moles           | --          |
|Ca++                   Aqueous solution         |Moles           | --          |
|Cl-                    Aqueous solution         |Moles           | --          |
|H+                     Aqueous solution         |Moles           | --          |
|HCO3-                  Aqueous solution         |Moles           | --          |
|Na+                    Aqueous solution         |Moles           | --          |
|O2(g)                  Aqueous solution         |Moles           | --          |
|H2(aq)                 Aqueous solution         |Make non-basis  | --          |
|O2(aq)                 Aqueous solution         |Make non-basis  | --          |
|-------------------------------------------------------------------------------|
```

```
|Mass Balance Totals (moles)                                                    |
|-------------------------------------------------------------------------------|
|Basis species (info. only)      |Equilibrium System    |Aqueous Solution       |
| (ubmtbi(n))                    | (mtbi(n))            | (mtbaqi(n))           |
|-------------------------------------------------------------------------------|
|H2O                    Aqueous | 5.517738617802162E+01| 5.517738617802162E+01|
|Ca++                   Aqueous | 1.999999809499604E-03| 1.999999809499604E-03|
|Cl-                    Aqueous | 9.999999999831260E-21| 9.999999999831260E-21|
|H+                     Aqueous | 3.310203403585786E-01| 3.310203403585786E-01|
|HCO3-                  Aqueous | 5.419934995134428E-01| 5.419934995134428E-01|
|Na+                    Aqueous | 9.999999817285050E-21| 9.999999817285050E-21|
|O2(g)                  Aqueous |-1.440297992685448E-21|-1.440297992685448E-21|
|H2(aq)                 Aqueous | 6.453034550681758E-24| 6.453034550681758E-24|
|O2(aq)                 Aqueous | 1.334396514945488E-46| 1.334396514945488E-46|
|Electrical imbalance           |-2.069731595358649E-01|-2.069731595358649E-01|
|-------------------------------------------------------------------------------|
|Ordinary Basis Switches (for numerical purposes only)    | (nobswt)            |
|-------------------------------------------------------------------------------|
|Replace |None                                            | (uobsw(1,n))        |
|   with |None                                            | (uobsw(2,n))        |
|-------------------------------------------------------------------------------|
|Matrix Column Variables and Values                                             |
|-------------------------------------------------------------------------------|
|Basis species (uzveci(n))                      |Log moles (zvclgi(n)) | --     |
|-------------------------------------------------------------------------------|
|H2O                    Aqueous solution        | 1.744358983526984E+00| --     |
|Ca++                   Aqueous solution        |-2.984809808191531E+00| --     |
|Cl-                    Aqueous solution        |-2.000003513039269E+01| --     |
|H+                     Aqueous solution        |-5.946383304897180E+00| --     |
|HCO3-                  Aqueous solution        |-6.778684965107792E-01| --     |
|Na+                    Aqueous solution        |-2.007119534237021E+01| --     |
|O2(g)                  Aqueous solution        |-4.296520729295643E+01| --     |
|H2(aq)                 Aqueous solution        |-2.319023600959763E+01| --     |
|O2(aq)                 Aqueous solution        |-4.587471510095538E+01| --     |
|-------------------------------------------------------------------------------|
|Phases and Species in the PRS                                                  |
|-------------------------------------------------------------------------------|
|Phase           |None                    | (uprphi(n))                         |
|-------------------------------------------------------------------------------|
|->|No. of Moles    | 0.000000000000000E+00| (mprphi(n))                         |
|-------------------------------------------------------------------------------|
|--->|Species                |No. of Moles          | --                       |
|--->| (uprspi(i,n))         | (mprspi(i,n))        | --                       |
|-------------------------------------------------------------------------------|
|--->|None                   | 0.000000000000000E+00| --                       |
|-------------------------------------------------------------------------------|
|End of problem                                                                 |
|-------------------------------------------------------------------------------|
```

A.3.2 Calcitauflösung mit Ausfällung von Halit

A.3.2.1 Eingabedatei für EQ3, geschlossenes System, Gleichgewicht mit Halit (data0.cmp)

```
|-------------------------------------------------------------------------------|
| Title                 | (utitl(n))                                            |
|-------------------------------------------------------------------------------|
|EQ3NR input file name= NaCl_geschlossen_Halit.3i                               |
|Description= „Calcite dissolution in NaCl solution and                         |
|              precipitation of Halite possible"                                |
|Version level= 8.0                                                             |
|Revised 12/10/10    Revisor= C. Haase                                          |
|                                                                               |
|                                                                               |
```

```
|Szenario NaCl: T= 25 °C, CO2= 0.5 mol                                          |
|Input für NaCl_geschlossen_Halit.6i                                            |
|Ca= 2.0 mmol und CO3= 4.0 mmol                                                 |
|                                                                               |
|-------------------------------------------------------------------------------|
|Special Basis Switches (for model definition only)       | (nsbswt)            |
|-------------------------------------------------------------------------------|
|Replace |None                                            | (usbsw(1,n))        |
|   with |None                                            | (usbsw(2,n))        |
|-------------------------------------------------------------------------------|
|Temperature (C)         | 2.50000E+01| (tempc)                                 |
|-------------------------------------------------------------------------------|
|Pressure option (jpres3):                                                      |
|  [ ] ( 0) Data file reference curve value                                     |
|  [x] ( 1) 1.013-bar/steam-saturation curve value                              |
|  [ ] ( 2) Value (bars) | 0.00000E+00| (press)                                 |
|-------------------------------------------------------------------------------|
|Density (g/cm3)         | 1.00000E+00| (rho)                                   |
|-------------------------------------------------------------------------------|
|Total dissolved solutes option (itdsf3):                                       |
|  [x] ( 0) Value (mg/kg.sol) | 0.00000E+00| (tdspkg)                         |
|  [ ] ( 1) Value (mg/L)      | 0.00000E+00| (tdspl)                          |
|-------------------------------------------------------------------------------|
|Electrical balancing option (iebal3):                                          |
|  [x] ( 0) No balancing is done                                                |
|  [ ] ( 1) Balance on species |Cl-                    | (uebal)              |
|-------------------------------------------------------------------------------|
|Default redox constraint (irdxc3):                                             |
|  [ ] (-3) Use O2(g) line in the aqueous basis species block                   |
|  [x] (-2) pe (pe units)      | 4.00000E+00| (pei)                             |
|  [ ] (-1) Eh (volts)         | 5.00000E-01| (ehi)                             |
|  [ ] ( 0) Log fO2 (log bars) | 0.00000E+00| (fo2lgi)                          |
|  [ ] ( 1) Couple (aux. sp.)  |None                   | (uredox)             |
|-------------------------------------------------------------------------------|
|Aqueous Basis Species/Constraint Species        |Conc., etc. |Units/Constraint|
| (uspeci(n)/ucospi(n))                          | (covali(n))|(ujf3(jflgi(n)))|
|-------------------------------------------------------------------------------|
|H+                                              |7.00000E+00|pH                  |
|Ca++                                            |2.00000E-03|Molality            |
|HCO3-                                           |1.00000E-00|Hetero. equil.      |
|->|Calcite                                          | (ucospi(n))           |
|Na+                                             |1.00000E-20|Molality            |
|Cl-                                             |1.00000E-20|Molality            |
|CO2(aq)                                         |5.00000E-01|Molality            |
|-------------------------------------------------------------------------------|
|Create Ion Exchangers  | (net)                                                 |
|-------------------------------------------------------------------------------|
|Advisory: no exchanger creation blocks follow on this file.                    |
|Option: on further processing (writing a PICKUP file or running XCON3 on the   |
|present file), force the inclusion of at least one such block (qgexsh):        |
|  [ ] (.true.)                                                                 |
|-------------------------------------------------------------------------------|
|Ion Exchanger Compositions      | (neti)                                       |
|-------------------------------------------------------------------------------|
|Exchanger phase |None                    | (ugexpi(n))                         |
|-------------------------------------------------------------------------------|
|->|Moles/kg.H2O    |  0.0000    | (cgexpi(n))                                 |
|-------------------------------------------------------------------------------|
|->|Exchange site   |None    | (ugexji(j,n))                                    |
|-------------------------------------------------------------------------------|
|--->|Exchange species        |Eq. frac.   | (this is a table header)          |
|-------------------------------------------------------------------------------|
```

```
|--->|None                    | 0.00000E+00| (ugexsi(i,j,n), egexsi(i,j,n))    |
|-------------------------------------------------------------------------------|
|Solid Solution Compositions     | (nxti)                                       |
|-------------------------------------------------------------------------------|
|Solid Solution          |None                    | (usoli(n))                  |
|-------------------------------------------------------------------------------|
|->|Component               |Mole frac.  | (this is a table header)            |
|-------------------------------------------------------------------------------|
|->|None                    | 0.00000E+00| (umemi(i,n), xbari(i,n))            |
|-------------------------------------------------------------------------------|
|Alter/Suppress Options  | (nxmod)                                              |
|-------------------------------------------------------------------------------|
|Species                                          |Option          |Alter value |
| (uxmod(n))                                      |(ukxm(kxmod(n)))| (xlkmod(n))|
|-------------------------------------------------------------------------------|
|None                                             |Suppress        | 0.00000E+00|
|-------------------------------------------------------------------------------|
|Iopt Model Option Switches („( 0)" marks default choices)                      |
|-------------------------------------------------------------------------------|
|iopt(4) - Solid Solutions:                                                     |
|  [x] ( 0) Ignore                                                              |
|  [ ] ( 1) Permit                                                              |
|-------------------------------------------------------------------------------|
|iopt(11) - Auto Basis Switching in pre-N-R Optimization:                       |
|  [x] ( 0) Turn off                                                            |
|  [ ] ( 1) Turn on                                                             |
|-------------------------------------------------------------------------------|
|iopt(17) - PICKUP File Options:                                                |
|  [ ] (-1) Don't write a PICKUP file                                           |
|  [x] ( 0) Write a PICKUP file                                                 |
|-------------------------------------------------------------------------------|
|iopt(19) - Advanced EQ3NR PICKUP File Options:                                 |
|  [x] ( 0) Write a normal EQ3NR PICKUP file                                    |
|  [ ] ( 1) Write an EQ6 INPUT file with Quartz dissolving, relative rate law   |
|  [ ] ( 2) Write an EQ6 INPUT file with Albite dissolving, TST rate law        |
|  [ ] ( 3) Write an EQ6 INPUT file with Fluid 1 set up for fluid mixing        |
|-------------------------------------------------------------------------------|
|Iopg Activity Coefficient Option Switches („( 0)" marks default choices)       |
|-------------------------------------------------------------------------------|
|iopg(1) - Aqueous Species Activity Coefficient Model:                          |
|  [ ] (-1) The Davies equation                                                 |
|  [x] ( 0) The B-dot equation                                                  |
|  [ ] ( 1) Pitzer's equations                                                  |
|  [ ] ( 2) HC + DH equations                                                   |
|-------------------------------------------------------------------------------|
|iopg(2) - Choice of pH Scale (Rescales Activity Coefficients):                 |
|  [ ] (-1) „Internal" pH scale (no rescaling)                                  |
|  [x] ( 0) NBS pH scale (uses the Bates-Guggenheim equation)                   |
|  [ ] ( 1) Mesmer pH scale (numerically, pH = -log m(H+))                      |
|-------------------------------------------------------------------------------|
|Iopr Print Option Switches („( 0)" marks default choices)                      |
|-------------------------------------------------------------------------------|
|iopr(1) - Print All Species Read from the Data File:                           |
|  [x] ( 0) Don't print                                                         |
|  [ ] ( 1) Print                                                               |
|-------------------------------------------------------------------------------|
|iopr(2) - Print All Reactions:                                                 |
|  [x] ( 0) Don't print                                                         |
|  [ ] ( 1) Print the reactions                                                 |
|  [ ] ( 2) Print the reactions and log K values                                |
|  [ ] ( 3) Print the reactions, log K values, and associated data              |
|-------------------------------------------------------------------------------|
```

```
|iopr(3) - Print the Aqueous Species Hard Core Diameters:                      |
|  [x] ( 0) Don't print                                                        |
|  [ ] ( 1) Print                                                              |
|------------------------------------------------------------------------------|
|iopr(4) - Print a Table of Aqueous Species Concentrations, Activities, etc.:  |
|  [x] (-3) Omit species with molalities < 1.e-8                               |
|  [ ] (-2) Omit species with molalities < 1.e-12                              |
|  [ ] (-1) Omit species with molalities < 1.e-20                              |
|  [ ] ( 0) Omit species with molalities < 1.e-100                             |
|  [ ] ( 1) Include all species                                                |
|------------------------------------------------------------------------------|
|iopr(5) - Print a Table of Aqueous Species/H+ Activity Ratios:                |
|  [x] ( 0) Don't print                                                        |
|  [ ] ( 1) Print cation/H+ activity ratios only                               |
|  [ ] ( 2) Print cation/H+ and anion/H+ activity ratios                       |
|  [ ] ( 3) Print ion/H+ activity ratios and neutral species activities        |
|------------------------------------------------------------------------------|
|iopr(6) - Print a Table of Aqueous Mass Balance Percentages:                  |
|  [x] (-1) Don't print                                                        |
|  [ ] ( 0) Print those species comprising at least 99% of each mass balance   |
|  [ ] ( 1) Print all contributing species                                     |
|------------------------------------------------------------------------------|
|iopr(7) - Print Tables of Saturation Indices and Affinities:                  |
|  [ ] (-1) Don't print                                                        |
|  [x] ( 0) Print, omitting those phases undersaturated by more than 10 kcal   |
|  [ ] ( 1) Print for all phases                                               |
|------------------------------------------------------------------------------|
|iopr(8) - Print a Table of Fugacities:                                        |
|  [ ] (-1) Don't print                                                        |
|  [x] ( 0) Print                                                              |
|------------------------------------------------------------------------------|
|iopr(9) - Print a Table of Mean Molal Activity Coefficients:                  |
|  [x] ( 0) Don't print                                                        |
|  [ ] ( 1) Print                                                              |
|------------------------------------------------------------------------------|
|iopr(10) - Print a Tabulation of the Pitzer Interaction Coefficients:         |
|  [x] ( 0) Don't print                                                        |
|  [ ] ( 1) Print a summary tabulation                                         |
|  [ ] ( 2) Print a more detailed tabulation                                   |
|------------------------------------------------------------------------------|
|iopr(17) - PICKUP file format („W" or „D"):                                   |
|  [x] ( 0) Use the format of the INPUT file                                   |
|  [ ] ( 1) Use „W" format                                                     |
|  [ ] ( 2) Use „D" format                                                     |
|------------------------------------------------------------------------------|
|Iodb Debugging Print Option Switches („( 0)" marks default choices)           |
|------------------------------------------------------------------------------|
|iodb(1) - Print General Diagnostic Messages:                                  |
|  [x] ( 0) Don't print                                                        |
|  [ ] ( 1) Print Level 1 diagnostic messages                                  |
|  [ ] ( 2) Print Level 1 and Level 2 diagnostic messages                      |
|------------------------------------------------------------------------------|
|iodb(3) - Print Pre-Newton-Raphson Optimization Information:                  |
|  [x] ( 0) Don't print                                                        |
|  [ ] ( 1) Print summary information                                          |
|  [ ] ( 2) Print detailed information (including the beta and del vectors)    |
|  [ ] ( 3) Print more detailed information (including matrix equations)       |
|  [ ] ( 4) Print most detailed information (including activity coefficients)  |
|------------------------------------------------------------------------------|
|iodb(4) - Print Newton-Raphson Iteration Information:                         |
|  [x] ( 0) Don't print                                                        |
|  [ ] ( 1) Print summary information                                          |
```

```
|  [ ] ( 2) Print detailed information (including the beta and del vectors)    |
|  [ ] ( 3) Print more detailed information (including the Jacobian)           |
|  [ ] ( 4) Print most detailed information (including activity coefficients)  |
|------------------------------------------------------------------------------|
|iodb(6) - Print Details of Hypothetical Affinity Calculations:                |
|  [x] ( 0) Don't print                                                        |
|  [ ] ( 1) Print summary information                                          |
|  [ ] ( 2) Print detailed information                                         |
|------------------------------------------------------------------------------|
|Numerical Parameters                                                          |
|------------------------------------------------------------------------------|
| Beta convergence tolerance      | 0.00000E+00| (tolbt)                       |
| Del convergence tolerance       | 0.00000E+00| (toldl)                       |
| Max. Number of N-R Iterations   |   0        | (itermx)                      |
|------------------------------------------------------------------------------|
|Ordinary Basis Switches (for numerical purposes only)    | (nobswt)           |
|------------------------------------------------------------------------------|
|Replace |None                                              | (uobsw(1,n))       |
|   with |None                                              | (uobsw(2,n))       |
|------------------------------------------------------------------------------|
|Sat. flag tolerance     | 0.00000E+00| (tolspf)                               |
|------------------------------------------------------------------------------|
|Aq. Phase Scale Factor  | 1.00000E+00| (scamas)                               |
|------------------------------------------------------------------------------|
|End of problem                                                                |
|------------------------------------------------------------------------------|
```

A.3.2.2 Eingabedatei für EQ6, geschlossenes System, Gleichgewicht mit Halit (data0.cmp)

```
|------------------------------------------------------------------------------|
| Main Title             | (utitl1(n))                                         |
|------------------------------------------------------------------------------|
|EQ6 input file name= NaCl_geschlossen_Halit.6i                                |
|Description= „Calcite dissolution in NaCl solution                            |
|                and precipitation of Halite possible"                         |
|Version level= 8.0                                                            |
|Revised 12/10/2010    Revisor= C.Haase                                        |
|                                                                              |
|Szenario NaCl: T= 25°C, CO2= 0.5 mol                                          |
|                                                                              |
|Database data0.cmp                                                            |
|                                                                              |
|------------------------------------------------------------------------------|
|Temperature option (jtemp):                                                   |
|  [x] ( 0) Constant temperature:                                              |
|             Value (C)          | 2.50000E+01| (tempcb)                       |
|  [ ] ( 1) Linear tracking in Xi:                                             |
|             Base Value (C)     | 0.00000E+00| (tempcb)                       |
|             Derivative         | 0.00000E+00| (ttk(1))                       |
|  [ ] ( 2) Linear tracking in time:                                           |
|             Base Value (C)     | 0.00000E+00| (tempcb)                       |
|             Derivative         | 0.00000E+00| (ttk(1))                       |
|  [ ] ( 3) Fluid mixing tracking (fluid 2 = special reactant):                |
|             T of fluid 1 (C)   | 0.00000E+00| (tempcb)                       |
|             T of fluid 2 (C)   | 0.00000E+00| (ttk(2))                       |
|             Mass ratio factor | 0.00000E+00| (ttk(1))                       |
|------------------------------------------------------------------------------|
|Pressure option (jpress):                                                     |
|  [ ] ( 0) Follow the data file reference pressure curve                      |
|  [x] ( 1) Follow the 1.013-bar/steam-saturation curve                        |
|  [ ] ( 2) Constant pressure:                                                 |
|             Value (bars)       | 0.00000E+00| (pressb)                       |
|  [ ] ( 3) Linear tracking in Xi:                                             |
```

```
|             Base Value (bars) | 0.00000E+00| (pressb)                        |
|             Derivative        | 0.00000E+00| (ptk(1))                        |
|  [ ] ( 4) Linear tracking in time:                                            |
|             Base Value (bars) | 0.00000E+00| (pressb)                        |
|             Derivative        | 0.00000E+00| (ptk(1))                        |
|-------------------------------------------------------------------------------|
|Reactants (Irreversible Reactions) | (nrct)                                    |
|-------------------------------------------------------------------------------|
|Reactant        |Calcite                | (ureac(n))                           |
|-------------------------------------------------------------------------------|
|->|Type         |Pure mineral           | (urcjco(jcode(n)))                   |
|-------------------------------------------------------------------------------|
|->|Status       |Saturated, reacting    | (urcjre(jreac(n)))                   |
|-------------------------------------------------------------------------------|
|->|Amount remaining (moles) | 1.00000E+01| (morr(n))                        |
|-------------------------------------------------------------------------------|
|->|Amount destroyed (moles) | 0.00000E+00| (modr(n))                        |
|-------------------------------------------------------------------------------|
|->|Surface area option (nsk(n)):                                               |
|->|  [x] ( 0) Constant surface area:                                           |
|->|             Value (cm2)       | 1.00000E+01| (sfcar(n))                   |
|->|  [ ] ( 1) Constant specific surface area:                                  |
|->|             Value (cm2/g)     | 0.00000E+00| (ssfcar(n))                  |
|->|  [ ] ( 2) n**2/3 growth law- current surface area:                         |
|->|             Value (cm2)       | 0.00000E+00| (sfcar(n))                   |
|-------------------------------------------------------------------------------|
|->|Surface area factor      | 1.00000E+01| (fkrc(n))                        |
|-------------------------------------------------------------------------------|
|->|Forward rate law          |Relative rate equation  | (urcnrk(nrk(1,n)))   |
|-------------------------------------------------------------------------------|
|--->|dXi(n)/dXi (mol/mol)      | 1.00000E+00| (rkb(1,1,n))                    |
|-------------------------------------------------------------------------------|
|--->|d2Xi(n)/dXi2 (mol/mol2)   | 0.00000E+00| (rkb(2,1,n))                    |
|-------------------------------------------------------------------------------|
|--->|d3Xi(n)/dXi3 (mol/mol3)   | 0.00000E+00| (rkb(3,1,n))                    |
|-------------------------------------------------------------------------------|
|->|Backward rate law         |Partial equilibrium     | (urcnrk(nrk(2,n)))   |
|-------------------------------------------------------------------------------|
|Reactant        |Halite                 | (ureac(n))                           |
|-------------------------------------------------------------------------------|
|->|Type         |Pure mineral           | (urcjco(jcode(n)))                   |
|-------------------------------------------------------------------------------|
|->|Status       |Saturated, reacting    | (urcjre(jreac(n)))                   |
|-------------------------------------------------------------------------------|
|->|Amount remaining (moles) | 0.00000E+00| (morr(n))                        |
|-------------------------------------------------------------------------------|
|->|Amount destroyed (moles) | 0.00000E+00| (modr(n))                        |
|-------------------------------------------------------------------------------|
|->|Surface area option (nsk(n)):                                               |
|->|  [x] ( 0) Constant surface area:                                           |
|->|             Value (cm2)       | 1.00000E+01| (sfcar(n))                   |
|->|  [ ] ( 1) Constant specific surface area:                                  |
|->|             Value (cm2/g)     | 0.00000E+00| (ssfcar(n))                  |
|->|  [ ] ( 2) n**2/3 growth law- current surface area:                         |
|->|             Value (cm2)       | 0.00000E+00| (sfcar(n))                   |
|-------------------------------------------------------------------------------|
|->|Surface area factor      | 1.00000E+01| (fkrc(n))                        |
|-------------------------------------------------------------------------------|
|->|Forward rate law          |Relative rate equation  | (urcnrk(nrk(1,n)))   |
|-------------------------------------------------------------------------------|
|--->|dXi(n)/dXi (mol/mol)      | 1.00000E+00| (rkb(1,1,n))                    |
|-------------------------------------------------------------------------------|
```

```
|--->|d2Xi(n)/dXi2 (mol/mol2)   | 0.00000E+00| (rkb(2,1,n))                    |
|-------------------------------------------------------------------------------|
|--->|d3Xi(n)/dXi3 (mol/mol3)   | 0.00000E+00| (rkb(3,1,n))                    |
|-------------------------------------------------------------------------------|
|->|Backward rate law         |Partial equilibrium     | (urcnrk(nrk(2,n)))    |
|-------------------------------------------------------------------------------|
|Reactant        |NaCl                    | (ureac(n))                          |
|-------------------------------------------------------------------------------|
|->|Type         |Special reactant        | (urcjco(jcode(n)))                  |
|-------------------------------------------------------------------------------|
|->|Status       |Reacting                | (urcjre(jreac(n)))                  |
|-------------------------------------------------------------------------------|
|->|Amount remaining (moles) | 4.00000E+00| (morr(n))                        |
|-------------------------------------------------------------------------------|
|->|Amount destroyed (moles) | 0.00000E+00| (modr(n))                        |
|-------------------------------------------------------------------------------|
|->|Molar volume (cm3/mol)   | 0.00000E+00| (vreac(n))                       |
|-------------------------------------------------------------------------------|
|->|Composition                                                                 |
|-------------------------------------------------------------------------------|
|--->|Element |Stoich. Number        | (this is a table header)                |
|-------------------------------------------------------------------------------|
|--->|Na      | 1.0000000000000000+00| (uesri(i,n), cesri(i,n))                |
|--->|Cl      | 1.0000000000000000+00| (uesri(i,n), cesri(i,n))                |
|-------------------------------------------------------------------------------|
|->|Reaction                                                                    |
|-------------------------------------------------------------------------------|
|--->|Species                |Reaction Coefficient  | (this is a table header)|
|-------------------------------------------------------------------------------|
|--->|NaCl                   |-1.000000000000000E+00| (ubsri(i,n), cbsri(i,n))|
|--->|Na+                    | 4.000000000000000E+00| (ubsri(i,n), cbsri(i,n))|
|--->|Cl-                    | 4.000000000000000E+00| (ubsri(i,n), cbsri(i,n))|
|-------------------------------------------------------------------------------|
|->|Surface area option (nsk(n)):                                              |
|->|  [x] ( 0) Constant surface area:                                          |
|->|             Value (cm2)       | 1.00000E+01| (sfcar(n))                 |
|->|  [ ] ( 1) Constant specific surface area:                                 |
|->|             Value (cm2/g)     | 0.00000E+00| (ssfcar(n))                |
|->|  [ ] ( 2) n**2/3 growth law- current surface area:                        |
|->|             Value (cm2)       | 0.00000E+00| (sfcar(n))                 |
|-------------------------------------------------------------------------------|
|->|Surface area factor      | 1.00000E+00| (fkrc(n))                        |
|-------------------------------------------------------------------------------|
|->|Forward rate law           |Relative rate equation | (urcnrk(nrk(1,n)))  |
|-------------------------------------------------------------------------------|
|--->|dXi(n)/dXi (mol/mol)      | 1.00000E+00| (rkb(1,1,n))                    |
|-------------------------------------------------------------------------------|
|--->|d2Xi(n)/dXi2 (mol/mol2)   | 0.00000E-00| (rkb(2,1,n))                    |
|-------------------------------------------------------------------------------|
|--->|d3Xi(n)/dXi3 (mol/mol3)   | 0.00000E-00| (rkb(3,1,n))                    |
|-------------------------------------------------------------------------------|
|->|Backward rate law         |Partial equilibrium     | (urcnrk(nrk(2,n)))    |
|-------------------------------------------------------------------------------|
|Starting, minimum, and maximum values of key run parameters.                   |
|-------------------------------------------------------------------------------|
|Starting Xi value        | 1.00000E-01| (xistti)                               |
|-------------------------------------------------------------------------------|
|Maximum Xi value         | 1.10000E+00| (ximaxi)                               |
|-------------------------------------------------------------------------------|
|Starting time (seconds)  | 0.00000E+00| (tistti)                               |
|-------------------------------------------------------------------------------|
|Maximum time (seconds)   | 1.00000E+38| (timmxi)                               |
```

Minimum value of pH	1.00000E-00	(phmini)
Maximum value of pH	1.00000E+10	(phmaxi)
Minimum value of Eh (v)	-1.00000E+38	(ehmini)
Maximum value of Eh (v)	1.00000E+38	(ehmaxi)
Minimum value of log fO2	-1.00000E+38	(o2mini)
Maximum value of log fO2	1.00000E+38	(o2maxi)
Minimum value of aw	-1.00000E+38	(awmini)
Maximum value of aw	1.00000E+38	(awmaxi)
Maximum number of steps	400	(kstpmx)
Print interval parameters.		
Xi print interval	2.00000E-02	(dlxprn)
Log Xi print interval	5.00000E-01	(dlxprl)
Time print interval	1.00000E+38	(dltprn)
Log time print interval	1.00000E+38	(dltprl)
pH print interval	1.00000E+38	(dlhprn)
Eh (v) print interval	1.00000E+38	(dleprn)
Log fO2 print interval	1.00000E+38	(dloprn)
aw print interval	1.00000E+38	(dlaprn)
Steps print interval	0.1	(ksppmx)
Plot interval parameters.		
Xi plot interval	2.00000E-01	(dlxplo)
Log Xi plot interval	2.00000E-01	(dlxpll)
Time plot interval	1.00000E+38	(dltplo)
Log time plot interval	1.00000E+38	(dltpll)
pH plot interval	2.00000E-01	(dlhplo)
Eh (v) plot interval	2.00000E-01	(dleplo)
Log fO2 plot interval	1.00000E+38	(dloplo)
aw plot interval	2.00000E-01	(dlaplo)
Steps plot interval	100	(ksplmx)
Iopt Model Option Switches („(0)“ marks default choices)		
iopt(1) - Physical System Model Selection:		

```
|   [x] ( 0) Closed system                                                      |
|   [ ] ( 1) Titration system                                                   |
|   [ ] ( 2) Fluid-centered flow-through open system                            |
|-------------------------------------------------------------------------------|
|iopt(2) - Kinetic Mode Selection:                                              |
|   [x] ( 0) Reaction progress mode (arbitrary kinetics)                        |
|   [ ] ( 1) Reaction progress/time mode (true kinetics)                        |
|-------------------------------------------------------------------------------|
|iopt(3) - Phase Boundary Searches:                                             |
|   [x] ( 0) Search for phase boundaries and constrain the step size to match   |
|   [ ] ( 1) Search for phase boundaries and print their locations              |
|   [ ] ( 2) Don't search for phase boundaries                                  |
|-------------------------------------------------------------------------------|
|iopt(4) - Solid Solutions:                                                     |
|   [x] ( 0) Ignore                                                             |
|   [ ] ( 1) Permit                                                             |
|-------------------------------------------------------------------------------|
|iopt(5) - Clear the ES Solids Read from the INPUT File:                        |
|   [x] ( 0) Don't do it                                                        |
|   [ ] ( 1) Do it                                                              |
|-------------------------------------------------------------------------------|
|iopt(6) - Clear the ES Solids at the Initial Value of Reaction Progress:       |
|   [x] ( 0) Don't do it                                                        |
|   [ ] ( 1) Do it                                                              |
|-------------------------------------------------------------------------------|
|iopt(7) - Clear the ES Solids at the End of the Run:                           |
|   [x] ( 0) Don't do it                                                        |
|   [ ] ( 1) Do it                                                              |
|-------------------------------------------------------------------------------|
|iopt(9) - Clear the PRS Solids Read from the INPUT file:                       |
|   [x] ( 0) Don't do it                                                        |
|   [ ] ( 1) Do it                                                              |
|-------------------------------------------------------------------------------|
|iopt(10) - Clear the PRS Solids at the End of the Run:                         |
|   [x] ( 0) Don't do it                                                        |
|   [ ] ( 1) Do it, unless numerical problems cause early termination           |
|-------------------------------------------------------------------------------|
|iopt(11) - Auto Basis Switching in pre-N-R Optimization:                       |
|   [x] ( 0) Turn off                                                           |
|   [ ] ( 1) Turn on                                                            |
|-------------------------------------------------------------------------------|
|iopt(12) - Auto Basis Switching after Newton-Raphson Iteration:                |
|   [x] ( 0) Turn off                                                           |
|   [ ] ( 1) Turn on                                                            |
|-------------------------------------------------------------------------------|
|iopt(13) - Calculational Mode Selection:                                       |
|   [x] ( 0) Normal path tracing                                                |
|   [ ] ( 1) Economy mode (if permissible)                                      |
|   [ ] ( 2) Super economy mode (if permissible)                                |
|-------------------------------------------------------------------------------|
|iopt(14) - ODE Integrator Corrector Mode Selection:                            |
|   [x] ( 0) Allow Stiff and Simple Correctors                                  |
|   [ ] ( 1) Allow Only the Simple Corrector                                    |
|   [ ] ( 2) Allow Only the Stiff Corrector                                     |
|   [ ] ( 3) Allow No Correctors                                                |
|-------------------------------------------------------------------------------|
|iopt(15) - Force the Suppression of All Redox Reactions:                       |
|   [x] ( 0) Don't do it                                                        |
|   [ ] ( 1) Do it                                                              |
|-------------------------------------------------------------------------------|
|iopt(16) - BACKUP File Options:                                                |
|   [ ] (-1) Don't write a BACKUP file                                          |
```

```
|   [x] ( 0) Write BACKUP files                                                |
|   [ ] ( 1) Write a sequential BACKUP file                                    |
|------------------------------------------------------------------------------|
|iopt(17) - PICKUP File Options:                                               |
|   [ ] (-1) Don't write a PICKUP file                                         |
|   [x] ( 0) Write a PICKUP file                                               |
|------------------------------------------------------------------------------|
|iopt(18) - TAB File Options:                                                  |
|   [ ] (-1) Don't write a TAB file                                            |
|   [x] ( 0) Write a TAB file                                                  |
|   [ ] ( 1) Write a TAB file, prepending TABX file data from a previous run   |
|------------------------------------------------------------------------------|
|iopt(20) - Advanced EQ6 PICKUP File Options:                                  |
|   [x] ( 0) Write a normal EQ6 PICKUP file                                    |
|   [ ] ( 1) Write an EQ6 INPUT file with Fluid 1 set up for fluid mixing      |
|------------------------------------------------------------------------------|
|Iopr Print Option Switches („( 0)" marks default choices)                     |
|------------------------------------------------------------------------------|
|iopr(1) - Print All Species Read from the Data File:                          |
|   [x] ( 0) Don't print                                                       |
|   [ ] ( 1) Print                                                             |
|------------------------------------------------------------------------------|
|iopr(2) - Print All Reactions:                                                |
|   [x] ( 0) Don't print                                                       |
|   [ ] ( 1) Print the reactions                                               |
|   [ ] ( 2) Print the reactions and log K values                              |
|   [ ] ( 3) Print the reactions, log K values, and associated data            |
|------------------------------------------------------------------------------|
|iopr(3) - Print the Aqueous Species Hard Core Diameters:                      |
|   [x] ( 0) Don't print                                                       |
|   [ ] ( 1) Print                                                             |
|------------------------------------------------------------------------------|
|iopr(4) - Print a Table of Aqueous Species Concentrations, Activities, etc.:  |
|   [ ] (-3) Omit species with molalities < 1.e-8                              |
|   [ ] (-2) Omit species with molalities < 1.e-12                             |
|   [ ] (-1) Omit species with molalities < 1.e-20                             |
|   [x] ( 0) Omit species with molalities < 1.e-100                            |
|   [ ] ( 1) Include all species                                               |
|------------------------------------------------------------------------------|
|iopr(5) - Print a Table of Aqueous Species/H+ Activity Ratios:                |
|   [x] ( 0) Don't print                                                       |
|   [ ] ( 1) Print cation/H+ activity ratios only                              |
|   [ ] ( 2) Print cation/H+ and anion/H+ activity ratios                      |
|   [ ] ( 3) Print ion/H+ activity ratios and neutral species activities       |
|------------------------------------------------------------------------------|
|iopr(6) - Print a Table of Aqueous Mass Balance Percentages:                  |
|   [ ] (-1) Don't print                                                       |
|   [x] ( 0) Print those species comprising at least 99% of each mass balance  |
|   [ ] ( 1) Print all contributing species                                    |
|------------------------------------------------------------------------------|
|iopr(7) - Print Tables of Saturation Indices and Affinities:                  |
|   [ ] (-1) Don't print                                                       |
|   [x] ( 0) Print, omitting those phases undersaturated by more than 10 kcal  |
|   [ ] ( 1) Print for all phases                                              |
|------------------------------------------------------------------------------|
|iopr(8) - Print a Table of Fugacities:                                        |
|   [ ] (-1) Don't print                                                       |
|   [x] ( 0) Print                                                             |
|------------------------------------------------------------------------------|
|iopr(9) - Print a Table of Mean Molal Activity Coefficients:                  |
|   [ ] ( 0) Don't print                                                       |
|   [x] ( 1) Print                                                             |
```

```
|-------------------------------------------------------------------------------|
|iopr(10) - Print a Tabulation of the Pitzer Interaction Coefficients:          |
|   [x] ( 0) Don't print                                                        |
|   [ ] ( 1) Print a summary tabulation                                         |
|   [ ] ( 2) Print a more detailed tabulation                                   |
|-------------------------------------------------------------------------------|
|iopr(17) - PICKUP file format („W" or „D"):                                    |
|   [x] ( 0) Use the format of the INPUT file                                   |
|   [ ] ( 1) Use „W" format                                                     |
|   [ ] ( 2) Use „D" format                                                     |
|-------------------------------------------------------------------------------|
|Iodb Debugging Print Option Switches („( 0)" marks default choices)            |
|-------------------------------------------------------------------------------|
|iodb(1) - Print General Diagnostic Messages:                                   |
|   [x] ( 0) Don't print                                                        |
|   [ ] ( 1) Print Level 1 diagnostic messages                                  |
|   [ ] ( 2) Print Level 1 and Level 2 diagnostic messages                      |
|-------------------------------------------------------------------------------|
|iodb(2) - Kinetics Related Diagnostic Messages:                                |
|   [x] ( 0) Don't print                                                        |
|   [ ] ( 1) Print Level 1 kinetics diagnostic messages                         |
|   [ ] ( 2) Print Level 1 and Level 2 kinetics diagnostic messages             |
|-------------------------------------------------------------------------------|
|iodb(3) - Print Pre-Newton-Raphson Optimization Information:                   |
|   [x] ( 0) Don't print                                                        |
|   [ ] ( 1) Print summary information                                          |
|   [ ] ( 2) Print detailed information (including the beta and del vectors)    |
|   [ ] ( 3) Print more detailed information (including matrix equations)       |
|   [ ] ( 4) Print most detailed information (including activity coefficients)  |
|-------------------------------------------------------------------------------|
|iodb(4) - Print Newton-Raphson Iteration Information:                          |
|   [x] ( 0) Don't print                                                        |
|   [ ] ( 1) Print summary information                                          |
|   [ ] ( 2) Print detailed information (including the beta and del vectors)    |
|   [ ] ( 3) Print more detailed information (including the Jacobian)           |
|   [ ] ( 4) Print most detailed information (including activity coefficients)  |
|-------------------------------------------------------------------------------|
|iodb(5) - Print Step-Size and Order Selection:                                 |
|   [x] ( 0) Don't print                                                        |
|   [ ] ( 1) Print summary information                                          |
|   [ ] ( 2) Print detailed information                                         |
|-------------------------------------------------------------------------------|
|iodb(6) - Print Details of Hypothetical Affinity Calculations:                 |
|   [x] ( 0) Don't print                                                        |
|   [ ] ( 1) Print summary information                                          |
|   [ ] ( 2) Print detailed information                                         |
|-------------------------------------------------------------------------------|
|iodb(7) - Print General Search (e.g., for a phase boundary) Information:       |
|   [x] ( 0) Don't print                                                        |
|   [ ] ( 1) Print summary information                                          |
|-------------------------------------------------------------------------------|
|iodb(8) - Print ODE Corrector Iteration Information:                           |
|   [x] ( 0) Don't print                                                        |
|   [ ] ( 1) Print summary information                                          |
|   [ ] ( 2) Print detailed information (including the betar and delvcr vectors)|
|-------------------------------------------------------------------------------|
|Mineral Sub-Set Selection Suppression Options | (nxopt)                        |
|-------------------------------------------------------------------------------|
|Option  |Sub-Set Defining Species| (this is a table header)                    |
|-------------------------------------------------------------------------------|
|All     |                        | (uxopt(n), uxcat(n))                       |
|-------------------------------------------------------------------------------|
```

```
|Exceptions to the Mineral Sub-Set Selection Suppression Options | (nxopex)    |
|-----------------------------------------------------------------------------|
|Mineral                | (this is a table header)                            |
|-----------------------------------------------------------------------------|
|Calcite                | (uxopex(n))                                         |
|-----------------------------------------------------------------------------|
|Fixed Fugacity Options | (nffg)                                              |
|-----------------------------------------------------------------------------|
|Gas                    |Moles to Add |Log Fugacity | --                      |
| (uffg(n))             | (moffg(n))  | (xlkffg(n)) | --                      |
|-----------------------------------------------------------------------------|
|None                   |  1.00000E+01| 0.000000E+00| --                      |
|-----------------------------------------------------------------------------|
|Numerical Parameters                                                         |
|-----------------------------------------------------------------------------|
|Max. finite-difference order               |   6        | (nordmx)           |
|Beta convergence tolerance                 | 0.00000E+00| (tolbt)            |
|Del convergence tolerance                  | 0.00000E+00| (toldl)            |
|Max. No. of N-R iterations                 |   0        | (itermx)           |
|Search/find convergence tolerance          | 0.00000E+00| (tolxsf)           |
|Saturation tolerance                       | 0.00000E+00| (tolsat)           |
|Max. No. of Phase Assemblage Tries         |   0        | (ntrymx)           |
|Zero order step size (in Xi)               | 0.00000E+00| (dlxmx0)           |
|Max. interval in Xi between PRS transfers  | 0.00000E+00| (dlxdmp)           |
|-----------------------------------------------------------------------------|
* Start of the bottom half of the input file                                  *
*-----------------------------------------------------------------------------*
| Secondary Title       | (utitl2(n))                                         |
|-----------------------------------------------------------------------------|
|EQ3NR input file name= NaCl_geschlossen_Halit.3i                             |
|Description= „Calcite dissolution in NaCl solution and                       |
|              precipitation of Halite possible“                              |
|Version level= 8.0                                                           |
|Revised 12/10/10    Revisor= C. Haase                                        |
|                                                                             |
|                                                                             |
|Szenario NaCl: T= 25 °C, CO2= 0.5 mol                                        |
|Input für NaCl_geschlossen_Halit.6i                                          |
|Ca= 2.0 mmol und CO3= 4.0 mmol                                               |
|                                                                             |
|-----------------------------------------------------------------------------|
|Special Basis Switches (for model definition only)       | (nsbswt)          |
|-----------------------------------------------------------------------------|
|Replace |None                                            | (usbsw(1,n))      |
|   with |None                                            | (usbsw(2,n))      |
|-----------------------------------------------------------------------------|
|Original temperature (C) | 2.50000E+01| (tempci)                             |
|-----------------------------------------------------------------------------|
|Original pressure (bars) | 1.01320E+00| (pressi)                             |
|-----------------------------------------------------------------------------|
|Create Ion Exchangers  | (net)                                               |
|-----------------------------------------------------------------------------|
|Advisory: no exchanger creation blocks follow on this file.                  |
|Option: on further processing (writing a pickup file or running XCON6 on the |
|present file), force the inclusion of at least one such block (qgexsh):      |
|  [ ] (.true.)                                                               |
|-----------------------------------------------------------------------------|
|Alter/Suppress Options  | (nxmod)                                            |
|-----------------------------------------------------------------------------|
|Species                                    |Option          |Alter value |
| (uxmod(n))                                |(ukxm(kxmod(n)))| (xlkmod(n))|
|-----------------------------------------------------------------------------|
```

```
|None                                                |None           | 0.00000E+00|
|----------------------------------------------------------------------------------|
|Iopg Activity Coefficient Option Switches („( 0)" marks default choices)          |
|----------------------------------------------------------------------------------|
|iopg(1) - Aqueous Species Activity Coefficient Model:                             |
|  [ ] (-1) The Davies equation                                                    |
|  [x] ( 0) The B-dot equation                                                     |
|  [ ] ( 1) Pitzer's equations                                                     |
|  [ ] ( 2) HC + DH equations                                                      |
|----------------------------------------------------------------------------------|
|iopg(2) - Choice of pH Scale (Rescales Activity Coefficients):                    |
|  [ ] (-1) „Internal" pH scale (no rescaling)                                     |
|  [x] ( 0) NBS pH scale (uses the Bates-Guggenheim equation)                      |
|  [ ] ( 1) Mesmer pH scale (numerically, pH = -log m(H+))                         |
|----------------------------------------------------------------------------------|
|Matrix Index Limits                                                               |
|----------------------------------------------------------------------------------|
|No. of chem. elements   |    6| (kct)                                            |
|No. of basis species    |   10| (kbt)                                            |
|Index of last pure min. |   10| (kmt)                                            |
|Index of last sol-sol.  |   10| (kxt)                                            |
|Matrix size             |   10| (kdim)                                           |
|PRS data flag           |    0| (kprs)                                           |
|----------------------------------------------------------------------------------|
|Mass Balance Species (Matrix Row Variables)     |Units/Constraint| --           |
| (ubmtbi(n))                                    |(ujf6(jflgi(n)))| --           |
|----------------------------------------------------------------------------------|
|H2O                    Aqueous solution         |Moles           | --           |
|Ca++                   Aqueous solution         |Moles           | --           |
|Cl-                    Aqueous solution         |Moles           | --           |
|H+                     Aqueous solution         |Moles           | --           |
|HCO3-                  Aqueous solution         |Moles           | --           |
|Na+                    Aqueous solution         |Moles           | --           |
|O2(g)                  Aqueous solution         |Moles           | --           |
|H2(aq)                 Aqueous solution         |Make non-basis  | --           |
|O2(aq)                 Aqueous solution         |Make non-basis  | --           |
|CO2(aq)                Aqueous solution         |Make non-basis  | --           |
|----------------------------------------------------------------------------------|
|Mass Balance Totals (moles)                                                       |
|----------------------------------------------------------------------------------|
|Basis species (info. only)      |Equilibrium System    |Aqueous Solution          |
| (ubmtbi(n))                    | (mtbi(n))            | (mtbaqi(n))              |
|----------------------------------------------------------------------------------|
|H2O                    Aqueous | 5.550843517294234E+01| 5.550843517294234E+01|
|Ca++                   Aqueous | 2.000000004567650E-03| 2.000000004567650E-03|
|Cl-                    Aqueous | 1.000000000013663E-20| 1.000000000013663E-20|
|H+                     Aqueous |-1.043859538452722E-05|-1.043859538452722E-05|
|HCO3-                  Aqueous | 5.728535851048820E-03| 5.728535851048820E-03|
|Na+                    Aqueous | 1.000000000178489E-20| 1.000000000178489E-20|
|O2(g)                  Aqueous |-4.636168198045946E-25|-4.636168198045946E-25|
|H2(aq)                 Aqueous | 7.838717489141694E-26| 7.838717489141694E-26|
|O2(aq)                 Aqueous | 9.730995588502664E-43| 9.730995588502664E-43|
|CO2(aq)                Aqueous | 5.000000000000000E-01| 5.000000000000000E-01|
|Electrical imbalance           |-1.738974437298047E-03|-1.738974437298047E-03|
|----------------------------------------------------------------------------------|
|Ordinary Basis Switches (for numerical purposes only)    | (nobswt)            |
|----------------------------------------------------------------------------------|
|Replace |None                                           | (uobsw(1,n))        |
|   with |None                                           | (uobsw(2,n))        |
|----------------------------------------------------------------------------------|
|Matrix Column Variables and Values                                                |
|----------------------------------------------------------------------------------|
```

```
|Basis species (uzveci(n))                      |Log moles (zvclgi(n)) | --   |
|-----------------------------------------------------------------------------|
|H2O                     Aqueous solution       | 1.744358983526984E+00| --   |
|Ca++                    Aqueous solution       |-2.719636084494143E+00| --   |
|Cl-                     Aqueous solution       |-2.000011964066534E+01| --   |
|H+                      Aqueous solution       |-6.965444153944126E+00| --   |
|HCO3-                   Aqueous solution       |-2.249322626609868E+00| --   |
|Na+                     Aqueous solution       |-2.000292867438012E+01| --   |
|O2(g)                   Aqueous solution       |-3.911283773692741E+01| --   |
|H2(aq)                  Aqueous solution       |-2.510575498743690E+01| --   |
|O2(aq)                  Aqueous solution       |-4.201184272432840E+01| --   |
|CO2(aq)                 Aqueous solution       |-3.010299956639812E-01| --   |
|-----------------------------------------------------------------------------|
|Phases and Species in the PRS                                                |
|-----------------------------------------------------------------------------|
|Phase          |None                  | (uprphi(n))                          |
|-----------------------------------------------------------------------------|
|->|No. of Moles    | 0.000000000000000E+00| (mprphi(n))                          |
|-----------------------------------------------------------------------------|
|--->|Species                |No. of Moles          | --                      |
|--->| (uprspi(i,n))         | (mprspi(i,n))        | --                      |
|-----------------------------------------------------------------------------|
|--->|None                   | 0.000000000000000E+00| --                      |
|-----------------------------------------------------------------------------|
|End of problem                                                               |
|-----------------------------------------------------------------------------|
```

Anhang B

Anhang B

Eingabedateien für PhreeqC und The Geochemist's Workbench zu Kapitel 5 (»Uncertainties of geochemical codes and thermodynamic databases for predicting geochemical impact of carbon dioxide on geologic formations«).

B.1 Eingabedateien für PhreeqC

B.1.1 Quaternary formation water

```
# Input files for PhreeqC are identical with the exception that the database is selected by
the following commands
DATABASE C:\phreeqc\database\phreeqc.dat
#DATABASE C:\phreeqc\database\wateq4f.dat
#DATABASE C:\phreeqc\databse\llnl.dat
#DATABASE C:\phreeqc\database\minteq.dat

TITLE 1-d model scenario for calculating anorthite dissolution time using the Quaternary
formation water

SELECTED_OUTPUT                         # User defined output file
-file C:\Buntsandstein\Output.xls
-saturation_indices Anorthite
-kinetic_reactants  Anorthite


RATES                                   # Rate law for anorthite dissolution
Anorthite
  -start
10  R = 8.314472
11  deltaT = 1/TK - 1/298.15
12  e = 2.7183
rem acidic mechanism
13  Ea = 16600
14  logK25 = -3.5
15  ny = 1.411
16  mech_a = (10^logK25) * (e^(-Ea/R*deltaT)) * (ACT("H+"))^ny
rem neutral mechanism
23  Ea = 17800
24  logK25 = -9.12
26  mech_b = (10^logK25) * (e^(-Ea/R*deltaT))
30  rate = mech_a + mech_b
40  teta = 1
41  eta = 1
42  Area = 1
70  rate = Area * rate * (1 - SR("Anorthite"))
80  moles = rate * time
100 save moles
  -end
END


SOLUTION 0                              # Definition of initial solution
-temp   7.0
-units  mol/kgw
-pH     7.0
Na              5.5E-04
K               1.1E-04
Ca              2.7E-03
Mg              2.8E-04
Cl              1.5E-03 charge
S(6)            1.3E-03
Alkalinity      1.0E-09
Si              5.0E-07
Al              1.0E-20
REACTION 0                              # Irreversibel reaction with 0.5 mol CO2
CO2             0.5
EQUILIBRIUM_PHASES 0                    # Equilibrium mineral phases
Calcite 0.0     1.0
```

```
Chalcedony      0.0     5.0
Kaolinite       0.0     159.0
SAVE SOLUTION 0
END

SOLUTION 1-100
-temp   7.0
-units  mol/kgw
-pH     7.0
Na              5.5E-04
K               1.1E-04
Ca              2.7E-03
Mg              2.8E-04
Cl              1.5E-03 charge
S(6)            1.3E-03
Alkalinity      1.0E-09
Si              5.0E-07
Al              1.0E-20
EQUILIBRIUM_PHASES 1-100      # Equilibrium reactions for model cells
Calcite         0.0     1.0
Chalcedony      0.0     5.0
Kaolinite       0.0     159.0
KINETICS 1-100                # Anorthite dissolution using rate law
Anorthite
-m0 2.0
SAVE SOLUTION 1-100
END


TRANSPORT                           # one-dimensional column (50m)
-cells                  100         # 100 cell model column
-lengths                0.5         # Column length = 0.5m*100 = 50m
-shifts                 50000       # Number of time steps
-time_step              86400       # Time step length [s]
-dispersivities         0.25        # unit [m}
-diffusion_coefficient 1E-20        # unit [m2/s]
-flow_direction         forward
-boundary_conditions    flux flux
END
```

B.1.2 Tertiary formation water

```
# Input files for PhreeqC are identical with the exception that the database is selected by
the following commands
DATABASE C:\phreeqc\database\phreeqc.dat
#DATABASE C:\phreeqc\database\wateq4f.dat
#DATABASE C:\phreeqc\databse\llnl.dat
#DATABASE C:\phreeqc\database\minteq.dat

TITLE 1-d model scenario for calculating anorthite dissolution time using the Tertiary for-
mation water

SELECTED_OUTPUT                     # User defined output file
-file C:\Buntsandstein\Output.xls
-saturation_indices Anorthite
-kinetic_reactants  Anorthite


RATES                               # Rate law for anorthite dissolution
Anorthite
  -start
10  R = 8.314472
```

```
11  deltaT = 1/TK - 1/298.15
12  e = 2.7183
rem acidic mechanism
13  Ea = 16600
14  logK25 = -3.5
15  ny = 1.411
16  mech_a = (10^logK25) * (e^(-Ea/R*deltaT)) * (ACT("H+"))^ny
rem neutral mechanism
23  Ea = 17800
24  logK25 = -9.12
26  mech_b = (10^logK25) * (e^(-Ea/R*deltaT))
30  rate = mech_a + mech_b
40  teta = 1
41  eta = 1
42  Area = 1
70  rate = Area * rate * (1 - SR("Anorthite"))
80  moles = rate * time
100 save moles
  -end
END


SOLUTION 0                    # Definition of initial solution
-temp   15.0
-units mol/kgw
-pH     5.9
Na              1.162
K               6.03E-03
Ca              8.61E-03
Mg              3.77E-02
Cl              1.250 charge
S(6)            1.38E-03
Alkalinity      6.46E-03
Al              1.08E-07
Fe              4.31E-04
REACTION 0                    # Irreversibel reaction with 0.5 mol CO2
CO2 0.5
EQUILIBRIUM_PHASES 0          # Equilibrium mineral phases
Chalcedony      0.0     159.0
Kaolinite       0.0     1.0
Calcite         0.0     5.0
SAVE SOLUTION 0
END

SOLUTION 100
-temp           15.0
-pH             5.9
-units  mol/kgw
Na              1.162
K               6.03E-03
Ca              8.61E-03
Mg              3.77E-02
Cl              1.250 charge
S(6)            1.38E-03
Alkalinity      6.46E-03
Al              1.076e-07
Fe              4.304e-04
KINETICS 1-100                # Anorthite dissolution using rate law
Anorthite
-m0 2.0
EQUILIBRIUM_PHASES 1-100      # Equilibrium reactions for model cells
Chalcedony      0.0     159.0
```

```
Kaolinite       0.0     1.0
Calcite         0.0     5.0
SAVE SOLUTION 1-100
END


TRANSPORT                               # one-dimensional column (50m)
-cells                  100             # 100 cell model colum
-lengths                0.5             # Column length = 0.5m*100 = 50m
-shifts                 40000           # Number of time steps
-time_step              86400           # Time step length
-dispersivities         0.25            # unit [m]
-diffusion_coefficient 1E-20            # unit [m2/s]
-flow_direction        forward
-boundary_conditions   flux flux
END
```

B.1.3 Keuper formation water

```
# Input files for PhreeqC are identical with the exception that the database is selected by
the following commands
DATABASE C:\phreeqc\database\phreeqc.dat
#DATABASE C:\phreeqc\database\wateq4f.dat
#DATABASE C:\phreeqc\databse\llnl.dat
#DATABASE C:\phreeqc\database\minteq.dat

TITLE 1-d model scenario for calculating anorthite dissolution time using the Keuper forma-
tion water

SELECTED_OUTPUT                         # User defined output file
-file C:\Buntsandstein\Output.xls
-saturation_indices Anorthite
-kinetic_reactants  Anorthite


RATES                                   # Rate law for anorthite dissolution
Anorthite
  -start
10  R = 8.314472
11  deltaT = 1/TK - 1/298.15
12  e = 2.7183
rem acidic mechanism
13  Ea = 16600
14  logK25 = -3.5
15  ny = 1.411
16  mech_a = (10^logK25) * (e^(-Ea/R*deltaT)) * (ACT("H+"))^ny
rem neutral mechanism
23  Ea = 17800
24  logK25 = -9.12
26  mech_b = (10^logK25) * (e^(-Ea/R*deltaT))
30  rate = mech_a + mech_b
40  teta = 1
41  eta = 1
42  Area = 1
70  rate = Area * rate * (1 - SR("Anorthite"))
80  moles = rate * time
100 save moles
  -end
END
```

```
SOLUTION 0                          # Definition of initial solution
-temp   50
-units mol/kgw
-pH     6.2
Na              2.668
K               0.006
Ca              0.058
Mg              0.030
Cl              2.824 charge
S(6)            0.012
Alkalinity      0.004
Si              1E-20
Al              1E-20
REACTION 0                          # Irreversibel reaction with 0.5 mol CO2
CO2             0.5
EQUILIBRIUM_PHASES 0                # Equilibrium mineral phases
Calcite         0.0     1.0
Chalcedony      0.0     5.0
Kaolinite       0.0     159.0
SAVE SOLUTION 0
END

SOLUTION 100
-temp   50
-units mol/kgw
-pH     6.2
Na              2.668
K               0.006
Ca              0.058
Mg              0.030
Cl              2.824  charge
S(6)            0.012
Alkalinity      0.004
Si              1E-20
Al              1e-20
KINETICS 1-100                      # Anorthite dissolution using rate law
Anorthite
-m0     2.0
EQUILIBRIUM_PHASES 1-100            # Equilibrium reactions for model cells
Calcite 0.0     1.0
Chalcedony      0.0     5.0
Kaolinite       0.0     159.0
SAVE SOLUTI     ON 1-100
END


TRANSPORT                           # one-dimensional column (50m)
-cells                  100         # 100 cell model column
-lengths                0.5         # Column length = 0.5m*100 = 50m
-shifts                 20000       # Number of time steps
-time_step              86400       # Time step length [s]
-dispersivities         0.25        # unit [m]
-diffusion_coefficient  1E-20       # unit [m2/s]
-flow_direction         forward
-boundary_conditions    flux flux
END
```

B.1.4 Buntsandstein formation water

```
# Input files for PhreeqC are identical with the exception that the database is selected by
the following commands
DATABASE C:\phreeqc\database\phreeqc.dat
```

```
#DATABASE C:\phreeqc\database\wateq4f.dat
#DATABASE C:\phreeqc\databse\llnl.dat
#DATABASE C:\phreeqc\database\minteq.dat

TITLE 1-d model scenario for calculating anorthite dissolution time using the Buntsandstein
formation water

SELECTED_OUTPUT                         # User defined output file
-file C:\Buntsandstein\Output.xls
-saturation_indices Anorthite
-kinetic_reactants  Anorthite

RATES                                   # Rate law for anorthite dissolution
Anorthite
  -start
10  R = 8.314472
11  deltaT = 1/TK - 1/298.15
12  e = 2.7183
rem acidic mechanism
13  Ea = 16600
14  logK25 = -3.5
15  ny = 1.411
16  mech_a = (10^logK25) * (e^(-Ea/R*deltaT)) * (ACT("H+"))^ny
rem neutral mechanism
23  Ea = 17800
24  logK25 = -9.12
26  mech_b = (10^logK25) * (e^(-Ea/R*deltaT))
30  rate = mech_a + mech_b
40  teta = 1
41  eta = 1
42  Area = 1
70  rate = Area * rate * (1 - SR("Anorthite"))
80  moles = rate * time
100 save moles
  -end
END

SOLUTION 0                              # Definition of initial solution
-temp   58.0
-units  mol/kgw
-pH     5.80
Na      4.7430
K       0.0207
Ca      0.4779
Mg      0.1123
Cl      5.9304 charge
S(6)    0.0046
C(4)    0.0011
Al      1.0E-20
REACTION 0                              # Irreversibel reaction with 0.5 mol CO2
CO2     0.5
EQUILIBRIUM_PHASES 0                    # Equilibrium mineral phases
Chalcedony      0.0     159.0
Kaolinite       0.0     1.0
Calcite 0.0     5.0
SAVE SOLUTION 0
END


SOLUTION 1-100
-temp   58.0
-units  mol/kgw
```

```
-pH     5.8
Na      4.7430
K       0.0207
Ca      0.4779
Mg      0.1123
Cl      5.9340 charge
S(6)    0.0046
C(4)    0.00112
Al      1.0E-20
KINETICS 1-100                      # Anorthite dissolution using rate law
Anorthite
-m0 2.0
EQUILIBRIUM_PHASES 1-100            # Equilibrium reactions for model cells
Chalcedony      0.0     159.0
Kaolinite       0.0     1.0
Calcite         0.0     5.0
END


TRANSPORT                           # one-dimensional column (50m)
-cells                  100         # 100 cell model column
-lengths                0.5         # Column length = 0.5m*100 = 50m
-shifts                 15000       # Number of time steps
-time_step              86400       # Lenth of time step [s]
-dispersivities         0.25        # unit [m]
-diffusion_coefficient 1.0E-20      # unit [m2/s]
-boundary_conditions   flux flux
-flow_direction        forward
END
```

B.2 Eingabedateien für The Geochemist's Workbench: Quaternary formation water

B.2.1 thermo_phreeqc.dat

```
# X1t script, saved Wed Mar 26 2014 by C.Haase
data = C:\Programme\Gwb\Gtdata\thermo_phreeqc.dat verify
time start      = 0 years,      end = 47900 days
length          = 50 m
width           = 0.5 m
height          = 0.01 m
Nx              = 50
discharge       = 0.1 m/day
permeability    intercept   = 15        porosity = -5
porosity                = 0.25
diffusion_coef          = 1.0E-20
thermal_cond            = 0
dispersivity            = 25 cm
temperature initial     = 7.0 C,        inlet = 7.0     constant = on
scope = initial
   H2O          = 1.0 free kg
   pH           = 7.0
   Ca++         = 0.00253 molal
   Mg++         = 0.00029 molal
   Na+          = 0.00056 molal
   K+           = 0.00011 molal
   Cl-          = 0.00153 molal
   SO4--        = 0.00132 molal
   swap Kaolinite for Al+++
   Kaolinite    = 1.0 free mol
   swap Calcite for CO3--
   Calcite      = 5.0 free mol
   swap Chalcedony for H4SiO4
   Chalcedony   = 159.0 free mol
```

```
   balance on Ca++
scope = inlet
   H2O          = 1.0 free kg
   swap CO2 for H+
   CO2          = 0.5 free molal
   Ca++         = 0.00253 molal
   Mg++         = 0.00029 molal
   Na+          = 0.00056 molal
   K+           = 0.00011 molal
   Cl-          = 0.00153 molal
   SO4--        = 0.00132 molal
   swap Kaolinite for Al+++
   Kaolinite    = 1.0 free mol
   swap Calcite for CO3--
   Calcite      = 5.0 free mol
   swap Chalcedony for H4SiO4
   Chalcedony   = 159.0 free mol
   balance on Ca++

kinetic Anorthite 2.0 mol
kinetic Anorthite rate_law = D:\Anorthite.bas
rate_con = 7.59E-10    surface = 1.0

suppress ALL
unsuppress Anorthite Calcite Chalcedony Kaolinite
extrapolate
printout on    minerals = long        basis = short
delxi          = 0.01
dxplot         = 0.01 exact linear
dxprint        = 0.01 exact linear
epsilon        = 1.0E-7
nswap          = 80
simax          = 10
theta          = 1
timax          = 10
```

B.2.2 thermo_wateq4f.dat

```
# X1t script, saved Fri Feb 21 2014 by C.Haase
data = C:\Programme\Gwb\Gtdata\thermo_wateq4f.dat verify
time start     = 0 years,     end = 47900 days
length         = 50 m
width          = 0.5 m
height         = 0.01 m
Nx             = 50
discharge      = 0.1 m/day
permeability   intercept   = 15        porosity = -5
porosity               = 0.25
diffusion_coef         = 1.0E-20
thermal_cond           = 0
dispersivity           = 25 cm
temperature initial    = 7.0 C,        inlet = 7.0,    constant = on
scope = initial
   H2O          = 1.0 free kg
   pH           = 7.0
   Ca++         = 0.00253 molal
   Mg++         = 0.00029 molal
   Na+          = 0.00056 molal
   K+           = 0.00011 molal
   Cl-          = 0.00153 molal
   SO4--        = 0.00132 molal
   swap Kaolinite for Al+++
```

```
   Kaolinite    = 1.0 free mol
   swap Calcite for CO3--
   Calcite      = 5.0 free mol
   swap Chalcedony for H4SiO4
   Chalcedony   = 159.0 free mol
   balance on Ca++
scope = inlet
   H2O          = 1.0 free kg
   swap CO2 for H+
   CO2          = 0.5 free molal
   Ca++         = 0.00253 molal
   Mg++         = 0.00029 molal
   Na+          = 0.00056 molal
   K+           = 0.00011 molal
   Cl-          = 0.00153 molal
   SO4--        = 0.00132 molal
   swap Kaolinite for Al+++
   Kaolinite    = 1.0 free mol
   swap Calcite for CO3--
   Calcite      = 5.0 free mol
   swap Chalcedony for H4SiO4
   Chalcedony   = 159.0 free mol
   balance on Ca++


kinetic Anorthite 2.0 mol
kinetic Anorthite rate_law = D:\Anorthite.bas
rate_con = 7.59E-10    surface = 1.0

suppress ALL
unsuppress  Anorthite Calcite Chalcedony Kaolinite
extrapolate
printout on    minerals = long        basis = short
delxi          = 0.01
dxplot         = 0.01 exact linear
dxprint        = 0.01 exact linear
epsilon        = 1.0E-7
nswap          = 80
simax          = 10
theta          = 1
timax          = 10
```

B.2.3 thermo.dat

```
# X1t script, saved Wed Feb 19 2014 by C.Haase
data = C:\Programme\Gwb\Gtdata\thermo.dat verify
time start     = 0 years,     end = 47700 days
length         = 50 m
width          = 0.5 m
height         = 0.01 m
Nx             = 50
discharge      = 0.1 m/day
permeability   intercept  = 15        porosity = -5
porosity               = 0.25
diffusion_coef         = 1.0E-20
thermal_cond           = 0
dispersivity           = 25 cm
temperature initial    = 7.0 C,       inlet = 7.0,   constant = on
scope = initial
   H2O         = 1.0 free kg
   pH          = 7.0
   Ca++        = 0.00253 molal
```

```
   Mg++          = 0.00029 molal
   Na+           = 0.00056 molal
   K+            = 0.00011 molal
   Cl-           = 0.00153 molal
   SO4--         = 0.00132 molal
   swap Kaolinite for Al+++
   Kaolinite     = 1.0 free mol
   swap Calcite for HCO3-
   Calcite       = 5.0 free mol
   swap Chalcedony for SiO2(aq)
   Chalcedony    = 159.0 free mol
   balance on Ca++
scope = inlet
   H2O           = 1.0 free kg
   swap CO2(aq) for H+
   CO2(aq)       = 0.5 free molal
   Ca++          = 0.00253 molal
   Mg++          = 0.00029 molal
   Na+           = 0.00056 molal
   K+            = 0.00011 molal
   Cl-           = 0.00153 molal
   SO4--         = 0.00132 molal
   swap Kaolinite for Al+++
   Kaolinite     = 1.0 free mol
   swap Calcite for HCO3-
   Calcite       = 5.0 free mol
   swap Chalcedony for SiO2(aq)
   Chalcedony    = 159.0 free mol
   balance on Ca++


kinetic Anorthite 2.0 mol
kinetic Anorthite rate_law = D:\Anorthite.bas
rate_con = 7.59E-10    surface = 1.0

suppress        ALL
unsuppress      Anorthite Calcite Chalcedony Kaolinite
extrapolate
printout on     minerals = long        basis = short
delxi           = 0.01
dxplot          = 0.01 exact linear
dxprint         = 0.01 exact linear
epsilon         = 1.0E-7
nswap           = 80
simax           = 10
theta           = 1
timax           = 10
```

B.2.4 thermo.com.v8.r6+.dat

```
# X1t script, saved Thu Feb 20 2014 by C.Haase
data = C:\Programme\Gwb\Gtdata\thermo.com.v8.r6+.dat verify
time start      = 0 years,      end = 48000 days
length          = 50 m
width           = 0.5 m
height          = 0.01 m
Nx              = 50
discharge       = 0.1 m/day
permeability    intercept   = 15        porosity = -5
porosity                = 0.25
diffusion_coef          = 1.0E-20
thermal_cond            = 0
```

```
dispersivity           = 25 cm
temperature initial = 7.0 C,          inlet = 7.0,    constant = on
scope = initial
   H2O          = 1.0 free kg
   pH           = 7.0
   Ca++         = 0.00253 molal
   Mg++         = 0.00029 molal
   Na+          = 0.00056 molal
   K+           = 0.00011 molal
   Cl-          = 0.00153 molal
   SO4--        = 0.00132 molal
   swap Kaolinite for Al+++
   Kaolinite    = 1.0 free mol
   swap Calcite for HCO3-
   Calcite      = 5.0 free mol
   swap Chalcedony for SiO2(aq)
   Chalcedony   = 159.0 free mol
   balance on Ca++
scope = inlet
   H2O          = 1.0 free kg
   swap CO2(aq) for H+
   CO2(aq)      = 0.5 free molal
   Ca++         = 0.00253 molal
   Mg++         = 0.00029 molal
   Na+          = 0.00056 molal
   K+           = 0.00011 molal
   Cl-          = 0.00153 molal
   SO4--        = 0.00132 molal
   swap Kaolinite for Al+++
   Kaolinite    = 1.0 free mol
   swap Calcite for HCO3-
   Calcite      = 5.0 free mol
   swap Chalcedony for SiO2(aq)
   Chalcedony   = 159.0 free mol
   balance on Ca++

kinetic Anorthite 2.0 mol
kinetic Anorthite rate_law = D:\Anorthite.bas
rate_con = 7.59E-10    surface = 1.0

suppress ALL
unsuppress  Anorthite Calcite Chalcedony Kaolinite
extrapolate
printout on    minerals = long       basis = short
delxi          = 0.01
dxplot         = 0.01 exact linear
dxprint        = 0.01 exact linear
epsilon        = 1.0E-7
nswap          = 80
simax          = 10
theta          = 1
timax          = 10
```

B.3 Eingabedateien für The Geochemist's Workbench: Tertiary formation water

B.3.1 thermo_phreeqc.dat

```
# X1t script, saved Wed Mar 26 2014 by C. Haase
data = C:\Programme\Gwb\Gtdata\thermo_phreeqc.dat verify
time start      = 0 years,      end = 39000 days
length          = 50 m
width           = 0.5 m
height          = 0.01 m
Nx              = 50
discharge       = 0.1 m/day
permeability    intercept   = 15        porosity = -5
porosity                = 0.25
diffusion_coef          = 1.0E-20
thermal_cond            = 0
dispersivity            = 25 cm
temperature initial     = 15 C,         inlet = 15,     constant = on
scope = initial
   H2O          = 1.0 free kg
   pH           = 5.9
   Ca++         = 0.0081 molal
   Mg++         = 0.0377 molal
   Na+          = 1.1620 molal
   K+           = 0.0060 molal
   Cl-          = 1.2500 molal
   SO4--        = 0.0014 molal
   swap Kaolinite for Al+++
   Kaolinite    = 1.0 free mol
   swap Calcite for CO3--
   Calcite      = 5.0 free mol
   swap Chalcedony for H4SiO4
   Chalcedony   = 159.0 free mol
   balance on Ca++
scope = inlet
   H2O          = 1.0 free kg
   swap CO2 for H+
   CO2          = 0.5 free molal
   Ca++         = 0.0086 molal
   Mg++         = 0.0377 molal
   Na+          = 1.1620 molal
   K+           = 0.0060 molal
   Cl-          = 1.2500 molal
   SO4--        = 0.0014 molal
   swap Kaolinite for Al+++
   Kaolinite    = 1.0 free mol
   swap Calcite for CO3--
   Calcite      = 5.0 free mol
   swap Chalcedony for H4SiO4
   Chalcedony   = 159.0 free mol
   balance on Ca++

kinetic Anorthite 2.0 mol
kinetic Anorthite rate_law = D:\Anorthite.bas
rate_con = 7.59E-10 surface = 1.0

suppress ALL
unsuppress  Anorthite Calcite Chalcedony Kaolinite
extrapolate
printout on     minerals = long         basis = short
delxi           = 0.01
dxplot          = 0.01 exact linear
dxprint         = 0.01 exact linear
```

```
epsilon         = 1.0E-7
nswap           = 80
simax           = 10
theta           = 1
timax           = 10
```

B.3.2 thermo_wateq4f.dat

```
# X1t script, saved Wed Mar 26 2014 by C.Haase
data = C:\Programme\Gwb\Gtdata\thermo_wateq4f.dat verify
time start      = 0 years,      end = 38900 days
length          = 50 m
width           = 0.5 m
height          = 0.01 m
Nx              = 50
discharge       = 0.1 m/day
permeability    intercept   = 15        porosity = -5
porosity                = 0.25
diffusion_coef          = 1.0E-20
thermal_cond            = 0
dispersivity            = 25 cm
temperature initial     = 15 C,         inlet = 15,     constant = on
scope = initial
   H2O          = 1.0 free kg
   pH           = 5.9
   Ca++         = 0.0086 molal
   Mg++         = 0.0377 molal
   Na+          = 1.1620 molal
   K+           = 0.0060 molal
   Cl-          = 1.2500 molal
   SO4--        = 0.0014 molal
   swap Kaolinite for Al+++
   Kaolinite    = 1.0 free mol
   swap Calcite for CO3--
   Calcite      = 5.0 free mol
   swap Chalcedony for H4SiO4
   Chalcedony   = 159.0 free mol
   balance on Ca++
scope = inlet
   H2O          = 1.0 free kg
   swap CO2 for H+
   CO2          = 0.5 free molal
   Ca++         = 0.0086 molal
   Mg++         = 0.0377 molal
   Na+          = 1.1620 molal
   K+           = 0.0060 molal
   Cl-          = 1.2500 molal
   SO4--        = 0.0014 molal
   swap Kaolinite for Al+++
   Kaolinite    = 1.0 free mol
   swap Calcite for CO3--
   Calcite      = 5.0 free mol
   swap Chalcedony for H4SiO4
   Chalcedony   = 159.0 free mol
   balance on Ca++

kinetic Anorthite 2.0 mol
kinetic Anorthite rate_law = D:\Anorthite.bas
rate_con = 7.59E-10    surface = 1.0

suppress ALL
unsuppress  Anorthite Calcite Chalcedony Kaolinite
```

```
extrapolate
printout on     minerals = long        basis = short
delxi           = 0.01
dxplot          = 0.01 exact linear
dxprint         = 0.01 exact linear
epsilon         = 1.0E-8
nswap           = 80
simax           = 10
theta           = 1
timax           = 10
```

B.3.3 thermo.dat

```
# X1t script, saved Wed Mar 26 2014 by Christoph
data = C:\Programme\Gwb\Gtdata\thermo.dat verify
time start      = 0 years,      end = 38700 days
length          = 50 m
width           = 0.5 m
height          = 0.01 m
Nx              = 50
discharge       = 0.1 m/day
permeability    intercept   = 15        porosity = -5
porosity                = 0.25
diffusion_coef          = 1.0E-20
thermal_cond            = 0
dispersivity            = 25 cm
temperature initial     = 15 C,         inlet = 15,     constant = on
scope = initial
   H2O          = 1.0 free kg
   pH           = 5.94
   Ca++         = 0.0086 molal
   Mg++         = 0.0377 molal
   Na+          = 1.162 molal
   K+           = 0.006 molal
   Cl-          = 1.250 molal
   SO4--        = 0.0014 molal
   swap Kaolinite for Al+++
   Kaolinite    = 1.0 free mol
   swap Calcite for HCO3-
   Calcite      = 5.0 free mol
   swap Chalcedony for SiO2(aq)
   Chalcedony   = 159.0 free mol
   balance on Ca++
scope = inlet
   H2O          = 1.0 free kg
   swap CO2(aq) for H+
   CO2(aq)      = 0.5 free molal
   Ca++         = 0.0086 molal
   Mg++         = 0.0377 molal
   Na+          = 1.1620 molal
   K+           = 0.0060 molal
   Cl-          = 1.2500 molal
   SO4--        = 0.0014 molal
   swap Kaolinite for Al+++
   Kaolinite    = 1.0 free mol
   swap Calcite for HCO3-
   Calcite      = 5.0 free mol
   swap Chalcedony for SiO2(aq)
   Chalcedony   = 159.0 free mol
   balance on Ca++
```

```
kinetic Anorthite 2.0 mol
kinetic Anorthite rate_law = D:\Anorthite.bas
rate_con = 7.59E-10    surface = 1.0

suppress ALL
unsuppress  Anorthite Calcite Chalcedony Kaolinite
extrapolate
printout on    minerals = long       basis = short
delxi          = 0.01
dxplot         = 0.01 exact linear
dxprint        = 0.01 exact linear
epsilon        = 1.0E-7
nswap          = 80
simax          = 10
theta          = 1
timax          = 10
```

B.3.4 thermo.com.v8.r6+.dat

```
# X1t script, saved Sat Sep 27 2014 by C.Haase
data = C:\Programme\Gwb\Gtdata\thermo.com.v8.r6+.dat verify
time start     = 0 years,     end = 38700 days
length         = 50 m
width          = 0.5 m
height         = 0.01 m
Nx             = 50
discharge      = 0.1 m/day
permeability   intercept  = 15       porosity = -5
porosity               = 0.25
diffusion_coef         = 1.0E-20
thermal_cond           = 0
dispersivity           = 25 cm
temperature initial    = 15,          inlet = 15,    constant = on
scope = initial
   H2O         = 1.0 free kg
   pH          = 5.9
   Ca++        = 0.0087 molal
   Mg++        = 0.0377 molal
   Na+         = 1.1620 molal
   K+          = 0.0060 molal
   Cl-         = 1.2500 molal
   SO4--       = 0.0014 molal
   swap Kaolinite for Al+++
   Kaolinite    = 1.0 free mol
   swap Calcite for HCO3-
   Calcite      = 5.0 free mol
   swap Chalcedony for SiO2(aq)
   Chalcedony   = 159.0 free mol
   balance on Ca++
scope = inlet
   H2O         = 1.0 free kg
   swap CO2(aq) for H+
   CO2(aq)     = 0.5 free molal
   Ca++        = 0.0086 molal
   Mg++        = 0.0377 molal
   Na+         = 1.1620 molal
   K+          = 0.0060 molal
   Cl-         = 1.2500 molal
   SO4--       = 0.0014 molal
   swap Kaolinite for Al+++
   Kaolinite   = 1.0 free mol
   swap Calcite for HCO3-
```

```
   Calcite     = 5.0 free mol
   swap Chalcedony for SiO2(aq)
   Chalcedony  = 159.0 free mol
   balance on Ca++


kinetic Anorthite 2.0 mol
kinetic Anorthite rate_law = C:\Anorthite.bas
rate_con = 7.59E-10    surface = 1.0

suppress ALL
unsuppress  Anorthite Calcite Chalcedony Kaolinite
extrapolate
printout on    minerals = long       basis = short
delxi          = 0.025
dxplot         = 0.025 exact linear
dxprint        = 0.01 exact linear
epsilon        = 1.0E-8
nswap          = 80
simax          = 10
theta          = 1
timax          = 10
```

B.4 Eingabedateien für The Geochemist's Workbench: Keuper formation water

B.4.1 thermo_phreeqc.dat

```
# X1t script, saved Mon Feb 17 2014 by C.Haase
data = C:\Programme\Gwb\Gtdata\thermo_phreeqc.dat verify
time start      = 0 years,      end = 16500 days
length          = 50 m
width           = 0.5 m
height          = 0.01 m
Nx              = 50
discharge       = 0.1 m/day
permeability    intercept   = 15        porosity = -5
porosity                = 0.25
diffusion_coef          = 1.0E-20
thermal_cond            = 0
dispersivity            = 25 cm
temperature initial = 50 C,             inlet = 50,     constant = on
scope = initial
   H2O          = 1.0 free kg
   pH           = 6.2
   Ca++         = 0.058 molal
   Mg++         = 0.030 molal
   Na+          = 2.668 molal
   K+           = 0.006 molal
   Cl-          = 2.824 molal
   SO4--        = 0.012 molal
   swap Kaolinite for Al+++
   Kaolinite    = 1.0 free mol
   swap Calcite for CO3--
   Calcite      = 5.0 free mol
   swap Chalcedony for H4SiO4
   Chalcedony   = 159.0 free mol
   balance on Cl-
scope = inlet
   H2O          = 1.0 free kg
   swap CO2 for H+
   CO2          = 0.5 free molal
   Ca++         = 0.058 molal
   Mg++         = 0.030 molal
   Na+          = 2.668 molal
   K+           = 0.006 molal
   Cl-          = 2.824 molal
   SO4--        = 0.012 molal
   swap Kaolinite for Al+++
   Kaolinite    = 1.0 free mol
   swap Calcite for CO3--
   Calcite      = 5.0 free mol
   swap Chalcedony for H4SiO4
   Chalcedony   = 159.0 free mol
   balance on Cl-

kinetic Anorthite 2.0 mol
kinetic Anorthite rate_law = D:\Anorthite.bas
rate_con = 7.59E-10    surface = 1.0

suppress ALL
unsuppress  Anorthite Calcite Chalcedony Kaolinite
extrapolate
printout on     minerals = long         basis = short
delxi           = 0.01
dxplot          = 0.01 exact linear
dxprint         = 0.01 exact linear
```

```
epsilon         = 1.0E-7
nswap           = 80
simax           = 10
theta           = 1
timax           = 10
```

B.4.2 thermo_wateq4f.dat

```
# X1t script, saved Tue Feb 18 2014 by Christoph
data = C:\Programme\Gwb\Gtdata\thermo_wateq4f.dat verify
time start      = 0 years,      end = 16500 days
length          = 50 m
width           = 0.5 m
height          = 0.01 m
Nx              = 50
discharge       = 0.1 m/day
permeability    intercept   = 15        porosity = -5
porosity                = 0.25
diffusion_coef          = 1.0E-20
thermal_cond            = 0
dispersivity            = 25 cm
temperature initial = 50 C,           inlet = 50,     constant = on
scope = initial
   H2O          = 1.0 free kg
   pH           = 6.2
   Ca++         = 0.058 molal
   Mg++         = 0.030 molal
   Na+          = 2.668 molal
   K+           = 0.006 molal
   Cl-          = 2.824 molal
   SO4--        = 0.012 molal
   swap Kaolinite for Al+++
   Kaolinite    = 1.0 free mol
   swap Calcite for CO3--
   Calcite      = 5.0 free mol
   swap Chalcedony for H4SiO4
   Chalcedony   = 159.0 free mol
   balance on Cl-
scope = inlet
   H2O          = 1.0 free kg
   swap CO2 for H+
   CO2          = 0.5 free molal
   Ca++         = 0.058 molal
   Mg++         = 0.030 molal
   Na+          = 2.668 molal
   K+           = 0.006 molal
   Cl-          = 2.824 molal
   SO4--        = 0.012 molal
   swap Kaolinite for Al+++
   Kaolinite    = 1.0 free mol
   swap Calcite for CO3--
   Calcite      = 5.0 free mol
   swap Chalcedony for H4SiO4
   Chalcedony   = 159.0 free mol
   balance on Cl-

kinetic Anorthite 2.0 mol
kinetic Anorthite rate_law = D:\Anorthite.bas
rate_con = 7.59E-10 surface = 1.0

suppress ALL
unsuppress  Anorthite Calcite Chalcedony Kaolinite
```

```
extrapolate
printout on     minerals = long        basis = short
delxi           = 0.01
dxplot          = 0.01 exact linear
dxprint         = 0.01 exact linear
epsilon         = 1.0E-7
nswap           = 80
simax           = 10
theta           = 1
timax           = 10
```

B.4.3 thermo.dat

```
# X1t script, saved Mon Feb 17 2014 by Christoph
data = C:\Programme\Gwb\Gtdata\thermo.dat verify
time start      = 0 years,      end = 17200 days
length          = 50 m
width           = 0.5 m
height          = 0.01 m
Nx              = 50
discharge       = 0.1 m/day
permeability    intercept = 15         porosity = -5
porosity                = 0.25
diffusion_coef          = 1.0E-20
thermal_cond            = 0
dispersivity            = 25 cm
temperature initial = 50 C,            inlet = 50,     constant = on
scope = initial
   H2O          = 1.0 free kg
   pH           = 5.8
   Ca++         = 0.058 molal
   Mg++         = 0.030 molal
   Na+          = 2.668 molal
   K+           = 0.006 molal
   Cl-          = 2.824 molal
   SO4--        = 0.012 molal
   swap Kaolinite for Al+++
   Kaolinite    = 1.0 free mol
   swap Calcite for HCO3-
   Calcite      = 5.0 free mol
   swap Chalcedony for SiO2(aq)
   Chalcedony   = 159.0 free mol
   balance on Cl-
scope = inlet
   H2O          = 1.0 free kg
   swap CO2(aq) for H+
   CO2(aq)      = 0.5 free molal
   Ca++         = 0.058 molal
   Mg++         = 0.030 molal
   Na+          = 2.668 molal
   K+           = 0.006 molal
   Cl-          = 2.824 molal
   SO4--        = 0.012 molal
   swap Kaolinite for Al+++
   Kaolinite    = 1.0 free mol
   swap Calcite for HCO3-
   Calcite      = 5.0 free mol
   swap Chalcedony for SiO2(aq)
   Chalcedony   = 159.0 free mol
   balance on Cl-
```

```
kinetic Anorthite 2.0 mol
kinetic Anorthite rate_law = D:\Anorthite.bas
rate_con = 7.59E-10    surface = 1.0

suppress ALL
unsuppress     Anorthite Calcite Chalcedony Kaolinite
extrapolate
printout on    minerals = long        basis = short
delxi          = 0.01
dxplot         = 0.01 exact linear
dxprint        = 0.01 exact linear
epsilon        = 1.0E-7
nswap          = 80
simax          = 10
theta          = 1
timax          = 10
```

B.4.4 thermo.com.v8.r6+.dat

```
# X1t script, saved Tue Feb 18 2014 by C.Haase
data = C:\Programme\Gwb\Gtdata\thermo.com.v8.r6+.dat verify
time start     = 0 years,     end = 16900 days
length         = 50 m
width          = 0.5 m
height         = 0.01 m
Nx             = 50
discharge      = 0.1 m/day
permeability   intercept = 15        porosity = -5
porosity               = 0.25
diffusion_coef         = 1.0E-20
thermal_cond           = 0
dispersivity           = 25 cm
temperature initial = 58,            inlet = 58,    constant = on
scope = initial
   H2O         = 1.0 free kg
   pH          = 5.8
   Ca++        = 0.058 molal
   Mg++        = 0.030 molal
   Na+         = 2.668 molal
   K+          = 0.006 molal
   Cl-         = 2.824 molal
   SO4--       = 0.012 molal
   swap Kaolinite for Al+++
   Kaolinite   = 1.0 free mol
   swap Calcite for HCO3-
   Calcite     = 5.0 free mol
   swap Chalcedony for SiO2(aq)
   Chalcedony  = 159.0 free mol
   balance on Cl-
scope = inlet
   H2O         = 1.0 free kg
   swap CO2(aq) for H+
   CO2(aq)     = 0.5 free molal
   Ca++        = 0.058 molal
   Mg++        = 0.030 molal
   Na+         = 2.668 molal
   K+          = 0.006 molal
   Cl-         = 2.824 molal
   SO4--       = 0.012 molal
   swap Kaolinite for Al+++
   Kaolinite   = 1.0 free mol
   swap Calcite for HCO3-
```

```
   Calcite     = 5.0 free mol
   swap Chalcedony for SiO2(aq)
   Chalcedony  = 159.0 free mol
   balance on Cl-

kinetic Anorthite 2.0 mol
kinetic Anorthite rate_law = D:\Anorthite.bas
rate_con = 7.59E-10    surface = 1.0

suppress ALL
unsuppress     Anorthite Calcite Chalcedony Kaolinite
extrapolate
printout on    minerals = long       basis = short
delxi          = 0.01
dxplot         = 0.01 exact linear
dxprint        = 0.01 exact linear
epsilon        = 1.0E-7
nswap          = 80
simax          = 10
theta          = 1
timax          = 10
```

B.5 Eingabedateien für The Geochemist's Workbench: Buntsandstein formation water

B.5.1 thermo_phreeqc.dat

```
# X1t script, saved Sat Sep 20 2014 by C.Haase
data = C:\Programme\Gwb\Gtdata\thermo_phreeqc.dat verify
time start      = 0 years,      end = 7100 days
length          = 100 m
width           = 0.5 m
height          = 0.01 m
Nx              = 50
discharge       = 0.1 m/day
permeability    intercept   = 15        porosity = -5
porosity                = 0.25
diffusion_coef          = 1.0E-20
thermal_cond            = 0
dispersivity            = 25 cm
temperature initial = 58,               inlet = 58,     constant = on
scope = initial
   H2O          = 1.0 free kg
   pH           = 5.8
   Ca++         = 0.478 molal
   Mg++         = 0.112 molal
   Na+          = 4.743 molal
   K+           = 0.021 molal
   Cl-          = 5.934 molal
   SO4--        = 0.005 molal
   swap Kaolinite for Al+++
   Kaolinite    = 1.0 free mol
   swap Calcite for CO3--
   Calcite      = 5.0 free mol
   swap Chalcedony for H4SiO4
   Chalcedony   = 159.0 free mol
   balance on Cl-
scope = inlet
   H2O          = 1.0 free kg
   swap CO2 for H+
   CO2          = 0.5 free molal
   Ca++         = 0.478 molal
   Mg++         = 0.112 molal
   Na+          = 4.740 molal
   K+           = 0.021 molal
   Cl-          = 5.934 molal
   SO4--        = 0.005 molal
   swap Kaolinite for Al+++
   Kaolinite    = 1.0 free mol
   swap Calcite for CO3--
   Calcite      = 5.0 free mol
   swap Chalcedony for H4SiO4
   Chalcedony   = 159.0 free mol
   balance on Cl-

kinetic Anorthite 2.0 mol
kinetic Anorthite rate_law = C:\Anorthite.bas
rate_con = 7.59E-10    surface = 1.0

suppress ALL
unsuppress  Anorthite Calcite Chalcedony Kaolinite
extrapolate
printout on     minerals = long         basis = short
delxi           = 0.025
dxplot          = 0.01 exact linear
dxprint         = 0.01 exact linear
```

```
epsilon         = 1.0E-7
nswap           = 80
simax           = 10
theta           = 1
timax           = 10
```

B.5.2 thermo_wateq4f.dat

```
# X1t script, saved Wed Feb 12 2014 by C.Haase
data = C:\Programme\Gwb\Gtdata\thermo_wateq4f.dat verify
time start      = 0 years,      end = 6400 days
length          = 50 m
width           = 0.5 m
height          = 0.01 m
Nx              = 50
discharge       = 0.1 m/day
permeability    intercept   = 15        porosity = -5
porosity                = 0.25
diffusion_coef          = 1.0E-20
thermal_cond            = 0
dispersivity            = 25 cm
temperature initial = 58 C,             inlet = 58,     constant = on
scope = initial
   H2O          = 1.0 free kg
   pH           = 5.8
   Ca++         = 0.478 molal
   Na+          = 4.743 molal
   Cl-          = 5.934 molal
   K+           = 0.021 molal
   Mg++         = 0.112 molal
   SO4--        = 0.005 molal
   swap Kaolinite for Al+++
   Kaolinite    = 1.0 free mol
   swap Calcite for CO3--
   Calcite      = 5.0 free mol
   swap Chalcedony for H4SiO4
   Chalcedony   = 159.0 free mol
   balance on Cl-
scope = inlet
   H2O          = 1.0 free kg
   swap CO2 for H+
   CO2          = 0.5 molal
   Ca++         = 0.478 molal
   Na+          = 4.743 molal
   Cl-          = 5.934 molal
   K+           = 0.021 molal
   Mg++         = 0.112 molal
   SO4--        = 0.005 molal
   swap Kaolinite for Al+++
   Kaolinite    = 1.0 free mol
   swap Calcite for CO3--
   Calcite      = 5.0 free mol
   swap Chalcedony for H4SiO4
   Chalcedony   = 159.0 free mol
   balance on Cl-

kinetic Anorthite 2.0 mol
kinetic Anorthite rate_law = „C:\Anorthite.bas“
rate_con = 7.59E-10    surface = 1.0

suppress ALL
unsuppress  Anorthite Calcite Chalcedony Kaolinite
```

```
extrapolate
printout on     minerals = long        basis = short
dxplot          = 0.01 exact linear
dxprint         = 0.01 exact linear
epsilon         = 1.0E-7
nswap           = 80
simax           = 10
theta           = 0.2
timax           = 10
```

B.5.3 thermo.dat

```
# X1t script, saved Tue Feb 11 2014 by C. Haase
data = C:\Programme\Gwb\Gtdata\thermo.dat verify
time start      = 0 years,      end = 13900 days
length          = 50 m
width           = 0.5 m
height          = 0.01 m
Nx              = 50
discharge       = 0.1 m/day
permeability    intercept = 15         porosity = -5
porosity                = 0.025
diffusion_coef          = 1.0E-20
thermal_cond            = 0
dispersivity            = 25 cm
temperature initial = 58,              inlet = 58,     constant = on
scope = initial
   H2O          = 1.0 free kg
   pH           = 5.8
   Ca++         = 0.478 molal
   Mg++         = 0.112 molal
   Na+          = 4.743 molal
   K+           = 0.021 molal
   Cl-          = 5.934 molal
   SO4--        = 0.005 molal
   swap Kaolinite for Al+++
   Kaolinite    = 1.0 free mol
   swap Calcite for HCO3-
   Calcite      = 5.0 free mol
   swap Chalcedony for SiO2(aq)
   Chalcedony   = 159.0 free mol
   balance on Cl-
scope = inlet
   H2O          = 1.0 free kg
   swap CO2(aq) for H+
   CO2(aq)      = 0.5 free molal
   Ca++         = 0.478 molal
   Mg++         = 0.112 molal
   Na+          = 4.743 molal
   K+           = 0.021 molal
   Cl-          = 5.934 molal
   SO4--        = 0.005 molal
   swap Kaolinite for Al+++
   Kaolinite    = 1.0 free mol
   swap Calcite for HCO3-
   Calcite      = 5.0 free mol
   swap Chalcedony for SiO2(aq)
   Chalcedony   = 159.0 free mol
   balance on Cl-

kinetic Anorthite 2.0 mol
kinetic Anorthite rate_law = D:\Anorthite.bas
```

```
rate_con = 7.59E-10    surface = 1.0

suppress ALL
unsuppress  Anorthite Calcite Chalcedony Kaolinite
extrapolate
printout on     minerals = long        basis = short
delxi           = 0.025
dxplot          = 0.025 exact linear
dxprint         = 0.025 exact linear
epsilon         = 1.0E-7
nswap           = 80
simax           = 10
```

B.5.4 thermo.com.v8.r6+.dat

```
# X1t script, saved Wed Feb 12 2014 by Christoph
data = C:\Programme\Gwb\Gtdata\thermo.com.v8.r6+.dat verify
time start      = 0 years,      end = 15000 days
length          = 50 m
width           = 0.5 m
height          = 0.01 m
Nx              = 50
discharge       = 0.1 m/day
permeability    intercept = 15         porosity = -5
porosity                = 0.025
diffusion_coef          = 1.0E-20
thermal_cond            = 0
dispersivity            = 25 cm
temperature initial = 58,              inlet = 58,     constant = on
scope = initial
   H2O          = 1.0 free kg
   pH           = 5.8
   Ca++         = 0.478 molal
   Mg++         = 0.112 molal
   Na+          = 4.743 molal
   K+           = 0.021 molal
   Cl-          = 5.934 molal
   SO4--        = 0.005 molal
   swap Kaolinite for Al+++
   Kaolinite    = 1.0 free mol
   swap Calcite for HCO3-
   Calcite      = 5.0 free mol
   swap Chalcedony for SiO2(aq)
   Chalcedony   = 159.0 free mol
   balance on Cl-
scope = inlet
   H2O          = 1.0 free kg
   swap CO2(aq) for H+
   CO2(aq)      = 0.5 free molal
   Ca++         = 0.478 molal
   Mg++         = 0.112 molal
   Na+          = 4.743 molal
   K+           = 0.021 molal
   Cl-          = 5.934 molal
   SO4--        = 0.005 molal
   swap Kaolinite for Al+++
   Kaolinite    = 1.0 free mol
   swap Calcite for HCO3-
   Calcite      = 5.0 free mol
   swap Chalcedony for SiO2(aq)
   Chalcedony   = 159.0 free mol
   balance on Cl-
```

```
kinetic Anorthite 2.0 mol
kinetic Anorthite rate_law = D:\Anorthite.bas
rate_con = 7.59E-10    surface = 1.0

suppress ALL
unsuppress  Anorthite Calcite Chalcedony Kaolinite
extrapolate
printout on    minerals = long        basis = short
delxi          = 0.01
dxplot         = 0.01 exact linear
dxprint        = 0.01 exact linear
epsilon        = 1.0E-7
nswap          = 80
simax          = 10
theta          = 1
timax          = 10
```

B.6 Anorthite rate law script file

```
rem 9: IF(-rate*Deltat+moles) < 1.0E-06 THEN rate=(moles/Deltat)*0.99

11: R = 8.314472
12: e = 2.7184
13: deltaT = 1/TK - 1/298.15
14: n = 1.411
rem acidic mechanism
20: Act_ac = -16600
21: ratenkonst = 3.16E-04
22: mech_a = exp(Act_ac/R*deltaT)*(1-Q/K)*ratenkonst*(activity(„H+“))^n
rem neutral mechanism
30: Act_neu = -17800
39: mech_n = exp(Act_neu/R*deltaT)*rate_con*(1 - Q/K)
40: rate = mech_a + mech_n
GOTO 60
50: rate = 0.0
60: RETURN rate
```

Anhang C

Anhang C

Eingabedateien für PHREEQC zu Kapitel 5 (»Suitability of Existing Numerical Model Codes and Thermodynamic Databases for the Prognosis of Calcite Dissolution Processes in Near-Surface Sediments Due to a CO_2 Leakage Investigated by Column Experiments«).

C.1 Eingabedatei für die Calcitlösung im Säulenversuch mit dem Ratengesetz nach Plummer et al. (1978) bei 6 bar und einer reaktiven Oberfläche von 700 und 5 550 dm^2/dm^3

```
DATABASE phreeqc.dat   # Database of PHREEQC version 2

TITLE Column Experiment with rate law of Plummer et al. (1978)

PRINT
  -reset false

SELECTED_OUTPUT
-file C:\Column_Experiment_7bar_Plummer.xls  # Excel output file path
-high_precision true
-totals Na Ca Mg K Cl C(4) Si S(6) Al
-equilibrium_phases    Calcite CO2(g)
-kinetic_reactants     Calcite
-saturation_indices    Calcite CO2(g)

RATES 1-120                   # Rate law from Plummer et al. (1978)
Calcite
 -start
  1   rem Calcite dissolution kinetics from Plummer et al. (1978)
  2   rem parm(1) = A/V, 1/dm         parm(2) = exponent for m/m0
  10  si_cc = si("Calcite")
  20  if (m <= 0  and si_cc < 0) then goto 200
  30  k1 = 10^(0.198 - 444.0 / (273.16 + tc))
  40  k2 = 10^(2.84 - 2177.0 / (273.16 + tc))
  50  if tc <= 25 then k3 = 10^(-5.86 - 317.0 / (273.16 + tc) )
  60  if tc > 25 then k3 = 10^(-1.10 - 1737.0 / (273.16 + tc) )
  70    t = 1
  80    if m0 > 0 then t = m/m0
  90    if t = 0 then t = 1
  100   moles = parm(1) * 0.1 * (t)^parm(2)
  110   moles = moles * (k1 * act("H+") + k2 * act("CO2") + k3 * act("H2O"))
  120   moles = moles * (1 - 10^(2/3 * si_cc))
  130   moles = moles * time
  140   if (moles > m) then moles = m
  150 if (moles >= 0) then goto 200
  160   temp = tot("Ca")
  170   mc = tot("C(4)")
  180   if mc < temp then temp = mc
  190   if -moles > temp then moles = -temp
  200 save moles
 -end
END

SOLUTION 0                    # Input solution: 0.1M NaCl solution in model column
-units mol/kgw
-temp   22
-pH     7.0
Na      0.1
Cl      0.1
EQUILIBRIUM_PHASES 0
CO2(g) 0.7782                 # Logarithm of fugacity of pCO2 at 7 bars
SAVE SOLUTION 0
END

SOLUTION 1-120                # 0.1M NaCl solution in model column
-units mol/kgw
-temp   22
-pH     7.0
Na      0.1
```

```
Cl      0.1
KINETICS 1-120
Calcite
-tol            1.0E-8
-m0             15.71
-m              15.71
-parms          700     0.6             # Set 5550 0.6 for larger surface area


TRANSPORT
-cells                  120             # Cell number
-lengths                0.0036          # Column length: 0.0036m * 120 = 0.43m
-shifts                 240             # Pore volume exchange: Two times
-time_step              37              # Flow velocity: 0.0036m/37s = 8.4m/d
-dispersivities         0.0024          # Longitudinal dispersivity, unit [m]
-diffusion_coefficient 0.3E-08         # Unit [m2/s]
-flow_direction         forward
-boundary_conditions    flux flux
-punch_frequency        240             # Output of 240th shift only

USER_GRAPH 1
-chart_title „Calcite dissolution in experimental column"
-axis_titles „Column length (m)" „Ca (mmol/L)"
-axis_scale y_axis      0       50
-axis_scale x_axis      0       0.43
-start
10 graph_x Dist                 # Column length in cm on x-axis
20 graph_y tot("Ca") * 1000     # Ca in mmol/L on y-axis
END
```

C.2 Eingabedatei für die Calcitlösung im Säulenversuch mit dem Ratengesetz nach Plummer et al. (1978) bei einem pCO_2 von 7 bar und einer reaktiven Oberfläche von 700 und 5 550 dm^2/dm^3

```
DATABASE phreeqc.dat            # Database of PHREEQC version 2

TITLE Column Experiment with rate law of Plummer et al. (1978)

PRINT
  -reset false

SELECTED_OUTPUT
-file C:\Column_Experiment_7bar_Plummer.xls  # Excel output file path
-high_precision true
-totals Na Ca Mg K Cl C(4) Si S(6) Al
-equilibrium_phases    Calcite CO2(g)
-kinetic_reactants     Calcite
-saturation_indices    Calcite CO2(g)

RATES 1-120                     # Rate law from Plummer et al. (1978)
Calcite
 -start
  1   rem Calcite dissolution kinetics from Plummer et al. (1978)
  2   rem parm(1) = A/V, 1/dm         parm(2) = exponent for m/m0
  10  si_cc = si("Calcite")
  20  if (m <= 0  and si_cc < 0) then goto 200
  30  k1 = 10^(0.198 - 444.0 / (273.16 + tc))
  40  k2 = 10^(2.84 - 2177.0 / (273.16 + tc))
  50  if tc <= 25 then k3 = 10^(-5.86 - 317.0 / (273.16 + tc) )
  60  if tc > 25 then k3 = 10^(-1.10 - 1737.0 / (273.16 + tc) )
  70    t = 1
  80    if m0 > 0 then t = m/m0
  90    if t = 0 then t = 1
```

```
  100   moles = parm(1) * 0.1 * (t)^parm(2)
  110   moles = moles * (k1 * act("H+") + k2 * act("CO2") + k3 * act("H2O"))
  120   moles = moles * (1 - 10^(2/3 * si_cc))
  130   moles = moles * time
  140   if (moles > m) then moles = m
  150   if (moles >= 0) then goto 200
  160   temp = tot("Ca")
  170   mc = tot("C(4)")
  180   if mc < temp then temp = mc
  190   if -moles > temp then moles = -temp
  200 save moles
 -end
END

SOLUTION 0             # Input solution: 0.1M NaCl solution in model column
-units mol/kgw
-temp   22
-pH     7.0
Na      0.1
Cl      0.1
EQUILIBRIUM_PHASES 0
CO2(g) 0.8325          # Logarithm of fugacity of pCO2 at 7 bars
SAVE SOLUTION 0
END

SOLUTION 1-120         # 0.1M NaCl solution in model column
-units mol/kgw
-temp   22
-pH     7.0
Na      0.1
Cl      0.1
KINETICS 1-120
Calcite
-tol           1.0E-8
-m0            15.71
-m             15.71
-parms         700     0.6            # Set 5550 0.6 for larger surface area


TRANSPORT
-cells                 120            # Cell number
-lengths               0.0036         # Column length: 0.0036m * 120 = 0.43m
-shifts                240            # Pore volume exchange: Two times
-time_step             92             # Flow velocity: 0.0036m/92s = 3.4m/d
-dispersivities        0.0024         # Longitudinal dispersivity, unit [m]
-diffusion_coefficient 0.3E-08        # Unit [m2/s]
-flow_direction        forward
-boundary_conditions   flux flux
-punch_frequency       240            # Output of 240th shift only

USER_GRAPH 1
-chart_title "Calcite dissolution in experimental column"
-axis_titles "Column length (m)" "Ca (mmol/L)"
-axis_scale y_axis     0       50
-axis_scale x_axis     0       0.43
-start
10 graph_x Dist                       # Column length in cm on x-axis
20 graph_y tot("Ca") * 1000           # Ca in mmol/L on y-axis
END
```

C.3 Eingabedatei für die Calcitlösung im Säulenversuch mit dem Ratengesetz nach Plummer et al. (1978) bei einem pCO_2 von 43 bar und einer reaktiven Oberfläche von 700 und 5 550 dm^2/dm^3

```
DATABASE phreeqc.dat   # Database of PHREEQC version 2

TITLE Column Experiment with rate law of Plummer et al. (1978)

PRINT
  -reset false

SELECTED_OUTPUT
-file C:\Column_Experiment_43bar_Plummer.xls  # Excel output file path
-high_precision true
-totals Na Ca Mg K Cl C(4) Si S(6) Al
-equilibrium_phases Calcite CO2(g)
-kinetic_reactants  Calcite
-saturation_indices Calcite CO2(g)

RATES 1-120            # Rate law from Plummer et al. (1978)
Calcite
 -start
  1   rem Calcite rate law from Plummer et al. (1978)
  2   rem parm(1) = A/V, 1/dm         parm(2) = exponent for m/m0
  10  si_cc = si("Calcite")
  20  if (m <= 0  and si_cc < 0) then goto 200
  30  k1 = 10^(0.198 - 444.0 / (273.16 + tc))
  40  k2 = 10^(2.84 - 2177.0 / (273.16 + tc))
  50  if tc <= 25 then k3 = 10^(-5.86 - 317.0 / (273.16 + tc) )
  60  if tc > 25 then k3 = 10^(-1.10 - 1737.0 / (273.16 + tc) )
  70    t = 1
  80    if m0 > 0 then t = m/m0
  90    if t = 0 then t = 1
  100   moles = parm(1) * 0.1 * (t)^parm(2)
  110   moles = moles * (k1 * act("H+") + k2 * act("CO2") + k3 * act("H2O"))
  120   moles = moles * (1 - 10^(2/3 * si_cc))
  130   moles = moles * time
  140   if (moles > m) then moles = m
  150 if (moles >= 0) then goto 200
  160   temp = tot("Ca")
  170   mc = tot("C(4)")
  180   if mc < temp then temp = mc
  190   if -moles > temp then moles = -temp
  200 save moles
 -end
END

SOLUTION 0             # Input solution: 0.1M NaCl solution in model column
-units mol/kgw
-temp   22
-pH     7.0
Na      0.1
Cl      0.1
EQUILIBRIUM_PHASES 0
CO2(g) 1.543           # Logarithm of CO2 fugacity at pCO2 of 43bars
SAVE SOLUTION 0
END


SOLUTION 1-120         # 0.1M NaCl solution in model column
-units mol/kgw
-temp   22
-pH     7.0
```

```
Na      0.1
Cl      0.1
KINETICS 1-120
Calcite
 -tol           1.0E-8
 -m0            15.71
 -m             15.71
 -parms         700     0.6             # Set 5550 0.6 for larger surface area
END


TRANSPORT
-cells                  120             # Cell number
-lengths                0.0036          # Column length: 0.0036m * 120 = 0.43m
-shifts                 240             # Exchange of pore water: Two times
-time_step              92              # Flow velocity: 0.0036m/92s = 3.4m/d
-dispersivities         0.0024          # Longitudinal dispersivity, unit [m]
-diffusion_coefficient 0.3E-08         # Unit [m2/s]
-flow_direction         forward
-boundary_conditions    flux flux
-punch_frequency        240             # Output of 240th shift only

USER_GRAPH 1
-chart_title „Calcite dissolution in experimental column"
-axis_titles „Column length (m)" „Ca (mmol/L)"
-axis_scale y_axis      0       50
-axis_scale x_axis      0       0.43
-start
10 graph_x Dist                         # Column length in cm on x-axis
20 graph_y tot(„Ca") * 1000             # Ca in mmol/L on y-axis
END
```

C.4 Eingabedatei für die Calcitlösung im Säulenversuch mit dem Ratengesetz nach Palandri & Kharaka (2004) bei einem pCO_2 6 bar und einer reaktiven Oberfläche von 700 und 5 550 dm^2/dm^3

```
DATABASE phreeqc.dat   # Database of PHREEQC version 2

TITLE Colum Experiment using rate law of Palandri & Kharaka (2004)

PRINT
  -reset false

SELECTED_OUTPUT
-file C:\Column_Experiment_6bar_Palandri_5550.xls   # Excel output file path
-high_precision true
-totals Na Ca Mg K Cl C(4) Si S(6) Al
-equilibrium_phases Calcite CO2(g)
-kinetic_reactants Calcite
-saturation_indices Calcite CO2(g)


RATES                   # Rate law from Palandri & Kharakha (2004)
Calcite
  -start
10  R = 8.314472
11  deltaT = 1/TK - 1/298.15
12  e = 2.7183
rem Acidic Mechanism
13  Ea = 14400
14  logK25 = -0.30
15  ny = 1.0
16  mech_a = (10^logK25) * (e^(-Ea/R*deltaT)) * (ACT(„H+"))^ny
```

```
rem Neutral Mechanism
21  Ea = 23500
22  logK25 = -5.81
23  mech_b = (10^logK25) * (e^(-Ea/R*deltaT))
rem Total Rate
50  rate = mech_b + mech_a
51  teta = 1.0
52  eta  = 1.0
53  Area = 55.5         # Surface area 700dm2/dm3
rem                     # 55.5 corresponds to 5550dm2/dm3
60  rate = Area * rate * (1 - SR("Calcite"))
61  moles = rate * time
62  save moles
  -end
END

SOLUTION 0              # Input solution: 0.1M NaCl solution in model column
-temp 22
-units mol/kgw
-pH     7.0
Na      0.1
Cl      0.1
EQUILIBRIUM_PHASES 0
CO2(g)  0.7782          # Logarithm of CO2 fugacity at pCO2 of 6bars
SAVE SOLUTION 0
END

SOLUTION 1-120          # 0.1M NaCl solution in model column
-temp 22
-units mol/kgw
-pH     7.0
Na      0.1
Cl      0.1

KINETICS 1-120
Calcite
-m      1.0
-m0     1.0
-tol    1.0E-12


TRANSPORT
-cells                  120             # Cell number
-length                 0.0036          # Column length 0.0036m * 120 = 0.43m
-shifts                 240             # Exchange of pore water: Two times
-time_step              37              # Flow velocity: 0.0036m/37s = 8.4m/d
-dispersivity           0.0024          # Longitudinal dispersivity, unit [m]
-diffusion_coefficient 0.3E-09         # Unit [m2/s]
-flow_direction        forward
-boundary_conditions   flux flux
-punch_frequency       240             # Output of 240th shift only

USER_GRAPH 1
-chart_title "Calcite dissolution in experimental column"
-axis_titles "Column length (m)" "Ca (mmol/L)"
-axis_scale y_axis     0       50
-axis_scale x_axis     0       0.43
-start
10 graph_x Dist                         # Column length in cm on x-axis
20 graph_y tot("Ca") * 1000             # Ca in mmol/L on y-axis
END
```

C.5 Eingabedatei für die Calcitlösung im Säulenversuch mit dem Ratengesetz nach Palandri & Kharaka (2004) bei einem pCO_2 von 7 bar und einer reaktiven Oberfläche von 700 und 5 550 dm^2/dm^3

```
DATABASE phreeqc.dat   # Database of PHREEQC version 2

TITLE Colum Experiment using rate law of Palandri & Kharaka (2004)

SELECTED_OUTPUT
-file C:\Column_Experiment_6bar_Palandri_5550.xls # Excel output file path
-high_precision true
-totals Na Ca Mg K Cl C(4) Si S(6) Al
-equilibrium_phases Calcite CO2(g)
-kinetic_reactants Calcite
-saturation_indices Calcite CO2(g)


RATES                  # Rate law from Palandri & Kharakha (2004)
Calcite
  -start
10  R = 8.314472
11  deltaT = 1/TK - 1/298.15
12  e = 2.7183rem Acidic Mechanism
13  Ea = 14400
14  logK25 = -0.30
15  ny = 1.0
16  mech_a = (10^logK25) * (e^(-Ea/R*deltaT)) * (ACT("H+"))^ny
rem Neutral Mechanism
23  Ea = 23500
24  logK25 = -5.81
26  mech_b = (10^logK25) * (e^(-Ea/R*deltaT))
rem Total Rate
50  rate = mech_a + mech_b
51  teta = 1.0
52  eta  = 1.0
53  Area = 7.0         # Surface area 700dm2/dm3
rem                    # 55.5 corresponds to 5550dm2/dm3
60  rate = Area * rate * (1 - SR("Calcite"))
61  moles = rate * time
62  save moles
  -end
END


SOLUTION 0             # Input solution: 0.1M NaCl solution in model column
-temp   22
-pH     7.0
-units mol/kgw
Na      0.1
Cl      0.1

EQUILIBRIUM_PHASES 0
CO2(g)   0.8325        # Logarithm of CO2 fugacity at pCO2 of 7 bars
SAVE SOLUTION 0
END

SOLUTION 1-120         # 0.1M NaCl solution in model column
-temp 22
-pH     7.0
-units mol/kgw
Na      0.1
Cl      0.1
```

```
KINETICS 1-120
Calcite
-m      1.0
-m0     1.0
-tol    1.0E-12
END


TRANSPORT
-cells                  120             # Cell number
-length                 0.0036          # Column length 0.0036m*120 = 0.43m
-shifts                 240             # Exchange of pore water: Two times
-time_step              92              # Flow velocity: 0.0036m/37s = 3.4m/d
-dispersivity           0.0024          # Longitudinal dispersivity, unit [m]
-diffusion_coefficient 0.3E-09         # Unit [m2/s]
-flow_direction        forward
-boundary_conditions   flux flux
-punch_frequency       240             # Output of 240th shift only

USER_GRAPH 1
-chart_title „Calcite dissolution in experimental column"
-axis_titles „Column length (m)" „Ca (mmol/L)"
-axis_scale y_axis     0       50
-axis_scale x_axis     0       0.43
-start
10 graph_x Dist                                 # Column length in cm on x-axis
20 graph_y tot(„Ca") * 1000             # Ca in mmol/L on y-axis
END
```

C.6 Eingabedatei für die Calcitlösung im Säulenversuch mit dem Ratengesetz nach Palandri & Kharaka (2004) bei einem pCO_2 von 43 bar und einer reaktiven Oberfläche von 700 und 5 550 dm^2/dm^3

```
DATABASE phreeqc.dat   # Database of PHREEQC version 2

TITLE Säulenversuch 43bar

SELECTED_OUTPUT
-file C:\Column_43bar_Palandri_5550.xls # file name
-high_precision true
-totals Na Ca Mg K Cl C(4) Si S(6) Al
-equilibrium_phases    Calcite CO2(g)
-kinetic_reactants     Calcite
-saturation_indices    Calcite CO2(g)

RATES                           # Rate law from Palandri & Kharakha (2004)
Calcite
  -start
10  R = 8.314472
11  deltaT = 1/TK - 1/298.15
12  e = 2.7183
rem Acidic Mechanism
13  Ea = 14400
14  logK25 = -0.30
15  ny = 1.0
16  mech_a = (10^logK25) * (e^(-Ea/R*deltaT)) * (ACT(„H+"))^ny
rem Neutral Mechanism
21  Ea = 23500
22  logK25 = -5.81
23  mech_b = (10^logK25) * (e^(-Ea/R*deltaT))
rem Total Rate
50  rate = mech_b + mech_a
51  teta = 1.0
```

```
52  eta  = 1.0
53  Area = 7.0                  # surface area 700dm2/dm3
rem                             # 55.5 corresponds to 5550dm2/dm3
60  rate = Area * rate * (1 - SR(„Calcite"))
61  moles = rate * time
62  save moles
  -end
END


SOLUTION 0                      # Input solution: 0.1M NaCl solution in model column
-temp   22
-units mol/kgw
-pH     7.0
Na      0.1
Cl      0.1
UILIBRIUM_PHASES 0
CO2(g) 1.543                    # Logarithm of CO2 fugacity at pCO2 of 43 bars
SAVE SOLUTION 0
END

SOLUTION 1-120                  # 0.1M NaCl solution in model column
-temp 22
-units mol/kgw
-pH     7.0
Na      0.1
Cl      0.1


KINETICS 1-120
Calcite
-m      1.0
-m0     1.0
-tol    1.0e-12
END


TRANSPORT
-cells                  120             # Cell number
-length                 0.0036          # Column length 0.0036m*120 = 0.43m
-shifts                 240             # Exchange of pore water: Two times
-time_step              92              # Flow velocity: 0.0036m/37s = 3.4m/d
-dispersivity           0.0024          # Longitudinal dispersivity, unit [m]
-diffusion_coefficient 0.3E-9          # Unit [m2/s]
-flow_direction        forward
-boundary_conditions   flux flux
-punch_frequency       240             # Output of 240th shift only

USER_GRAPH 1
-chart_title „Calcite dissolution in experimental column"
-axis_titles „Column length (m)" „Ca (mmol/L)"
-axis_scale y_axis     0       50
-axis_scale x_axis     0       0.43
-start
10 graph_x Dist                         # Column length in cm on x-axis
20 graph_y tot(„Ca") * 1000             # Ca in mmol/L on y-axis
END
```

C.7 Eingabedatei für die Calcitlösung im Säulenversuch bei einem pCO_2 von 6 bar

```
DATABASE phreeqc.dat   # Database of PHREEQC version 2
# DATABASE wateq4f.dat # Selection of thermodynamic database
# DATABASE llnl.dat
# DATABASE minteq.dat
# DATABASE minteq.v4.dat
# DATABASE sit.dat
# DATABASE pitzer.dat
# DATABASE theredata.dat

TITLE Column experiment conducted at 6bars. Surface area 30dm2/dm3.

SELECTED_OUTPUT
-file C:\Column_Experiment_6bar.xls   # Path for Excel Output File
-high_precision true
-totals Na Ca Mg K Cl C(4) Si S(6) Al
-equilibrium_phases    Calcite CO2(g)
-kinetic_reactants     Calcite
-saturation_indices    Calcite CO2(g)


RATES                          # Rate law from Palandri & Kharakha (2004)
Calcite
  -start
10  R = 8.314472
11  deltaT = 1/TK - 1/298.15
12  e = 2.7183
rem Acidic Mechanism
13  Ea = 14400
14  logK25 = -0.30
15  ny = 1.0
16  mech_a = (10^logK25) * (e^(-Ea/R*deltaT)) * (ACT("H+"))^ny
rem Neutral Mechanism
23  Ea = 23500
24  logK25 = -5.81
26  mech_b = (10^logK25) * (e^(-Ea/R*deltaT))
rem Total Rate
50  rate = mech_a + mech_b
51  teta = 1.0
52  eta  = 1.0
53  Area = 0.30                # Corresponding to surface area of 30dm2/dm3
60  rate = Area * rate * (1 - SR("Calcite"))
61  moles = rate * time
62  save moles
  -end
END

SOLUTION 0                     # Input solution: 0.1M NaCl solution in model column
-temp   22
-pH     7.0
-units mol/kgw
Na      0.1
Cl      0.1
EQUILIBRIUM_PHASES 0
CO2(g) 0.7782                  # Logarithm of CO2 fugacity at a pCO2 of 6 bars
SAVE SOLUTION 0
END


SOLUTION 1-120                         # 0.1M NaCl solution in model column
-temp   22
```

```
-pH     7.0
-units mol/kgw
Na      0.1
Cl      0.1

KINETICS 1-120
Calcite
-m      1.0
-m0     1.0
-tol    1.0E-12
END


TRANSPORT
-cells                  120                     # Cell number
-length                 0.0036                  # Column length: 0.0036m*120= 0.43m
-shifts                 240                     # Exchange of pore water: Two times
-time_step              37                      # Flow velocity = 0.0036m/37s = 8.4m/d
-dispersivity           0.0024                  # Longitudinal dispersivity, unit [m]
-diffusion_coefficient 0.3E-09                 # Unit [m2/s]
-flow_direction        forward
-boundary_conditions   flux flux
-punch_frequency       240                     # Output of 240th shift only

USER_GRAPH 1
-chart_title „Calcite dissolution in experimental column"
-axis_titles „Column length (m)" „Ca (mmol/L)"
-axis_scale y_axis     0       50
-axis_scale x_axis     0       0.43
-start
10 graph_x Dist                                 # Column length in cm on x-axis
20 graph_y tot(„Ca") * 1000           # Ca in mmol/L on y-axis
END
```

C.8 Eingabedatei für die Calcitlösung im Säulenversuch bei einem pCO_2 von 7 bar

```
DATABASE phreeqc.dat   # Database of PHREEQC version 2
# DATABASE wateq4f.dat # Selection of thermodynamic database
# DATABASE llnl.dat
# DATABASE minteq.dat
# DATABASE minteq.v4.dat
# DATABASE sit.dat
# DATABASE pitzer.dat
# DATABASE theredata.dat

TITLE Column Experiment conducted at 7bars. Surface Area 6.5 dm2/dm3.

SELECTED_OUTPUT
-file                   C:\Column_7bar.xls     # Path for Excel Output File
-high_precision         true
-totals         Na Ca Mg K Cl C(4) Si S(6) Al
-equilibrium_phases     Calcite CO2(g)
-kinetic_reactant               Calcite
-saturation_indices Calcite CO2(g)


RATES                           # Rate law from Palandri & Kharakha (2004)
Calcite
  -start
10  R   = 8.314472
11  deltaT = 1/TK - 1/298.15
12  e   = 2.7183
```

```
rem Acidic Mechanism
13  Ea  = 14400
14  logK25      = -0.30
15  ny  = 1.0
16  mech_a = (10^logK25) * (e^(-Ea/R*deltaT)) * (ACT("H+"))^ny
rem Neutral Mechanism
23  Ea  = 23500
24  logK25      = -5.81
26  mech_b = (10^logK25) * (e^(-Ea/R*deltaT))
rem Total Rate:
50  rate = mech_a + mech_b
51  teta        = 1.0
52  eta = 1.0
53  Area        = 0.065 # Corresponding to surface area of 6.5 dm2/dm3
60  rate = Area * rate * (1 - SR("Calcite"))
61  moles = rate * time
62  save moles
  -end
END


SOLUTION 0                    # Input solution: 0.1M NaCl solution in model column
-temp   22
-units mol/l
-pH     7.0
Na      0.1
Cl      0.1
EQUILIBRIUM_PHASES 0
CO2(g) 0.8451                 # Logarithm of CO2 fugacity at pCO2 of 7 bars
SAVE SOLUTION 0
END


SOLUTION 1-120                        # 0.1M NaCl solution in model column
-temp   22
-units mol/l
-pH     7.0
Na      0.1
Cl      0.1

KINETICS 1-120
Calcite
-m      1.0
-m0     1.0
-tol    1.0E-12
END


TRANSPORT
-cells          120                   # Cell number
-length         0.0036                # Column length: 120*0.005 = 0.43m
-shifts         240                   # Exchange of pore water: Two times
-time_step              92                    # Flow velocity = 0.0036m/92s = 8.4m/d
-dispersivity                  0.0024         # Longitudinal dispersivity, unit [m]
-diffusion_coefficient 0.3E-9         # Unit [m2/s]
-flow_direction                forward
-boundary_conditions   flux flux
-punch_frequency               240            # Output of 240th shift only


USER_GRAPH 1                                  # Plot chart after simulation
-chart_title "Calcite dissolution in experimental column"
```

```
-axis_titles „Column length (m)“ „Ca (mmol/L)“
-axis_scale y_axis     0       50
-axis_scale x_axis     0       0.43
-start
10 graph_x Dist                        # Column length in cm on x-axis
20 graph_y tot(„Ca“) * 1000            # Ca in mmol/L on y-axis
END
```

C.9 Eingabedatei für die Calcitlösung im Säulenversuch bei einem pCO_2 von 43 bar

```
DATABASE phreeqc.dat   # Database of PHREEQC version 2
# DATABASE wateq4f.dat # Selection of thermodynamic database
# DATABASE llnl.dat
# DATABASE minteq.dat
# DATABASE minteq.v4.dat
# DATABASE sit.dat
# DATABASE pitzer.dat
# DATABASE theredata.dat

TITLE Column Experiment 43 bar Surface Area?

SELECTED_OUTPUT
-file C:\Column_43bar.xls      # Path for Excel Output File
-high_precision true
-totals Na Ca Mg K Cl C(4) Si S(6) Al
-equilibrium_phases    Calcite CO2(g)
-kinetic_reactant              Calcite
-saturation_indices    Calcite CO2(g)


RATES                          # Rate law from Palandri & Kharakha (2004)
Calcite
  -start
10  R   = 8.314472
11  deltaT = 1/TK - 1/298.15
12  e   = 2.7183
rem Acidic Mechanism
13  Ea  = 14400
14  logK25      = -0.30
15  ny  = 1.0
16  mech_a = (10^logK25) * (e^(-Ea/R*deltaT)) * (ACT(„H+“))^ny
rem Neutral Mechanism
23  Ea  = 23500
24  logK25      = -5.81
26  mech_b = (10^logK25) * (e^(-Ea/R*deltaT))
rem Total Rate:
50  rate = mech_a + mech_b
51  teta        = 1.0
52  eta = 1.0
53  Area        = 0.02             # Correponds to surface area of 2 dm2/dm3
60  rate = Area * rate * (1 - SR(„Calcite“))
61  moles = rate * time
62  save moles
  -end
END


SOLUTION 0                     # Input solution: 0.1M NaCl solution in model column
-temp 22
-units mol/kgw
-pH   7.0
Na      0.1
```

```
Cl      0.1
EQUILIBRIUM_PHASES 0
CO2(g) 1.543                    # Logarithm of CO2 fugacity at pCO2 of 43bars
SAVE SOLUTION 0
END


SOLUTION 1-120                  # 0.1M NaCl solution in model column
-temp   22
-units mol/kgw
-pH     7.0
Na      0.1
Cl      0.1

KINETICS 1-120
Calcite
-m      1.0
-m0     1.0
-tol    1.0E-12
END

TRANSPORT
-cells                  120
-shifts                 240                     # Flow velocity = 0.0036m/92s = 8.4m/d
-time_step              92                      # Total time = 92s*240shifts = 22080s
-length                 0.0036                  # Column length: 120*0.036 = 0.43m
-dispersivity           0.0024                  # Longitudinal dispersivity, unit [m]
-diffusion_coefficient 0.3E-9                  # Unit [m2/s]
-flow_direction         forward
-boundary_conditions    flux flux
-punch_frequency        240                     # Output of 240th shift only


USER_GRAPH 1                                    # Plot chart after simulation
-chart_title „Calcite dissolution in experimental column"
-axis_titles „Column length (m)" „Ca (mmol/L)"
-axis_scale y_axis     0       50
-axis_scale x_axis     0       0.43
-start
10 graph_x Dist                                 # Column length in cm on x-axis
20 graph_y tot(„Ca") * 1000                     # Ca in mmol/L on y-axis
END
```

C.10 Eingabedatei für die Calcitlösung im »field scale model« bei einem pCO_2 von 6 bar und einer Strömungsgeschwindigkeit von 1.0 m/d.

```
DATABASE phreeqc.dat   # Database of PHREEQC version 2
# DATABASE pitzer.dat

TITLE Field scale model at 6bars pCO2 and a flow velocity of 1m/d

SELECTED_OUTPUT
-file C:\Field scale_6bars.xls
-high_precision        true
-totals         Na Ca Mg K Cl C(4) Si S(6) Al
-equilibrium_phases    Calcite CO2(g)
-kinetic_reactant      Calcite
-saturation_indices Calcite CO2(g)


RATES                          # Rate law from Palandri & Kharakha (2004)
Calcite
```

```
  -start
10  R = 8.314472
11  deltaT = 1/TK - 1/298.15
12  e = 2.7183
rem Acidic Mechanism
13  Ea = 14400
14  logK25 = -0.30
15  ny = 1.0
16  mech_a = (10^logK25) * (e^(-Ea/R*deltaT)) * (ACT("H+"))^ny
rem Neutral Mechanism
23  Ea = 23500
24  logK25 = -5.81
26  mech_b = (10^logK25) * (e^(-Ea/R*deltaT))
rem Total Rate
50  rate = mech_a + mech_b
51  teta = 1.0
52  eta  = 1.0
53  Area = 0.30               # Corresponding to surface area of 30dm2/dm3
60  rate = Area * rate * (1 - SR("Calcite"))
61  moles = rate * time
62  save moles
  -end
END


SOLUTION 0                  # Input solution: 0.1M NaCl solution in model column
-temp 22
-pH     7.0
-units mol/kgw
Na      0.1
Cl      0.1
EQUILIBRIUM_PHASES 0
CO2(g) 0.7782               # Logarithm of CO2 fugacity at a pCO2 of 6bars
SAVE SOLUTION 0
END


SOLUTION 1-1000             # 0.1M NaCl solution in model column
-temp 22
-units mol/kgw
pH      7.0
Na      0.1
Cl      0.1

KINETICS 1-1000
Calcite
-m      1.0
-m0     1.0
-tol    1.0E-12
END


TRANSPORT
-cells                 100
-length                0.1                  # Column length 100*0.1m = 10m
-shift                 2000                 # 2000/100 = pore volumes replacd
-time_step             8640                 # Flow velocity = 0.1m/8640s = 1m/d
-dispersivity          0.05                 # Longitudinal dispersivity, unit [m]
-diffusion_coefficient 0.3E-09 # Unit [m2/s]
-flow_direction        forward
-boundary_conditions   flux flux
-print_frequency               2000          # Output of 2000th shift only
```

```
USER_GRAPH 1                                    # Plot chart after simulation
-chart_title „Calcite dissolution in experimental column"
-axis_titles „Column length (m)" „Ca (mmol/L)"
-axis_scale y_axis     0       50
-axis_scale x_axis     0       10
-start
10 graph_x Dist                                 # Column length in cm on x-axis
20 graph_y tot(„Ca") * 1000           # Ca in mmol/L on y-axis
END
```

C.11 Eingabedatei für die Calcitlösung im »field scale model« bei einem pCO_2 von 43 bar und einer Strömungsgeschwindigkeit von 1.0 m/d.

```
DATABASE phreeqc.dat   # Database of PHREEQC version 2
# DATABASE pitzer.dat

TITLE Field scale model at 43bars pCO2 and a flow velocity of 1m/d

SELECTED_OUTPUT
-file C:\Field scale_43bars.xls
-high_precision        true
-totals        Na Ca Mg K Cl C(4) Si S(6) Al
-equilibrium_phases    Calcite CO2(g)
-kinetic_reactant              Calcite
-saturation_indices    Calcite CO2(g)


RATES                          # Rate law from Palandri & Kharakha (2004)
Calcite
  -start
10  R = 8.314472
11  deltaT = 1/TK - 1/298.15
12  e = 2.7183
rem Acidic Mechanism
13  Ea = 14400
14  logK25 = -0.30
15  ny = 1.0
16  mech_a = (10^logK25) * (e^(-Ea/R*deltaT)) * (ACT(„H+"))^ny
rem Neutral Mechanism
23  Ea = 23500
24  logK25 = -5.81
26  mech_b = (10^logK25) * (e^(-Ea/R*deltaT))
rem Total Rate
50  rate = mech_b + mech_a
51  teta = 1.0
52  eta  = 1.0
53  Area = 0.30                # Corresponding to surface area of 30dm2/dm3
60  rate = Area * rate * (1 - SR(„Calcite"))
61  moles = rate * time
62  save moles
  -end
END


SOLUTION 0                     # Input solution: 0.1M NaCl solution in model column
-temp   22
-units mol/kgw
-pH     7.0
Na      0.1
Cl      0.1
EQUILIBRIUM_PHASES 0
```

```
CO2(g) 1.543                    # Logarithm of CO2 fugacity at a pCO2 of 43bars
SAVE SOLUTION 0
END


SOLUTION 1-1000                 # 0.1M NaCl solution in model column
-temp   22
-units mol/kgw
-pH     7.0
Na      0.1
Cl      0.1

KINETICS 1-1000
Calcite
-m      1.0
-m0     1.0
-tol    1.0E-12
END


TRANSPORT
-cells                  100
-length                 0.1                     # column length 100*0.1m = 10m
-shift                  2000                    # 2000/100 = pore volumes replacd
-time_step              8640                    # flow velocity = 0.1m/8640s = 1m/d
-dispersivity           0.05                    # unit [m]
-diffusion_coefficient 0.3E-09                 # longitudinal dispersivity, unit [m]
-flow_direction        forward
-boundary_conditions   flux flux
-print_frequency               2000             # Output of 2000th shift only


USER_GRAPH 1                                    # Plot chart after simulation
-chart_title „Calcite dissolution in experimental column“
-axis_titles „Column length (m)“ „Ca (mmol/L)“
-axis_scale y_axis     0       50
-axis_scale x_axis     0       10
-start
10 graph_x Dist                                 # Column length in cm on x-axis
20 graph_y tot(„Ca“) * 1000                     # Ca in mmol/L on y-axis
END
```

Anhang D

D.1 Aktivitätsgleichungen und ihre Gültigkeitsbereiche

1. Davies-Gleichung (Davies, 1938)

$$\log \gamma_i = -Az_i^2 \frac{\sqrt{I}}{1+\sqrt{I}} - 0.3I$$ gültig bei I < 0.5 ~ 0.7 mol/kgw

2. Debye-Hückel-Gleichung (Debye & Hückel, 1923)

$$\log \gamma_i = -A \times z_i^2 \times \sqrt{I}$$ gültig bei I < 0.005 mol/kgw

3. Erweiterte Debye-Hückel-Gleichung

$$\log \gamma_i = -Az_i^2 \frac{\sqrt{I}}{1+B \times a_0 \times \sqrt{I}}$$ gültig bei I < 0.1 mol/kgw

4. WATEQ Debye-Hückel-Gleichung

$$\log \gamma_i = \frac{-Az_i^2 \times \sqrt{I}}{1+B \times a_0 \times \sqrt{I}} - b_0 I$$ gültig bei I < 1.0 mol/kgw

5. Setchenow equation

$$\log \gamma_i = b_0 \times I$$ gültig bei I < 1.0 mol/kgw

Veröffentlichungsrechte

Haase, C., Dethlefsen, F., Ebert, M. & Dahmke. A, 2013. Uncertainty in geochemical modelling of CO_2 and calcite dissolution in NaCl solutions due to different modelling codes and thermodynamic databases. Applied Geochemistry 33(June 2013), 306–317. doi: *10.1016/j.apgeochem.2013.03.001*

Für den Artikel wird keine gesonderte Erlaubnis für den Abdruck in einer Dissertation benötigt. Auf der Webseite wird folgender Rechtehinweis angegeben:

As an Elsevier journal author, you retain various rights including Inclusion of the article in a thesis or dissertation whether in part or in toto; see http://www.elsevier.com/about/policies/author-agreement/lightbox_scholarly-purposes for more information. As this is a retained right, no written permission is necessary provided that proper acknowledgement is given.

Elsevier:
Published Journal Article
Policies for sharing published journal articles differ for subscription and gold open access articles:

Subscription articles

If you are an author, please share a link to your article rather than the full-text. Millions of researchers have access to the formal publications on ScienceDirect, and so links will help your users to find, access, cite, and use the best available version.

Theses and dissertations which contain embedded PJAs as part of the formal submission can be posted publicly by the awarding institution with DOI links back to the formal publications on ScienceDirect.

If you are affiliated with a library that subscribes to ScienceDirect you have additional private sharing rights for others' research accessed under that agreement. This includes use for classroom teaching and internal training at the institution (including use in course packs and courseware programs), and inclusion of the article for grant funding purposes.

Haase, C., Dahmke, A., Ebert, M., Schäfer, D. & Dethlefsen, F. 2014. Suitability of existing numerical model codes and thermodynamic databases for the prognosis of calcite dissolution processes in near-surface sediments due to a CO_2 leakage investigated by column experiments. Aquatic Geochemistry 20(6), 639–661.

SPRINGER LICENSE
TERMS AND CONDITIONS

Jul 15, 2015

This is a License Agreement between Christoph Haase („You“) and Springer („Springer“) provided by Copyright Clearance Center („CCC“). The license consists of your order details, the terms and conditions provided by Springer, and the payment terms and conditions.

All payments must be made in full to CCC. For payment instructions, please see information listed at the bottom of this form.

License Number	3615230577546
License date	Apr 24, 2015
Licensed content publisher	Springer
Licensed content publication	Aquatic Geochemistry
Licensed content title	Suitability of Existing Numerical Model Codes and Thermodynamic Databases for the Prognosis of Calcite Dissolution Processes in Near-Surface Sediments Due to a CO_2 Leakage Investigated by Column Experiments
Licensed content author	Christoph Haase
Licensed content date	Jan 1, 2014
Volume number	20
Issue number	6
Type of Use	Thesis/Dissertation
Portion	Full text
Number of copies	4
Author of this Springer article	Yes and you are a contributor of the new work
Order reference number	None
Title of your thesis / dissertation	Hydrogeochemische Modellierung der CO2-Speicherung in salinen Aquiferen
Expected completion date	Jun 2015
Estimated size(pages)	170
Total	0.00 USD
Terms and Conditions	

Introduction
The publisher for this copyrighted material is Springer Science + Business Media. By clicking „accept“ in connection with completing this licensing transaction, you agree that the following terms and conditions apply to this transaction (along with the Billing and Payment terms and conditions established by Copyright Clearance

Institut für Geowissenschaften
Christian-Albrechts-Universität zu Kiel
Kiel, 2015

Textsatz mit Adobe Indesign CS 2.0
Minion Pro/Myriad Pro
Druck & Herstellung:
ksh diedruckerin.de & Buchbinderei Zach
gedruckt auf Inacopia Elite Colour Plus 100g/m²
chlorarm gebleicht
alterungsbeständig nach DIN 9706